1995

Wheat hardness by near infrared (NIR) spectroscopy: New insights

Manley, Marena

Wheat hardness by near infrared (NIR) spectroscopy: New insights

by

Marena Manley

A thesis submitted to the University of Plymouth
in partial fulfilment for the degree of

DOCTOR OF PHILOSOPHY

Department of Agriculture and Food Studies
Seale-Hayne Faculty of Agriculture, Food and Land Use

July 1995

Abstract

Wheat hardness by near infrared (NIR) spectroscopy: New insights

by

Marena Manley

The determination of wheat hardness by the evaluation of whole wheat grain would be of considerable value to the UK Milling Industry. Until now, accurate whole wheat grain hardness predictions by NIR spectroscopy have only been reported for North American wheats. By the evaluation of selected samples of UK and North American wheats this study showed that the prediction of whole wheat grain hardness by NIR spectroscopy depends only on the scattering properties of the sample and that there is no direct relationship with chemical composition. The scattering effect, in case of whole wheat grain reflectance and transmittance spectra, was found not to be multiplicative as in the case of ground wheat grain spectra.

Empirical NIR spectroscopy calibrations are often performed without knowing what is measured or understanding the basis of the measurement. In other words the NIR spectrophotometer is often used as a "black box". Empirical calibrations were performed using three different software packages i.e. Infrasoft International (ISI) Software, NIRSystems Spectral Analysis Software (NSAS) and UNSCRAMBLER. Successful NIR spectroscopy hardness measurements on ground wheat are based on light scattering. Separating the scattering effect from whole wheat grain spectra mathematically allowed predictions not significantly different to empirical calibrations, with the benefit of a theoretical explanation and fewer terms used.

Although hardness predictions for whole wheat grain were not as accurate as in the case of ground wheat grain, it did prove to predict hardness with an acceptable accuracy with practical use as screening methods for grain trading.

This study did not completely solve the problem of predicting whole wheat grain hardness by NIR spectroscopy, but new insights were provided which would hopefully encourage further work in this area and lead to a more complete fundamental understanding of the properties of whole wheat grain hardness using NIR spectroscopy.

List of Contents

List of Tables

List of Figures

List of Appendices

List of Abbreviations

AACC	American Association of Cereal Chemists
ADAS	Agricultural Development and Advisory Service
AJS	Air Jet Sieve
AREA	Area under the second derivative curve
ca.	*circa*, about
CAP	Common Agricultural Policy
CCA	Canonical Correlation Analysis
CGC	Canadian Grain Commission
CCFRA	Campden-Chorleywood Food Research Association
Corr.	Correlation
CV	Canonical variates
CWRS	Canadian Western Red Spring
Dev.	Deviation
e.g.	for example
FGIS	Federal Grain Inspection Service
FMBRA	Flour Milling and Baking Research Association
ICC	International Association for Cereal Science and Technology
i.e.	that is
IR	Infrared
ISI	Infrasoft International Software
kDa	Kilo-Dalton
lab	Laboratory
mb	Moisture base
MH	Mean of hard samples
MLR	Multiple linear regression
MS	Mean of soft samples
MSC	Multiplicative scatter correction

2nd	Second
NIR	Near infrared
NSAS	NIRSystems Spectral Analysis Software
PbS	Lead sulphide
PC	Principal component
PCA	Principal components analysis
PCR	Principal components regression
PLS	Partial least squares
PSI	Particle Size Index
r	Correlation coefficient
R	Reflectance
RMS	Root mean square
RMS(C)	Root mean square corrected for bias
RMSEP	Root mean square error of prediction (performance)
RPD	Ratio of SEP to standard deviation of validation set
RSQ	Coefficient of multiple determination
SDS	Sodium dodecyl sulphate
SEC	Standard error of calibration
SEP	Standard error of prediction (performance)
Si	Silicon
1st	First
Std.	Standard
T	Transmittance
UK	United Kingdom
UNSCR	UNSCRAMBLER
USA	United States of America
USDA	United States Department of Agriculture

List of Definitions

Absorbance (A)	The logarithm to the base 10 of the reciprocal of the transmittance (T) or reflectance (R). $A = \log_{10}(1/T)$ or $A = \log_{10}(1/R)$
Absorption band	A region of the absorption spectrum in which the absorbance passes through a maximum
Absorption spectrum	A plot, or other representation, of absorbance, or any function of absorbance, against wavelength, or any function of wavelength
Baseline	Any line drawn on an absorption spectrum to establish a reference point representing a function of the radiant power incident on a sample at a given wavelength
Bias	A systematic error that contributes to the difference between a population mean of the measurements or test results and an accepted or reference value
Coefficient of multiple determination	The amount of variation in the data which is adequately modeled by the calibration equation
Conditioning	The process of adding water to dry grain and allowing the grain to rest for a period of time before it is milled
Correlation coefficient	A measure of the strength of the linear relationship between X and Y
Extraction rate (flour yield)	The percentage of flour by weight produced from a given mass of wheat milled
Grist	An appropriate blend of wheats to produce uniform flours of defined characteristics
Principal Components Analysis	A mathematical procedure for resolving sets of data into orthogonal components whose linear combinations approximate the original data to any desired degree of accuracy
Reflectance	The ratio of the radiant power reflected by the sample to the radiant power incident on the sample
Simple linear regression	A statistical method of estimating the linear relationship between a dependent variable y and an independent variable x using the linear model
Transmittance	The ratio of radiant power transmitted by the sample to the radiant power incident on the sample
Wavelength	The distance measured along the line of propagation, between two points that are in phase on adjacent waves
Wavenumber	The number of waves per unit length

The standard mathematical equations and unreferenced figures reproduced in this thesis were taken from the following sources:

BANWELL, C.N., 1983. *Fundamentals of molecular spectroscopy.* 3rd Edition. McGraw-Hill Book Company (UK) Limited. pp 338.

BURNS, D.A. & CIURCZAK, E.W. (eds), 1992. *Handbook of Near-Infrared Analysis.* Practical Spectroscopy Series, Volume 13, Marcel Dekker, Inc. New York, pp 681.

OSBORNE, B.G., FEARN, T. & HINDLE, P.H., 1993. *Practical NIR Spectroscopy with application in food and beverage analysis.* 2nd Edition. Longman, Scientific and Technical, Harlow. pp 227.

WORKMAN, J.J., 1993. A brief review of the near infrared measurement technique. *NIR news*, **4**, 8-9,15-16.

Acknowledgements

I wish to express my sincere gratitude towards the following for their contributions towards the completion of this study:

- **Dr Brian Osborne**, without whom this study would not have been possible, for all his useful advice and ideas during the time of supervising this study as well as the time spent and his help towards the completion of my thesis.

- **Prof Albert McGill** for his constant motivation and support since 1987, his supervision during the course of this study and for giving me the opportunity to experience a "whole new world".

- **Ralph Barnes** for giving me my first few lessons on an NIR monochromator.

- **Dr Tom Fearn** for many statistical tutorials, advice and useful discussions during the course of this study.

- **Dr Phil Williams** for the opportunity to spend time with him in his laboratory and many discussions on cereal science and wheat hardness.

- **Dr Marie-Françoise Devaux** and **Dr Paul Robert** for the performance of and discussions on canonical correlation analysis as well as the canonical variate plots provided.

- **Debbie Sobering** for her assistance and help with Particle Size Index analysis, mailing many wheat samples to and fro and conversion of Infratec data.

- My dear parents, **Naughty and Martie Manley**, for their support and constant encouragement throughout my studies all these years. "Baie, baie dankie Pa en Ma - sommer vir alles".

Author's declaration

I declare that at no time during the registration for the degree of Doctor of Philosophy at the University of Plymouth have I been registered for any other University award.

This study was financed through a University of Plymouth Research Studentship.

In this study the physical property measurements have been referred to as Parameter A and Parameter B due to confidentiality restrictions.

Relevant scientific Seminars and Conferences were attended regularly at which work was often presented.

Papers were prepared for publication and external institutions were visited for consultation purposes.

Publications:

Refereed:

MANLEY, M., McGILL, A.E.J. & OSBORNE, B.G., 1994. The effect of light scattering on NIR reflectance and transmittance spectra of wheat. *J. Near infrared Spectrosc.*, **2**, 93-99.

Not Refereed:

MANLEY, M., McGILL, A.E.J. & OSBORNE, B.G., 1995. Wheat hardness by NIR: New Insights. In: Batten, G.D., Flinn, P.C., Welsh, L.A. & Blakeney, A.B. (eds). *Leaping ahead with near infrared spectroscopy.* NIR spectroscopy Group, Royal Australian Chemical Institute, North Melbourne, Australia, 178-180.

Conferences Attended and Presentations:

Research Seminar, May 1993. Seale-Hayne Faculty of Agriculture and Food Studies, Newton Abbot, UK.

Analytical applications of near infrared (NIR) spectroscopy with particular reference to wheat hardness.

Research Seminar, May 1994. Seale-Hayne Faculty of Agriculture and Food Studies, Newton Abbot, UK
Wheat hardness by NIR: New insights.

14th ICC Congress, June 1994. The Hague, Netherlands.
MANLEY, M#., McGILL, A.E.J. & OSBORNE, B.G.
Wheat hardness by NIR: New insights.

7th International Diffuse Reflectance Conference, August 1994. Chambersburg, PA, USA.
MANLEY, M#., McGILL, A.E.J. & OSBORNE, B.G.
Wheat Milling Quality by NIR: Part 1. New insights into hardness measurements.
Wheat Milling Quality by NIR: Part II. Prediction of damaged starch in flour.

International Conference on Wheat structure, Biochemistry and Functionality, April 1995. Reading, UK.

Research Seminar, July 1995. Seale-Hayne Faculty of Agriculture and Food Studies, Newton Abbot, UK.
Wheat hardness by near infrared (NIR) spectroscopy: New insights.

Royal Australian Chemical Institute (RACI) NIR Spectroscopy Conference, Gordonvale, Queensland, Australia.
MANLEY, M., McGILL, A.E.J., OSBORNE, B.G#. & WILLIAMS, P.C.
NIR calibration using different software packages.

Accepted to be presented at future Conferences

9th World Congress of Food Science and Technology, July/August 1995. Budapest, Hungary.
MANLEY, M#., McGILL, A.E.J. & OSBORNE, B.G.
Application of NIR spectroscopy to whole wheat grain hardness measurements.

7th International Conference on NIR Spectroscopy, August 1995. Montreal, Canada.
MANLEY, M#., McGILL, A.E.J. & OSBORNE, B.G.
Whole wheat grain hardness by NIR.

presented or to be presented by

External Contacts:

Dr Tom Fearn
University College London, London, UK.

Dr Phil Williams
Canadian Grain Commission, Winnepeg, Canada.

Dr Tony Evers & Dr Martin Whitworth
Campden-Chorleywood Food Research Association, Chorleywood, UK.

Dr Marie-Françoise Devaux and Dr Paul Robert
INRA, Nantes, France.

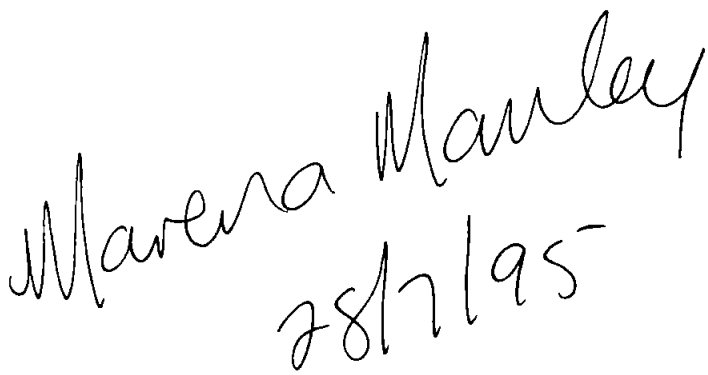

Chapter 1

Introduction

CHAPTER 1

1.0 INTRODUCTION

Cereals form the most important source of carbohydrates and protein for the nutrition of humans and livestock (Shewry & Miflin, 1985) and can be regarded as the most important of all food crops. Wheat (*Triticum aestivum, Triticum compactum, Triticum durum*) is expected to remain foremost among the staple crops for man, being a concentrated carbohydrate source with useful protein, fat, mineral, vitamin and fibre content (Wibberley, 1989). The ability to form a visco-elastic, gas-retaining dough also distinguishes wheat flour from that of maize, barley and to a lesser extent rye, and the attractiveness of the resulting foods gives this crop much of its economic significance (Wall, 1979). More than 70 % of the world's cultivated surface is under cereals of which more than 30 % comprises wheat, followed by maize, rice and barley (Manley, 1983; Kent & Evers, 1994). The importance of wheat, apart from being a staple crop, can be explained in terms of the following (Wibberley, 1989):

Wheat is

- adaptable, as different varieties tolerate a wide range of soil types, climatic and agricultural conditions.
- relatively easy to produce under favourable climatic conditions with a harvesting procedure that is easily mechanised.
- suitable for long term storage under appropriate conditions.
- multipurpose and versatile providing both human diet and livestock feeds.
- suitable for various uses in the food industry. Having a bland taste, it can carry different flavours e.g. as thickeners in soup and in snack foods.

Wheat is usually consumed in its ground form i.e. flour. The whole wheat grain is reduced to flour fineness in a flour mill whose primary function therefore is to grind an appropriate blend of wheats (grist) to produce uniform flours of defined characteristics (Kent-Jones & Amos, 1967). The composition of the grist is very important in controlling flour quality and protein content which in turn depend on the properties of the different types or varieties of wheat.

Until recently, more than 60 % of the wheats used for flour milling in the UK were imported, of which almost 60 % came from Canada and the USA. This wheat has been of quite uniform milling quality and there was little need to optimise grists based on milling performance. Today, for most flours in the UK, the major component of the grist is UK home-grown wheat. Due to import levies on Third Country produce under the European Union (Community) Common Agricultural Policy (CAP), it can be prohibitively expensive to import wheat from Canada and the USA. Figure 1.1 shows the decrease in usage of Third Country (Northern America) wheat and the increase in usage of UK home-grown wheat since 1975/76. Hence the quality of this component of home-grown wheats is of crucial importance to the UK Milling Industry.

The essential requirements for making white flour are

- to condition the wheat by adding water so that the distribution of moisture among the constituents of the grain is optimal for clean separation of the bran from the endosperm,
- to separate the white endosperm from the brownish bran and the yellow germ and
- to reduce the separated endosperm to flour fineness (Osborne, 1991; Kent & Evers, 1994).

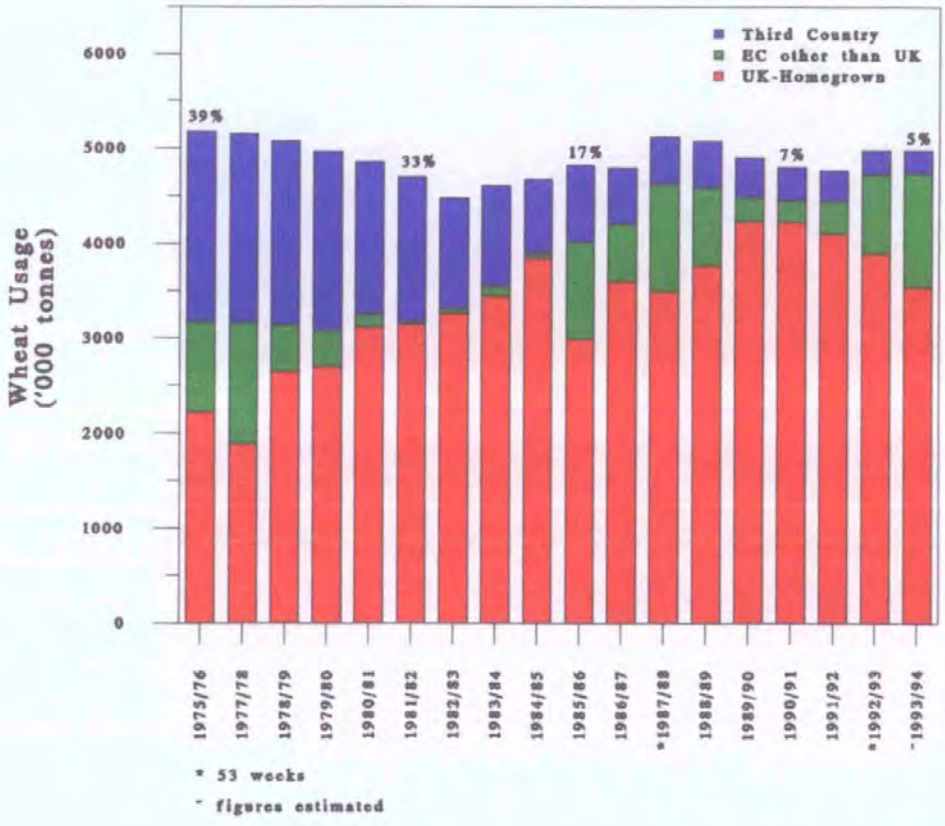

Figure 1.1 Wheat Usage by Millers ('000 tonnes). Percentages shown refer to Third Country wheat usage (NABIM, 1994)

Wheat grain hardness is one of the most important characteristics that influence the milling process, its efficiency and the end-use properties of the flour. The hardness of the wheat grain influences the ease with which the endosperm is separated from the bran during the milling process, and also controls some of the properties of the flour produced (Blackman & Payne, 1987). If sufficient pressure and shear is applied during reduction of the endosperm, the starch granules of hard wheats are more likely to become mechanically damaged. The flour from hard wheats would therefore have greater proportions of damaged starch grains than the flours of soft wheats. This will influence the end-use of flours from wheats of differing hardness (Blackman & Payne, 1987; Osborne, 1991).

The measurement of wheat hardness is very important for predicting milling quality and end-use properties (Norris, Hruschka, Bean & Slaughter, 1989) and is clearly an important measurement for millers to make. Wheat hardness and other typical quality tests that are performed on wheat on intake at the flour mills are shown in Table 1.1.

Table 1.1 Quality tests performed on whole and ground wheat on intake at flour mills (FMBRA, 1992)

Whole Grain Samples	**Ground Grain Samples** (ground on hammer mill)
Wheat Sampling	Moisture content
Visual Inspection	Protein content (14 % mb)
Specific Weight	Hagberg Falling Number
Screenings	NIR Wheat Hardness
	SDS-Sedimentation test
	Gluten Washing test

Wheat is traded against these specifications which indicate its potential for particular end-uses such as breadmaking or biscuit making. Since acceptance or rejection of a load and the price to be paid may be determined by these properties, rapid testing is important.

1.1 Wheat Hardness

Despite wide use of the term, wheat hardness is a concept for which no definition has been accepted universally (Norris *et al.*, 1989). Wheat hardness has been defined by various people as 'the state of being hard', 'not easily penetrated or separated into parts' or 'difficult to penetrate or separate into fragments'. Softness is not so clearly defined and has been defined as 'easily disintegrating under stress' (Pomeranz & Williams, 1990).

In this study the terms **hard wheat(s)** and **soft wheat(s)** will refer to **genetically hard** and **soft wheats** and *wheat grain hardness*, *wheat hardness* or *hardness* will refer to the *degree of hardness* and *softness* of the endosperm.

1.1.1 Significance of wheat hardness

Wheat hardness is the most important single characteristic that affects the functionality of a common wheat.

Wheat hardness affects

- the way in which the wheat must be conditioned for milling,
- the ease of milling,
- the extraction rate,
- the particle size, shape and density of flour particles,
- the level of damaged starch,
- therefore, the water absorption capacity of the flour,
- of which both will have an affect on the breadmaking process and
- the production of soft wheat products.

- *Conditioning*

Conditioning is the process of adding water to dry grain and allowing the grain to rest for a period of time before it is milled (Hoseney, 1994). Varieties of soft or mealy wheats have cavities in the endosperm and absorb water faster, requiring a much shorter conditioning time than hard wheats. The higher quantitative water absorbing capacity of hard wheat varieties and the longer conditioning times required are due to the large amount of proteinaceous substance between the starch granules (Pomeranz & Williams, 1990; Hoseney, 1994).

- *Ease of milling*

More power is consumed in milling hard wheat varieties, but they are generally easier to mill, causing far fewer problems in the conveying and sifting sections of the mill than soft wheat varieties. Hard wheat varieties yield a greater proportion of larger flour particles which have a well-defined shape. These particles flow freely, sieve easily and pack closely together. Soft wheat varieties, on the other hand, yield flour that has poor flow properties, takes much longer to sieve and packs loosely. Having such poor flow and sieving properties, soft wheat milling quite often causes "chokes" in flour mills which could be costly (Pomeranz & Williams, 1990; Osborne, 1991).

- *Extraction rate*

The percentage extraction rate is the percentage of flour by mass produced from a given mass of wheat milled. It is also known as the flour yield (Kent & Evers, 1994). In hard wheats, the endosperm is separated readily from the bran, due to the manner in which hard wheats fracture, giving high extraction rates. In contrast soft wheats tend to give much lower extraction rates (Blackman & Payne 1987).

- *Particle size*

During the milling process the break rolls splinter the endosperm, according to the hardness of the wheat, breaking it into particles of varying sizes (Bennion, 1969). Due to the nature of the wheat grains, hard wheat breaks down yielding coarser flour, consisting of regular-shaped particles, whereas soft wheats give very fine flour consisting of irregular-shaped particles (Kent & Evers, 1994).

- *Damaged starch*

More energy is required to reduce hard wheats to a fine particle size. The result of this

energy input is that a greater percentage of the starch is damaged during milling. A linear relationship exists between energy consumed during grinding and flour starch damage content which shows that, under a given set of conditions, higher levels of starch damage are obtained from milling of hard wheats than soft wheats. In hard wheats, milling causes fractures along the endosperm cell walls or through the cell contents in which case the starch granules are damaged due to stronger adhesion between the protein matrix and the starch granules, while in soft wheats, the granules are more readily freed from their cells and consequently undergo less damage. The degree of damaged starch obtained will influence the end-use properties of flours and so governs which type of wheat is used (Blackman & Payne, 1987; Osborne, 1991; Kent & Evers, 1994). Endosperm from hard wheat flour have starch granules with a large quantity of protein adhering to them whereas in the case of soft wheat starch is relatively free of adhering protein (Pomeranz & Williams, 1990).

- *Water absorption*

The ability of flour to take up water during dough making is largely influenced by the protein and damaged starch contents. Flours milled from hard wheats have a higher level of damaged starch and subsequent water absorption than do those milled from soft wheats (Pomeranz & Williams, 1990; Osborne, 1991).

- *Breadmaking*

It is desirable that the content of damaged starch should be maintained at a reasonably high level, and this requirement can be met by adjustments to the milling process and the use of a specific type of wheat (Kent & Evers, 1994). During breadmaking it is also important that the dough remains in a form which is easy to handle and retains a consistently economic quantity of water, as the water absorption is directly related to the amount of

bread the baker can produce from a given weight of flour (Pomeranz & Williams, 1990). The water absorption also has a profound influence on crumb softness and breadkeeping characteristics (Tipples, Kilborn & Preston, 1994).

- *Soft wheat products*

Flours with low damaged starch contents and subsequent lower water absorbing characteristics are required for biscuit making. The factor that makes hard wheats hard also apparently has an effect upon the texture of the products made from the flour of those wheats. Biscuits made from hard wheat flour are almost invariably hard in texture (Hoseney, 1994). Although no correlation has been found between the damaged starch content of the flour and the hardness of the finished product, damaged starch does affect the processing of biscuit dough by increasing the water absorption and reducing the biscuit spread (Faridi, Finley & Leveille, 1987).

1.1.2 Theories of wheat hardness

Wheat types may be classified as hard wheats or soft wheats which differ significantly in terms of functionality. Hoseney & Seib (1973) raised the question of "why are hard wheats harder than soft wheats if both hard and soft wheats contain the same two major components, protein and starch" and discussed three possibilities in terms of

- the variation in the ratio of protein to starch components,
- the intrinsic hardness of the starch and protein components and
- the binding forces between the starch and protein components.

- *Variation in the ratio of protein to starch components*

The ratio of starch to protein differs between hard and soft wheats, but there is experimental evidence that this variation is not responsible for the differences in hardness.

Soft wheats grown under conditions to produce high proteins, still proved to be relatively soft and a low protein hard wheat will still be relatively hard (Hoseney & Seib, 1973). It has also been shown that a hard wheat tended to become softer at high protein whereas a soft wheat showed the opposite tendency (Symes, 1961).

- *The intrinsic hardness of the starch and protein components*

There is convincing evidence that the difference in wheat hardness is not due to the intrinsic hardness of the starch and protein components, respectively. Barlow, Buttrose, Simmonds & Vesk (1973) conducted micropenetrometer tests on purified starch and storage protein preparations of hard and soft wheats. It was reported that no significant difference existed in the hardness of either the protein or the starch from different varieties.

- *The binding forces between the starch and protein components*

When Barlow *et al.* (1973) reported that the individual storage components do not differ in hardness between varieties, they concluded that the adhesion between starch and protein does differ. This was supported by scanning electron microscopy results. In hard wheats, fractures during milling tend to pass along endosperm cell walls to yield clean, well-defined particles. Fracture through cell content in these wheats, when it occurs, involves both starch granules and storage protein, resulting in a high proportion of damaged and broken starch granules. Because of the lower adhesion between starch and protein, soft wheats tend to release starch granules more freely during milling, with fractures occurring around rather than through granules (Barlow *et al.*, 1973). This phenomenon suggests a pattern of areas of mechanical strength and weakness in hard wheats, but fairly uniform mechanical weakness in soft wheats and resulted in much less starch damage in the latter case (Kent & Evers, 1994). Simmonds, Barlow & Wrigley (1973) confirmed the results of Barlow *et al.* (1973) that wheat grain hardness is related to the degree of adhesion between the starch

and the surrounding protein in the endosperm. The interface was shown to be rich in water-extractable proteins, although no specific biochemical component that might control the adhesion between starch granules surface and protein matrix was identified (Kent & Evers, 1994). This is still the currently accepted theoretical basis for wheat grain hardness.

Glenn & Saunders (1990) discussed wheat grain hardness in terms of two theories which stimulated considerable interest. One theory attributed hardness to the degree of starch-protein adhesion as discussed earlier (Barlow *et al.*, 1973). The authors found no difference in hardness of protein fragments or starch granules between hard and soft wheat varieties and concluded that starch-protein adhesion accounts for wheat hardness and gave little consideration to the structural features of the protein matrix. Simmonds *et al.* (1973) isolated a starch extract that they proposed could function in hard wheat varieties as a adhesive that binds starch and protein. Glenn & Saunders (1990) suggested that starch-protein adhesion could vary in hard and soft wheat endosperm as a result of quantitative differences in cellular products deposited at the starch-protein interface.

The second theory was based on the physical structure of the protein matrix. Stenvert & Kingswood (1977) attributed wheat hardness to the physical structure of the protein matrix and placed little importance on starch-protein adhesion. This theory holds that the wheat grain hardness is determined by the continuity of the protein matrix, its structure and the strength with which it physically entraps starch granules. Both these theories are supported by Glenn & Saunders (1990). Stenvert & Kingswood (1977) also reported that starch granules do not adhere to protein but are merely entrapped within the protein matrix. Glenn & Saunders (1990), however, suggested that starch-protein adhesion occurs and is associated with a continuous matrix.

The starch-protein adhesion has been attributed to a biochemical "cement" (Simmonds *et al.*, 1973) or "non-stick" protein (Greenwell & Schofield, 1986). Greenwell & Schofield (1986) reported a 15-kDa polypeptide in sodium dodecyl sulphate (SDS) extracts of soft wheat starch preparations that was much less prevalent in hard wheat samples. They suggested that the polypeptide functions as a "non-stick" protein that is genetically linked to hard or soft varieties and that it is important in conferring endosperm softness to wheat. This polypeptide was thought to weaken the starch-protein adhesion, inducing softening. Glenn & Saunders (1990) supported the claim that this polypeptide is associated with soft wheat varieties. However, the textural hardness of wheat is not directly attributable to the presence of the 15-kDA polypeptide.

1.1.3 Factors affecting wheat hardness

The following factors are most likely to affect wheat hardness (Pomeranz & Williams, 1990):

- genotype
- environment
- protein content
- moisture content
- kernel size

- *Genotype*

The most important factor affecting the hardness of a wheat variety is its genetic constitution i.e., the hardness of a given variety of wheat is genetically controlled. Although hardness is genetically controlled, the growing environment also has some influence on hardness. However, wheats that are clearly genetically hard may vary in hardness, but never to the extent of becoming soft, and vice versa (Pomeranz & Williams,

1990).

- *Environment*

In addition to the differences in hardness, another important characteristic of the wheat endosperm is its appearance. Some wheats are vitreous, hornlike, or translucent in appearance, while others are opaque, mealy, or floury. Wheat endosperm therefore varies both in texture (hardness) and appearance (vitreousness). Traditionally, vitreousness has been associated with hardness and high protein content and opacity with softness and low protein. However, the causes of vitreousness and hardness are different, and the two do not always go together (Hoseney, 1994), but it has recently been shown that within a given variety the degree of hardness caused by environment has been linked to the percentage of vitreous kernels present (Dobraszczyk, 1994). It is entirely possible to have hard wheats that are opaque and soft wheats that are vitreous, although these are somewhat unusual (Hoseney, 1994).

Hardness is caused by the genetically controlled strength of the association between protein and starch in the endosperm. Vitreousness, on the other hand, results from lack of air spaces in the kernel. The controlling mechanism is not clear but appears to be related to the amount of protein in the sample which in turn is mainly controlled by the environment. For example, high-protein soft wheats are more vitreous than low-protein soft wheats and low-protein hard wheats have more opacity than their high-protein counterparts (Hoseney, 1994).

The air spaces in the kernel diffract and diffuse light and make the kernel appear opaque or floury. In tightly packed kernels, with no air spaces, light is diffracted at the air-grain interface but then travels through the grain without being diffracted again. The result is

a translucent or vitreous kernel. As expected, the presence of air spaces within the grain makes the opaque grain less dense. The air spaces are apparently formed during the drying of the grain. As the grain loses water, the protein shrinks, ruptures, and leaves air spaces. With vitreous endosperm, the protein shrinks but remains intact, giving a dense kernel. If grain is harvested before it matures and is dried by freeze-drying, it is opaque. This shows that the vitreous character results during final drying in the field. It is also well known that vitreous grain that is wet and dried in the field, or for that matter in the laboratory, will lose its vitreousness (Hoseney, 1994).

Wheat samples may be entirely vitreous, entirely mealy or may consist of a mixture of vitreous and mealy grains, with one type predominating. Individual grains are generally completely vitreous or completely mealy, but grains which are partly vitreous and partly mealy are frequently encountered. Mealiness is favoured by heavy rainfall, light sandy soils and crowded planting and is more dependent on these conditions than on the type of grain grown and is positively correlated with high grain-yielding capacity. Vitreousness can be induced by nitrogenous manuring or commercial fertilizing and is positively correlated with high protein (Kent & Evers, 1994).

- *Protein content*

No direct correlation has been found between protein content and wheat hardness (Pomeranz & Williams, 1990). Pomeranz, Peterson & Mattern (1985) reported that if protein content did affect hardness it would be within a variety, rather than across all varieties.

- *Moisture content*

Moisture content would affect wheat hardness in the sense that most methods of measuring

wheat grain hardness will be affected by variation in moisture content (Pomeranz & Williams, 1990).

- *Kernel size*

Again kernel size would affect wheat hardness in the sense that some methods of measuring wheat grain hardness will be affected by variation in kernel size. Methods involving grinding do not seem to be affected by kernel size, however, tests involving single kernels might be affected (Pomeranz & Williams, 1990)

1.1.4 Methods for measuring wheat hardness

Wheat grain hardness testing has been a factor in wheat quality assessment for about 100 years. Over 100 different methods for the determination of wheat hardness have been documented and date back to 1896, when Cobb first assigned a numerical value to the hardness of Australian wheats (Cobb, 1896). Practically all of the methods differ from each other to some degree. The earlier methods of evaluating wheat hardness has been summarized and discussed in detail by Pomeranz & Williams (1990).

Most of the earlier reports on wheat hardness refer to visual observations made on the appearance of the grain. The 'biting' type of device is the oldest form of apparatus to be employed in the evaluation of wheat hardness. Another method expressed the texture of whole wheat in terms of granularity. The particle size index test on whole wheat kernels which involves grinding a sample of wheat by a standard grinding procedure, sifting a known weight of the whole meal for a standard time, then weighing the throughs. The pearling test is based on the fact that hard wheats are more resistant to the action of the pearler than are soft wheats. Other tests are based on differences in the energy used to grind or crush the kernel, abrasion, indentation, microscopic observation, tensile strength,

and acoustic methods (Pomeranz & Williams, 1990).

Referring to the described methods of measurement it is clear that the measurements of wheat grain hardness usually employ the following different characteristics of wheats:

- hard wheat on grinding gives coarser products than soft wheat
- hard wheats require more energy in grinding
- soft wheats are abraded more during the same time of pearling than are hard wheats

The disadvantages of all these tests are that they describe the effects of hardness without actually measuring hardness itself and are destructive in that they involve some form of measurement of either the resistance of the kernel to breakage or the granularity of the meal resulting from grinding (Williams, 1991). The reason for this is that the absolute hardness of wheat is difficult to measure. Therefore, how the grain breaks is usually measured, rather than the absolute hardness as it has been known for many years that soft wheat breaks into a fine powder and hard wheat breaks into angular fragments and gives a coarser product (Pomeranz & Williams, 1990). These tests therefore fail to characterize wheat endosperm texture in terms of fundamental physical properties (Glenn, Younce & Pitts, 1991).

(i) Fracture mechanics of wheat grain

Because of the complex geometry of wheat grains and the possible effect of moisture content on the measurement, it is difficult to characterize the physical properties of wheat. In spite of this Glenn *et al.* (1991) conducted a study to characterize fundamental physical properties of wheat endosperm and to investigate their relationship to wheat hardness. They established significant positive correlations between the variation in fracture mechanic

measurements at various moisture levels within a wheat class (soft, hard and durum) and wheat hardness as measured by near infrared (NIR) spectroscopy. A highly significant positive, although non-linear, relationship was found between endosperm (compression) strength and NIR. NIR wheat hardness scores increased at a greater rate than endosperm strength. The variation in moisture content markedly altered the physical properties of the endosperm and again stressed the need to condition wheat before milling.

Recently, Dobraszczyk (1994) conducted a study to develop methods for measuring the fracture toughness of individual wheat grains in order to develop a better understanding of the fracture process of wheat endosperm during milling. Very little is known about the relationship between the fundamental material properties of wheat endosperm and the fracture of wheat grains. Vitreous grains were separated from the mealy grains of a commercially grown variety on the basis of their appearance. The vitreous grains showed a higher fracture toughness than mealy grains in a single variety. Dobraszczyk (1994) suggested that as fracture mechanics measure the energy to separate two surfaces it is possible, in principle, to relate fracture toughness to the strength of the interparticle adhesion if the fracture plane passes around particles through the particle-matrix interface. If the fracture area and fracture path can be measured accurately, then fracture toughness can be related directly to the interparticle adhesion. Dobraszczyk (1994) then concluded that the particle sizes produced during fracture of vitreous grains should be larger than for mealy grains. These results suggested that the higher the ratio of vitreous kernels in a given variety the harder the wheat.

A related study was the OPTIMILL LINK Programme (Food Processing Sciences LINK number 75) in which a consortium of researchers investigated the application of fracture mechanics to optimise flour milling and aimed to measure hardness in a more fundamental

way on single kernels or pieces of endosperm instead of measuring average properties of several grains as do most of the milling hardness tests. Studies to investigate the physical properties of different endosperm samples were conducted with the aim of explaining the causes of variation in hardness.

(ii) Single kernel analysis

Single kernels have been examined through the use of optical microscopy (Mattern, 1988), stress-strain behaviour during crushing (Lai, Rousser, Brabec & Pomeranz, 1985; Pomeranz, Martin, Rousser, Brabec & Lai, 1988), force of slicing (Eckhoff, Supak & Davis, 1988), the use of a single kernel crushing device (Martin, Rousser & Brabec, 1993) and acoustical properties during grinding (Massie, Slaughter, Abbot & Hruschka, 1993). These methods, however, are destructive, eliminating multiple readings on the sample kernels and the kernels cannot be used in breeding trials. This led to Delwiche (1993) conducting a study to investigate whether hardness is measurable by near infrared transmittance measurements of intact kernels. He concluded that using multiple single kernels it was possible to separate hard and soft varieties, however, the order of hardness within a hardness group was not predicted correctly. On a single kernel basis, spectral overlap occurred between hard and soft varieties. This phenomenon that the range in hardness of individual kernels can overlap even though their bulk hardness scores do not, was also observed by Glenn & Johnston (1992).

Delwiche (1993) suggested that one term models appear to base classification on the vitreousness of the kernel, therefore higher order models were needed to improve on hardness models over that achievable through the correlation to vitreousness. Soft wheat varieties tend to have a wider range of single-kernel hardness than hard varieties. Delwiche (1993) attributed the wider range in hardness of soft varieties to a greater inherent variation

in vitreousness of soft wheats compared to that of hard wheats. He concluded that there remains a biochemical property of the kernel that is responsible for hardness which is not easily measured by intact single kernel transmittance spectroscopy.

Currently the most popular working methods are based on grinding resistance and sieving. No method for measuring wheat hardness has been accepted, as yet, by the International Association for Cereal Science and Technology (ICC) .

During 1985-1986, hardness began to attain the status of a major factor in the description of wheat because of the need of the United States Department of Agriculture's (USDA) Federal Grain Inspection Service (FGIS) to use an objective hardness test as a means of differentiating the hard and soft wheat classes. Crossing of the classes in wheat breeding programmes had obscured the differences to the point where it was no longer possible to visually identify the classes. Various procedures for measuring hardness were proposed, one of which was measuring wheat grain hardness by near infrared (NIR) spectroscopy on ground grain (Halverson & Zeleny, 1988).

1.2 Near infrared (NIR) spectroscopy

1.2.1 Development of NIR spectroscopy

In the early 1800s William Herschel built a reflective telescope, but as with all reflective telescopes, it reflected both light and heat. While conducting an experiment to find out which part of the light spectrum is responsible for this reflected heat, he discovered the near infrared region (Herschel, 1800).

The first study of infrared (IR) spectroscopy was carried out in the early 1900s by Coblentz (1905). He recorded the absorption spectra of many materials and showed that certain

atomic groupings have characteristic absorption bands. By observing these bands the chemical constituents in a product could be identified. Nearly all the spectra he recorded showed weak but distinctive bands near 840 nm and 1200 nm and a stronger one at 1700 nm. He speculated that 840 nm and 1200 nm were part of a harmonic series and that these bands were related to the presence of C-H bonds. This work laid the foundation for the concept that different chemical bonds could be associated with infrared group frequencies.

The Beer-Lambert law describes the quantitative relationship between the absorption of energy to the concentration of an absorbing molecule in a sample:

$$\log\frac{I_o}{I}=A=\log\frac{1}{T}=\epsilon bc \qquad \text{.....} \quad 1.1$$

where I_o is the intensity of the radiation falling on the sample and I that part transmitted. A is the fraction of radiation transmitted through the sample expressed as absorbance, b is the thickness through which the radiation passes or path length and c is the concentration of the molecules in the sample. If c is expressed in mol l^{-1} and b in cm, then ε in mol^{-1} $l\ cm^{-1}$, is the molar absorptivity constant for a particular compound at a chosen wavelength.

Spectrophotometric analysis rapidly gained popularity after the Second World War and Harry Willis used NIR to make analytical measurements on intact samples of polymers and plastics. A more detailed description of this earlier work is given in Miller (1991).

In the 1950s the US Department of Agriculture (USDA) Instrumentation Research Laboratory, headed by Karl Norris, became heavily involved with the optical analysis of agricultural products. In the mid 1960s, Karl Norris set out to build a new moisture meter

using NIR absorption measurements, after recognising the potential of the diffuse reflectance measurement in the NIR region for rapid analysis of grains. Cereal grains were found to exhibit specific absorption bands in the NIR region. However, his work was frustrated by the interferences caused by other constituents in the grain, such as oil, protein, and starch. Using computer correlation techniques, he was able to select a set of wavelengths for absorption or reflectance measurements in the near infrared region that not only eliminated the interferences, but also permitted the measurement of those constituents. Norris suggested that NIR instruments could be used to measure protein and moisture in grains and protein, oil and moisture in soybeans and that these instruments were to utilise, at a minimum, the following wavelengths: 1680, 1940, 2100, 2180, 2230, 2310 nm as shown in Figure 1.2 (Norris, 1962; Norris, 1964; Ben-Gera & Norris, 1968a; Ben-Gera & Norris, 1968b).

Moisture has a strong absorption band at 1940 nm which is not overlapped by bands due to other constituents of flour. Calibration therefore is straightforward since only a single reference wavelength (2310 nm) is required. The protein measurement wavelength is 2180 nm while 2100 nm allows a correction to be made for the effect of starch absorption at 2180 nm. 1680 nm and 2230 nm are neutral wavelengths which have the function of correcting for the particle size of the sample. This demonstrates one of the strengths of NIR spectroscopy i.e. its ability to enable the simultaneous determination of several constituents to be carried out on the same sample (Osborne, 1992).

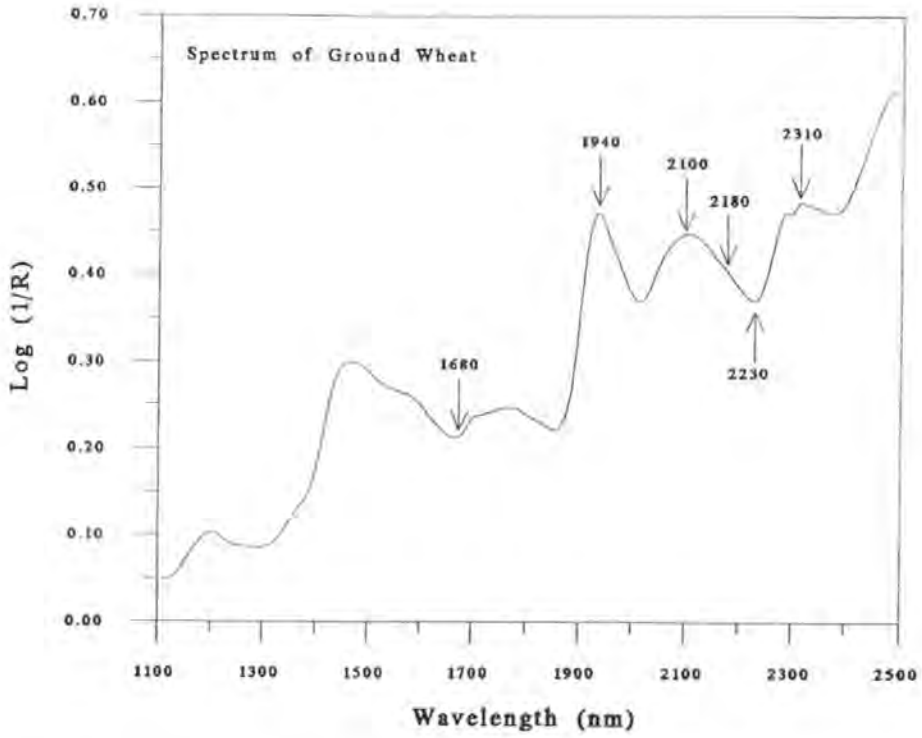

Figure 1.2 Wavelengths suggested by Karl Norris to be used in NIR instruments

The only commercially available NIR instruments at that time were those developed to optimise measurements in the ultraviolet and visible region with the NIR capability only as an added feature. Karl Norris decided that since none of the commercially available instruments were designed specifically for making NIR measurements, he and co-workers would design a system and subsequently the first commercial unit was produced and introduced by Dickey-John in 1971. Since then Karl Norris has been considered by many to be the "father" of NIR (Figure 1.3). A more detailed description of the development of NIR can be found in Osborne, Fearn & Hindle (1993).

Figure 1.3 Karl Norris, the "father" of NIR at the Chambersburg Conference, 1994

Near infrared (NIR) spectroscopy was given credibility by the grain industry and has now been applied to the analysis of cereal grains for more than 20 years (Williams, 1973; Williams & Sobering, 1993). The value of NIR spectroscopy for the quantitative analysis of cereal products has been demonstrated and discussed in several review articles and books (Stark, Luchter & Margoshes, 1986; Williams & Norris, 1987; Burns & Ciurczak, 1992; Osborne *et al.*, 1993). Despite the low contrast of absorption bands in NIR cereal spectra, NIR spectroscopy has become a standard technique for performing rapid analyses of protein, fat and moisture in cereal samples.

As is the case with most measurements by analytical instruments, NIR spectroscopy has its advantages and disadvantages (Osborne *et al.*, 1993):

Advantages of NIR spectroscopy

- low running costs and bench space requirements
- non-destructive
- little or no sample preparation

- simple and safe to use
- environmentally friendly
- rapid measurements thus suitable for on-line use
- multiple analyses are possible
- precise

Disadvantages of NIR spectroscopy

- specific instrumentation requirements
- requires calibration procedures
- complexity in choice of data treatment
- lack of sensitivity for minor constituents

1.2.2 Theoretical aspects of NIR spectroscopy

Near infrared spectra result from energy absorption by organic molecules. All the absorption bands are the result of overtones and combinations of overtones originating in the fundamental mid-infrared region of the spectrum. The part of the electromagnetic spectrum visible to the human eye extends from about 400-700 nm while the infrared (IR) extends from 2500-15000 nm. The intermediate region between the IR and the visible is termed the near infrared (NIR) as illustrated in Figure 1.4.

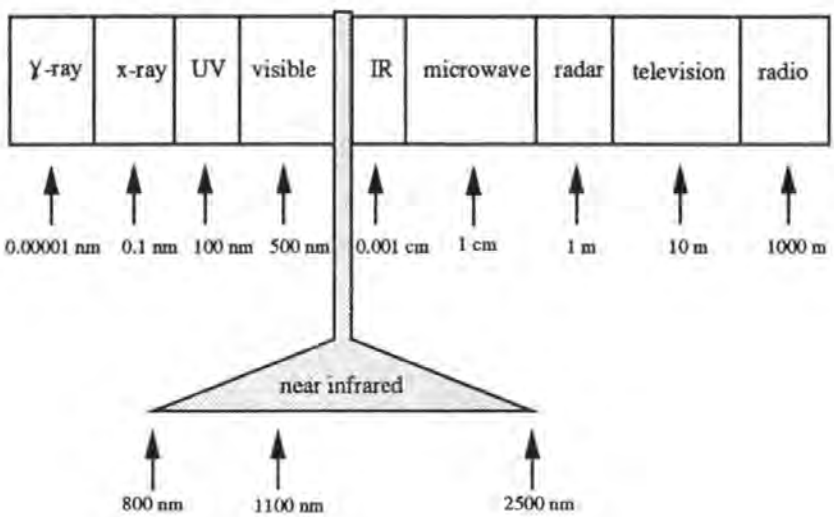

Figure 1.4 Electromagnetic spectrum indicating the NIR region

Electromagnetic radiation, of which the IR forms a part, may be considered as a simple harmonic wave. It can also be characterised in terms of its wavenumber ($\bar{\nu}$) which is the reciprocal of the wavelength, λ, when λ is expressed in centimetres (i.e. cm^{-1}), therefore

$$\bar{\nu} = \frac{1}{\lambda} cm^{-1}1 \qquad \text{..... 1.2}$$

Molecular vibrations

- *Harmonic oscillator*

Interatomic bonds behave like springs, have elastic properties and will vibrate at a certain frequency depending on the bond strength and the atomic masses of the atoms bonded together. The total energy in the bond is proportional to the frequency of the vibration. Hooke's law illustrate the properties of the two atoms with a spring like bond between them. It states that the restoring force (F) exerted by the spring is proportional to the distance (y) that it has travelled from the equilibrium position:

$$F = -ky \qquad \text{..... 1.3}$$

where k is the force constant.

The significance of spectroscopic measurements lies in the association between the frequency of radiant energy and the frequencies of molecular motions. The frequency of vibration for a bond between two atoms is given by

$$\nu = \frac{1}{2\pi}\sqrt{\frac{K}{\mu}} \qquad \text{..... 1.4}$$

where k is the force constant and

$$\mu = \frac{(m_1 m_2)}{(m_1 + m_2)} \qquad \text{..... 1.5}$$

where m_1 = the mass of atom 1 and m_2 = the mass of atom 2.

Quantum mechanical theory shows that the vibrational energy of bonds in a molecule is quantized into discrete energy levels. The discrete vibrational energy levels for any molecule are given by

$$E = (\upsilon + \frac{1}{2})\, h\nu \qquad \text{..... 1.6}$$

where h is Plank's constant, ν is the vibrational frequency of the bond and υ is the vibrational quantum number which may have the number 0, 1, 2, 3, ...

Quantum theory indicates that the only allowed vibrational transitions are those in which υ changes by one ($\Delta\upsilon = \pm 1$). Spectral bands will only be observed if the vibration interacts with the radiation and the interaction depends upon the existence of an electric moment across the vibrating bond.

- *Anharmonic oscillator*

Real molecules do not obey exactly the laws of simple harmonic motion and real bonds, although elastic, do not obey Hooke's law. The anharmonic oscillator behaves like the harmonic oscillator but with an oscillation frequency which decreases steadily with increasing υ. The vibrational energy levels for a molecule are now given by

$$E=\left(\frac{h\nu}{2}\right)\left(1-\frac{1}{2}x\right) \quad \text{..... 1.7}$$

where x is an anharmonicity constant. The energy associated with a transition from υ to $(\upsilon + \Delta\upsilon)$ is given by

$$\Delta E=h\nu\left[1-(2\upsilon+\Delta\upsilon+1)x\right] \quad \text{..... 1.8}$$

and the selection rules are $\Delta\upsilon = \pm 1, \pm 2, \pm 3, \ldots\ldots$. These selection rules are the same as for the harmonic oscillator, but with the additional possibility of larger "jumps". Figure 1.5 show the energy of a diatomic molecule undergoing simple harmonic motion and anharmonic vibrations. In practice only bands due to $\Delta\upsilon = \pm 1, \pm 2$ and ± 3 at the most have observable intensity. Transitions where $\Delta\upsilon = \pm 2, \pm 3, \ldots\ldots$ give rise to overtone bands in the NIR region and vibrational modes of complex molecules can combine to produce combination bands. Overtones can be found by dividing the wavelengths in the infrared region by approximately 2, 3 or 4 and provides the advantage of a dilution series. The features in NIR spectra of organic compounds are therefore orders of magnitude weaker than those in the mid-IR, involving vibrations in functional groups e.g. C-H, O-H and N-H as shown in Figure 1.6. The NIR spectrum therefore contains information about the major X-H chemical bonds in an agricultural product.

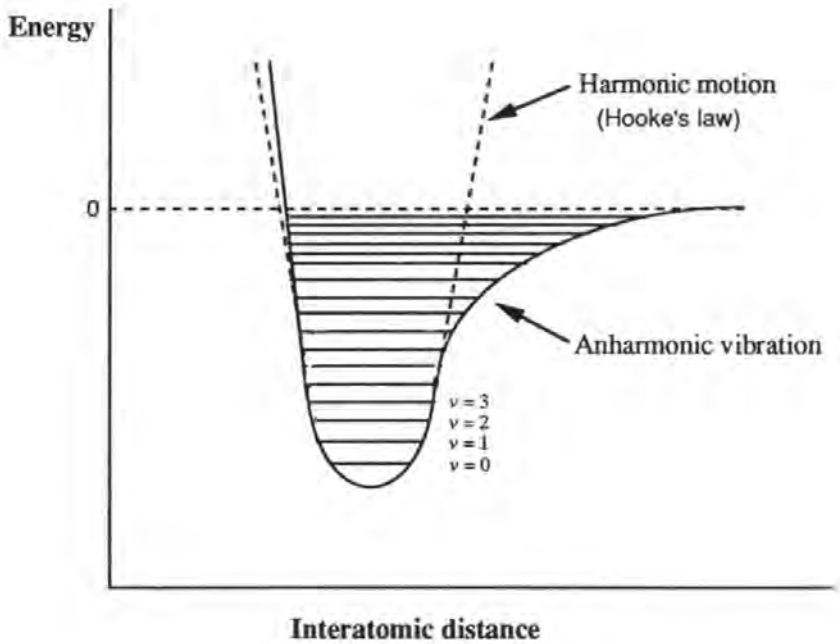

Figure 1.5 The energy diagram of a diatomic molecule undergoing harmonic motion (dotted line) and anharmonic vibrations (solid line)

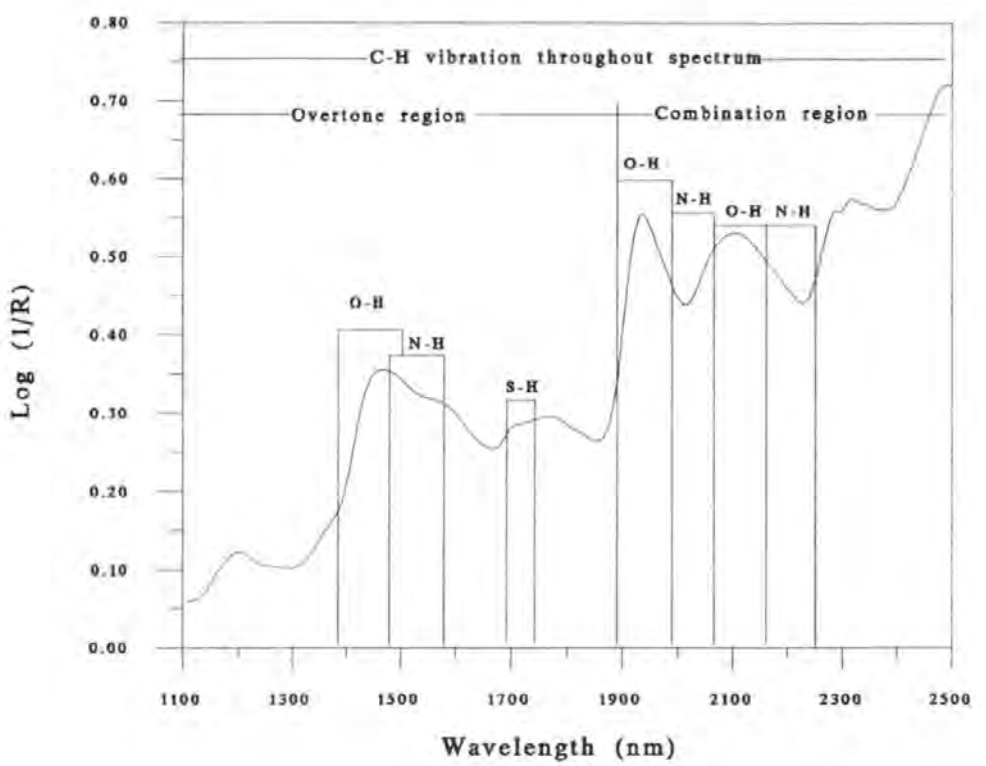

Figure 1.6 A general representation of X-H vibrational information available throughout a wheat spectrum

Molecules that absorb NIR energy vibrate in two fundamental modes, stretching and bending. Stretching is defined as a continuous change in the interatomic distance along the axis between two atoms and bending is defined as a change in the bond angle between atoms as shown in Figure 1.7. Almost all the absorption bands observed in the NIR arise from overtones of hydrogenic stretching vibrations involving XH_y functional groups or combinations involving stretching and bending modes of vibration of such groups. The theory of NIR is described in more detail by Ciurczak (1992) and Osborne *et al.* (1993).

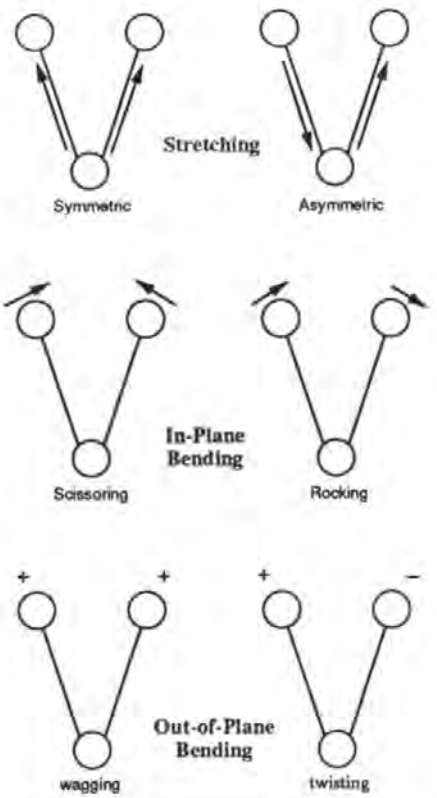

Figure 1.7 Molecular vibrational modes observed in the NIR region

Kubelka-Munk function

The NIR spectrum is dependent by definition on all the functional groups that absorb NIR radiation, which in turn are correlated to the major chemical, physical and or sensory components of a substance. Additionally, the spectrum also contains all the information due to radiation interaction with the sample as well as instrumental artifacts, data collection and computational errors (Shenk, Workman & Westerhaus, 1992).

Kubelka and Munk (Kubelka & Munk, 1931; Kubelka, 1948) proposed a theory to describe mathematically the path or radiation for diffuse reflectance. They proposed that the power of reflected radiation could be described by means of the scattering (s) and absorption (k) constants, respectively. The power of reflected radiation in the case of a layer of infinite thickness may be described as

$$\frac{(1-R\infty)^2}{2R\infty} = \frac{k}{s} \qquad \text{..... 1.9}$$

where R∞ is the reflectance of the infinite thick layer and the term on the left hand side is the Kubelka-Munk function also expressed as F(R∞). The absorption coefficient is equal to the concentration multiplied by the absorptivity defined by the Beer-Lambert law. If all the diffusely reflected radiation is collected and measured, the Kubelka-Munk function may be related to sample concentration i.e.

$$F(R\infty) = \frac{ac}{s} \qquad \text{..... 1.10}$$

and therefore

$$\log\frac{1}{R} = \frac{ac}{s} \qquad \text{..... 1.11}$$

as well as

$$\log\frac{1}{T} = \frac{ac}{s} \qquad \text{..... 1.12}$$

The reflectance which is measurable is a function only of the ratio of two constants k and s and not of their absolute values. For quantitative analyses equation 1.10 can be used in

an analogous way to Beer's law (equation 1.1) to determine concentration c where a is the absorptivity. However, s is not constant and depends on properties like particle size and moisture content and also varies with wavelength. In NIR spectra selection of measurements and reference wavelength should be made in such a way that s is nearly equal. The Kubelka-Munk function is explained in more detail by Olinger & Griffiths (1992).

1.2.3 NIR spectroscopy instrumentation

The basic component requirements for an NIR spectrophotometer are as follows (Workman & Burns, 1992; Osborne *et al.*, 1993):

- a light source (tungsten-halogen monofilament) to generate the necessary NIR radiation
- a wavelength selector or monochromator to provide a narrow band of wavelengths
- a sample holder or sample cell holder to keep the sample during recording of spectra
- detectors to measure the radiation after interaction with the sample (lead sulphide (PbS) for the 1100 - 2500 nm region and silicon (Si) for the 800 - 1098 nm region.

The arrangements of these components differ between instruments. The basic configurations for reflectance and transmittance are shown schematically in Figure 1.8.

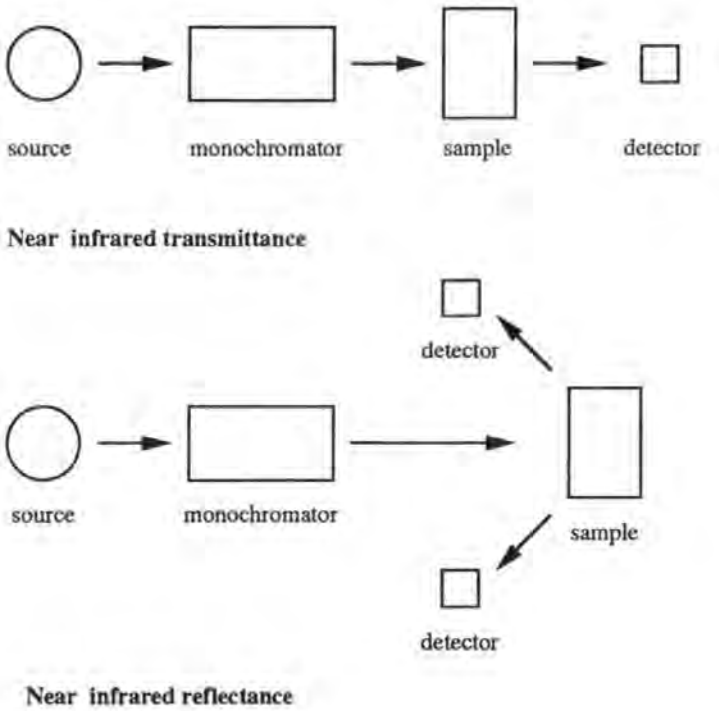

Figure 1.8 Basic instrument configurations for reflectance and transmittance (Workman & Burns, 1992)

- ***Scan Modes***

If electromagnetic radiation is directed onto a sample it may either be transmitted or reflected. When the radiation interacts with the sample, the amount of reflected or transmitted energy received at the detector is dependent on both the chemical (molecular absorbance) and physical (scattering) properties of the sample as well as the measurement geometry (Workman, 1992). Figure 1.9 show the radiant energy interaction with a solid sample i.e. ground or whole grain wheat.

- *Transmittance*

In transmittance spectrophotometry all the incident light (I_o) is either absorbed (I_a), transmitted (I_t) or reflected (I_r):

$$I_o = I_a + I_t + I_r \qquad \text{1.13}$$

The reflected component (I_r) is eliminated by a control or solvent blank. Since the path length of the cell can be kept constant, the absorbance is linearly related to concentration provided the refractive index remains constant (Murray, 1988). In transmittance measurements the entire path length of samples is integrated into spectral measurement, thereby reducing errors due to non-homogeneity of samples (Workman & Burns, 1992).

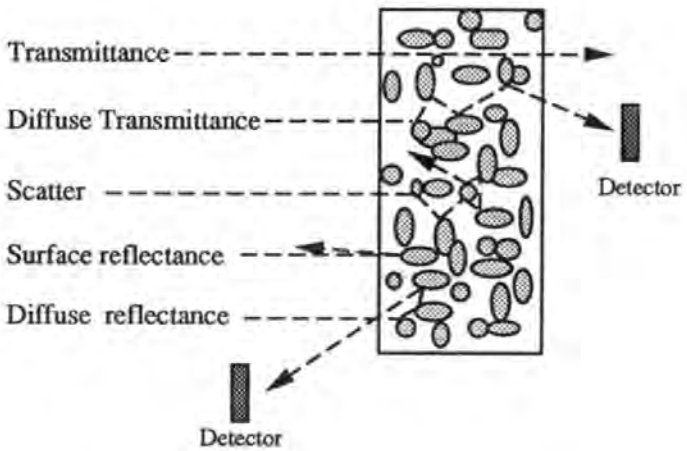

Figure 1.9 The radiant energy interaction with the sample (Shenk & Westerhaus, 1993)

During transmittance through fine particles, the front surface brings about a loss of energy transmitted through a sample with the net effect being a decrease in the signal-to-noise of the instrument. Higher frequency energy is most commonly used due to its greater depth of penetration into the sample. The higher frequency energy, 800-1400 nm, is more susceptible to front surface scattering than lower frequency energy. In transmittance measurements, particle size can be small enough to begin to scatter most of the energy striking the sample. If the particle size is sufficiently small, the instrument will not transmit enough energy through the sample for the detectors to record a signal (Workman & Burns, 1992).

- *Reflectance*

In reflectance the same relationship as in equation 1.13 holds except that I_t is eliminated by using a sample thickness such that all the light is either absorbed or reflected and none gets through the sample. The solvent blank is replaced by a white ceramic reference tile. However, there is no control over path length traversed by the light. This will vary with particle size and refractive index of the voids (Murray, 1988).

Near infrared spectral information is presented as log 1/R (R = reflectance) or log 1/T (T = transmittance). In these relationships absorption is assumed to vary linearly with concentration. To control any possible drift due to environmental changes during measurement periods the sample spectrum is compared with a ceramic tile in the case of reflectance and a solvent blank in the case of transmittance (Coventry, 1988). Data are therefore actually recorded as log R'/R, where R' is constant because a reference is chosen such that its reflectance does not change with wavelength, and therefore log 1/R or log 1/T, eventually carries all the information (Osborne, 1981). Figures 1.10 and 1.11 show two commercial NIR spectrophotometers.

As with the majority of measuring instruments, NIR spectrophotometers require calibration before they can be used for quantitative measurements. In NIR spectroscopy the instrument/computer system is "taught" what to look for in a given type of sample, then the hardware/software combination is expected to produce valid answers when it is presented with unknown samples of the same type (Burns, 1992). Separate calibration development for specific constituents are therefore necessary.

Figure 1.10 An NIRSystems Model 6500 spectrophotometer operating in reflectance and transmittance modes

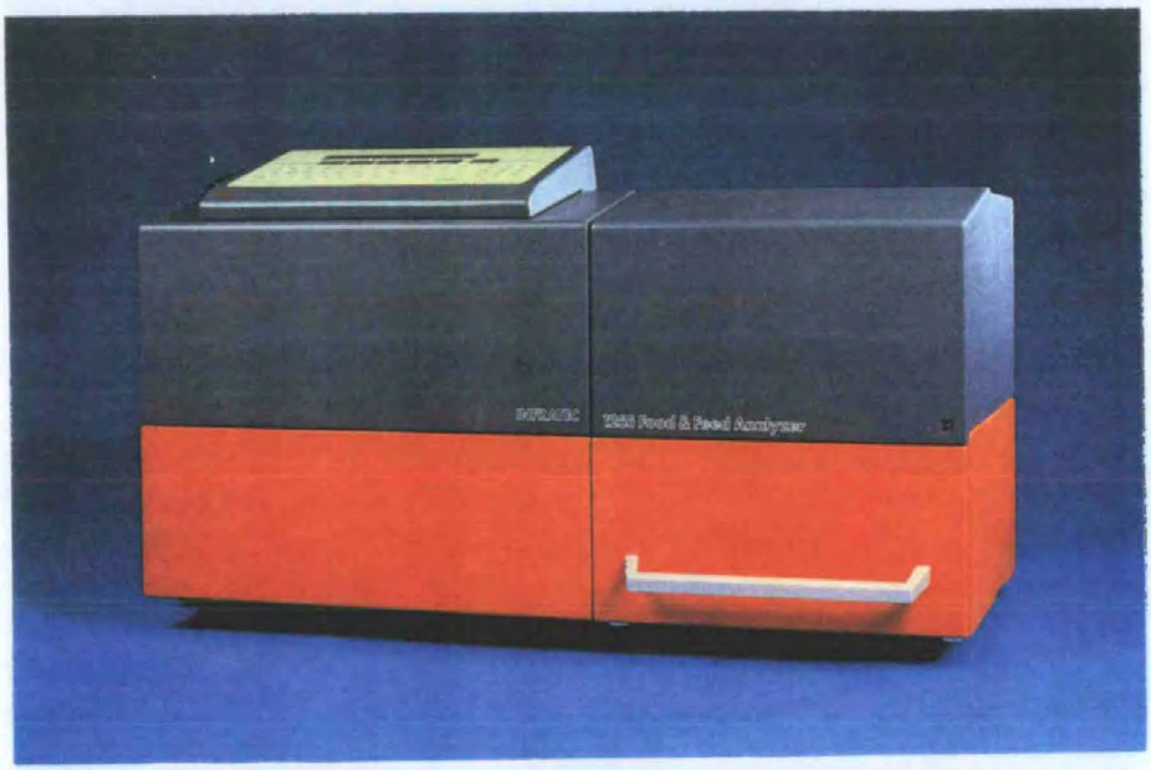

Figure 1.11 An Infratec Food and Feed Analyzer Model 1225 operating only in transmittance mode

1.2.4 NIR spectroscopy calibrations

The ultimate goal of calibration is to calculate a mathematical model of the calibration data which is most sensitive to changes in concentration of the sample and least sensitive to non-concentration related factors, such as physical, chemical and instrumental variables (Workman, 1992). In other words, the purpose of the calibration model is to relate the concentration of some analyte found in a sample (measured by a reference method) to the spectral data collected from that sample. However, it is important to appreciate that the accuracy of the results obtained by NIR is highly dependent on the accuracy of the method used (reference method) to calibrate the spectrophotometer. It is commonly assumed that the results obtained by NIR can never be better than those obtained by the reference method (Reeve & White, 1988). However, this was recently reported by DiFoggio (1995) to be a misconception. He showed that it was possible for NIR to perform better than the primary reference method. DiFoggio (1995) demonstrated this by using example calibrations on sets of real and synthetic spectra that had varying amounts of simulated laboratory error.

The accuracy of NIR protein determination on flour has been demonstrated by Osborne, Douglas, Fearn & Willis (1982). The accuracy was shown to be excellent compared with Kjeldahl and to be consistently maintained over a number of routine laboratories. The standard deviation of differences of 357 samples examined over 8 months was 0.20 %. However, the standard deviation of replicates for Kjeldahl was 0.12 %. Taking this into consideration the accuracy of NIR was recalculated to 0.16 % which is close to the accuracy of a single Kjeldahl determination.

Differences in the NIR optical response of samples with different compositions are very small compared to typical mid-IR analytical curves. However, they are reproducibly

measurable and are the basis of the success of NIR as a quantitative technique (Wetzel, 1983).

The original approach to the calibration of NIR spectrophotometers involves the use of multiple linear regression (MLR) to identify a combination of points in the spectrum where the original data correlate highly with the concentration of a specific constituent. More recently, alternative approaches which use all of the spectral data have been explored. Partial least squares (PLS) regression and principal components regression (PCR) have both been shown to provide viable alternatives which provide regression models to predict composition (Cowe, McNicol & Cuthbertson, 1990). Another recent development is the application of artificial neural networks to NIR calibration problems. According to Osborne *et al.* (1993) the feature that makes neural networks worth studying is their ability to model non-linearities in the calibration. They suggested that if non-linearity turned out not to be an important problem, neural networks would be unlikely to improve on PCR or PLS.

In spite of the successful use of NIR spectroscopy on a number of agricultural products to determine their composition, many of the factors determining this success are still not fully understood. This is partly because the technique has been developed with an emphasis on solving practical problems with immediate commercial potential (Cowe & McNicol, 1985).

1.2.5 NIR spectra of wheat

NIR reflectance spectra of agricultural products are characterised by poorly defined absorbance bands. Additionally, spectra of agricultural products in ground form e.g. ground wheat grain are also characterised by baseline shifts due to particle size influences as shown in Figure 1.12. Conventional spectroscopic evaluation as used in the mid-IR region is therefore not the solution. A statistical approach is usually adopted to determine where

measurements should be made in order to predict the composition of samples (Cowe *et al.*, 1990).

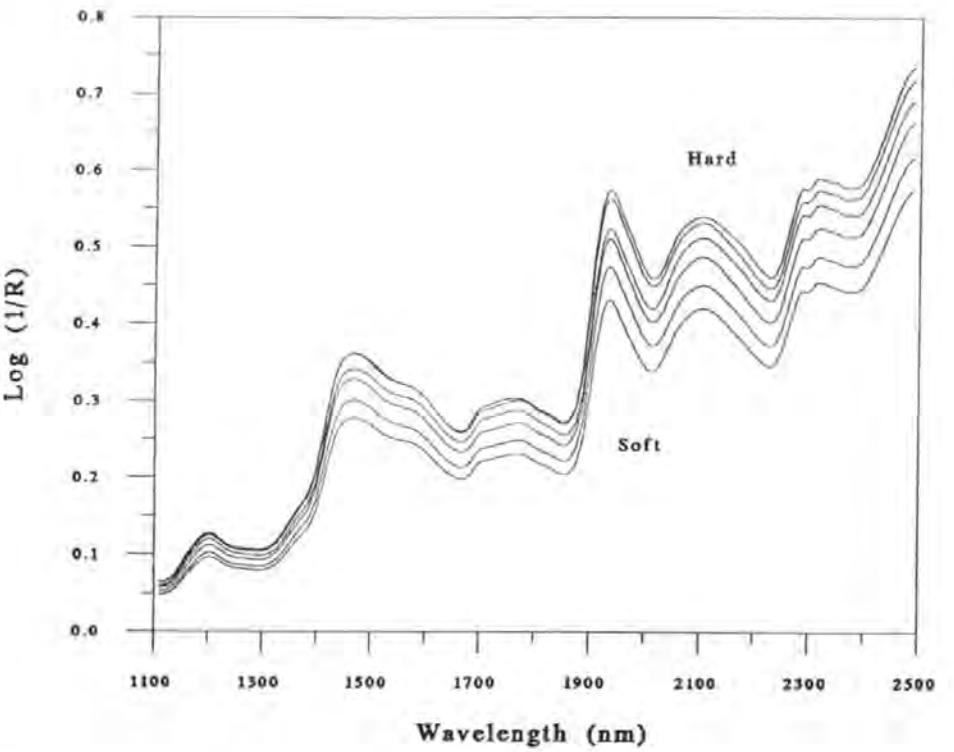

Figure 1.12 Spectra of ground wheat grain to illustrate the baseline shift due to differences in particle size

In diffuse reflectance and transmittance, light will be reflected and transmitted when the refractive index changes. Typically this happens when the light meets a particle surface in a powder. The light interaction with an analyte (scattering of light) will thus be a function of

- the number of light and surface interactions (depending on the particles' size and shape) and
- the actual differences in refractive indices (Næs & Isaksson, 1994).

The particles in food samples have a distribution of sizes and particle size has a pronounced effect on log 1/R values. It has been demonstrated by Norris & Williams (1984) that the effect of scatter on the NIR spectra of ground grain at a given wavelength

was proportional to the magnitude of log 1/R and this property is referred to as multiplicative. This effect can be seen in Figure 1.12. Due to the different particle sizes in ground wheat grain samples, when collecting spectra of these samples the effect of light scattering is multiplicative. Multiplicative light scatter also means that differences in scatter between two "equal" samples can be compensated for by multiplying each of one of the samples by the same constant. There is also an additive scatter component (Næs & Isaksson, 1994).

To ensure the best possible correlation between reference data and spectral data when calibrating to measure the composition of ground samples, it is essential to remove all or most to this effect of particle size. The simplest suggestion is dividing log 1/R at each wavelength by log 1/R at some reference wavelength. This method and other more sophisticated procedures to remove the effect of particle size have been summarised by Osborne *et al.* (1993) e.g. mathematical ballmilling (Murray & Hall, 1983). The most widely used method, however, is multiplicative scatter correction developed by Martens and co-workers (Martens, Jensen & Geladi, 1983; Geladi, MacDougal & Martens, 1985; Ilari, Martens & Isaksson, 1988).

- *Multiplicative scatter correction*

Multiplicative scatter correction (MSC) rotates each spectrum so that it fits as closely as possible to the mean spectrum and so removes at least some of the effect of light scattering on NIR spectra.. This is achieved, as summarised previously (Osborne *et al.*, 1993) for the spectrum of the i^{th} sample by fitting the equation

$$y_{iw} = a_i + b_i m_w \qquad w = 1,\ldots,p \qquad \ldots\ldots\ldots\ldots\ldots\ldots \quad 1.14$$

where y_{iw} is the log 1/R value for the i^{th} sample at the w^{th} of p wavelengths and m_w is the mean log 1/R value at wavelength w for all samples in the calibration set. The fitted

constants a_i and b_i are then used to compute the corrected spectrum as

$$y_{iw}^{c} = (y_{iw} - a_i)/b_i \qquad w = 1,.....,p \qquad \text{.....} \quad 1.15$$

Previous workers have shown that a multiplicative model applied to NIR reflectance spectra of ground wheat grain resulted in significant improvements to protein analysis (Martens *et al.*, 1983). This model has also been used for the measurement of particle size of powdered samples based on a direct correlation with the scatter effect (Ilari *et al.*, 1988).

In the discussion of wheat hardness (section 1.1.1) it was concluded that wheat hardness can be defined as how the wheat grain breaks down during the milling process and that wheats of different hardness break down to different particle sizes. When collecting NIR spectra of ground wheat grain the effect of particle size on the spectra is obvious. When measuring moisture and protein of ground wheat grain, it is important to remove some or all of this effect. As particle size has a pronounced effect on spectral values, it follows that it can be measured by NIR spectroscopy. This effect emphasises the differences between hard and soft wheats and as these differences can be measured by NIR spectroscopy, it is therefore possible to measure wheat hardness by NIR spectroscopy.

1.3 NIR spectroscopy and wheat hardness

The application of NIR reflectance and transmittance spectroscopy to the analysis of wheat is well established and is the basis of approved methods of both the American Association of Cereal Chemists (AACC) and International Association for Cereal Science and Technology (ICC).

1.3.1 NIR spectroscopy measurements of ground wheat grain

The effect of the mean particle size and particle size distribution on analysis of ground

wheat samples by NIR reflectance spectroscopy is well known (Williams 1975; Williams & Thompson, 1978). If wheat samples are ground to a meal or flour under standard conditions they will exhibit different light scattering properties due to different particle sizes. When particle size increases, so will the log 1/R at every wavelength. As a result, the log 1/R values will be higher the harder the wheat as shown earlier in Figure 1.12.

Williams & Sobering (1986) used this principle to calibrate an NIR instrument to predict hardness of ground wheat samples against particle size index (PSI) values. They derived an NIR hardness index for instruments with a limited number of filters by using a calibration set of hard and soft wheat varieties and taking log 1/R measurements at two wavelengths selected *a priori* (1680 nm & 2230 nm). In a later development, Norris *et al.* (1989) achieved the measurement of hardness by NIR spectroscopy without calibrating it against a reference method. Using the same wavelengths, they chose coefficients to maximize the precision of the measurement, while achieving discrimination between hard and soft wheats. This became AACC method 39-70A (AACC, 1989).

This NIR hardness index can therefore be defined as

$$\text{Hardness index} = a + b(\log 1/R_{1680}) + c(\log 1/R_{2230}) \quad \ldots\ldots\ldots\ldots\ldots\ldots\ldots\ldots\ldots\ldots\ldots\ldots \quad 1.16$$

with b and c optimized to maximize the precision of the measurement.

NIR hardness as measured according to AACC Method 39-70A is based on an empirical scale and generally ranges from about 10 (very soft) to 110 (very hard). The USDA has recently adopted a hardness index based solely on NIR reflectance measurements on ground wheat.

It has to be stressed that this method (AACC Method 39-70A) of measuring NIR hardness is based on the relationship between scatter and particle size and not on the concentrations of constituents in the samples. Brown, Curtis & Osborne (1993) have shown that the AACC method is affected by wheat moisture and protein content and by growing season when applied to UK wheats. The response of UK wheat NIR hardness scores to moisture content was found to be greater and more variable than that of North American wheats.

Until recently, NIR spectroscopy was an accepted technique for the accurate and rapid determination of quality parameters in cereals only in its most well-known form, reflectance. In this mode it suffers from the disadvantage that grain samples require grinding before analysis. This is inconvenient and leads to a significant source of error. NIR spectroscopy is already used as a method of discriminating between hard and soft wheat cultivars since ground samples of these exhibit different light scattering properties as described earlier. Successful predictions of wheat hardness by NIR spectroscopy on ground wheat grain have been reported by various previous workers (Miller, Afework, Pomeranz, Bruinsma & Booth, 1982; Williams, 1979; Williams & Sobering, 1986; Randall, Krieg & McGill, 1992). NIR reflectance spectroscopy is, however, not applicable to the wheat end of the mill without incorporating an on-line grinder into the system.

The whole grain NIR transmittance instrument has already been adapted for on-line use. Technology therefore exists for on-line measurement of NIR transmittance spectra of whole wheat grains and clearly it would be more convenient to be able to make measurements directly on the whole grain particularly if the method is to be used on-line to control wheat blending at the mill.

1.3.2 NIR spectroscopy measurements of whole wheat grain

In 1983, Norris introduced a new technique based on transmission through intact grain kernels which led to the development of commercial instruments which have been used to determine the protein and moisture contents of both wheat and barley. In 1988, an NIR transmittance monochromator designed for whole grain became commercially available and this opened the way for further research into the application of the NIR transmittance technique (Williams, 1991). Williams (1991) used the Infratec Model 1225 Food and Feed Analyzer, an NIR transmittance instrument, introduced by the Tecator Company which operates in the near-visible range of 850 - 1050 nm to perform non-destructive measurements of wheat kernel texture. As the tests are performed on whole grain, the moisture level will have less impact on the results than is the case with test methods that involve grinding (Williams, 1991). This investigation showed that the NIR transmittance instrument is capable of predicting wheat kernel texture with precision equal to that of the reference (PSI) method and that it is slightly superior to the NIR method for PSI prediction.

In 1993, Williams & Sobering again reported successful NIR calibrations for predicting wheat grain hardness on whole grains. This time they used the Infratec Model 1225 Food and Feed Analyzer in transmittance mode as well as the NIRSystems Model 6500 spectrophotometer in reflectance mode. They also introduced the concept of using ground grain calibrations to monitor the accuracy of whole grain analysis. Apart from this, no other successful NIR calibrations on whole grain samples has been reported so far. It has to be stressed that these calibrations have been performed only on Canadian home-grown wheats.

1.3.3 NIR spectroscopy measurements of UK home-grown whole wheat grain

Wheat grain hardness is the most important milling characteristic. Currently grists are

optimised mainly on the basis of compositional factors such as protein content and Falling Number and variation in milling quality has to be tackled by fine-tuning of the mill which may have to be achieved at the expense of increased energy consumption. Supplementation of flours with dried wheat gluten (although at high costs) has somewhat diminished the importance of protein content as a criterion of wheat quality and, in consequence, milling behaviour has become relatively more important as an economic factor.

Wheats grown in the UK are variable in their milling behaviour, partly due to environmental reasons and partly as a result of the diversity of varieties sown. Neither of these sources of variation is likely to diminish.

In a milling system, subject to a variable grist, millers need to make best use of the available wheat in terms of extracting the full potential yield of white flour. Due regard must also be paid to flour quality for the desired end-use. Flour for breadmaking requires a certain level of damaged starch granules which are produced on the reduction rolls and milling of wheat of non-optimum quality results in a need to narrow the roll gaps with an increase in energy usage and roll wear.

Ideally, a fixed milling system optimised for minimum energy consumption would be based on maximum extraction rate for wheat of consistent quality. An on-line method of measuring milling quality of whole grain wheat so as to control blending would enable such consistent raw material to be fed to the mill. This would therefore improve extraction rate and optimise starch damage while minimising energy consumption. The milling quality of wheat is largely dependent on the wheat grain hardness, hard wheat giving rise to more efficient separation of endosperm from the bran and freer-flowing flour of higher starch damage levels.

What is lacking is a fundamental understanding of NIR spectroscopy as a means to assess whole grain wheat hardness and thus milling quality of wheat in relation to its behaviour in the mill. This study investigated the measurement of whole wheat grain hardness by NIR in order to develop a hardness index which could be monitored on-line as a basis for automatically optimising grists in terms of milling performance and to attempt to provide this fundamental understanding of the measurement by NIR on whole wheat grains.

NIR hardness measurements of wheat hardness on whole grain cannot be based on particle size as no grinding is involved. However, particle size (Air Jet Sieve, Particle Size Index, AACC NIR wheat hardness scores) has been used as the reference method for empirical calibrations. Currently, measurement of wheat hardness on Canadian home-grown whole grain has been achieved using the so called "black box" approach to optimise the accuracy of prediction.

Assuming that hardness measurements of whole grains are also based on the scattering properties of the samples, there are several possible methods for separating the effects of scatter and absorption. Previously these methods have not been applied to whole grain spectra and are the following: multiplicative scatter correction (Ilari *et al.*, 1988), principal components analysis (Cowe & McNicol, 1985) and the area between the second derivative curve and the wavelength axis (Norris & Kuenstner, 1995).

- *Multiplicative scatter correction*

Multiplicative scatter correction (MSC) has already been discussed in detail under section 1.3.4 as a method to remove the multiplicative scattering effect due to differences in particle size. Subsequently, this allows separation of the effect of scatter and could be employed to measure hardness.

- *Principal components analysis*

Principal components analysis (PCA) is a standard statistical technique which describes the variation in multidimensional data by means of a few uncorrelated variables. Principal components are linear combinations of the original spectral data which represent in turn, the maximum unexplained variation in the spectral data. PCA is therefore a data compression technique (Cowe & McNicol, 1985).

Two terms are important as far as PCA is concerned: Principal component loadings (or weights) and principal component scores. The loadings extracted by PCA define a rotation of the original wavelength axes which positions spectral values on principal component axes. Each wavelength has its own loading. Some plots of these loadings display remarkable similarities to both the spectra of the samples and the spectra of their constituents. Where several constituents correlate with a single component the shape of the component may reveal influences from more than one constituent. Scores define the position of the samples on the principal component axes. They are derived by summing the loadings times the centred log 1/R or log 1/T values across the spectrum, and are the basis for principal components regression (PCR) models for predicting the composition (Cowe & McNicol, 1985).

Thus PCA attempts to describe the variation in multidimensional data by means of a small number of uncorrelated variables. Spectral data are intercorrelated to a high degree i.e. the various wavelengths correlate with each other much more than with, for example, the protein content of the samples. The use of principal components resolves completely this problem of multicollinearity between reflectance values, reduces the spectra to a small number of computed values and in addition provides information as to the nature of the underlying chemical factors affecting variation in the spectra. This information is presented

in a simple graphical form which relates directly to the original spectra (Cowe & McNicol, 1985).

In ground wheat samples, the first principal component has been found to be associated with variation in particle size, the second with variation in moisture, the third with variation in protein levels, the fourth and fifth with interaction between water and other constituents and the sixth principal component with the variability caused by varietal and environmental differences (Delwiche & Norris, 1993).

Discriminant analysis models can be developed using the loadings of the spectra as derived from principal component analysis (PCA). In application, samples from the calibration set are expressed initially in terms of their principal components. The principal components reduce the dimension of the variability space from the number of wavelengths per spectrum (eg. 700) down to a user selected number. Generally, between one and 10 factors (i.e. eigenvectors) are selected. Essentially each spectrum can be represented as a linear combination of these factors in which a spectrum's unique shape is a function of the coefficients (i.e. scores) applied to the factors. Once the spectra are expressed in terms of their principal components, the scores are then expressed in a normalised Mahalanobis distance space (Mahalanobis, 1936; Mark & Tunnel, 1985). A linear discriminant function is developed from the normalised scores (Delwiche & Norris, 1993).

Canonical correlation analysis (CCA) is a multivariate statistical analysis that studies linear relations between two sets of variables observed on the same sample set (Krzanowski, 1988). The objective of CCA is to find wavelengths in both variables that vary in a similar way. Certain difficulties, however, arise from the considerable intercorrelations across the wavelengths of the NIR spectra. Devaux, Robert, Qannari, Safar & Vigneau (1993)

adapted the CCA method to overcome this problem as suggested by Muller (1982) by performing CCA on the principal components instead of the raw spectral data.

- *Area under the second derivative curve*

Derivatives were originally described in the literature by Norris & Williams (1984) and remove, although not entirely, the effects of particle size. The idea of derivatives is to calculate differences between nearby points of the spectrum. This process, however, would be sensitive to noise in the original data. It cancels the "signal" that is in common between the two points and doubles the "noise". In order to reduce the effect of noise, segments of the spectrum are smoothed and these values are used in the calculation of the derivative.

The most popular way to calculate derivatives on spectra collected on monochromators is the segment-gap method. The segment is the range of data points averaged together and the gap is the distance between averages being subtracted. A first derivative is the difference between two averages separated by the specified gap. A first derivative with a six point gap is computed as average 1 minus average 7, average 2 minus average 8, and so on. A second derivative can be computed by applying the first derivative procedure to the first derivative data.

It is difficult to interpret first derivative spectra because band peaks and valleys do not follow the log 1/R spectral pattern. The second derivative calculation results in a spectral pattern display of absorbance peaks which were inverse in comparison to the raw spectral pattern and is easier to interpret than first derivative spectra.

Recently, during the course of this study, Norris & Kuenstner (1995) has suggested that the area between the second derivative curve and the wavelength axis (AREA), is a function

of path length and therefore scatter. This measurement could therefore be used to measure hardness.

1.4 Objectives

The main objectives of this study were thus to:

- investigate the measurement of whole wheat grain hardness by NIR spectroscopy
- investigate the measurement of whole wheat grain hardness by NIR spectroscopy on UK home-grown samples only
- predict damaged starch by NIR spectroscopy
- investigate the dependence of NIR wheat hardness measurements on chemical composition and scatter
- investigate the scatter properties of whole wheat grain as measured by NIR transmittance and reflectance spectroscopy
- attempt to provide a fundamental understanding of the measurement by NIR spectroscopy on whole wheat grains

Chapter 2

Materials and Methods

CHAPTER 2

2.0 MATERIALS AND METHODS

2.1 Materials

The wheat samples used were kindly provided by the Flour Milling Baking Research Association (FMBRA), Chorleywood (currently the Campden-Chorleywood Research Association (CCFRA), Chorleywood) and the Canadian Grain Commission (CGC), Winnepeg, Canada. The wheat varieties used are as listed in Tables 1 to 4, Appendix 1.

2.2 Methods

2.2.1 Wheat hardness measurements

The hardness of 104 wheat samples, covering a wide range of hardness, was determined by two conventional methods: The Air Jet Sieve test (currently used by the CCFRA) and the Particle Size Index test (currently used by the CGC). Both of these tests are grinding/sieving tests based on the fact that wheat grain, depending on the hardness of the grain, breaks down to different particle sizes during grinding (Cutler & Brinson, 1935; Williams & Sobering, 1986). In addition to these conventional tests, the wheat hardness of these samples was also measured on the ground grain by the AACC NIR wheat hardness test (currently used by the UK Milling Industry) (AACC, 1989).

(i) Air Jet Sieve test (AJS) (Appendix 2)

The ground grain samples were obtained by passing the whole wheat grain through a Model 3100 hammer mill (Falling Number AB, Huddinge, Sweden) fitted with a 1 mm screen. Wheat hardness was determined as the percentage of ground wheat (10 g) passing through a 75μm air jet sieve in 90 seconds. The AJS test was performed in duplicate.

(ii) Particle Size Index test (PSI) (Appendix 3)

The ground grain samples were obtained by passing the whole grain wheat through a UDY Cyclone sample mill equipped with a sample feed regulator and fitted with a 1 mm screen. Wheat hardness was determined as the percentage of ground wheat (10 g) passing through a 74 μm sieve in 10 minutes on an automatic sieve shaker. The PSI test was only performed as a single test but 3 reference samples of known hardness (soft, hard and durum wheats) were tested at the same time as controls.

(iii) AACC NIR wheat hardness test (AACC) (Appendix 4)

The AACC NIR wheat hardness test (AACC Method 39-70A) is based on the relationship between light scatter and particle size and not on the concentrations of constituents in the samples. If wheat samples are ground to a meal or flour under standard conditions, the log 1/R (R = reflectance) values will be higher the harder the wheat. NIR hardness scores can be derived for instruments with a limited number of filters by using a calibration set of hard and soft wheat varieties and taking log 1/R measurements at two wavelengths selected *a priori* (1680 nm & 2230 nm). A hardness index can be defined as

$$\text{NIR hardness score} = a + b(\log 1/R_{1680}) + c(\log 1/R_{2230}) \quad \ldots\ldots\ldots\ldots\ldots 2.1$$

with *b* and *c* optimised to maximise the precision of the measurement (AACC, 1989).

The twenty samples as listed in Table 1, Appendix 1 were used to construct the AACC NIR wheat hardness calibration. The initial calibration was constructed by entering the NIR constants detailed in Appendix 4 into the instrument. The hardness scores of samples 1 - 10 (as listed in Table 1, Appendix 1) were recorded and the means of the hard (MH) and the soft (MS) samples were calculated and corrected to read 75 and 25, respectively,

using the equations in Appendix 4. The new constants calculated were entered into the instrument and a further set (samples 11 - 20 as listed in Table 1, Appendix 1) was used to validate the new calibration. The AACC NIR wheat hardness scores were then measured for all of the 104 samples.

2.2.2 NIR spectroscopy measurements

(i) Determination of accuracy and precision of the NIR spectrophotometer

The NIR reflectance and transmittance spectra were recorded using a Model 6500 spectrophotometer (NIRSystems Inc., Silver Spring MD, USA) and an Infratec Food and Feed Analyzer Model 1225 (Tecator AB, Höganäs, Sweden). The instrument specifications for these two spectrophotometers are listed in Tables 2.1 & 2.2, respectively.

Instrument standardisation is a unique feature in Infrasoft International (ISI) software. It ensures that calibrations produced on ISI's master instrument are reproduced in host instruments. In addition, after an instrument is repaired at the factory it guarantees that the spectra produced by the repaired instrument are the same as before the instrument failed. Instrument standardisation is also necessary to move spectra files or calibration equations from one instrument to another (ISI, 1991).

The four main parameters of a spectrophotometer that a user may wish to check, are (Freeman, 1992):

- NIR repeatability
- wavelength accuracy
- bandwidth
- the amount of stray flux

Table 2.1 Specifications of the NIRSystems Model 6500 (Workman & Burns, 1992; ISI, 1991)

Optical configurations	Holographic, diffraction grating
Source type	Near infrared
	Tungsten-halogen monofilament
Wavelength range	400-2500 nm
Data interval	2.0 nm
Scan speed	1.8 scans/second
Detectors	Lead sulphide, 1100-2500 nm
	Silicon, 400-1100 nm
Spectral bandwidth	10 nm ± 1 nm in reflectance
	8.5 nm ± 1 nm in transmission
Wavelength accuracy	Based on instrument-to-instrument repeatability: 0.15 nm
	Based on currently accepted wavelength standards: 0.30 nm
Instrument wavelength	Short term 0.01 nm
Precision	Long term 0.01 nm
Linearity	1% of reading
Stray light	Less than 0.1% at 2300 nm

Table 2.2 Specifications of the Infratec Model 1225 (Workman & Andren, 1993)

Optical configurations	Mechanically ruled grating
Source type	Tungsten-halogen lamp
Wavelength range	800 - 1100 nm
Data interval	2.0 nm
Detectors	Silicon
Spectral bandwidth	6 nm
Signal handling	up to 5 Absorbance units

Diagnostics can be made easily using the ISI software to determine the **accuracy and precision** of the instrument. These diagnostics range from a daily use of a sealed check cell to instrument diagnostics of NIR repeatability, wavelength accuracy and instrument response (ISI, 1991). It is therefore not necessary to obtain any additional standards (Freeman, 1992).

The Model 6500 is supplied with a **check cell** which is the simplest overall test of instrument performance. It provides information on the accuracy and precision of the instrument. Accuracy is provided by the mean analysis of four constituents and precision by the standard deviation of the analysis over time. This sample is the most important link with the performance change of the instrument over time and is the only verification that the instrument is standardised to the master monochromator (ISI, 1991).

NIR repeatability is a measure of the repeatability of the spectral data points. It is sometimes referred to as noise. The importance of measuring noise has been demonstrated by Norris (1992). It is a measure of the deviations in optical (log 1/R) data at each wavelength. The tests are accomplished by scanning the internal ceramic as a reference, then as a sample, and again as a reference. This sequence is repeated and the two complete scans are subtracted. The statistic calculated is referred to as root mean square (RMS) and root mean square corrected for bias (RMS(C)). Using a 16,16,16 revolution sequence (ceramic or reference tile scanned 16 times as a reference, then 16 times as a sample and again 16 times as a reference), the average RMS(C) of five scans should be less than 20 in a room with stable temperature (ISI, 1991).

Wavelength accuracy for any spectrophotometer is the difference between the measured wavelength of a wavelength standard and the nominal wavelength reported for that

wavelength standard (Workman & Burns, 1992). It is determined by internal standards of polystyrene for the NIR region and didymium for the visible region (ISI, 1991).

Instrument response measures the absolute reflectance from the ceramic tile. The instrument should have a maximum value of between 55 000 and 58 000 for both the NIR and visible range (ISI, 1991).

For grating instruments, **bandwidth** is the full width at half maximum of the bandshape of monochromatic radiation passing through a monochromator. Bandwidth determines the resolution of the instrument and the smaller the bandwidth, the higher the resolution (Workman & Burns, 1992).

Stray flux sometimes termed stray radiant energy is the major cause of non-linearity for most instruments. It is defined as the sum total of any energy or light other than the wavelength of interest that reaches the sample and detector (Workman & Burns, 1992).

NIR repeatability or noise tests were carried out regularly to monitor the performance of the Model 6500 with regard to noise, accuracy and precision.

(ii) NIR spectra of wheat samples

Three sets of spectra for each of the 104 samples of wheat were recorded using the NIRSystems Model 6500 spectrophotometer. The three sets consisted of ground grain spectra recorded in reflectance mode and whole grain spectra recorded in reflectance and transmittance mode, respectively. Spectra were recorded as log 1/R or log 1/T, respectively, at 2 nm intervals from 400-2500 nm in case of reflectance on ground grain and reflectance on whole grain and in the case of transmittance on whole grain from 850-

1050 nm. The scan speed of the Model 6500 was 1.8 scans/second and 4-Point Fourier smoothing was applied. The ground samples were obtained by passing the whole wheat grain through the Falling Number Model 3100 hammer mill fitted with a 1 mm screen as described in section 2.2.1(i). The ground wheat grain spectra were collected using the standard sample cell (ca. 25 g). The NIRSystems Model 6500 is equipped with a sample transport mechanism which allows scanning of the whole grain sample while the sample cell is in motion. The coarse sample cell (full cell, ca. 120 g) was used and each whole wheat grain sample was scanned only once. The transport speed was adjusted to make only one downward pass of the entire sample, while taking 25 sub-scans. The standard and coarse sample cells are shown in Figure 2.1. Whole wheat grain spectra were also recorded for each of the 104 samples using the Infratec Food and Feed Analyzer Model 1225 spectrophotometer. These whole grain spectra were recorded in transmittance mode as log 1/T at 2 nm intervals from 850 - 1050 nm.

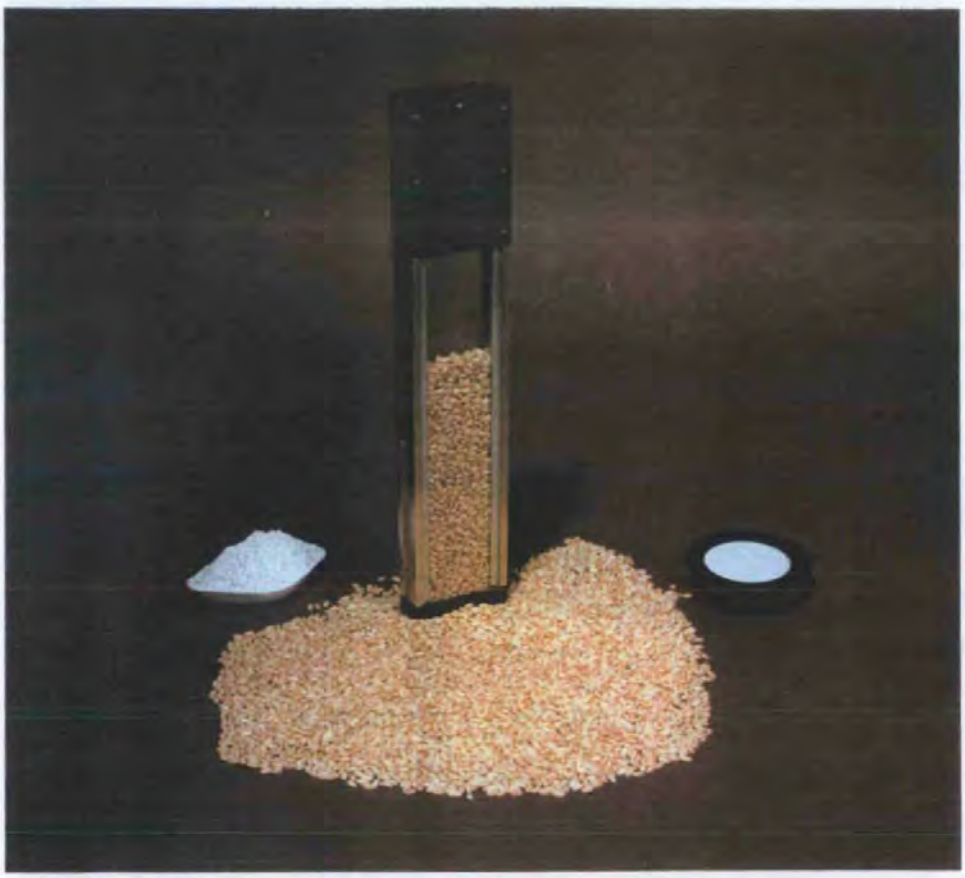

Figure 2.1 Standard and coarse sample cells of NIRSystems Model 6500 for ground and whole wheat grain, respectively

2.2.3 NIR spectroscopy calibrations

Empirical and alternative calibration equations were derived to predict wheat hardness on ground and whole grain, respectively, using both AJS and PSI tests as reference methods. The AACC NIR wheat hardness test was also used as a reference method to derive calibration equations for whole grain. All the samples as listed in Tables 1 to 4, Appendix 1 were used and consisted of:

Table 1: The samples used to construct the AACC NIR wheat hardness calibration equation.

Table 2: UK home-grown wheat varieties from different localities.

Table 3: The varieties, Mercia and Riband at two different protein levels from two different harvests.

Table 4: Canadian home-grown wheat varieties

The samples were divided into a calibration set and a prediction set in order to be able to monitor the validity of these equations on an unknown sample set. After sorting the samples in order of increasing AJS values, the set of 104 wheat samples were divided into a calibration set (63 samples) and a prediction set (41 samples) as shown in Table 2.3. The first three samples were selected into the calibration set, the following two into the validation set, the next three into the calibration set until all the samples had been allocated. Row one in Table 2.3 shows that the first three samples in the calibration set came from Table 4, Appendix 1, as well as the first sample of the prediction set. The next sample in the prediction set came from Table 2, Appendix 1, as well as the next sample in the calibration set.

Table 2.3 Matrix to show split of samples in calibration and predictions sets, respectively (**calibration set is in bold** and *prediction set in italics*)

Calibration			*Prediction*		**Calibration**			*Prediction*	
Z	**Z**	**Z**	*Z*	*Y*	**Y**	**Z**	**Z**	*Z*	*Z*
Y	**Z**	**Y**	*Z*	*Y*	**Z**	**Y**	**Y**	*Y*	*Z*
Y	**O**	**Z**	*Y*	*O*	**O**	**Y**	**Y**	*Y*	*Y*
X	***Y***	***Z***	*Y*	*O*	***Y***	***Y***	***Y***	*X*	*Y*
Y	***Y***	***Y***	*Y*	*Y*	***Y***	***Y***	***Y***	*X*	*Y*
X	**Y**	**Y**	*Y*	*X*	**X**	**Y**	**X**	*Y*	*Y*
X	**X**	**Y**	*Z*	*Y*	**Z**	**Y**	**X**	*Y*	*Y*
Y	**Y**	**Y**	*Y*	*Y*	**X**	**Y**	**Y**	*O*	*Y*
Y	***Y***	***Y***	*Z*	*O*	***Y***	***Y***	***O***	*O*	*Y*
X	***X***	***X***	*Z*	*X*	***X***	***Z***	***Z***	*X*	*X*
Z	***X***	***Z***	*X*						

X = Samples in Table 1, Appendix 1
Y = Samples in Table 2, Appendix 1
O = Samples in Table 3, Appendix 1
Z = Samples in Table 4, Appendix 1

(i) Empirical calibrations

Empirical calibration equations for the sets of spectra as listed in Table 2.4 were derived by means of Partial Least Square (PLS) regressions using the calibration set as described above. This calibration technique is described by Martens & Næs (1987). The equations were then validated using the validation set as described above. The reference methods used were the three hardness measurements as described in section 2.2.1. The AJS and PSI hardness tests were used as reference methods for all three sets of spectra whereas the AACC NIR wheat hardness measurements were only used as reference method in the case of the whole grain spectra.

Table 2.4 Sets of spectra for which empirical calibration equations were derived by PLS, with AJS, PSI and AACC as reference methods using different software packages

	ISI No cross - validations	**ISI** 20 cross - validations	**NSAS** No cross - validations	**NSAS** 20 cross - validations	**UNSCR** No cross - validations	**UNSCR** 20 cross - validations
Ground grain Reflectance	AJS	AJS	AJS	AJS	AJS	AJS
	PSI	PSI	PSI	PSI	PSI	PSI
Whole grain Reflectance	AJS	AJS	AJS	AJS	AJS	AJS
	PSI	PSI	PSI	PSI	PSI	PSI
	AACC	AACC	AACC	AACC	AACC	AACC
Whole grain Transmittance	AJS	AJS	AJS	AJS	AJS	AJS
	PSI	PSI	PSI	PSI	PSI	PSI
	AACC	AACC	AACC	AACC	AACC	AACC

ISI = Infrasoft International software

NSAS = NIRSystems Spectral Analysis software

UNSCR = UNSCRAMBLER software

The PLS regressions were performed over the wavelength ranges 1120 - 2480 nm for reflectance and 850 - 1050 nm for transmittance, respectively, using every data point. The spectra were not corrected for scattering and no mathematical treatment was applied. As this exercise included comparisons to be made, no outliers were removed. The calibrations were thus performed on the raw data as measured.

The 'best' equation was selected in two different ways:

- equation with lowest standard error of performance (SEP)
- equation selected by software after 20 internal cross-validations

- *equation with lowest SEP*

A number of equations were derived, each with a different number of terms (up to 15 terms). All these equations were then validated using the validation set. The equation that proved to give the lowest SEP was selected as the 'best' equation.

- *equation selected by software after 20 internal cross-validations*

Internal cross-validations during calibration were used to select the 'best' equation. The selected equation was then validated using the validation set.

Infrasoft International (ISI) software, (ISI, 1991), NIRSystems Spectral Analysis software (NSAS) (NSAS, 1991) and UNSCRAMBLER software (UNSCRAMBLER, 1993) (Environmental Sciences, University of Plymouth) packages were used, respectively, to derive calibration equations as shown in Table 2.4.

(ii) Empirical calibrations on UK home-grown wheat

Calibration equations were derived from a sample set containing only UK home-grown wheat samples to monitor the performance of the calibrations in comparison with the sample set also containing Canadian home-grown samples. The Canadian home-grown samples were removed from the sample set as described in section 2.2.3(i) and the remaining samples were divided into a calibration set and validation set following the same principle as shown in Table 2.3. Calibration equations were derived as described in section 2.2.3(i) using only the ISI software.

(iii) Alternative calibrations

Assuming that hardness measurements of whole grains are also based on the scattering properties of the samples, there are several possible methods for separating the effects of

scatter and absorption. These methods are based on algorithms which have not previously been applied to whole grain spectra. Multiplicative scatter correction (MSC), principal component analysis (PCA) and the area between the second derivative curve and the wavelength axis (AREA) were investigated, therefore, attempting calibrations to predict wheat hardness, with the empirical calibrations as comparisons. The sets of spectra analysed where as shown in Table 2.5.

Table 2.5 Sets of spectra for which alternative calibration equations were derived by MSC, principal components and AREA with AJS, PSI and AACC as reference methods

	MSC	**1st PC**	**2nd PC**	**1st PC & 2nd PC**	**AREA**
Ground grain Reflectance	AJS	AJS	AJS	AJS	AJS
	PSI	PSI	PSI	PSI	PSI
Whole grain Reflectance	AJS	AJS	AJS	AJS	AJS
	PSI	PSI	PSI	PSI	PSI
	AACC	AACC	AACC	AACC	AACC
Whole grain Transmittance	AJS	AJS	AJS	AJS	AJS
	PSI	PSI	PSI	PSI	PSI
	AACC	AACC	AACC	AACC	AACC

Multiplicative scatter correction (MSC)

Multiplicative scatter correction can be used to measure hardness on ground grain by separating the effect of scatter. The fact that the scattering of whole grain might not be multiplicative does not necessarily mean that it would not correlate with hardness. This

application has therefore been investigated in the case of whole grain as well.

(a) Method of calibration

The mean spectrum for the calibration set was calculated. A simple linear regression for each spectrum of the calibration set against the mean spectrum of the calibration set was performed to derive the intercept and slope for each sample spectrum.

Thus, by fitting the equation

$$y_{iw} = a_i + b_i m_w \qquad w = 1,.....,p \qquad \text{..... 2.2}$$

for the spectrum of the i^{th} sample where y_{iw} is the log 1/R value for the i^{th} sample at the w^{th} of p wavelengths and m_w is the mean log 1/R value at wavelength w for all samples in the calibration set, the constants a_i (intercept) and b_i (slope) were derived and used as raw data and regressed against the AJS, PSI and AACC test results, respectively, to derive a calibration equation to predict wheat hardness.

(b) Method of validation

The equation was validated using the unknown sample set. A simple linear regression for each spectrum of the prediction set against the mean spectrum of the calibration set was performed as described above to derive the intercept and slope for each prediction sample spectrum. The intercept and slope were substituted in the calibration equation to predict the wheat hardness.

Principal component analysis (PCA)

As the first principal component (1st PC) accounts for almost all of the variation within the data set, which in turn is known to be caused by scatter, it was chosen *a priori* to predict

wheat hardness. However, the plot of the loadings (or weights) of the second principal component (2nd PC) was found to be similar to the spectrum of the whole grain sample. It is known that these plots can be interpreted spectroscopically and that the shape of the principal component spectrum could refer to the "constituent" of interest. Therefore, both the 1st and 2nd PC were used in the whole grain calibrations. The means of the respective spectra, the standard deviations and the loadings of the 1st and 2nd principal components were plotted for spectral information interpretation.

The first and second principal component scores were derived, using the ISI software. Components are defined in terms of the wavelength data by loadings, which represent the amount of rotation from each wavelength axis to a component axis. Each component will therefore conform to the general equation:

$$P_n = C_{n,1}E_1 + C_{n,2}E_2 + C_{n,3}E_3 + \ldots\ldots\ldots\ldots + C_{n,700}E_{700} \qquad \ldots\ldots\ldots\ldots 2.3$$

where $C_{n,1}$ ..... $C_{n,700}$ are component loadings scaled so that the sum of loadings across the spectrum is 1; E_1 ..... E_{700} are centred spectral values across the spectrum and P_n is the n^{th} component.

The scores can then be found by substituting the spectral values for the sample in the equation. Thus

$$S_{i,n} = C_{n,1}E_{i,1} + C_{n,2}E_{i,2} + C_{n,3}E_{i,3} + \ldots\ldots\ldots\ldots + C_{n,700}E_{i,700} \qquad \ldots\ldots\ldots\ldots 2.4$$

where $S_{i,n}$ is the score for the i^{th} sample on the n^{th} component, $C_{n,1}$ ..... $C_{n,700}$ are loadings on the n^{th} selected component and $E_{i,1}$ ..... $E_{i,700}$ are the spectral values for the i^{th} sample.

(a) Method of calibration

Calibration equations were derived by regressing the 1st PC scores against AJS and PSI hardness results in the case of ground grain and the 1st and 2nd PCs against AJS, PSI and AACC NIR hardness results in case of the whole grain samples.

(b) Method of validation

The raw log 1/R or log 1/T data of the prediction set were multiplied by the loadings of the calibration set at each wavelength. The values obtained were summed up to give the principal component scores, as described above, which were used in the calibration equations to predict hardness.

Area under the second derivative curve (AREA)

Norris & Kuenstner (1995) have suggested that the area between the second derivative curve and the wavelength axis is a function of path length (therefore scatter). AREA was thus used to predict hardness as well.

The second derivatives were calculated by means of the segment-gap method. The segment is the range of data points averaged together and the gap is the distance between averages being subtracted. A first derivative is the difference between two averages separated by the specified gap. A first derivative with a six point gap is computed as average 1 minus average 7, average 2 minus average 8, and so on. A second derivative can be computed by applying the first derivative procedure to the first derivative data.

The second-order derivative spectra were calculated by smoothing the data over four data points and calculating the difference over a gap of six averages. The difference spectra were calculated over the wavelength range of 1100 - 2500 nm and 850 - 1050 nm in

reflectance and transmittance, respectively. The AREA between the second derivative curve and the wavelength axis was calculated by summing the absolute values of all the data points for each spectrum (sample).

(a) Method of calibration

The calibration equation was derived by performing a simple linear regression of the AREA values against the wheat hardness results.

(b) Method of validation

The equation was validated by substituting the AREA values of the prediction set in the calibration equation and predicting AJS and PSI wheat hardness.

Calibration and validation results were expressed as standard error of calibration (SEC), correlation coefficient (r) and standard error of performance (SEP). The algorithms are shown in equations 2.5, 2.6 & 2.7, respectively.

$$SEC = \sqrt{\frac{\sum_{i=1}^{n} (y_i - \hat{y}_i)^2}{n-2}} \qquad \text{..... 2.5}$$

$$r = \sqrt{\frac{\sum_{i=1}^{n} (\hat{y}_i - \bar{y}_i)^2}{\sum_{i=1}^{n} (y_i - \bar{y}_i)^2}} \qquad \text{..... 2.6}$$

$$SEP = \sqrt{\frac{\sum_{i=1}^{n} (y_i - \hat{y}_i)^2}{n}} \qquad \text{..... 2.7}$$

Where y is the actual value, $\hat{y}$ the predicted, y the mean and n the number of samples.

(iv) NIR calibration of damaged starch in flour

Calibration equations were derived to predict damaged starch of flour of UK home-grown wheat varieties from different localities (Table 2, Appendix 1) by AACC NIR wheat hardness, 1st PC scores and the area under the second derivative curve as derived from the raw NIR data, respectively. Damaged starch measurements by NIR have been reported by Osborne & Douglas (1981) and more recently by Morgan & Williams (1995). A revised Farrand (1964) method, with the malt flour replaced by fungal α-amylase, was used as the reference method. The sample set was split into a calibration set and prediction set and the calibrations performed as described in section 2.2.3(i), (ii) & (iii). The results were expressed in terms of the SEC, r and SEP as shown in equations 2.5, 2,6 & 2.7.

2.2.4 The dependence of NIR wheat hardness measurements on chemical composition and scatter

Canonical correlation analysis (CCA) assesses linear combinations of the wavelengths of two variables such that these combinations are highly correlated. However, because of the considerable intercorrelations across the wavelengths of the NIR spectra the method was adapted by Devaux *et al.* (1993) to overcome these problems.

In this study CCA was applied to the 104 samples as described in section 2.2.1. Only

reflectance spectra for ground and whole wheat grain were analysed. The problem of intercorrelations between wavelengths were overcome by applying principal component analysis to the two sets of data. The frequencies highly correlated were now condensed in the same PC. Canonical correlation analysis was performed by replacing the spectral data with the principal components.

The principal components were derived as described in section 2.2.3(iii) and correlation coefficients obtained between the first 10 principal components and the hardness measurements (AJS, PSI and AACC NIR wheat hardness). Similarity maps (scatter plots of two chosen principal components) were plotted between the principal components correlating the highest with hardness measurements in each case. These plots indicate the ability of the spectral data to measure hardness. The principal component loadings were plotted to investigate the spectral information regarding chemical composition.

The different steps of CCA applied to the two spectral data sets were as follows:

- The principal components were derived from the two data sets .
- The canonical variates (CV) were assessed and interpreted.

  The first canonical variates of the two data sets, respectively, are linear combinations of the two variables. These two canonical variates have the highest correlation coefficient that could be found for the principal components of the two variables or data sets. The next canonical variates are assessed in a similar way so that they are orthogonal with the previous ones. Correlation coefficients of the linear combinations point out the principal components which is the most important in the assessment of the linear combinations.
- The CV similarity maps and CV plots were interpreted. Canonical variates similarity maps will show the distribution of the samples for the two spectral data sets.

2.2.5 The effect of light scattering on whole wheat grain

(i) NIR spectroscopy measurements

The samples used were samples 1-20 in Table 1, Appendix 1. Three sets of spectra of each of the 20 samples of wheat were recorded using the NIRSystems Model 6500 spectrophotometer. The three sets consist of ground grain spectra recorded in reflectance mode and whole grain spectra recorded in reflectance and transmittance mode, respectively. A fourth set of spectra on the same set of 20 samples was recorded in transmittance mode using the Infratec Food and Feed Analyzer Model 1225 spectrophotometer. Spectra were recorded as log 1/R or log 1/T, respectively, as described in section 2.2.2(ii)

(ii) Hardness measurements

The ground samples were obtained by passing the whole grain wheat through the Model 3100 hammer mill, fitted with a 1 mm screen. Wheat hardness was determined as the percentage of ground wheat (10 g) passing through a 75μm air jet sieve in 90 seconds as described in section 2.2.1(i).

(iii) Data treatment and analysis

Multiplicative scatter correction (MSC) rotates each spectrum so that it fits as closely as possible to the mean spectrum. This is achieved, as summarized previously for the spectrum of the ith sample, by fitting the equation 2.2 i.e.

$$y_{iw} = a_i + b_i m_w \qquad w = 1,\ldots,p \qquad \ldots\ldots\ldots\ldots \quad 2.2$$

where y_{iw} is the log 1/R value for the i^{th} sample at the w^{th} of p wavelengths and m_w is the mean log 1/R value at wavelength w for all samples in the calibration set. The fitted constants a_i and b_i are then used to compute the corrected spectrum according to equation

1.15 i.e.

$$y_{iw}^{c} = (y_{iw} - a_i)/b_i \qquad w = 1,.....,p \qquad \text{..... 1.15}$$

The spectra of all four data sets were corrected according to this method to investigate the multiplicative effect of scatter in each case (Osborne *et al.*, 1993).

Each set of spectra was normalised by subtracting the spectrum having the lowest overall log 1/R or log 1/T values. Regressions of log 1/R or log 1/T versus Air Jet Sieve data were carried out for different wavelengths and for different absorbance values as described by Norris & Williams (1984).

2.2.6 The effect of protein content and growing season on the apparent hardness of two wheat varieties

Two home-grown wheat varieties Riband (soft) and Mercia (hard) (Table 3, Appendix 1) at two protein contents and from two growing seasons (1991 and 1992) were analysed as described by Brown *et al.* (1993).

Therefore for each year:

Sample	Hardness	Protein
1	soft	low
2	soft	high
3	hard	low
4	hard	high

Three spectra of each sample were recorded in both reflectance and transmittance modes, as described in section 2.2.2(ii). These samples were analysed in a random order for each of the two seasons. The replicate spectra were averaged, resulting in four spectra for each season. Using the ISI software the data were reduced to the 1st and 2nd principal components. The interaction between AACC hardness scores, wheat protein content and

growing season was investigated as well as the effect of the protein content and growing season on the first principal component in the case of ground samples and the first two principal components in the case of the whole grain samples.

2.2.7 Relationship between NIR measurements and physical property measurements

The eight samples as listed in Table 3, Appendix 1, being eight UK home-grown wheat samples were analysed. These samples comprised Mercia and Riband at two protein contents and from two growing seasons (1991 and 1992).

(i) NIR Measurements

Three spectra of each sample were recorded in both reflectance and transmittance modes, as described in section 2.2.5 and the data reduced to the 1st principal component.

(ii) Physical property measurements

In trying to explain the causes of variation in hardness, the consortium of researchers of the OPTIMILL LINK programme conducted studies to investigate the physical properties of different endosperm samples. They measured a physical property phenomenon labelled as Parameter A (labelled as such due to confidentiality restrictions - see Author's Declaration). A second phenomenon was measured labelled as Parameter B. It was shown that the soft wheat grain tended to have low parameter B values with a wide distribution, whereas hard wheat grains tended to have higher Parameter B values with a narrower distribution.

These physical property (PP) measurements could be used to predict milling performance of wheat, but the measurements are difficult and time consuming. Therefore the possibility of relating NIR measurements to the PP measurements either directly or indirectly was

investigated, the benefit of NIR being the speed of the measurements, possible on-line measurements in the flour mill and the fact that most mills already have NIR instruments.

Data sets derived from Parameter A and Parameter B, as measured on the eight samples as described above, were kindly supplied by the OPTIMILL LINK Programme consortium. Correlations were attempted between NIR measurements in terms of the 1st PC scores and these two sets of data.

2.2.8 Single kernel analysis

Twenty single kernels of each of the 42 samples (Tables 1 & 4, Appendix 1) were analysed using the Infratec Food and Feed Analyzer Model 1225 spectrophotometer in transmittance mode as well as the NIRSystems Model 6500 spectrophotometer in reflectance mode. Kernels were orientated as such that the crease was facing away from the incident energy at a 90° angle and analysed only once. Spectra were collected from 850 - 1050 nm. The commercially supplied, single kernel sample holder, which was used for transmittance measurements can scan up to 23 single kernels consecutively. There is no commercially available single kernel cell for the NIRSystems Model 6500. In order to be able to analyse single kernels, butyl rubber were use to construct a single kernel holder that would fit into the standard cell for ground samples. An O-ring, of the right size to hold a single kernel was attached to the centre of the round piece of butyl rubber. The standard sample cell, without the quartz lens, was used to hold the butyl rubber. The results were analysed over the specified wavelength range in order to compare the diffuse reflectance and diffuse transmittance measurements and to investigate the path the light beam follows in either case. The analyses were performed in terms of principal component analysis.

Chapter 3

Results

3.0 RESULTS

3.1 Wheat hardness measurements

The Air Jet Sieve (AJS) and Particle Size Index (PSI) results and AACC NIR wheat hardness scores, measured for all 104 wheat samples were as presented in Tables 3.1 to 3.4.

Table 3.1 Air Jet Sieve (AJS) and Particle Size Index (PSI) results (expressed as percentage throughs) and AACC NIR wheat hardness scores (AACC) as measured for each sample used to construct the AACC NIR wheat hardness calibration equation

Sample Number	Variety	AJS	PSI	AACC
1	Riband	48.7	71.3	24.0
2	Fresco	33.0	55.3	73.0
3	Mercia	36.9	57.4	74.3
4	Apollo	47.5	70.0	21.1
5	Hereward	34.9	55.4	76.6
6	Hunter	48.0	73.5	15.7
7	Mercia	36.1	56.9	76.4
8	Acier	35.2	53.1	68.2
9	Galahad	46.1	68.6	28.2
10	Admiral	46.4	70.2	22.9
11	Festival	38.3	59.3	75.7
12	Apollo	49.2	71.8	15.4
13	Admiral	45.7	67.2	32.8
14	Alexandria	34.8	54.8	76.6
15	Beaver	49.6	72.0	17.0
16	Wasp	41.4	62.0	47.9
17	Torfrida	33.6	56.2	65.8
18	Riband	46.8	71.8	32.4
19	Talon	37.0	61.5	53.3
20	CWRS[#]	35.3	58.5	85.7

[#] Canadian Western Red Spring (class)

Table 3.2 Air Jet Sieve (AJS) and Particle Size Index (PSI) results (expressed as percentage throughs) and AACC NIR wheat hardness scores (AACC) as measured for UK home-grown varieties from different localities

Sample Number	Variety	AJS	PSI	AACC
1	Cadenza	28.5	58.0	91.2
2	Hunter	38.6	66.3	38.7
3	Spark	35.2	57.3	68.8
4	Andante	43.9	66.6	29.7
5	Hereward	38.3	62.0	58.3
6	Flame	31.6	57.5	77.5
7	Hunter	39.0	68.5	36.3
8	Cadenza	28.0	56.4	87.6
9	Riband	42.9	71.5	21.4
10	Brigadier	33.0	58.2	54.9
11	Mercia	33.4	58.3	75.6
12	Andante	42.9	67.4	39.2
13	Flame	34.2	57.8	70.6
14	Prophet	35.2	59.5	76.4
15	Cadenza	31.8	55.5	79.0
16	Mercia	37.6	58.1	63.2
17	Genesis	37.2	59.4	49.0
18	Cadenza	31.6	53.0	70.7
19	Mercia	36.3	59.9	66.7
20	Spark	33.4	55.4	63.8
21	Spark	33.2	57.4	71.7
22	Rialto	34.5	58.6	61.7
23	Hunter	40.2	65.4	29.1
24	Flame	33.6	55.9	69.2
25	Riband	45.2	66.7	23.7
26	Prophet	34.4	58.3	71.7
27	Brigadier	30.6	57.1	70.6
28	Mercia	34.1	58.7	71.1
29	Riband	41.9	68.8	38.2
30	Hereward	36.8	60.6	71.0
31	Hereward	32.9	58.6	62.3
32	Rialto	34.1	57.2	62.1
33	Hunter	42.8	68.8	27.8
34	Andante	40.7	65.5	34.6
35	Riband	43.2	69.1	29.8
36	Prophet	34.6	58.7	61.3
37	Mercia	33.5	57.6	79.9
38	Flame	35.1	59.1	60.6
39	Cadenza	34.5	57.5	82.4
40	Genesis	34.9	60.2	59.7
41	Genesis	32.9	60.7	63.6
42	Hunter	38.7	68.4	31.6
43	Hereward	38.0	58.2	59.9
44	Brigadier	31.5	58.6	66.0
45	Rialto	33.1	58.3	67.3
46	Rialto	31.6	55.5	60.4
47	Riband	43.7	71.7	27.0
48	Genesis	34.7	59.2	63.5
49	Spark	35.4	58.7	73.7
50	Andante	41.4	67.5	35.1
51	Brigadier	32.5	59.2	52.2
52	Andante	41.9	68.6	28.7
53	Hereward	32.8	60.1	69.8
54	Brigadier	31.4	57.9	59.0

Table 3.3 Air Jet Sieve (AJS) and Particle Size Index (PSI) results (expressed as percentage throughs) and AACC NIR wheat hardness scores (AACC) as measured for Mercia and Riband at two different protein levels from two different harvests

Sample Number	Variety	AJS	PSI	AACC
1	Riband	43.5	72.7	25.9
2	Riband	42.7	71.7	33.5
3	Mercia	33.3	59.2	71.8
4	Mercia	32.7	59.2	79.5
5	Riband	44.5	73.6	23.4
6	Riband	44.3	72.7	19.9
7	Mercia	32.8	60.9	75.2
8	Mercia	32.2	60.0	62.5

Table 3.4. Air Jet Sieve (AJS) and Particle Size Index (PSI) results (expressed as percentage throughs) and AACC NIR wheat hardness scores (AACC) as measured for Canadian home-grown wheat varieties.

Sample Number	Variety	AJS	PSI	AACC
1	URBAN	31.6	58.3	89.4
2	CREW	47.8	73.2	31.6
3	DAWS	49.2	73.9	27.0
4	Len	31.5	57.7	81.3
5	Wheaton	31.5	54.5	89.9
6	Marshall	30.5	60.3	87.3
7	Perlo	32.5	58.3	73.8
8	Absolvent	37.3	60.8	76.3
9	Max	30.3	55.5	93.9
10	Frankenmuth	43.3	70.3	34.8
11	Vic 1985	19.7	45.7	133.0
12	Vic 1987	22.9	43.0	92.5
13	Augusta	46.4	74.0	26.8
14	HRS PC86	28.8	55.5	93.7
15	Fielder 85 HP	47.9	73.1	29.6
16	2 CPS CK	37.9	66.8	47.7
17	ICEWW	49.6	72.5	20.7
18	1CWAD	19.6	43.0	112.5
19	2CWAD	20.2	41.7	114.4
20	ARW	31.2	62.5	83.4
21	ARW	29.3	60.7	78.5
22	unknown	33.2	59.8	64.3

The correlations between AJS and PSI and AJS, PSI and AACC NIR wheat hardness scores are shown in Figures 3.1 & 3.2, respectively.

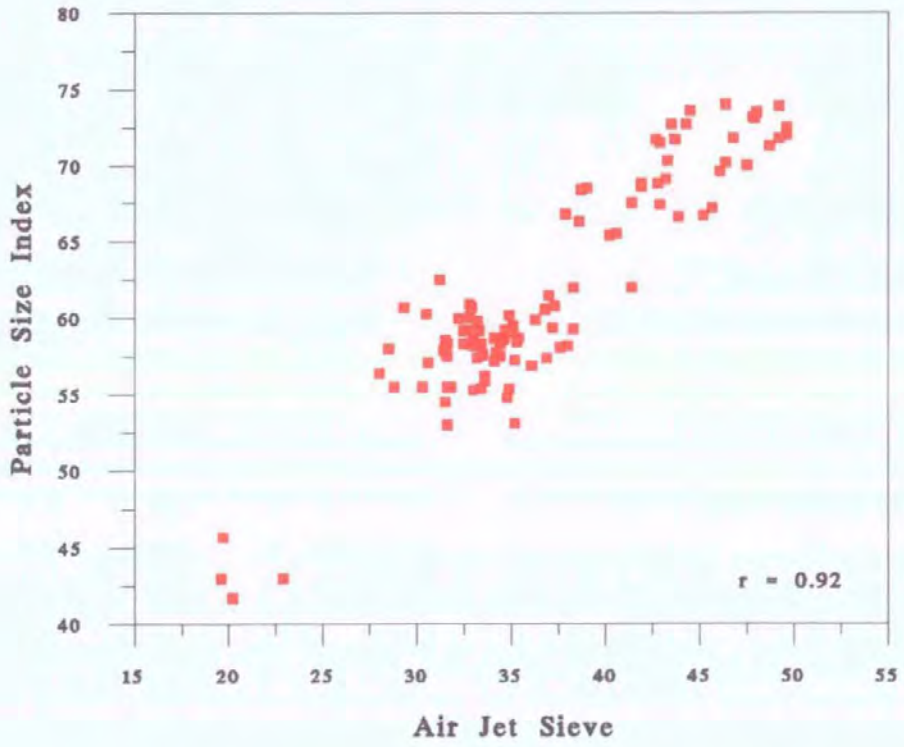

Figure 3.1 Correlation plot of Air Jet Sieve test results versus Particle Size Index test results

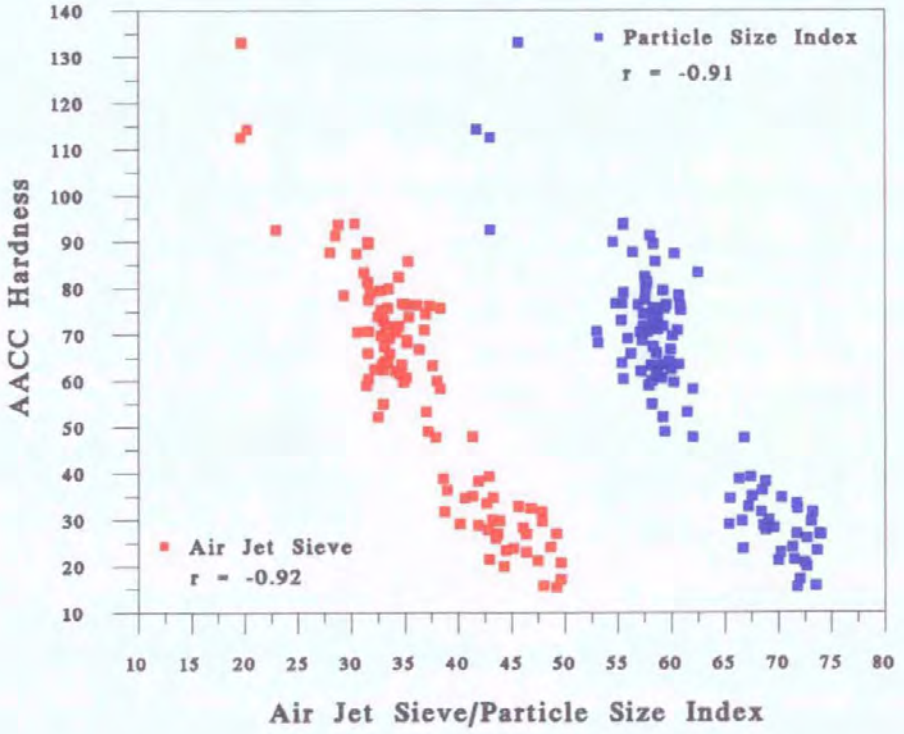

Figure 3.2 Correlation plots of Air Jet Sieve test results and Particle Size Index test results versus AACC NIR wheat hardness scores.

Table 3.5 summarises the AJS, PSI and the AACC NIR wheat hardness test results for all of the 104 samples.

Table 3.5 Summary of wheat hardness results as measured by Air Jet Sieve, Particle Size Index and AACC NIR wheat hardness methods, respectively

	AJS (% throughs)	**PSI** (% throughs)	**AACC** (scores)
n	104	104	104
Mean	36.76	61.61	58.38
Range	19.60 - 49.55	41.70 - 74.00	15.38 - 132.99
Standard deviation	6.59	7.04	24.81
Standard Error	0.65	0.69	2.43
Coefficient of variation	17.93	11.43	42.50
r	---	0.92	0.92

Tables 3.6 & 3.7 summarises similar comparative wheat hardness measurement results for the calibration set and validation set as used for the NIR wheat hardness calibrations.

Table 3.6 Summary of wheat hardness results, for the calibration set, as measured by Air Jet Sieve, Particle Size Index and AACC NIR wheat hardness methods, respectively

	AJS (% throughs)	**PSI** (% throughs)	**AACC** (scores)
n	63	63	63
Mean	36.57	61.44	58.76
Range	19.60 - 49.55	41.70 - 73.9	15.38 - 132.99
Standard deviation	6.86	7.05	25.55
Standard Error	0.86	0.89	3.22
Coefficient of variation	18.76	11.47	43.48

Table 3.7 Summary of wheat hardness results, for the validation set, as measured by Air Jet Sieve, Particle Size Index and AACC NIR wheat hardness methods, respectively

	AJS (% throughs)	**PSI** (% throughs)	**AACC** (scores)
n	41	41	41
Mean	37.05	61.86	57.80
Range	22.85 - 49.55	43.00 - 74.00	15.70 - 93.92
Standard deviation	6.22	7.12	23.92
Standard Error	0.97	1.11	3.74
Coefficient of variation	16.79	11.51	41.38

3.2 NIR spectroscopy measurements

3.2.1 Determination of accuracy and precision of the NIR spectrophotometer

Reflectance and transmittance noise spectra for the NIRSystems Model 6500 are displayed in Figures 3.3 & 3.5, respectively, as five replicates measured at the same time. Average reflectance and transmittance noise spectra of five replicates measured at the same time over a four month period are displayed in Figures 3.4 & 3.6, respectively.

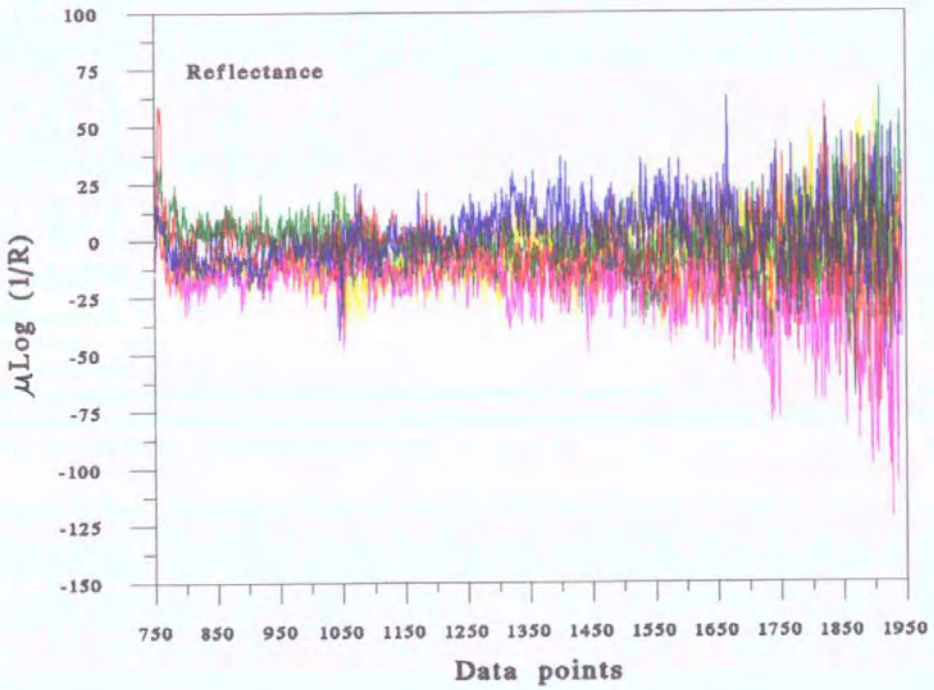

Figure 3.3 NIR reflectance noise spectra recorded at the same time

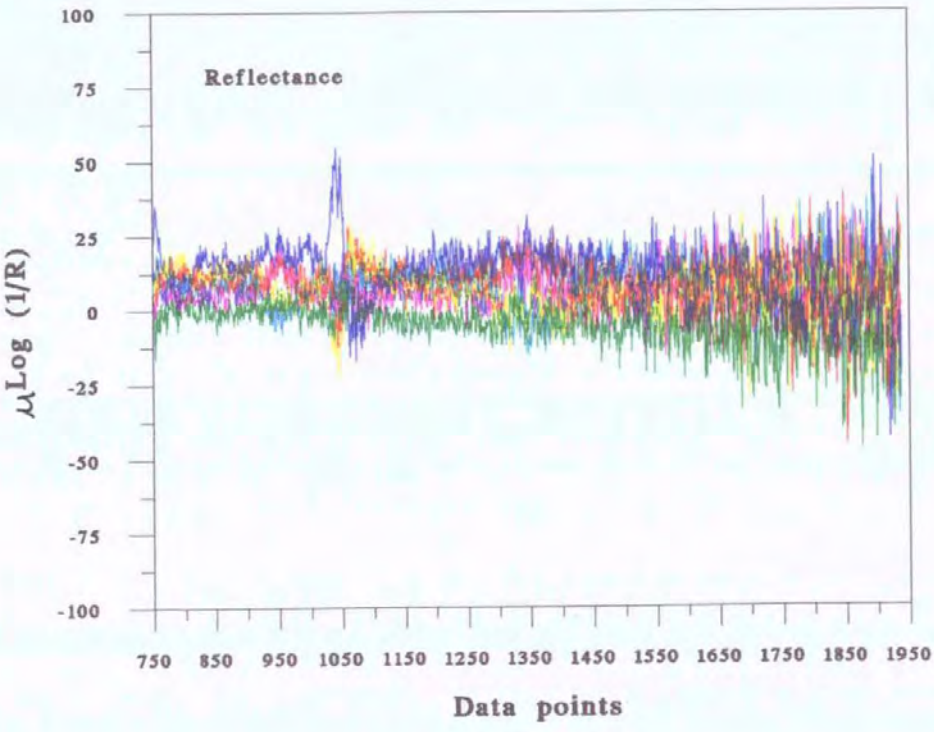

Figure 3.4 Averages of five NIR reflectance noise spectra recorded over a four month period

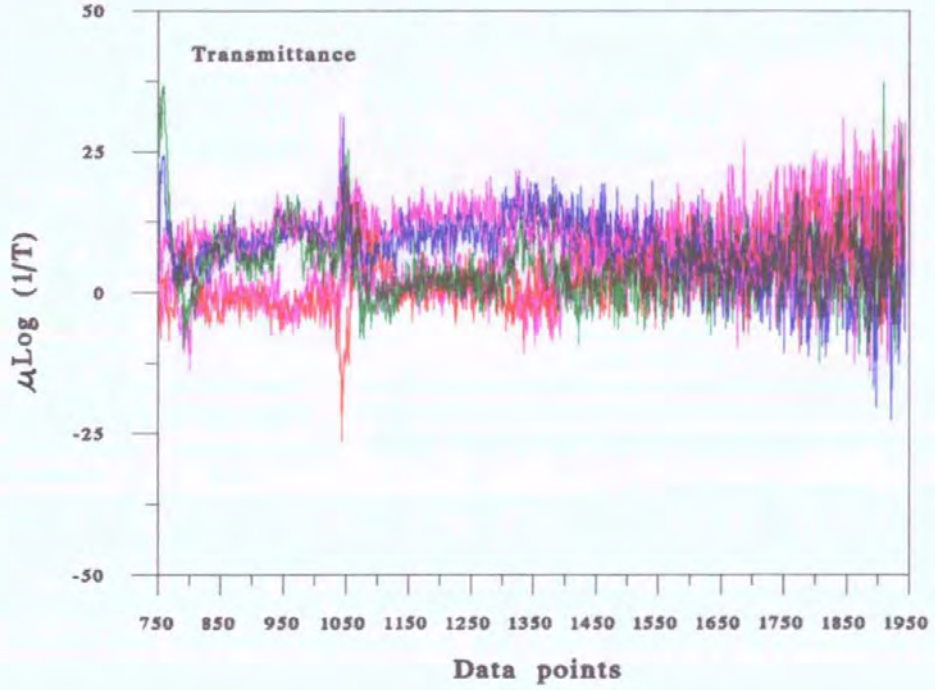

Figure 3.5 NIR transmittance noise spectra recorded at the same time

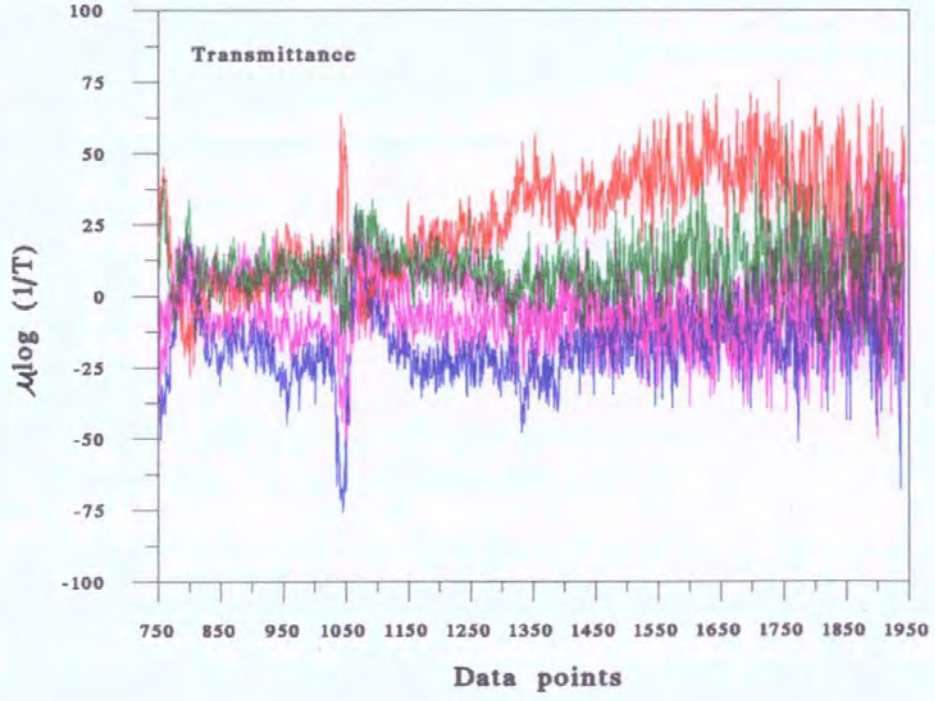

Figure 3.6 Averages of five NIR transmittance noise spectra recorded over a four month period

3.2.2 NIR measurements of wheat samples

The reflectance spectra of the ground wheat grain and the reflectance and transmittance spectra of the whole wheat grain samples are presented in Figures 3.7 to 3.26.

Figures 3.7 to 3.10 show the spectra of the 20 samples (Table 1, Appendix 1) as used for the AACC wheat hardness calibration.

Figures 3.11 to 3.14 show representative spectra of the 12 UK home-grown varieties from different localities (Table 2, Appendix 1).

Figures 3.15 to 3.22 show the spectra of the eight home-grown wheat samples (Riband and Mercia) (Table 3, Appendix 1) at two different protein levels from two different harvests.

Figures 3.23 to 3.26 show the spectra of the 21 Canadian home-grown wheat samples (Table 4, Appendix 1).

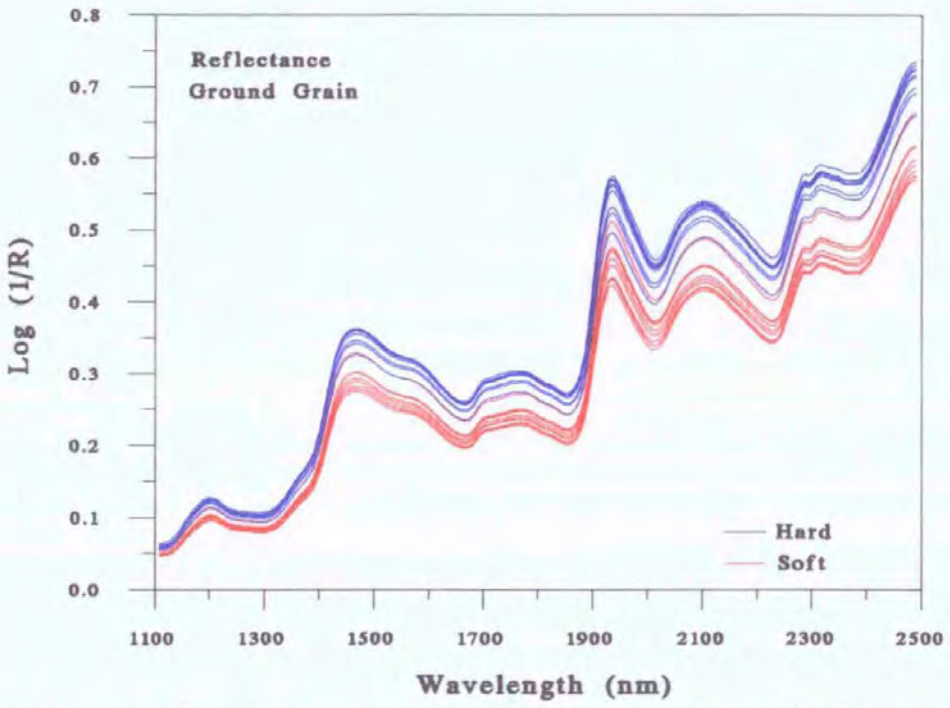

Figure 3.7 Ground grain, reflectance spectra of AACC wheat hardness calibration samples (Table 1, Appendix 1)

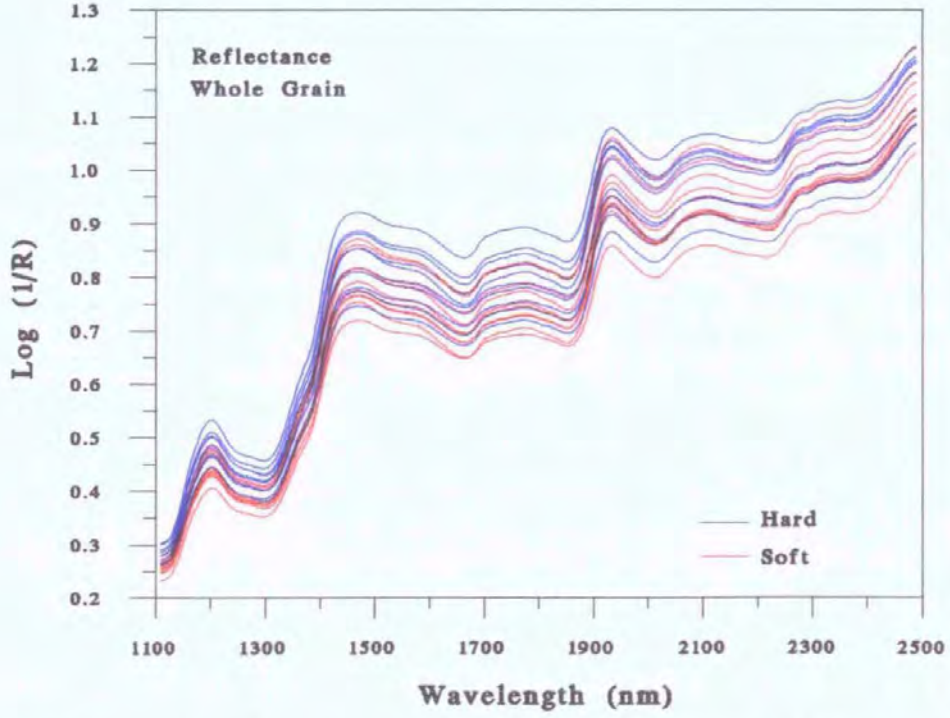

Figure 3.8 Whole grain, reflectance spectra of AACC wheat hardness calibration samples (Table 1, Appendix 1)

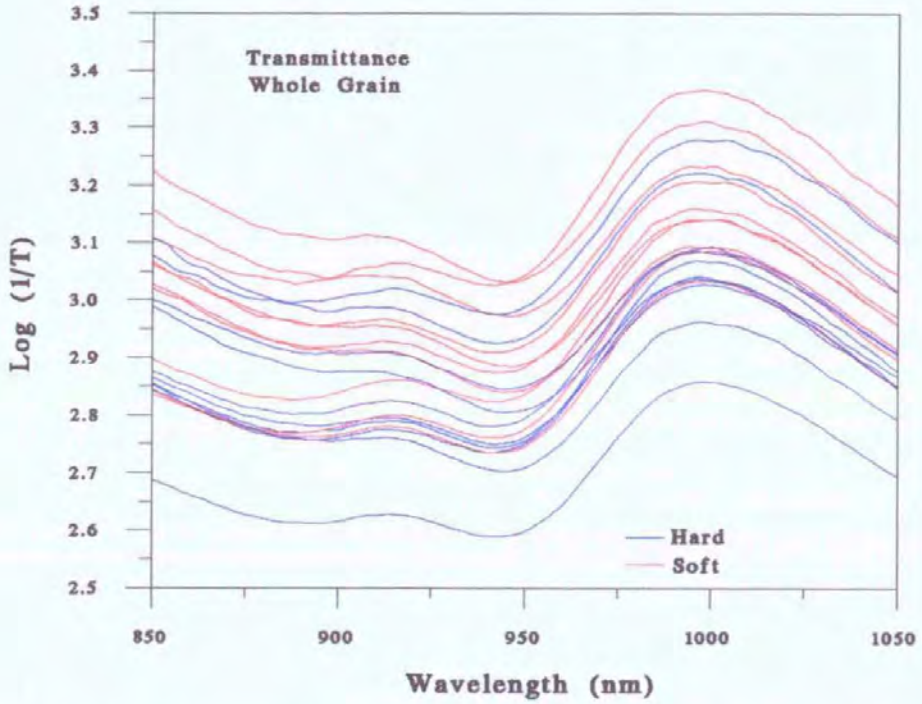

Figure 3.9 Whole grain, transmittance spectra of AACC wheat hardness calibration samples (Table 1, Appendix 1), recorded on NIRSystems Model 6500 spectrophotometer

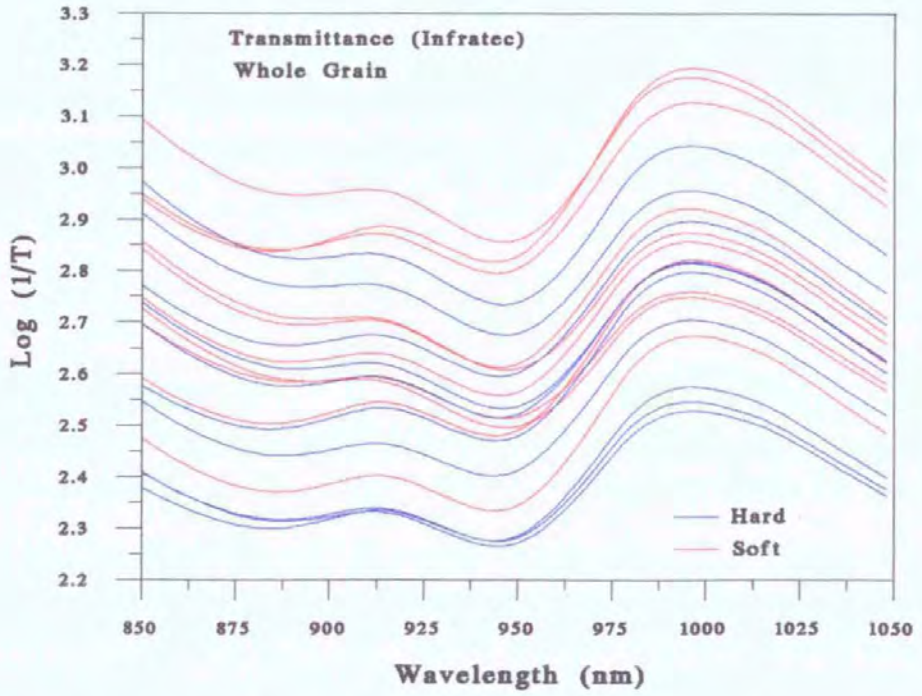

Figure 3.10 Whole grain, transmittance spectra of AACC wheat hardness calibration samples (Table 1, Appendix 1), recorded on Infratec Model 1225 spectrophotometer

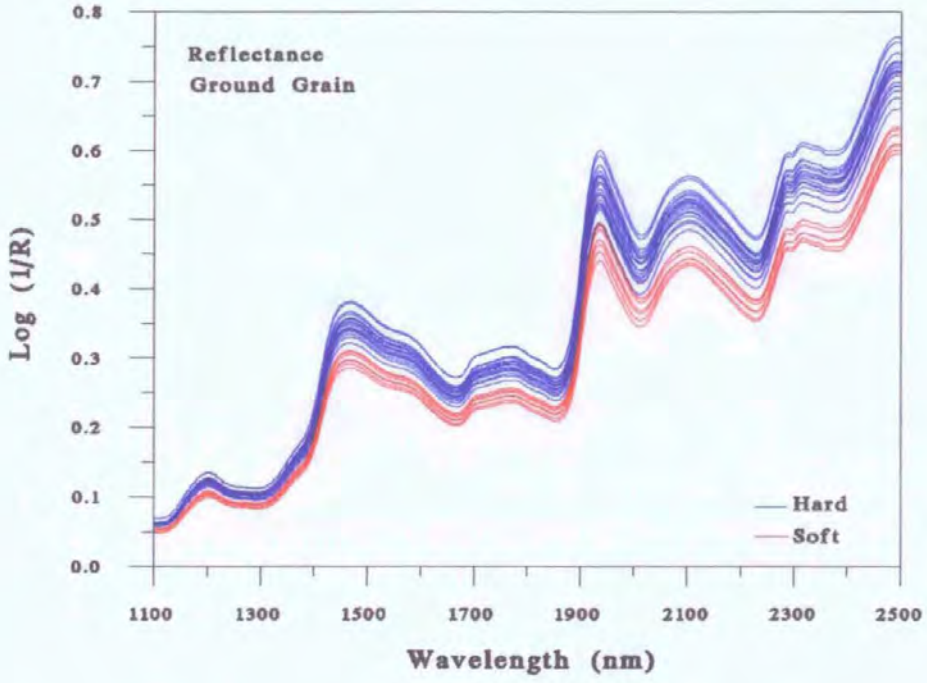

Figure 3.11 Representative ground grain, reflectance spectra of UK home-grown wheat varieties from different localities (Table 2, Appendix 1)

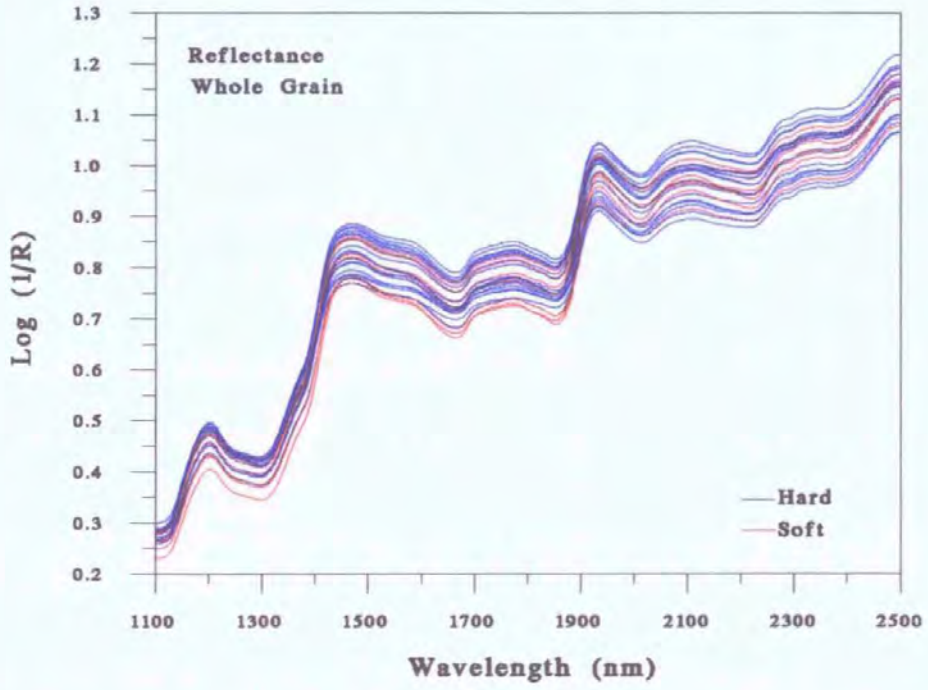

Figure 3.12 Representative whole grain, reflectance spectra of UK home-grown wheat varieties from different localities (Table 2, Appendix 1)

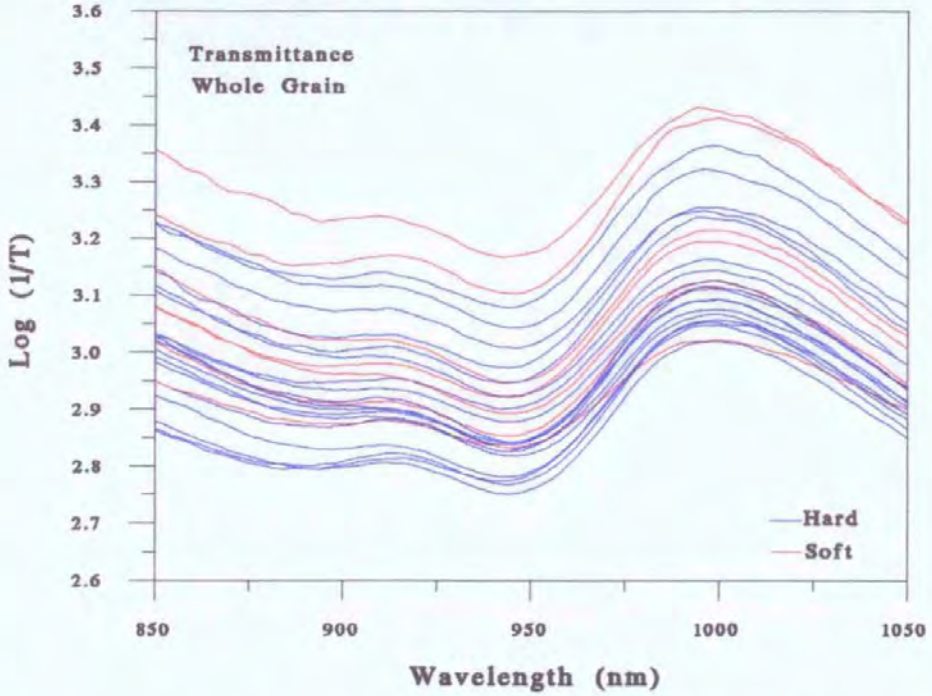

Figure 3.13 Representative whole grain, transmittance spectra of UK home-grown wheat varieties from different localities (Table 2, Appendix 1), recorded on NIRSystems Model 6500 spectrophotometer

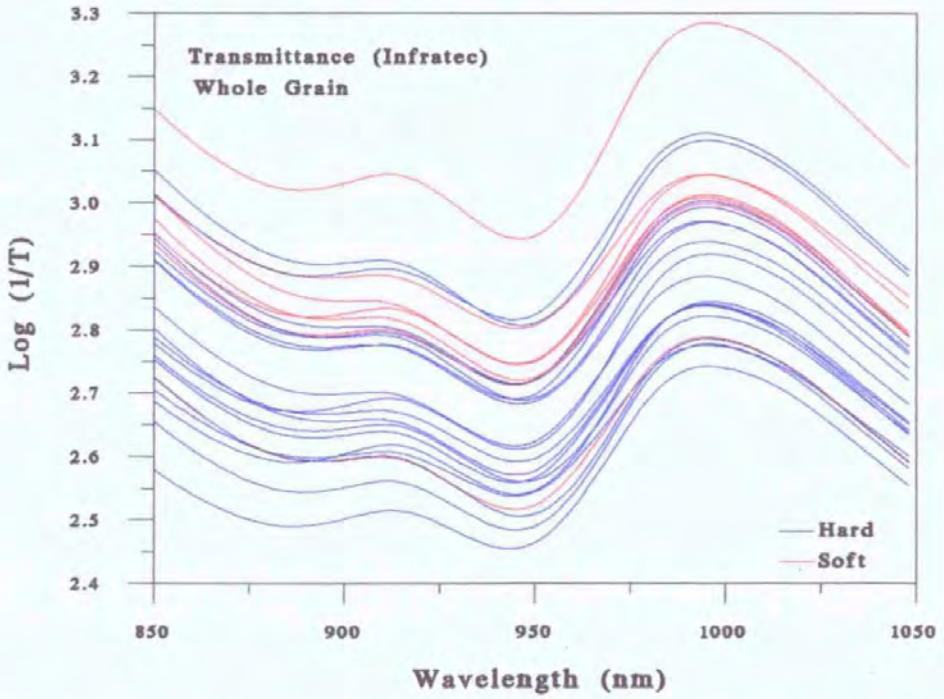

Figure 3.14 Representative whole grain, transmittance spectra of UK home-grown wheat varieties from different localities (Table 2, Appendix 1), recorded on Infratec Model 1225 spectrophotometer

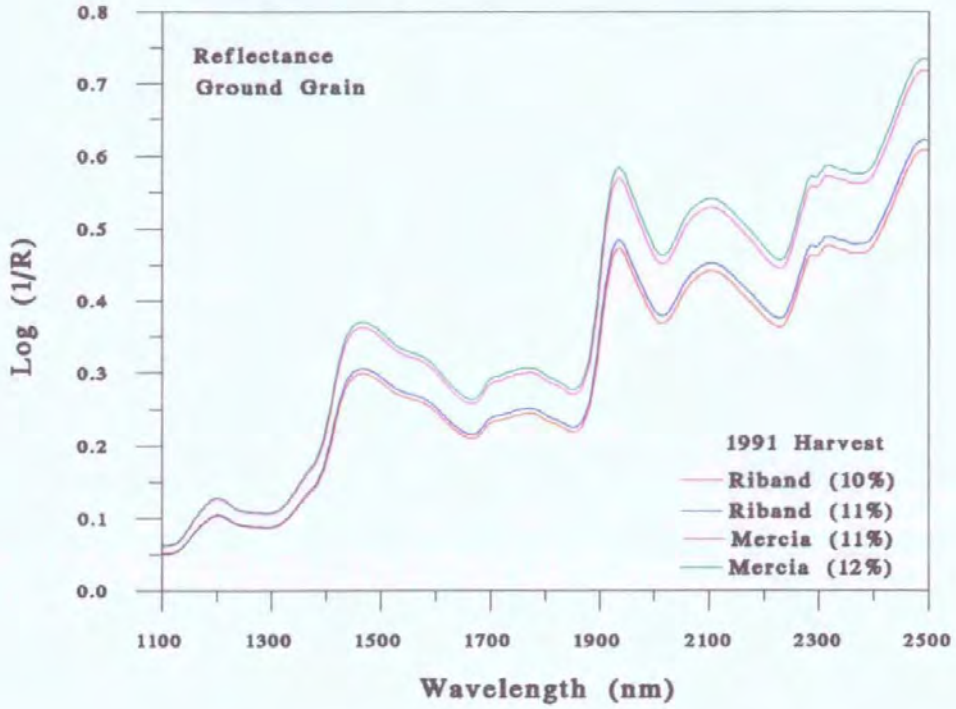

Figure 3.15 Ground grain, reflectance spectra of Riband and Mercia, 1991 harvest (Table 3, Appendix 1)

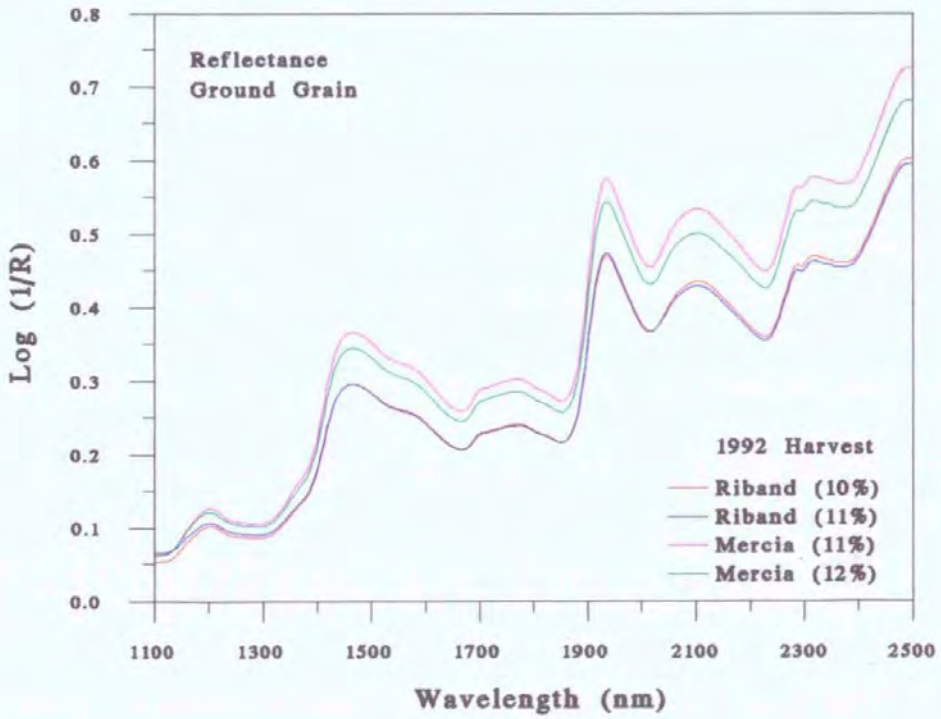

Figure 3.16 Ground grain, reflectance spectra of Riband and Mercia, 1992 harvest (Table 3, Appendix 1)

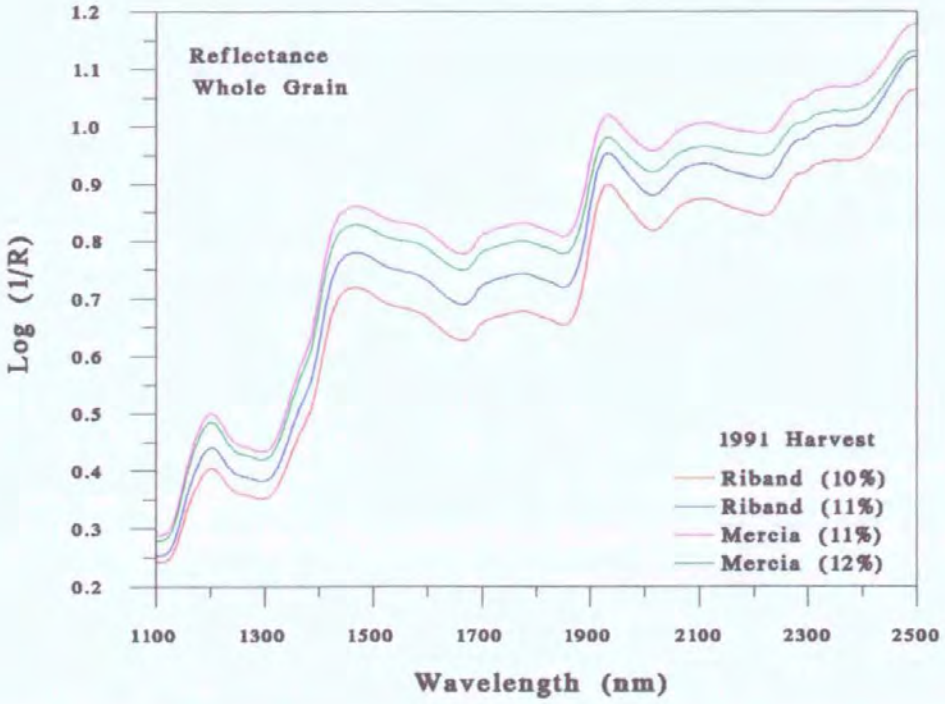

Figure 3.17 Whole grain, reflectance spectra of Riband and Mercia, 1991 harvest (Table 3, Appendix 1)

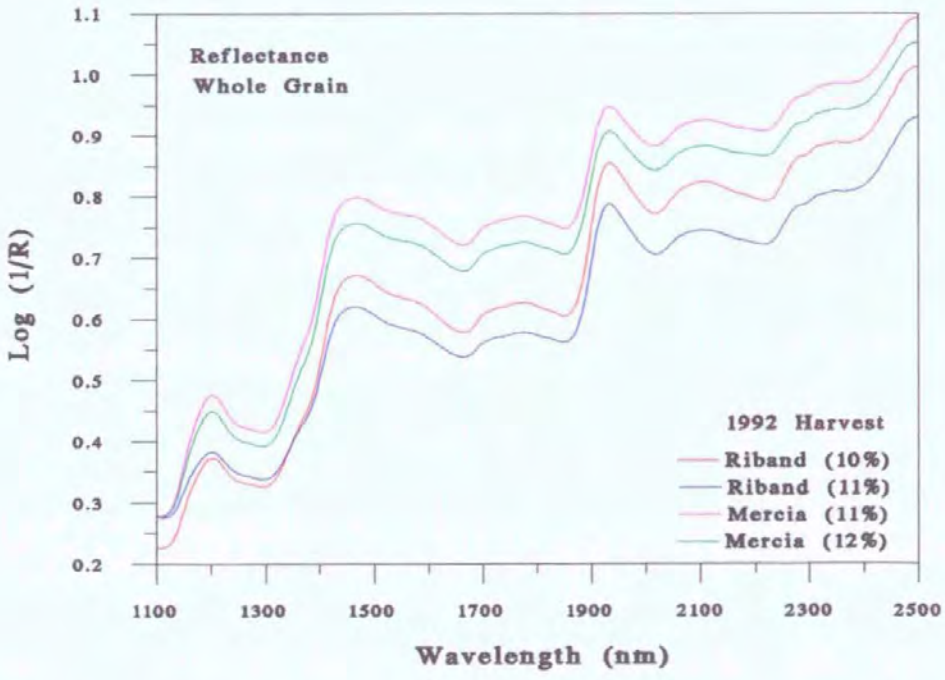

Figure 3.18 Whole grain, reflectance spectra of Riband and Mercia, 1992 harvest (Table 3, Appendix 1)

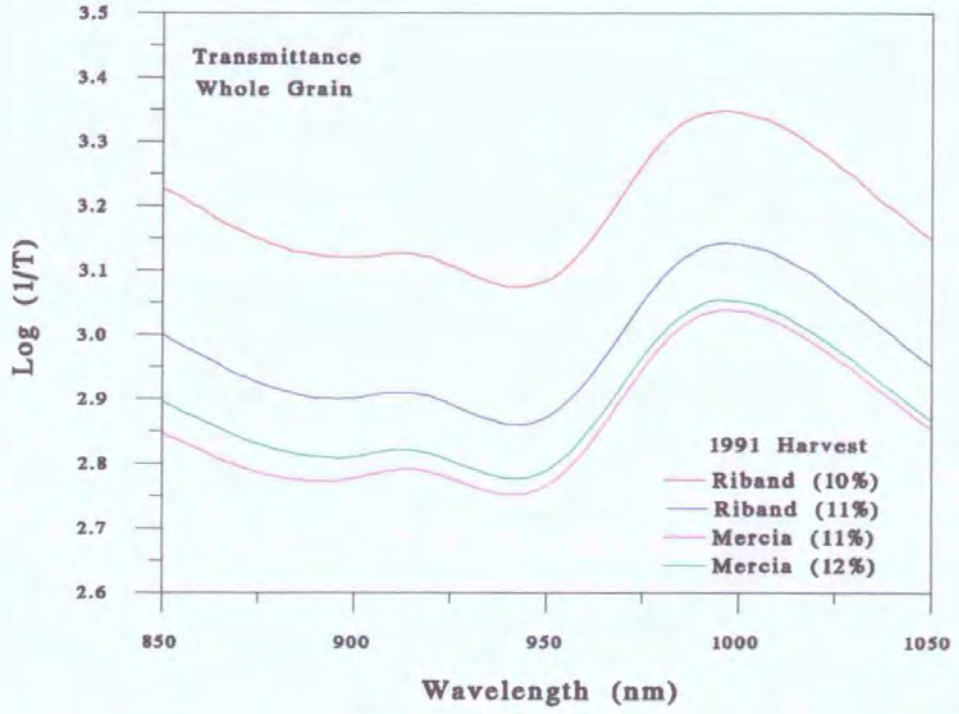

Figure 3.19 Whole grain, transmittance spectra of Riband and Mercia, 1991 harvest (Table 3, Appendix 1), recorded on NIRSystems Model 6500 spectrophotometer

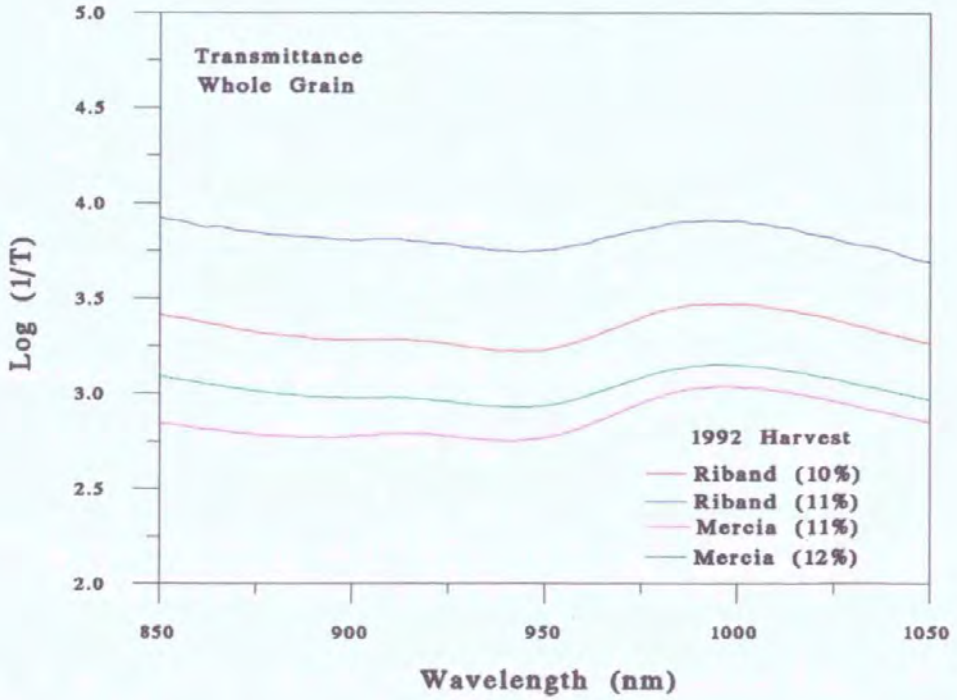

Figure 3.20 Whole grain, transmittance spectra of Riband and Mercia, 1992 harvest (Table 3, Appendix 1), recorded on NIRSystems Model 6500 spectrophotometer

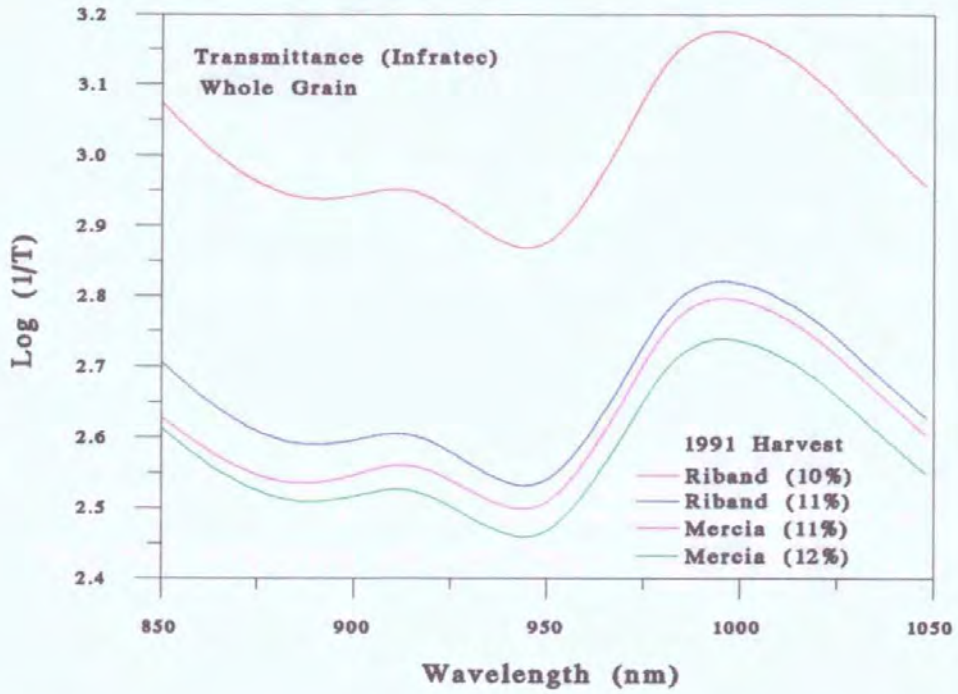

Figure 3.21 Whole grain, transmittance spectra of Riband and Mercia, 1991 harvest (Table 3, Appendix 1), recorded on Infratec Model 1225 spectrophotometer

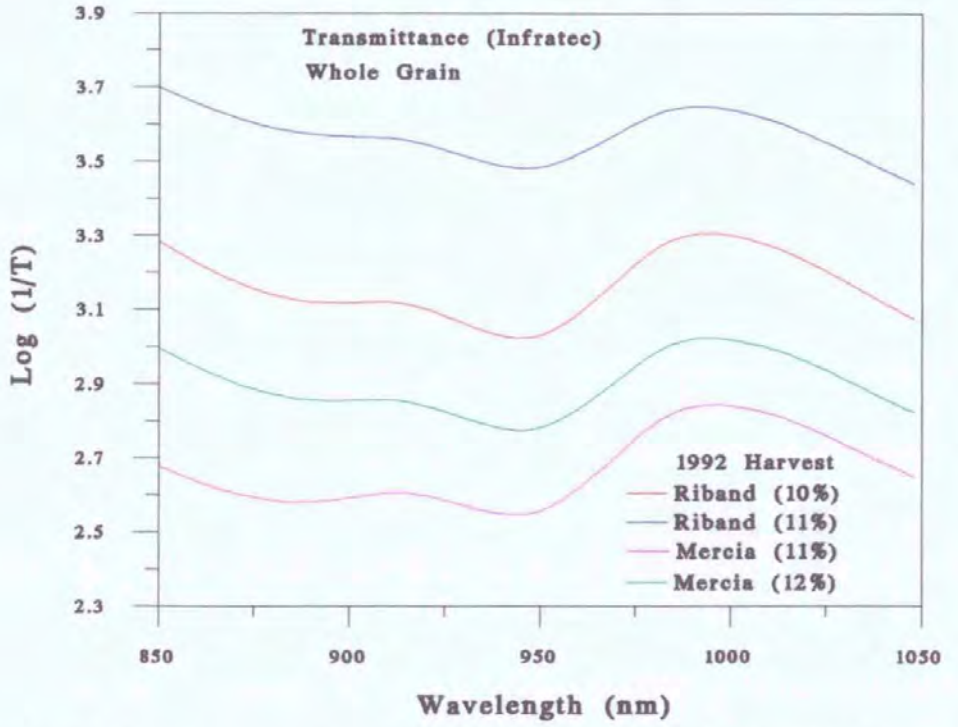

Figure 3.22 Whole grain, transmittance spectra of Riband and Mercia, 1992 harvest (Table 3, Appendix 1), recorded on Infratec Model 1225 spectrophotometer

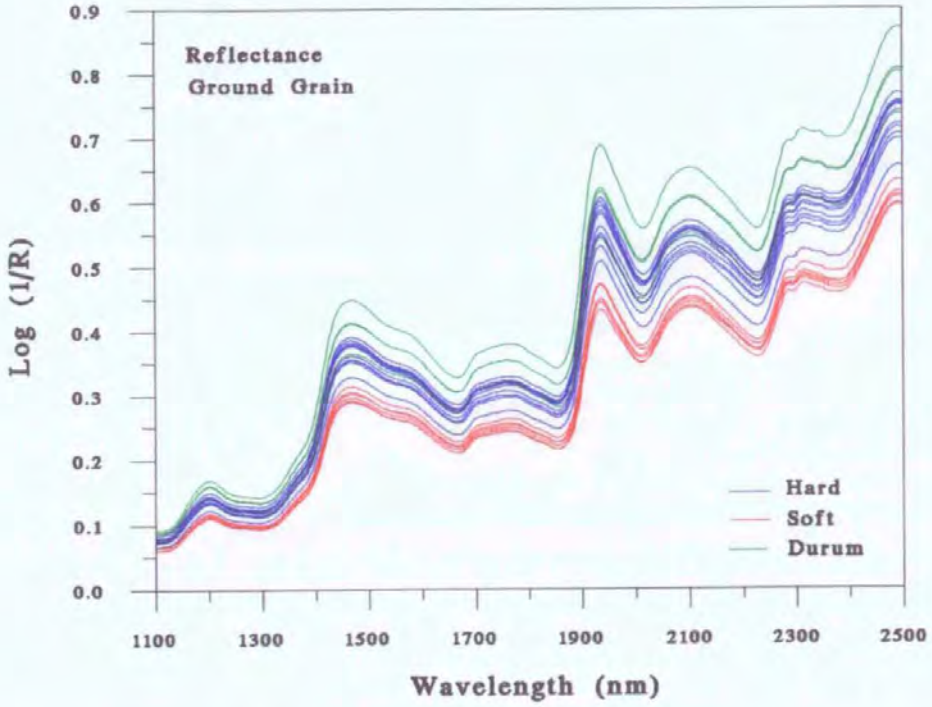

Figure 3.23 Ground grain, reflectance spectra of Canadian home-grown wheat samples (Table 4, Appendix 1)

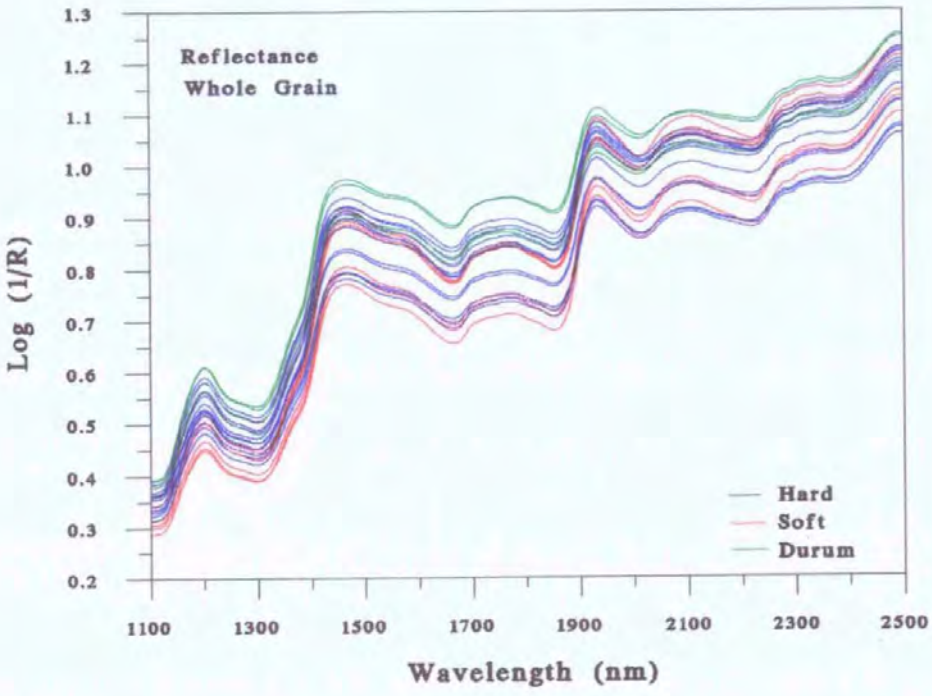

Figure 3.24 Whole grain, reflectance spectra of Canadian home-grown wheat samples (Table 4, Appendix 1)

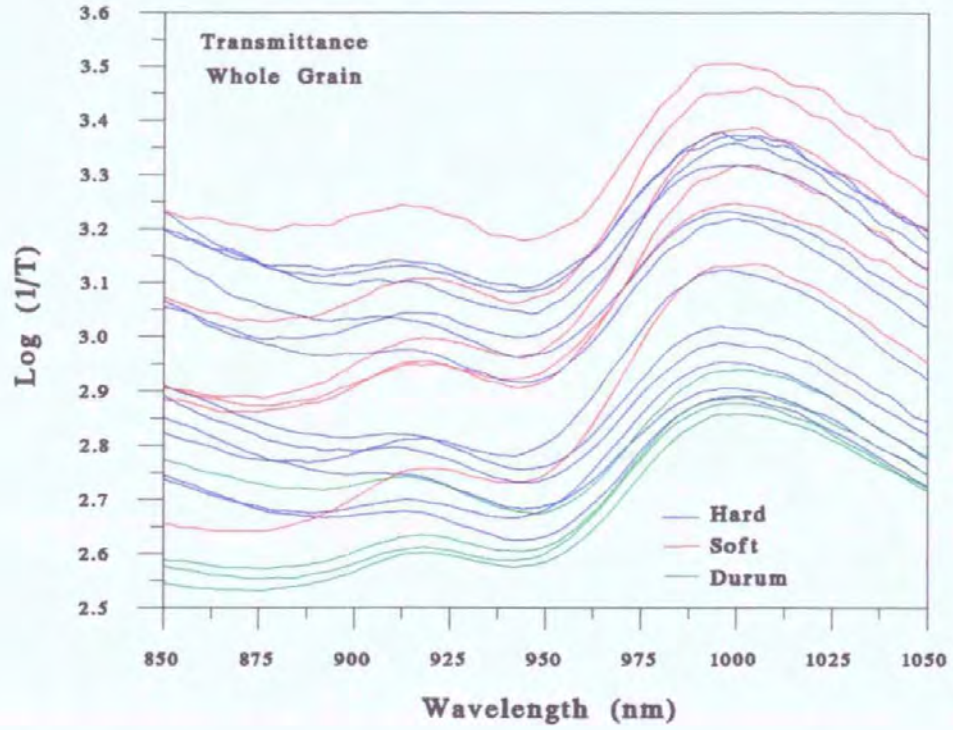

Figure 3.25 Whole grain, transmittance spectra of Canadian home-grown wheat samples (Table 4, Appendix 1), recorded on NIRSystems Model 6500 spectrophotometer

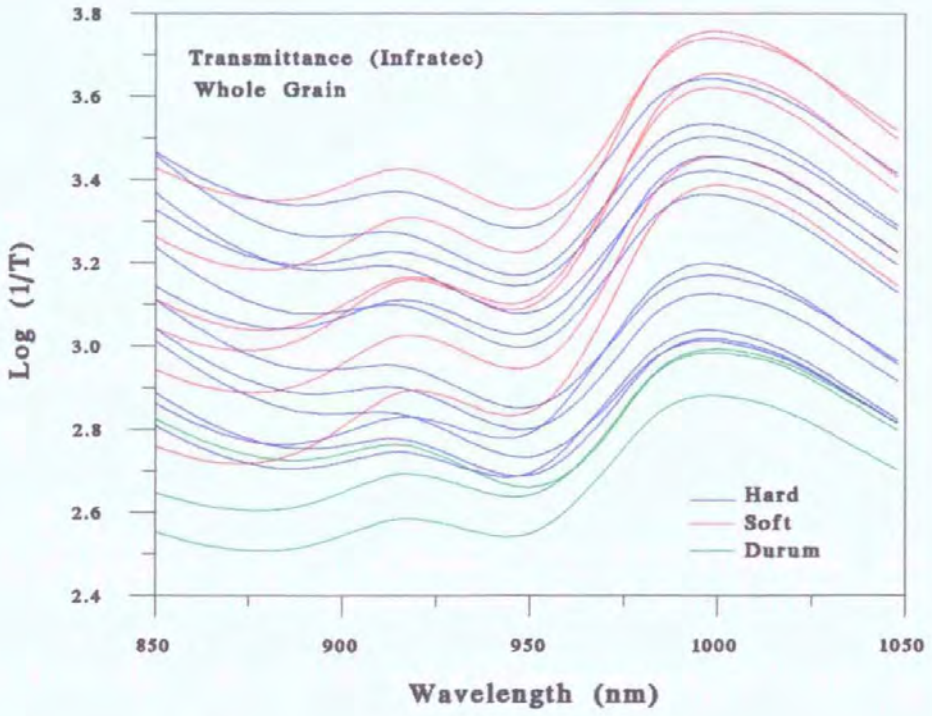

Figure 3.26 Whole grain, transmittance spectra of Canadian home-grown wheat samples (Table 4, Appendix 1), recorded on Infratec Model 1225 spectrophotometer

3.3 NIR spectroscopy calibrations

3.3.1 Empirical calibrations

NIR wheat hardness calibration and validation results obtained for the empirical NIR calibrations for ground grain reflectance, whole grain reflectance and whole grain transmittance are displayed in Tables 3.8, 3.9 & 3.10, respectively.

Table 3.8 NIR wheat hardness calibration and validation statistics for ground grain reflectance

Ground grain Reflectance	**ISI** No cross - validations	**ISI** 20 cross - validations	**NSAS** No cross - validations	**NSAS** 20 cross - validations	**UNSCR** No cross - validations	**UNSCR** 20 cross - validations
AJS	SEC = 1.37 r = 0.98 SEP = 1.45 9 terms	SEC = 1.26 r = 0.98 SEP = 1.55 11 terms	SEC = 1.37 r = 0.98 SEP = 1.47 9 terms	SEC =1.53 r = 0.98 SEP = 1.75 5 terms	SEC = 1.26 r = 0.98 SEP = 1.45 9 terms	SEC = 1.50 r = 0.98 SEP = 1.81 4 terms
PSI	SEC = 1.74 r = 0.97 SEP = 1.94 9 terms	SEC = 1.63 r = 0.97 SEP = 1.99 11 terms	SEC = 1.74 r = 0.97 SEP = 1.96 9 terms	SEC = 2.07 r = 0.96 SEP = 2.25 5 terms	SEC = 1.60 r = 0.97 SEP = 1.94 9 terms	SEC = 1.97 r = 0.96 SEP = 2.22 5 terms

ISI = Infrasoft International software
NSAS = NIRSystems Spectral Analysis software
UNSCR = UNSCRAMBLER software

Table 3.9 NIR wheat hardness calibration and validation statistics for whole grain reflectance

Whole grain Reflectance	**ISI** No cross - validations	**ISI** 20 cross - validations	**NSAS** No cross - validations	**NSAS** 20 cross - validations	**UNSCR** No cross - validations	**UNSCR** 20 cross - validations
AJS	SEC = 3.01 r = 0.90 SEP = 3.76 11 terms	SEC = 2.84 r = 0.91 SEP = 4.18 12 terms	SEC = 3.01 r = 0.92 SEP = 3.81 11 terms	SEC = 3.60 r = 0.87 SEP = 3.90 8 terms	SEC = 2.71 r = 0.92 SEP = 3.76 11 terms	SEC = 2.53 r = 0.93 SEP = 4.18 12 terms
PSI	SEC = 3.31 r = 0.88 SEP = 3.96 11 terms	SEC = 3.27 r = 0.88 SEP = 4.19 12 terms	SEC = 3.31 r = 0.90 SEP = 4.01 11 terms	SEC = 3.51 r = 0.89 SEP = 4.07 10 terms	SEC = 2.98 r = 0.91 SEP = 3.96 11 terms	SEC = 2.92 r = 0.91 SEP = 4.19 12 terms
AACC	SEC = 16.82 r = 0.75 SEP = 12.97 4 terms	SEC =17.24 r = 0.74 SEP = 13.24 2 terms	SEC = 16.82 r = 0.77 SEP = 13.10 4 terms	SEC = 17.24 r = 0.75 SEP = 13.40 2 terms	SEC = 16.14 r = 0.77 SEP = 12.97 4 terms	SEC = 16.83 r = 0.75 SEP = 13.24 2 terms

ISI = Infrasoft International software

NSAS = NIRSystems Spectral Analysis software

UNSCR = UNSCRAMBLER software

Table 3.10 NIR wheat hardness calibration and validation statistics for whole grain transmittance

Whole grain Transmittance	ISI No cross - validations	ISI 20 cross - validations	NSAS No cross - validations	NSAS 20 cross - validations	UNSCR No cross - validations	UNSCR 20 cross - validations
AJS	SEC = 3.85 r = 0.83 SEP = 5.06 6 terms	SEC = 5.31 r = 0.63 SEP = 5.90 3 terms	SEC = 3.85 r = 0.85 SEP = 5.12 6 terms	SEC = 5.81 r = 0.54 SEP = 5.84 1 term	SEC = 3.63 r = 0.85 SEP = 5.06 6 terms	SEC = 5.14 r = 0.66 SEP = 5.90 3 terms
PSI	SEC = 4.09 r = 0.81 SEP = 5.25 6 terms	SEC = 5.59 r = 0.61 SEP = 5.92 3 terms	SEC = 4.09 r = 0.83 SEP = 5.32 6 terms	SEC = 5.80 r = 0.58 SEP = 6.14 1 term	SEC = 3.86 r = 0.83 SEP = 5.25 6 terms	SEC = 5.41 r = 0.63 SEP = 5.92 3 terms
AACC	SEC = 14.50 r = 0.82 SEP = 20.26 6 terms	SEC = 20.18 r = 0.62 SEP = 22.05 3 terms	SEC = 14.50 r = 0.84 SEP = 20.5 6 terms	SEC = 21.01 r = 0.58 SEP = 21.40 1 term	SEC = 13.67 r = 0.84 SEP = 20.26 6 terms	SEC = 19.52 r = 0.64 SEP = 22.05 3 terms

ISI = Infrasoft International software
NSAS = NIRSystems Spectral Analysis software
UNSCR = UNSCRAMBLER software

The RPD statistics calculated for the equations with the lowest SEP as well as the RPD statistics reported by Williams & Sobering (1993) are listed in Table 3.11. In Table 3.11 is also included the RPD statistics for whole grain transmittance using the Infratec Food and Feed Analyzer Model 1225.

Table 3.11 RPD statistics for NIR wheat hardness empirical calibrations to standardise the SEP

	Ground grain reflectance		Whole grain reflectance		Whole grain transmittance (NIRSystems)		Whole grain transmittance (Infratec)	
AJS	4.29	--	1.65	--	1.23	--	1.52	--
PSI	3.67	--	1.80	3.32[#]	1.36	--	1.62	3.29[#]
AACC	--	--	1.84	--	1.18	--	1.60	--

[#] RPD statistics reported by Williams & Sobering (1993)

Tables 3.12, 3.13 & 3.14 illustrate the different ways in which the ISI, NSAS and UNSCRAMBLER software packages summarise the validation statistics, respectively.

Table 3.12 Statistical summary for prediction of AJS hardness using ISI software for ground grain reflectance (9 term equation)

	pair 1	
	lab AJS	nir AJS
SEP	1.45	
Means	37.05	36.60
BIAS	0.45	
BIAS Limit	0.82	
SEP(C)	1.39	
SEP(C) Limit	1.79	
Stand Devs	6.22	5.92
Slope	1.02	
RSQ	0.95	
Average H		0.95
N	41	

Table 3.13 Statistical summary for prediction of AJS hardness using NSAS software for ground grain reflectance (9 term equation)

STATISTICAL SUMMARY

Bias = -0.452
Std. Dev. of Differences = 1.39 Std. Error of Bias = 0.219
Root Mean Square (RMS) = 1.47

** Information for Slope and Intercept Corrections **

Slope Adjustment = 1.024 Std. Error of Slope = 0.0352
Intercept Adjustment = -0.423 Std Error of Performance = 1.39
Simple correlation = 0.975

** Results Achievable by Eliminating Special Causes **

Achievable Std. Error of Prediction = 1.41
Prediction Stability Coefficient = 0.959

Table 3.14 Statistical summary for prediction of AJS hardness using UNSCRAMBLER software for ground grain reflectance (9 term equation)

RMSEP	:	1.45
Bias	:	0.45
SEP	:	1.39
Slope	:	1.02
Offset	:	0.42
Corr.	:	0.98

Figures 3.27 to 3.34 illustrate the empirical calibration results (calibration equation selected based on lowest SEP) in Tables 3.8, 3.9 & 3.10 as bar graphs.

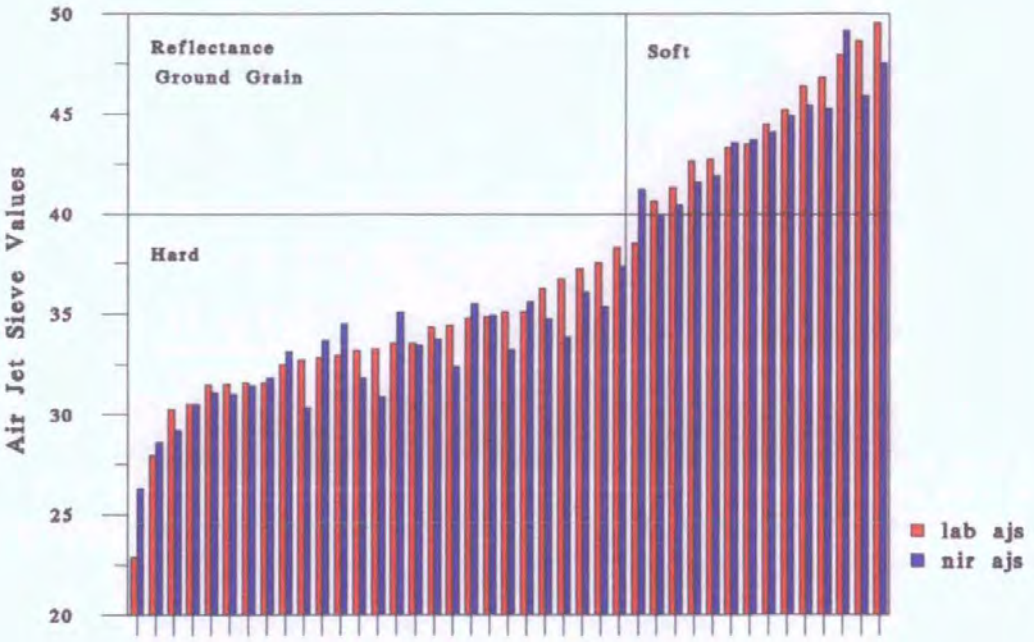

Figure 3.27 Bar graph illustrating separation of hard and soft wheats using empirical PLS calibrations (soft > 40) for ground grain reflectance and AJS as reference method

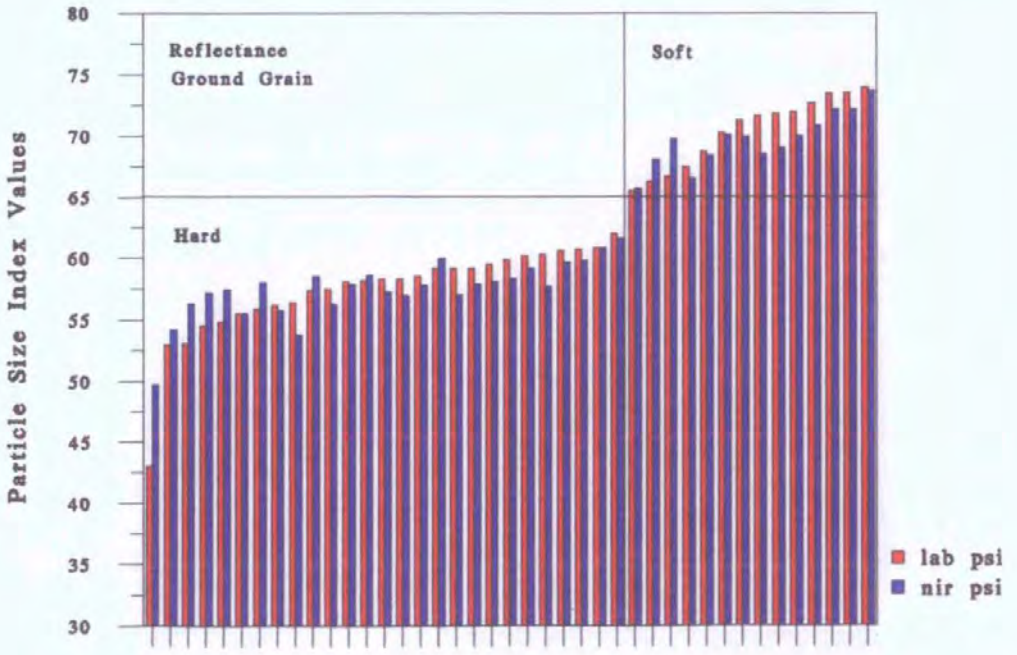

Figure 3.28 Bar graph illustrating separation of hard and soft wheats using empirical PLS calibrations (soft > 65) for ground grain reflectance and PSI as reference method

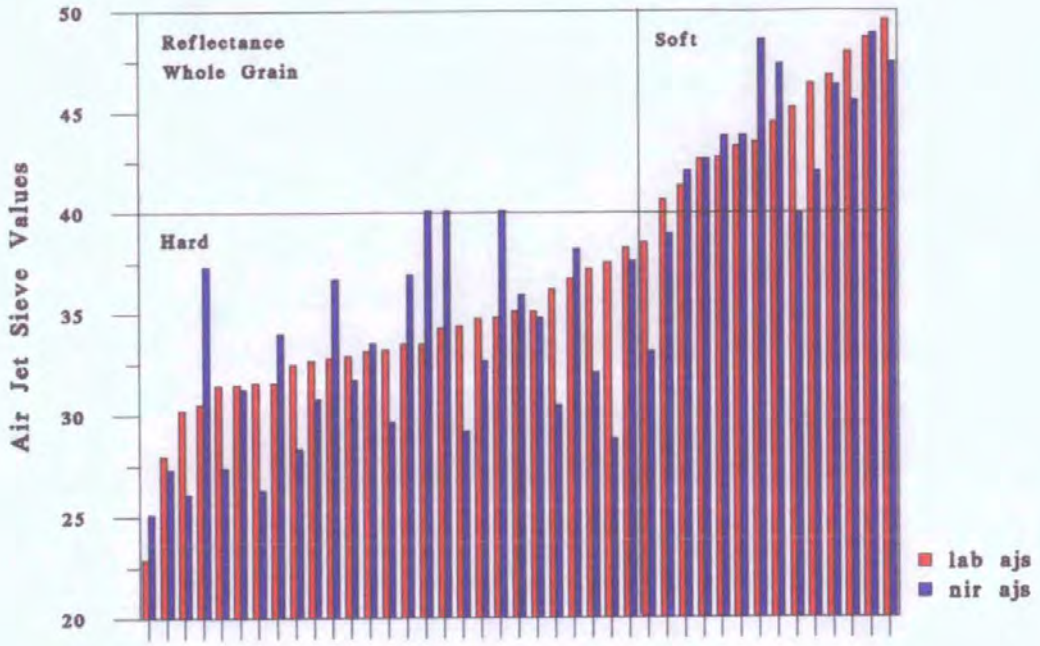

Figure 3.29 Bar graph illustrating separation of hard and soft wheats using empirical PLS calibrations (soft > 40) for whole grain reflectance and AJS as reference method

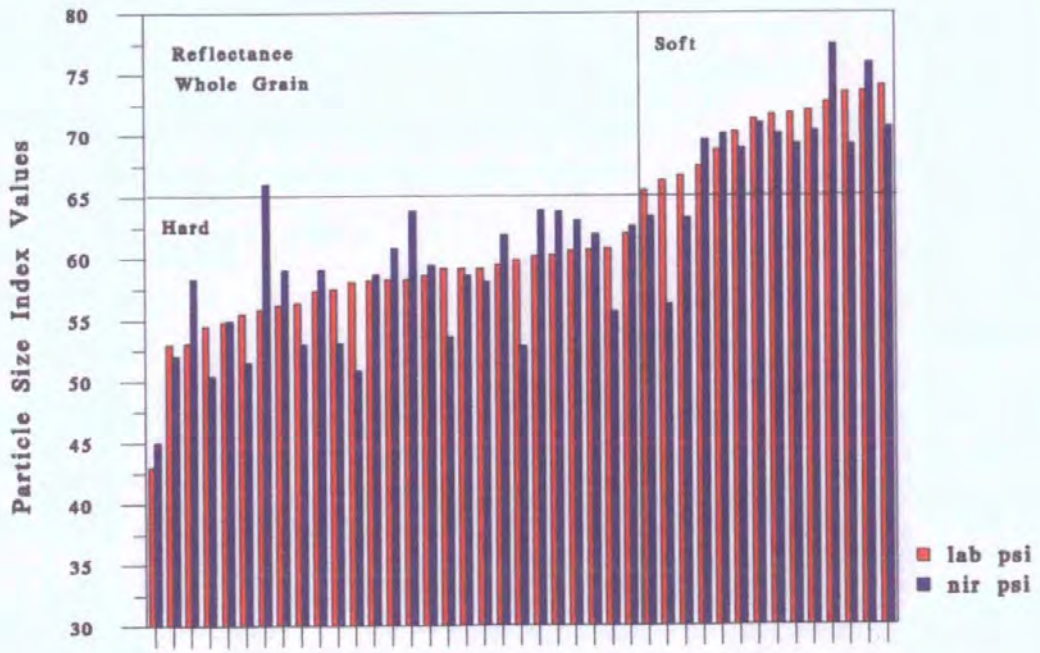

Figure 3.30 Bar graph illustrating separation of hard and soft wheats using empirical PLS calibrations (soft > 65) for whole grain reflectance and PSI as reference method

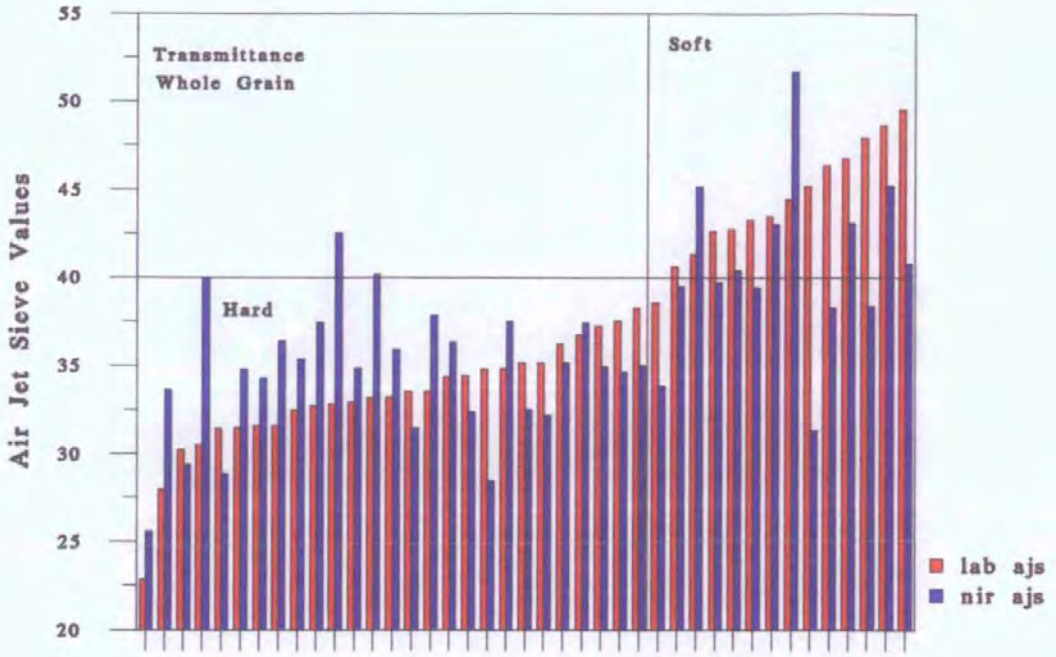

Figure 3.31 Bar graph illustrating separation of hard and soft wheats using empirical PLS calibrations (soft > 40) for whole grain transmittance and AJS as reference method

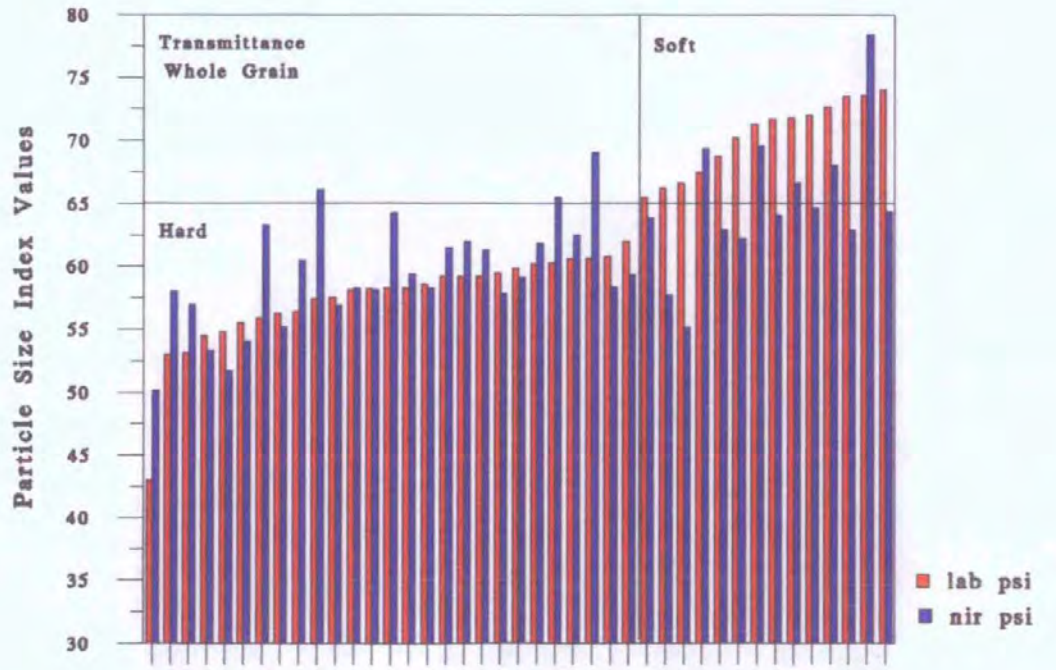

Figure 3.32 Bar graph illustrating separation of hard and soft wheats using empirical PLS calibrations (soft > 65) for whole grain transmittance and PSI as reference method

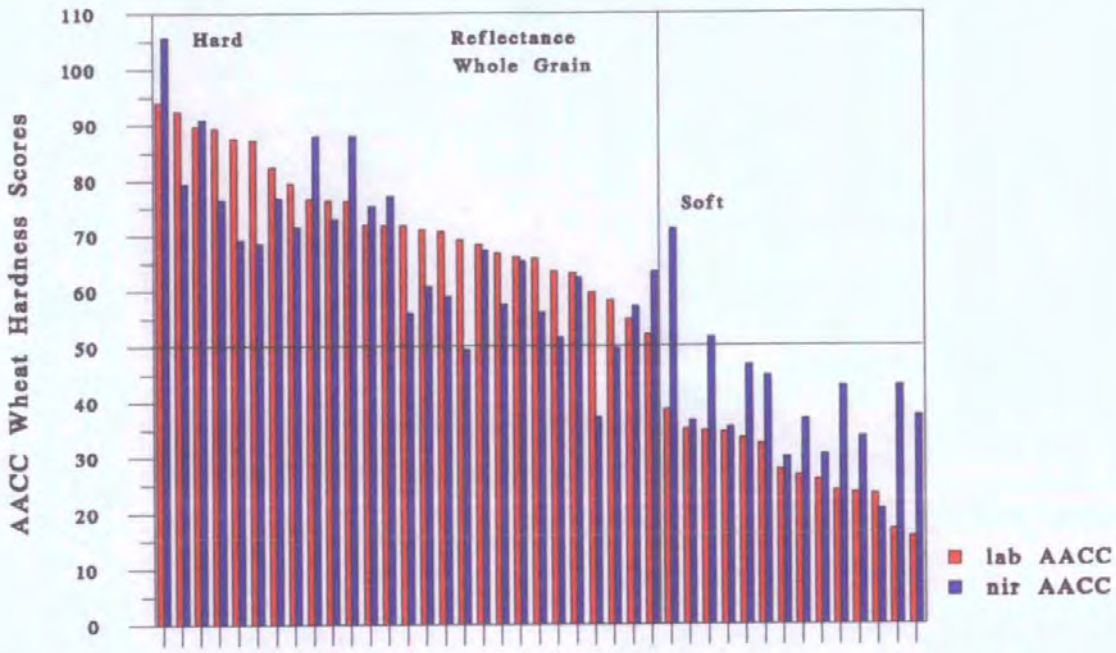

Figure 3.33 Bar graph illustrating separation of hard and soft wheats using empirical PLS calibrations (soft < 50) for whole grain reflectance and AACC NIR wheat hardness as reference method

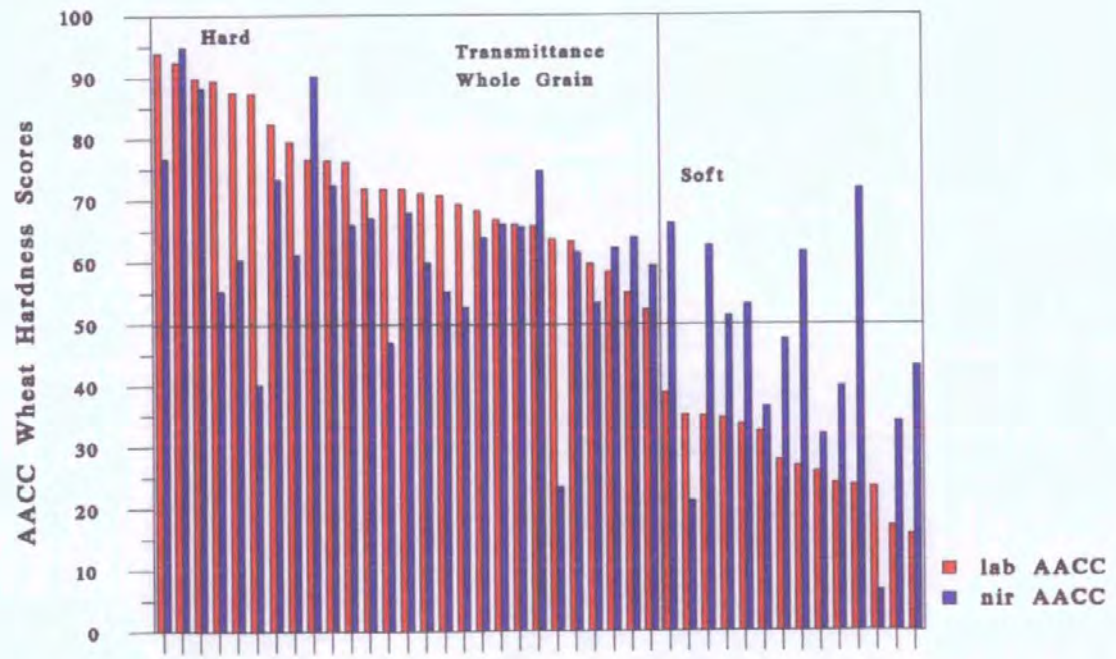

Figure 3.34 Bar graph illustrating separation of hard and soft wheats using empirical PLS calibrations (soft < 50) for whole grain transmittance and AACC NIR wheat hardness as reference method

3.3.2 Empirical calibrations for UK home-grown wheat

Table 3.15 summarises the AJS, PSI and AACC NIR wheat hardness test results for the 54 UK home-grown samples as shown in Table 3.2.

Table 3.15 Summary of UK home-grown wheat hardness results as measured by Air Jet Sieve, Particle Size Index and AACC NIR wheat hardness methods, respectively

	AJS (% throughs)	**PSI** (% throughs)	**AACC** (scores)
n	82	82	82
Mean	37.45	62.02	54.75
Range	27.95 - 49.55	53.00 - 73.60	15.38 - 91.23
Standard deviation	5.37	5.87	21.21
Standard Error	0.59	0.65	2.34
Coefficient of variation	14.33	9.46	38.74

Tables 3.16 & 3.17 summarises similar comparative wheat hardness measurement results for the calibration set and validation set as used for the NIR wheat hardness calibrations

Table 3.16 Summary of UK home-grown wheat hardness results, for the calibration set, as measured by Air Jet Sieve, Particle Size Index and AACC NIR wheat hardness methods, respectively

	AJS (% throughs)	**PSI** (% throughs)	**AACC** (scores)
n	50	50	50
Mean	37.37	62.12	54.85
Range	27.95 - 49.55	53.00 - 73.60	15.37 - 91.23
Standard deviation	5.53	6.18	22.28
Standard Error	0.78	0.87	3.15
Coefficient of variation	14.80	9.95	40.62

Table 3.17 Summary of UK home-grown wheat hardness results, for the validation set, as measured by Air, Jet Sieve, Particle Size Index and AACC NIR wheat hardness methods, respectively

	AJS (% throughs)	**PSI** (% throughs)	**AACC** (scores)
n	32	32	32
Mean	37.57	61.89	54.60
Range	31.35 - 48.65	57.90 - 71.30	23.99 - 58.99
Standard deviation	5.21	5.45	19.75
Standard Error	0.92	0.96	3.49
Coefficient of variation	13.87	8.81	36.17

Calibration and validation results obtained for the empirical NIR calibrations for ground grain reflectance, whole grain reflectance and whole grain transmittance for UK home-grown varieties are displayed in Tables 3.18, 3.19 & 3.20, respectively.

Table 3.18 NIR wheat hardness calibration and validation statistics for ground grain reflectance for UK home-grown varieties

Ground grain Reflectance	**ISI** No cross - validations	**ISI** 20 cross - validations	**RPD Statistic** No cross - validations
AJS	SEC = 1.27 r = 0.97 SEP = 1.43 8 terms	SEC = 1.46 r = 0.96 SEP = 1.46 6 terms	3.64
PSI	SEC = 1.40 r = 0.97 SEP = 1.43 8 terms	SEC = 1.37 r = 0.97 SEP = 1.49 9 terms	3.81

Table 3.19 NIR wheat hardness calibration and validation statistics for whole grain reflectance for UK home-grown varieties

Whole grain Reflectance	**ISI** No cross - validations	**ISI** 20 cross - validations	**RPD Statistic** No cross - validations
AJS	SEC = 2.77 r = 0.87 SEP = 3.32 10 terms	SEC = 3.61 r = 0.75 SEP = 4.03 5 terms	1.56
PSI	SEC = 3.91 r = 0.77 SEP = 3.78 7 terms	SEC = 2.63 r = 0.91 SEP = 4.36 12 terms	1.44
AACC	SEC = 11.70 r = 0.85 SEP = 13.68 10 terms	SEC = 14.44 r = 0.76 SEP = 14.05 6 terms	1.44

Table 3.20 NIR wheat hardness calibration and validation statistics for whole grain transmittance for UK home grown varieties

Whole grain Transmittance	**ISI** No cross - validations	**ISI** 20 cross - validations	**RPD Statistic** No cross - validations
AJS	SEC = 5.09 r = 0.39 SEP = 4.53 2 terms	SEC = 5.06 r = 0.40 SEP = 4.74 1 term	1.15
PSI	SEC = 5.30 r = 0.52 SEP = .73 1 term	SEC = 5.30 r = 0.52 SEP = 4.73 1 term	1.15
AACC	SEC = 19.58 r = 0.48 SEP = 16.66 1 term	SEC = 19.58 r = 0.48 SEP = 16.66 1 term	1.19

3.3.3 Alternative calibrations

Calibration and validation results obtained for the alternative NIR wheat hardness calibrations (MSC, PCA & AREA) for ground grain reflectance, whole grain reflectance and whole grain transmittance are displayed in Tables 3.21, 3.22 & 3.23, respectively.

Table 3.21 Alternative NIR wheat hardness calibration and validation statistics for ground grain reflectance

Ground grain Reflectance	MSC	1st PC	2nd PC	1st & 2nd PC	AREA
AJS	SEC = 2.61 r = 0.93 SEP = 2.59	SEC = 2.62 r = 0.93 SEP = 2.08	SEC = 6.92 r = 0.00 SEP = 5.01	SEC = 2.62 r = 0.93 SEP = 2.12	SEC = 3.02 r = 0.90 SEP = 2.24
PSI	SEC = 2.80 r = 0.92 SEP = 3.55	SEC = 3.02 r = 0.91 SEP = 2.98	SEC = 7.10 r = 0.04 SEP = 6.38	SEC = 3.01 r = 0.91 SEP = 4.20	SEC = 2.90 r = 0.91 SEP = 2.92

Table 3.22 Alternative NIR wheat hardness calibration and validation statistics for whole grain reflectance

Whole grain Reflectance	MSC	1st PC	2nd PC	1st & 2nd PC	AREA
AJS	SEC = 5.08 r = 0.68 SEP = 4.40	SEC = 6.21 r = 0.44 SEP = 4.41	SEC = 5.76 r = 0.56 SEP = 3.92	SEC = 4.89 r = 0.71 SEP = 3.53	SEC = 6.68 r = 0.26 SEP = 4.70
PSI	SEC = 5.45 r = 0.64 SEP = 4.90	SEC = 6.17 r = 0.50 SEP = 4.74	SEC = 6.31 r = 0.46 SEP = 4.72	SEC = 5.24 r = 0.68 SEP = 3.84	SEC = 7.00 r = 0.17 SEP = 5.52
AACC	SEC = 17.67 r = 0.73 SEP = 13.65	SEC = 22.00 r = 0.52 SEP = 15.75	SEC = 21.79 r = 0.53 SEP = 13.91	SEC = 10.74 r = 0.75 SEP = 17.18	SEC = 25.17 r = 0.21 SEP = 18.14

Table 3.23 Alternative NIR wheat hardness calibration and validation statistics for whole grain transmittance

Whole grain Transmittance	MSC	1st PC	2nd PC	1st & 2nd PC	AREA
AJS	SEC = 6.26 r = 0.42 SEP = 5.73	SEC = 5.82 r = 0.54 SEP = 4.66	SEC = 6.76 r = 0.21 SEP = 4.85	SEC = 5.63 r = 0.58 SEP = 4.57	SEC = 6.10 r = 0.47 SEP = 4.91
PSI	SEC = 6.30 r = 0.46 SEP = 6.14	SEC = 5.81 r = 0.57 SEP = 4.90	SEC = 6.99 r = 0.17 SEP = 5.50	SEC = 5.68 r = 0.60 SEP = 4.71	SEC = 6.57 r = 0.38 SEP = 5.46
AACC	SEC = 23.18 r = 0.44 SEP = 21.72	SEC = 21.01 r = 0.58 SEP = 17.04	SEC = 25.73 r = 0.14 SEP = 18.91	SEC = 20.97 r = 0.58 SEP = 16.89	SEC = 18.61 r = 0.33 SEP = 24.27

- *multiplicative scatter correction (MSC)*

A summary of the MSC linear regression results compared with empirical calibrations are shown in Table 3.24. Slope and intercept details are listed in Tables 5 & 6 in Appendix 5.

Table 3.24 SEP results for empirical calibrations (ISI software) and MSC regressions

	Ground grain Reflectance		Whole grain Reflectance		Whole grain Transmittance	
	ISI#	MSC	ISI#	MSC	ISI#	MSC
AJS	1.45 (1.55)	2.59	3.76 (4.18)	4.40	5.06 (5.90)	5.73
PSI	1.94 (1.99)	3.55	3.96 (4.19)	4.90	5.25 (5.92)	6.14
AACC	---	---	12.97 (13.24)	13.65	20.26 (22.05)	21.72

Figures in brackets show SEP for equations selected by cross-validations

- *principal component analysis (PCA)*

A summary of the PCA linear regression results compared with empirical calibrations are shown in Table 3.25. The loadings of the 1st & 2nd principal components are listed in Tables 7 & 8 in Appendix 6.

Table 3.25 SEP results for empirical calibrations (ISI software) and principal components regressions

	Ground grain Reflectance		Whole grain Reflectance		Whole grain Transmittance	
	ISI#	1st PC	ISI#	1st & 2nd PC	ISI#	1st & 2nd PC
AJS	1.45 (1.55)	2.08	3.76 (4.18)	3.53	5.06 (5.90)	4.57
PSI	1.94 (1.99)	2.98	3.96 (4.19)	3.84	5.25 (5.92)	4.71
AACC	---	---	12.97 (13.24)	17.18	20.26 (22.05)	16.89

Figures in brackets show SEP for equations selected by cross-validations

Figure 3.35 illustrates the mean spectrum and the standard deviation for ground grain reflectance, Figure 3.36 show the mean spectrum and the plot of the loadings of the 1st PC and Figure 3.37 the mean spectrum and the plot of the loadings of the 2nd PC.

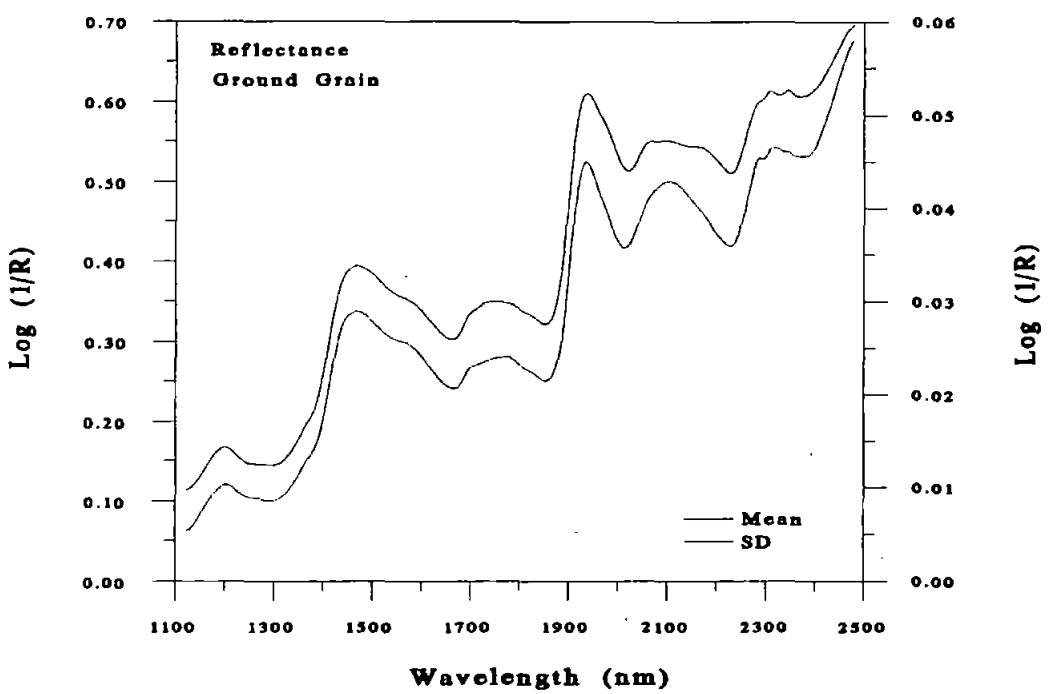

Figure 3.35 Plots of the mean spectrum and the standard deviation for ground grain reflectance

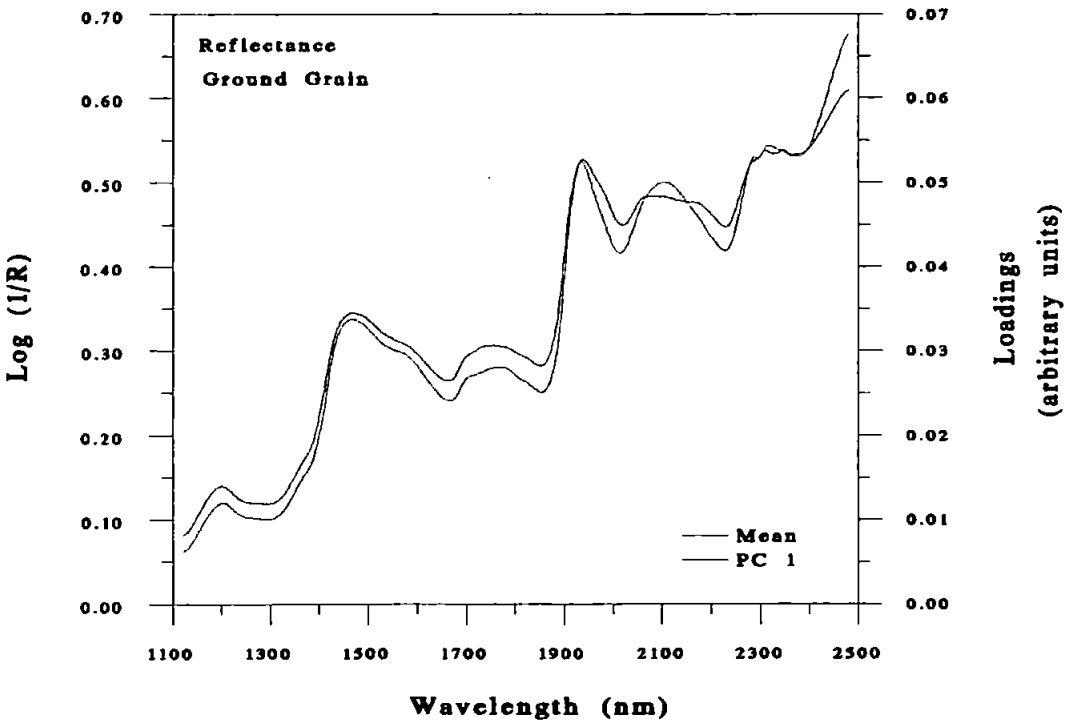

Figure 3.36 Plots of the mean spectrum and the loadings of the 1st PC for ground grain reflectance

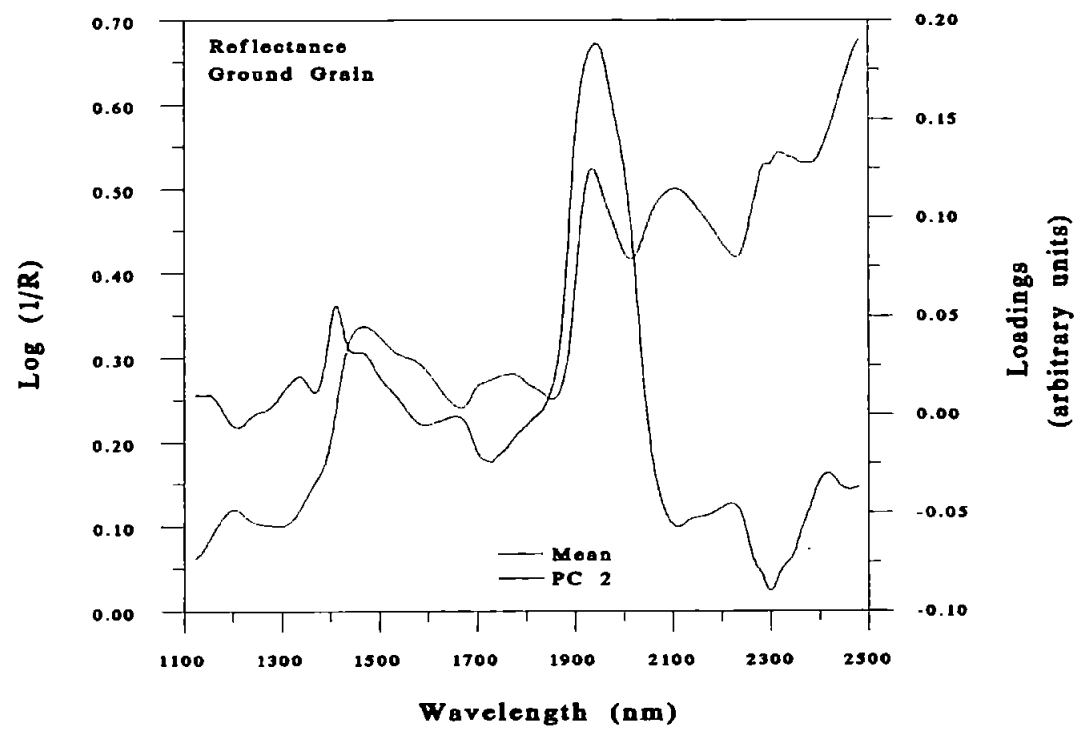

Figure 3.37 Plots of the mean spectrum and the loadings of the 2nd PC for ground grain reflectance

Figures 3.38, 3.39 & 3.40 illustrate similar figures for whole grain reflectance.

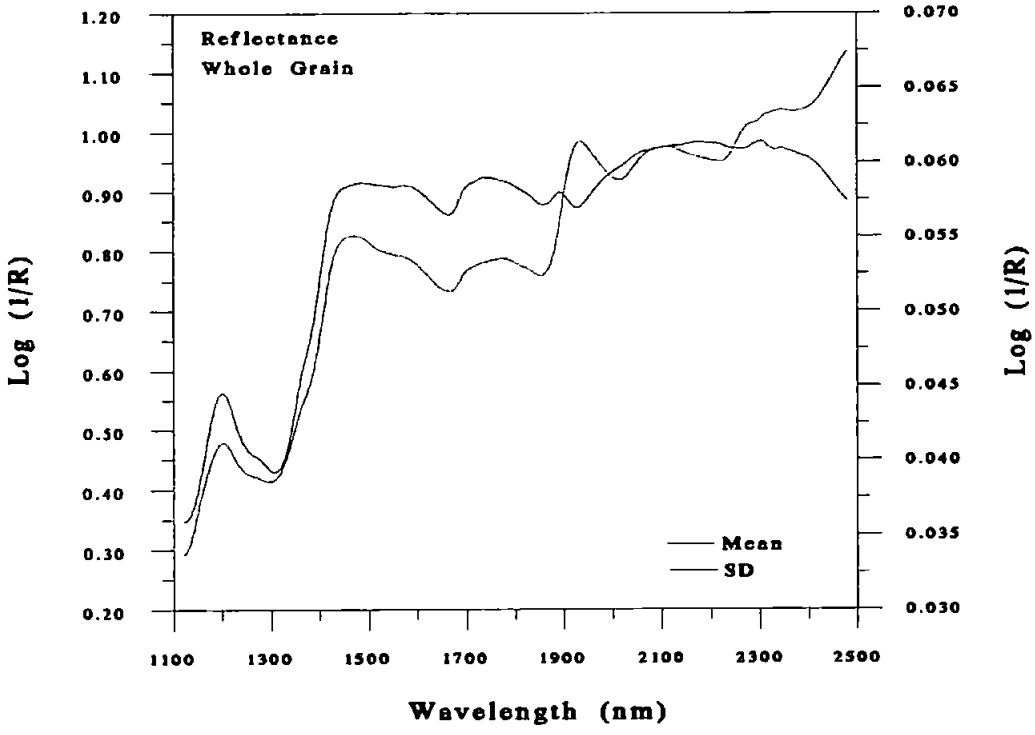

Figure 3.38 Plots of the mean spectrum and standard deviation for whole grain reflectance

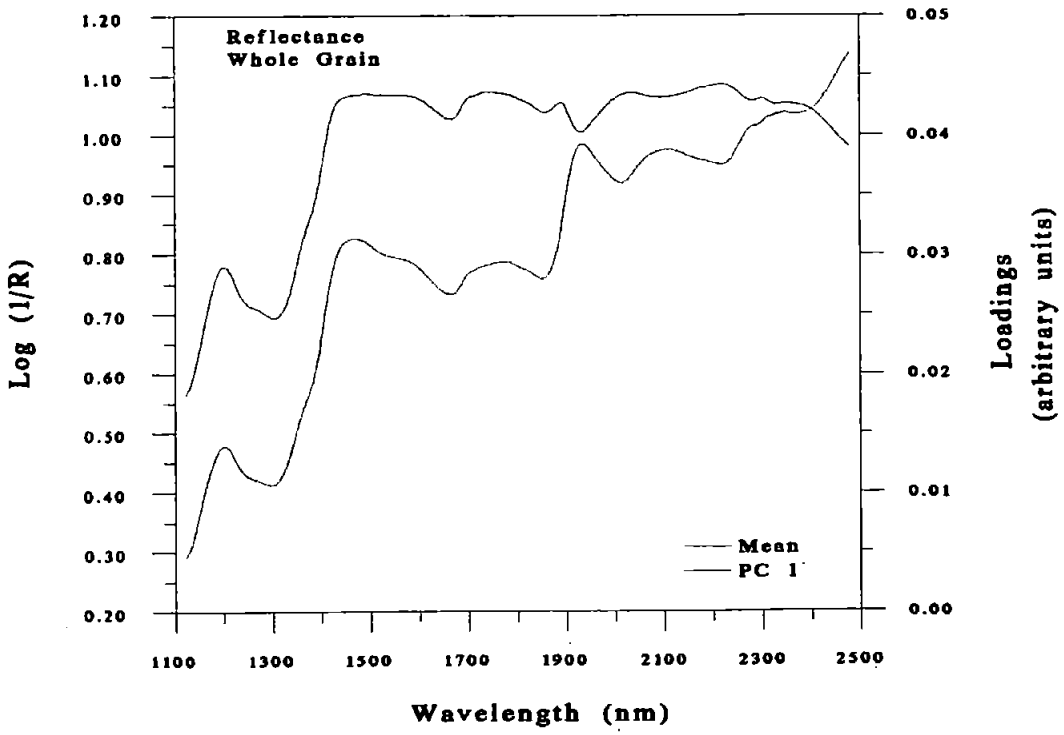

Figure 3.39 Plots of the mean spectrum and the loadings of the 1st PC for whole grain reflectance

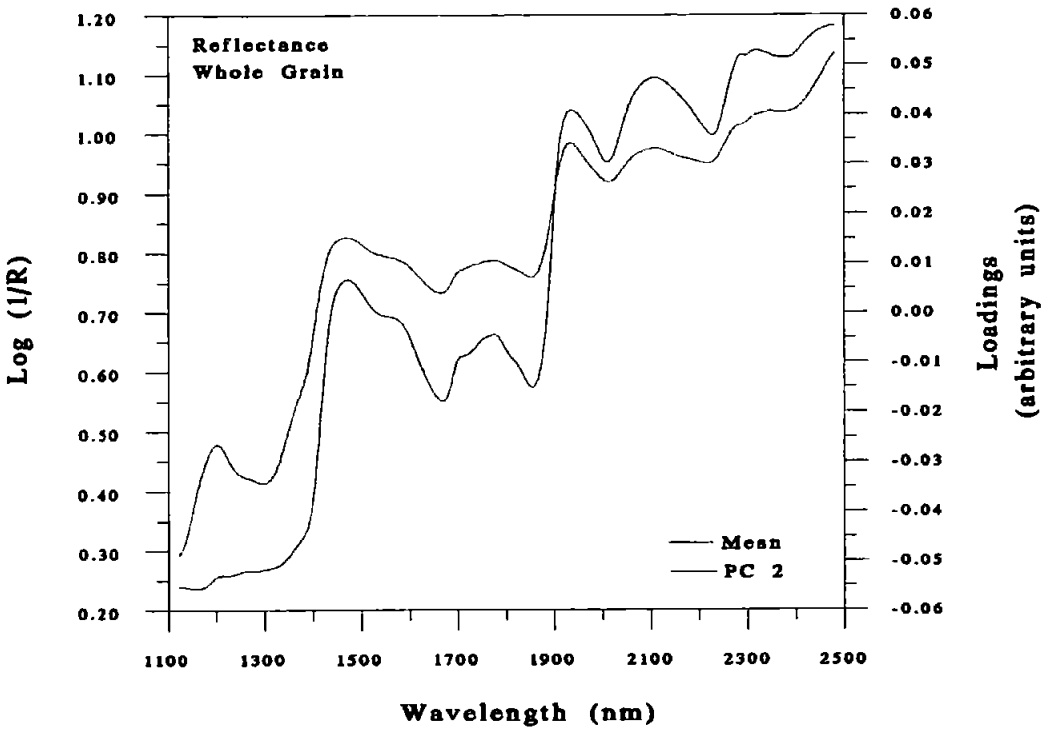

Figure 3.40 Plots of the mean spectrum and the loadings of the 2nd PC for whole grain reflectance

Figures 3.41, 3.42 & 3.43 show, respectively, the mean spectrum and standard deviation, the mean spectrum and the plot of the loadings of the 1st PC and the mean spectrum and the plot of the loadings of the 2nd PC for whole grain transmittance.

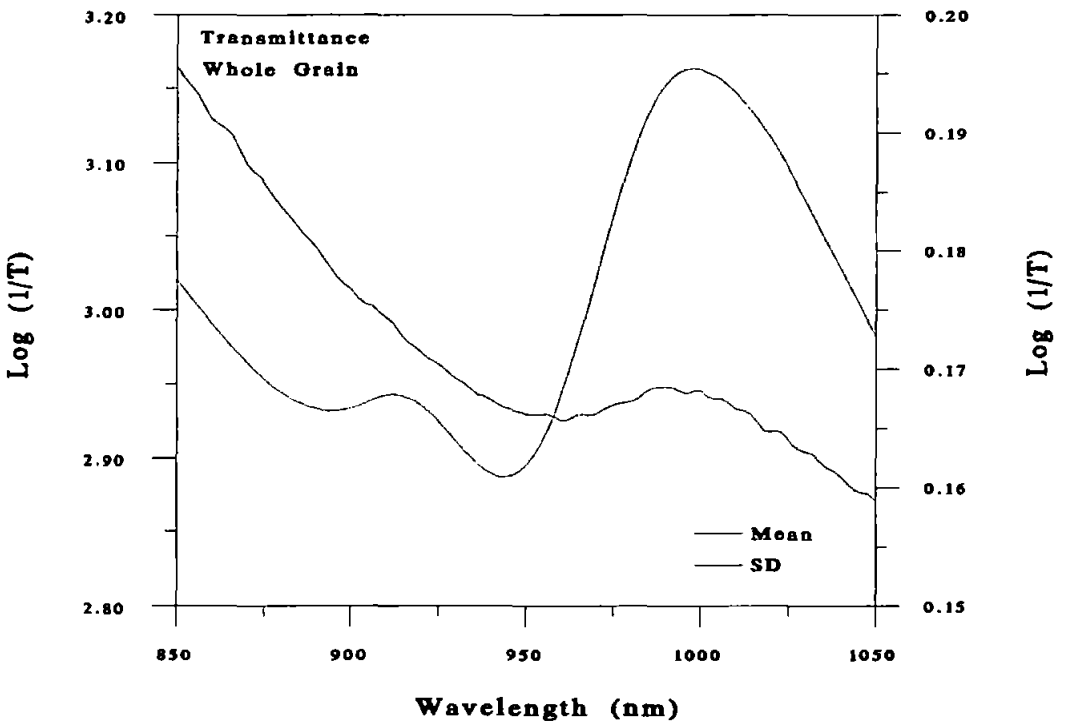

Figure 3.41 Plots of the mean spectrum and the standard deviation for whole grain transmittance

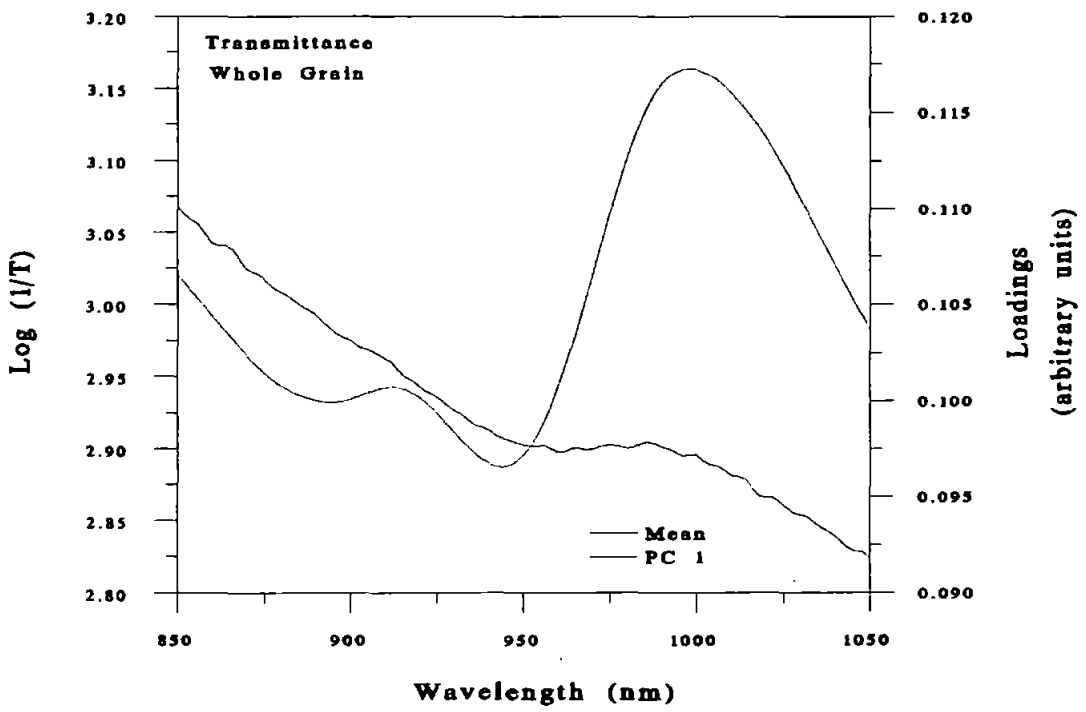

Figure 3.42 Plots of the mean spectrum and the loadings of the 1st PC for whole grain transmittance

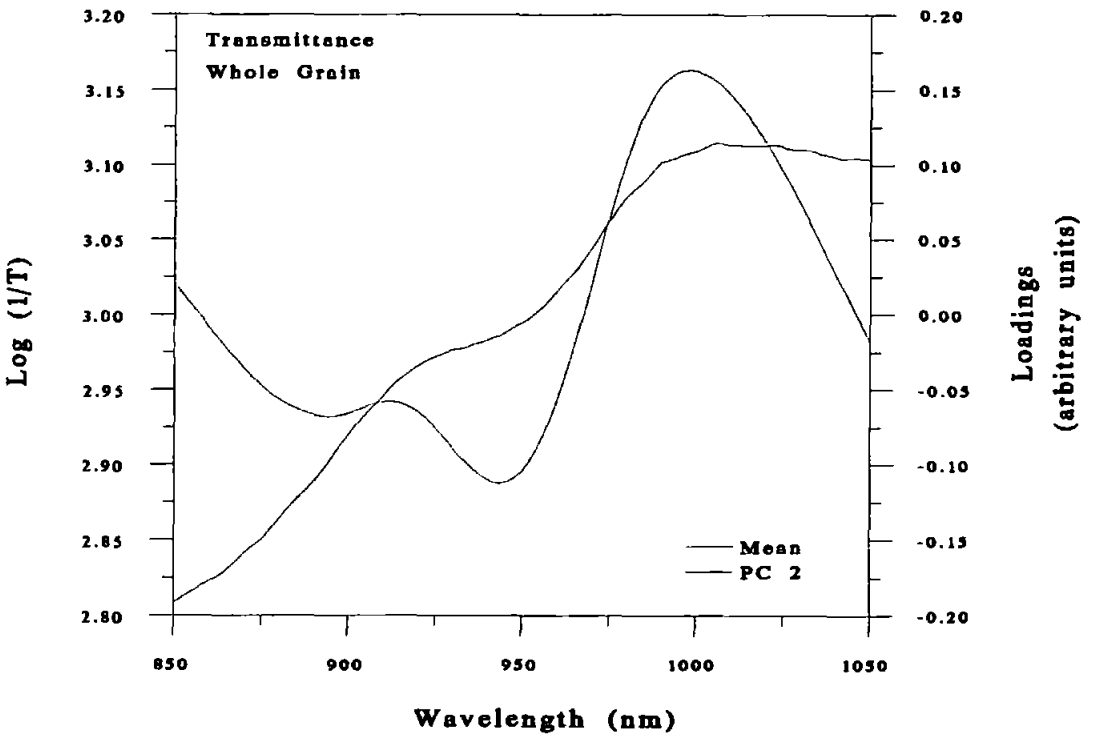

Figure 3.43 Plots of the mean spectrum and the loadings of the 2nd PC for whole grain transmittance

- *Area under the second derivative curve (AREA)*

A summary of the AREA linear regression results compared with empirical calibrations are shown in Table 3.26. Detailed results of the AREA are listed in Tables 9 & 10 in Appendix 7.

Table 3.26 SEP results for empirical calibrations (ISI software) and AREA regressions

	Ground grain Reflectance		Whole grain Reflectance		Whole grain Transmittance	
	ISI#	AREA	ISI#	AREA	ISI#	AREA
AJS	1.45 (1.55)	2.24	3.76 (4.18)	4.70	5.06 (5.90)	4.91
PSI	1.94 (1.99)	2.92	3.96 (4.19)	5.52	5.25 (5.92)	5.46
AACC	---	---	12.97 (13.24)	18.14	20.26 (22.05)	24.27

Figures in brackets show SEP for equations selected by cross-validations

3.3.4 NIR calibrations of damaged starch on flour

The damaged starch and AACC NIR wheat hardness test results, measured for the 54 UK home-grown wheat samples are presented in Table 3.27

Table 3.28 summarises the damaged starch and the AACC NIR wheat hardness test results for all of the 54 samples.

Tables 3.29 & 3.30 summarises similar comparative damaged starch and AACC NIR wheat hardness test results for the calibration set and validation set as used for the damaged starch calibrations.

Table 3.27 Damaged starch and AACC NIR wheat hardness results of UK home-grown varieties from different localities

Sample Number	Variety	Damaged starch	AACC
1	Cadenza	30	28.5
2	Hunter	30	38.6
3	Spark	26	35.2
4	Andante	21	43.9
5	Hereward	26	38.3
6	Flame	39	31.6
7	Hunter	22	39.0
8	Cadenza	40	28.0
9	Riband	17	42.9
10	Brigadier	38	33.0
11	Mercia	34	33.4
12	Andante	27	42.9
13	Flame	28	34.2
14	Prophet	38	35.2
15	Cadenza	33	31.8
16	Mercia	36	37.6
17	Genesis	39	37.2
18	Cadenza	42	31.6
19	Mercia	34	36.3
20	Spark	35	33.4
21	Spark	32	33.2
22	Rialto	34	34.5
23	Hunter	26	40.2
24	Flame	40	33.6
25	Riband	23	45.2
26	Prophet	36	34.4
27	Brigadier	49	30.6
28	Mercia	29	34.1
29	Riband	26	41.9
30	Hereward	30	36.8
31	Hereward	39	32.9
32	Rialto	31	34.1
33	Hunter	17	42.8
34	Andante	27	40.7
35	Riband	15	43.2
36	Prophet	30	34.6
37	Mercia	41	33.5
38	Flame	36	35.1
39	Cadenza	40	34.5
40	Genesis	30	34.9
41	Genesis	32	32.9
42	Hunter	17	38.7
43	Hereward	28	38.0
44	Brigadier	40	31.5
45	Rialto	46	33.1
46	Rialto	40	31.6
47	Riband	23	43.7
48	Genesis	39	34.7
49	Spark	40	35.4
50	Andante	16	41.4
51	Brigadier	29	32.5
52	Andante	23	41.9
53	Hereward	35	32.8
54	Brigadier	48	31.4

Table 3.28 Summary of damaged starch and AACC NIR wheat hardness results for UK home-grown varieties

	Damaged starch (Farrand Units)	**AACC** (scores)
n	54	54
Mean	31.89	57.69
Range	15 - 49	21.40 - 91.20
Standard deviation	8.24	18.40
Standard Error	1.12	2.50
Coefficient of variation	25.83	31.89

Table 3.29 Summary of damaged starch and AACC NIR wheat hardness results, for the calibration set, for UK home-grown varieties

	Damaged starch (Farrand units)	**AACC** (scores)
n	33	33
Mean	31.7	58.08
Range	15 - 48	28.7 - 87.6
Standard deviation	8.33	17.51
Standard Error	1.45	3.05
Coefficient of variatioin	26.28	30.15

Table 3.30 Summary of damaged starch and AACC NIR wheat hardness results, for the prediction set, for UK home-grown varieties

	Damaged starch (Farrand units)	**AACC** (scores)
n	21	21
Mean	32.19	57.09
Range	17 - 49	21.4 - 91.2
Standard deviation	8.29	20.15
Standard Error	1.81	4.40
Coefficient of variation	25.75	35.3

The damage starch calibration and validation statistics are shown in Table 3.31. NIR calibration equations were derived for damaged starch against AACC NIR wheat hardness, 1st PC scores and the area under the second derivative curve.

Table 3.31 Calibration and validation statistics for damaged starch

Ground grain Reflectance	
AACC	SEC = 5.86 r = 0.72 SEP = 5.89
1st PC	SEC = 5.97 r = 0.71 SEP = 5.76
AREA	SEC = 5.97 r = 0.71 SEP = 5.58

3.4 The dependence of NIR wheat hardness measurements on chemical composition and scatter

The correlation coefficients between the first 10 principal components of the ground and whole wheat grain and AJS, PSI and AACC NIR wheat hardness data are listed in Tables 3.32 & 3.33, respectively.

The principal component similarity maps for ground wheat grain (scatter plots of 1st PC & 3rd PC) and whole wheat grain (scatter plots of 1st PC & 2nd PC) are shown in Figures 3.44 & 3.45, respectively. The plots of the loadings of the 1st and 2nd principal components for ground and whole wheat grain have been shown in section 3.3.3 in Figures 3.36, 3.37, 3.39 & 3.40, respectively.

The plots of the first three canonical variates for ground and whole wheat grain are shown in Figures 3.46 to 3.48.

Table 3.32 Correlations (r) between the first ten principal components of the ground grain reflectance spectra and AJS, PSI and AACC NIR wheat hardness data

	AJS	PSI	AACC
PC1	-0.93	-0.91	0.99
PC2	0	0.03	-0.01
PC3	-0.01	-0.23	0.07
PC4	-0.01	0.04	0.06
PC5	-0.01	-0.07	0.04
PC6	-0.31	0.18	-0.02
PC7	0.06	0.09	0
PC8	0	-0.05	0.01
PC9	0.02	0.02	0
PC10	-0.03	-0.07	0

Table 3.33 Correlations (r) between the first ten principal components of the whole grain reflectance spectra and AJS, PSI and AACC NIR wheat hardness data

	AJS	PSI	AACC
PC1	-0.44	-0.49	0.52
PC2	-0.55	-0.45	0.53
PC3	-0.15	-0.26	0.14
PC4	0.16	0.03	-0.16
PC5	-0.01	0.09	-0.02
PC6	0.11	0.08	-0.04
PC7	0.07	0.03	0.07
PC8	0.05	0.08	-0.01
PC9	0.19	0.07	-0.01
PC10	0.29	0.26	-0.23

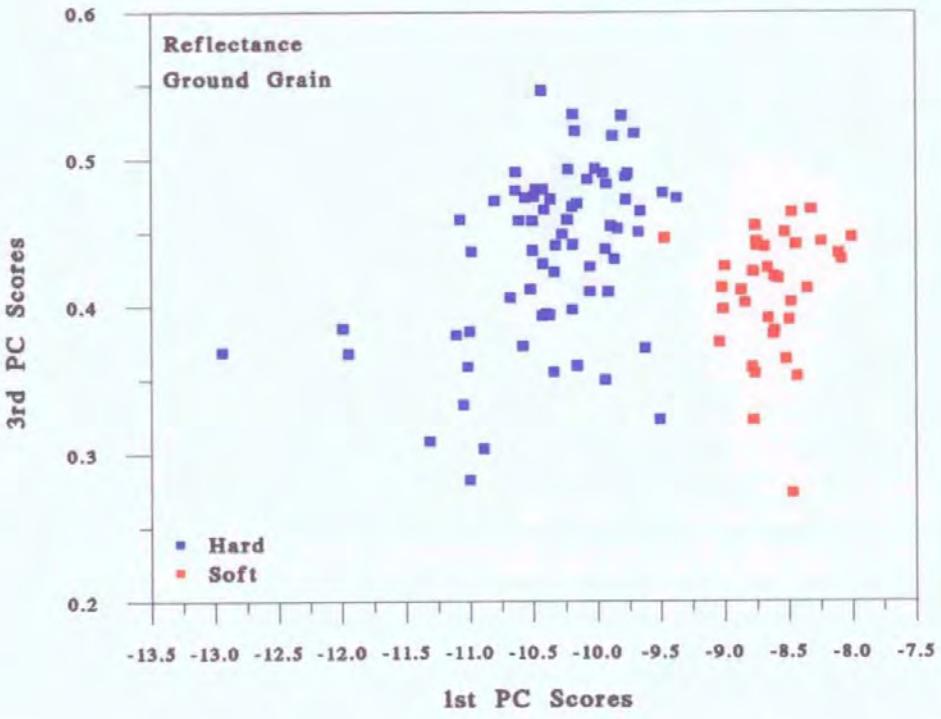

Figure 3.44 Plot of the 1st PC scores versus the 3rd PC scores (similarity map) for ground grain reflectance

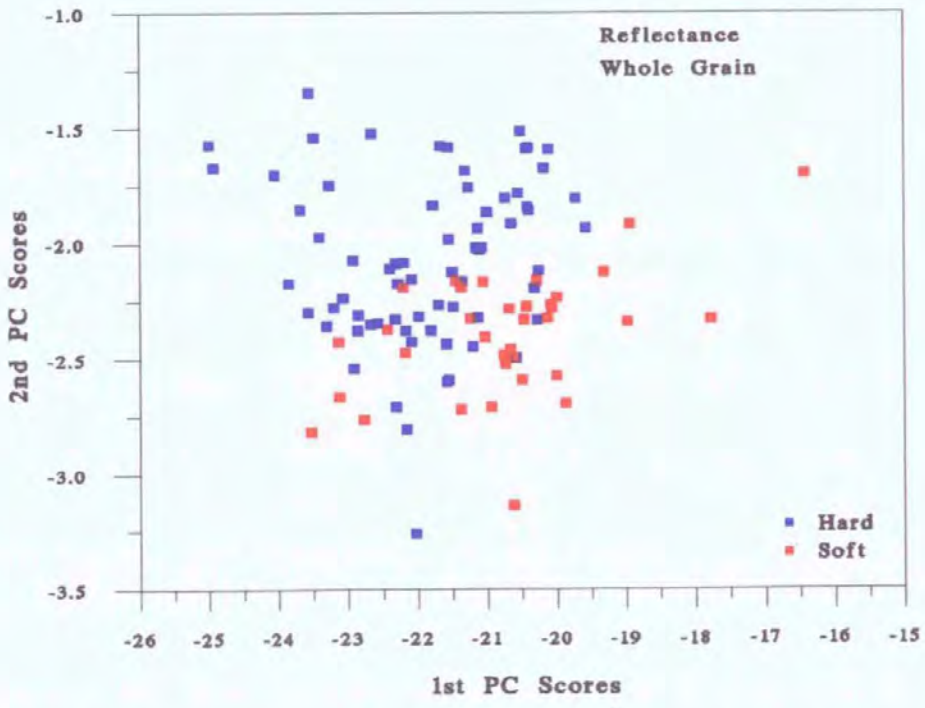

Figure 3.45 Plot of the 1st PC scores versus the 2nd PC scores (similarity map) for whole grain reflectance

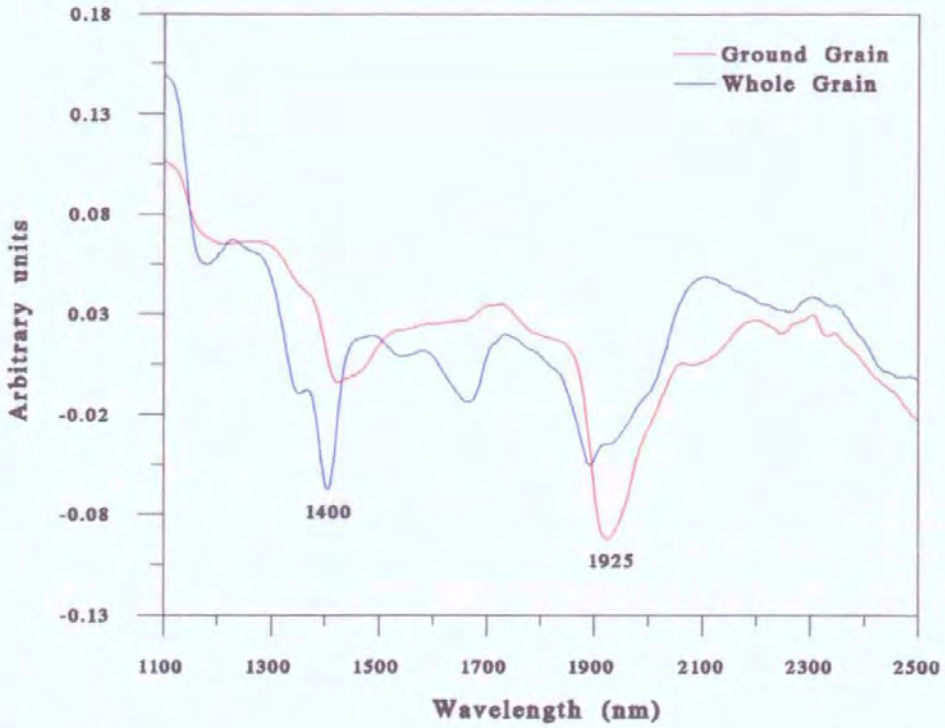

Figure 3.46 Plots of the 1st canonical variates for both ground and whole grain reflectance

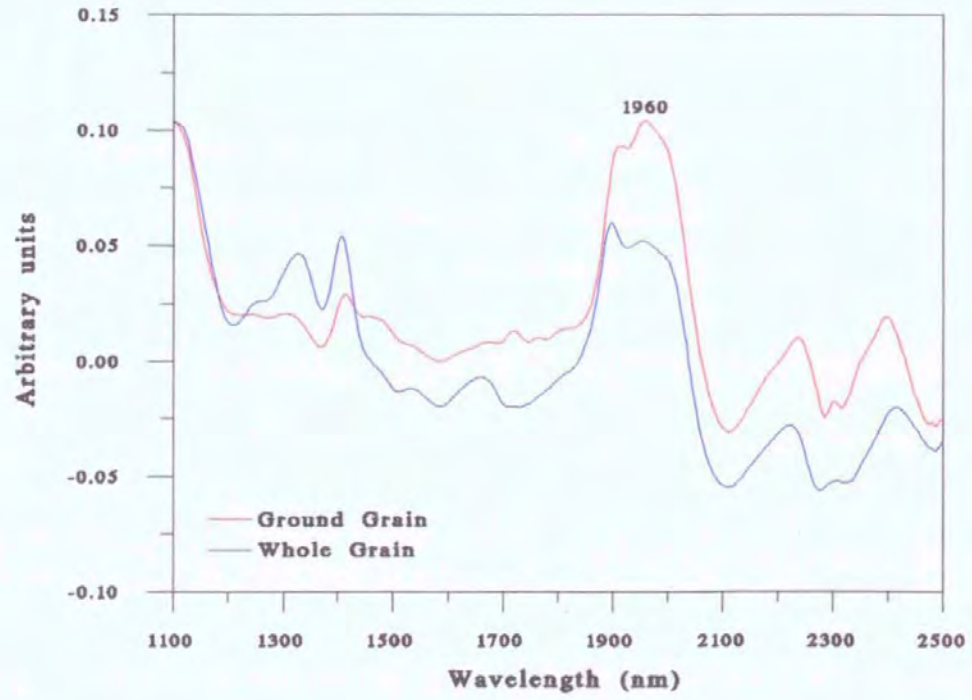

Figure 3.47 Plots of the 2nd canonical variates for both ground and whole grain reflectance

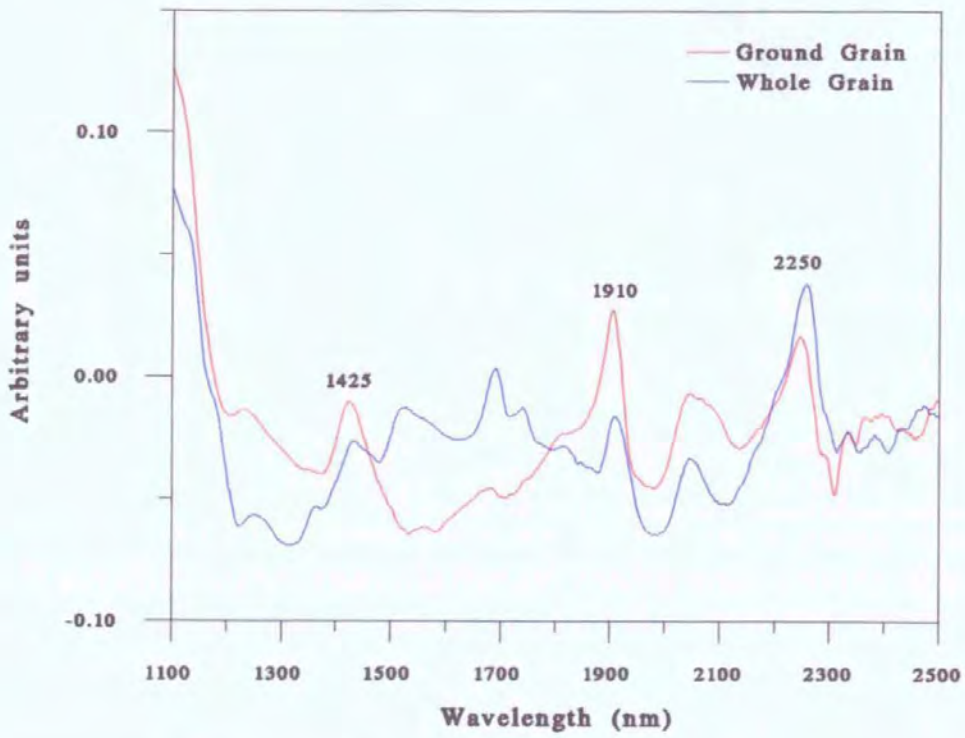

Figure 3.48 Plots of the 3rd canonical variates for both ground and whole grain reflectance

3.5 The effect of light scattering on whole wheat grain

The spectra of the four sets of data are shown in Figures 3.7 to 3.10 (section 3.2.2), with the spectra after correction for multiplicative scattering, shown in Figures 3.49 to 3.52.

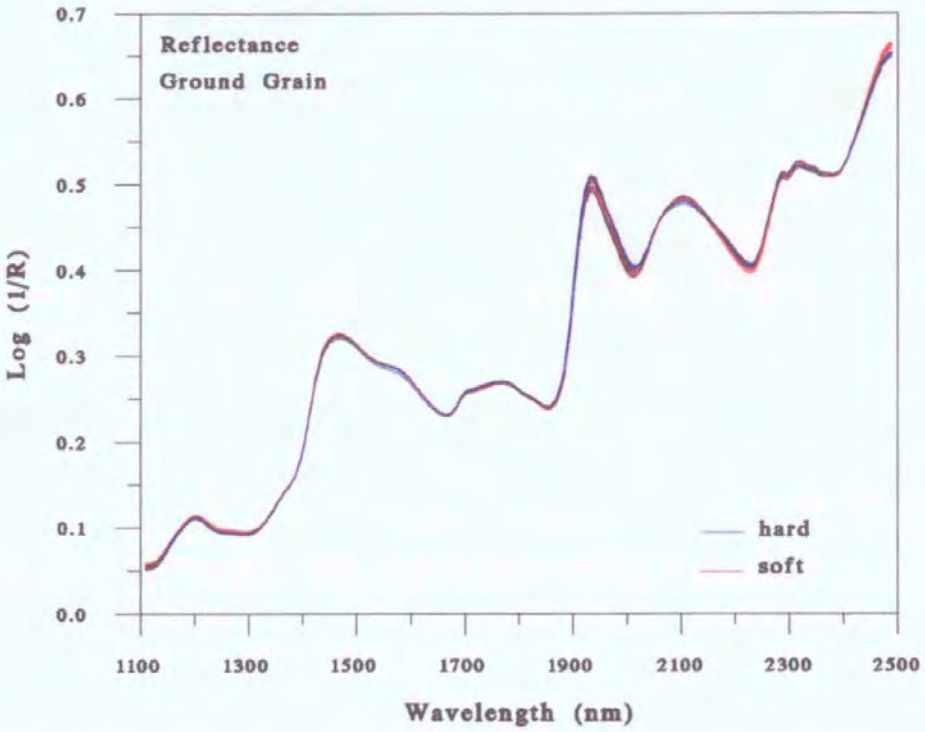

Figure 3.49 NIR reflectance spectra of ground wheat grain after correction for multiplicative scattering

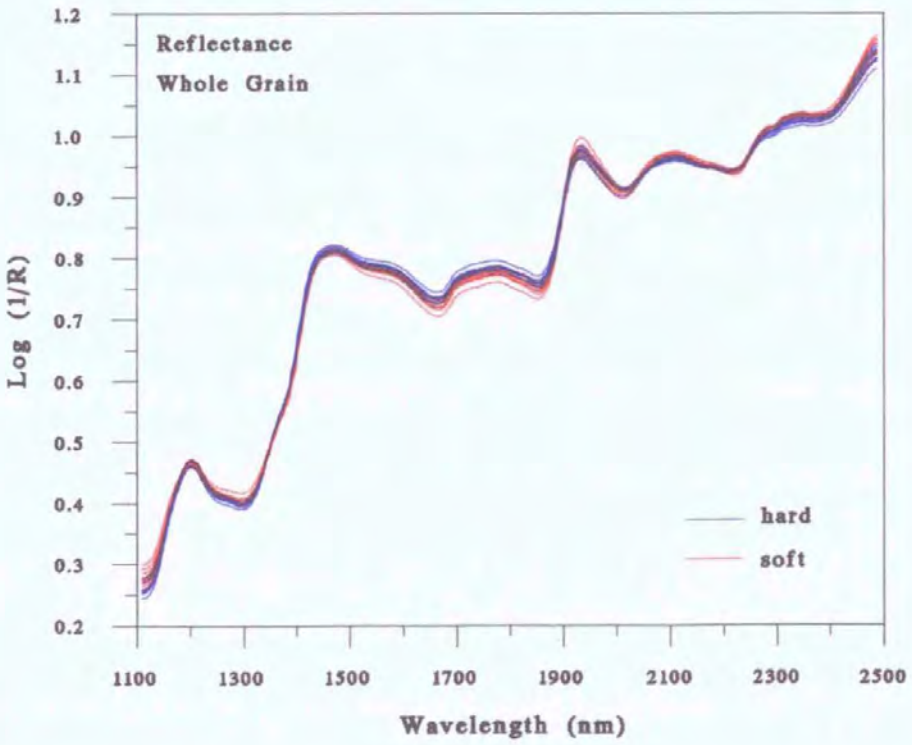

Figure 3.50 NIR reflectance spectra of whole wheat grain after correction for multiplicative scattering

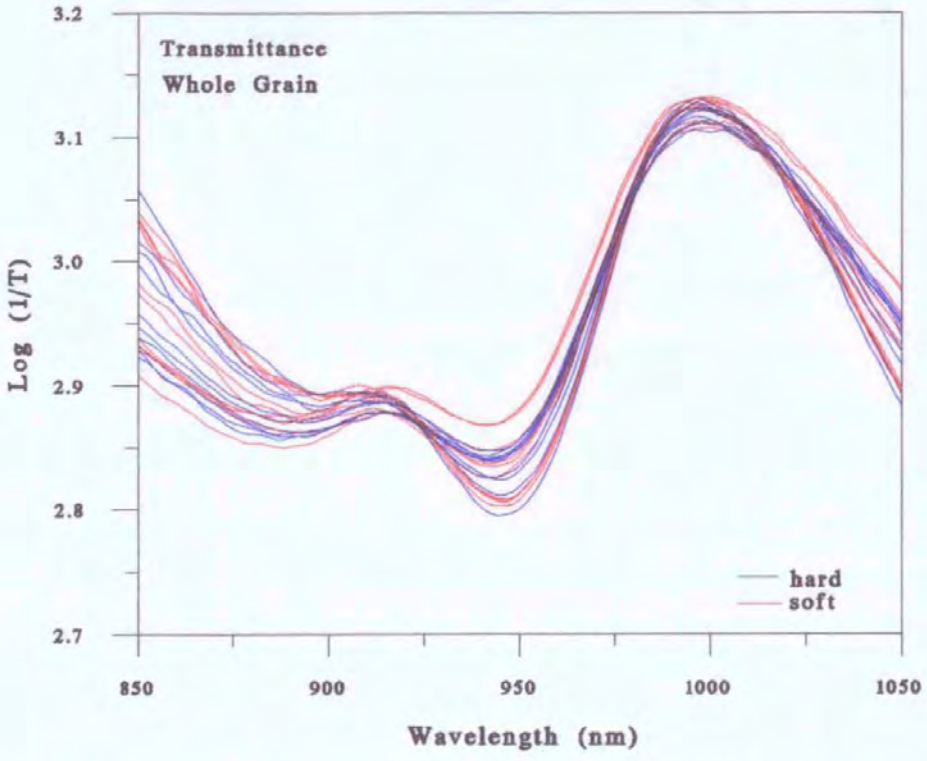

Figure 3.51 NIR transmittance spectra recorded on NIRSystems Model 6500 spectrophotometer of whole wheat grain after correction for multiplicative scattering

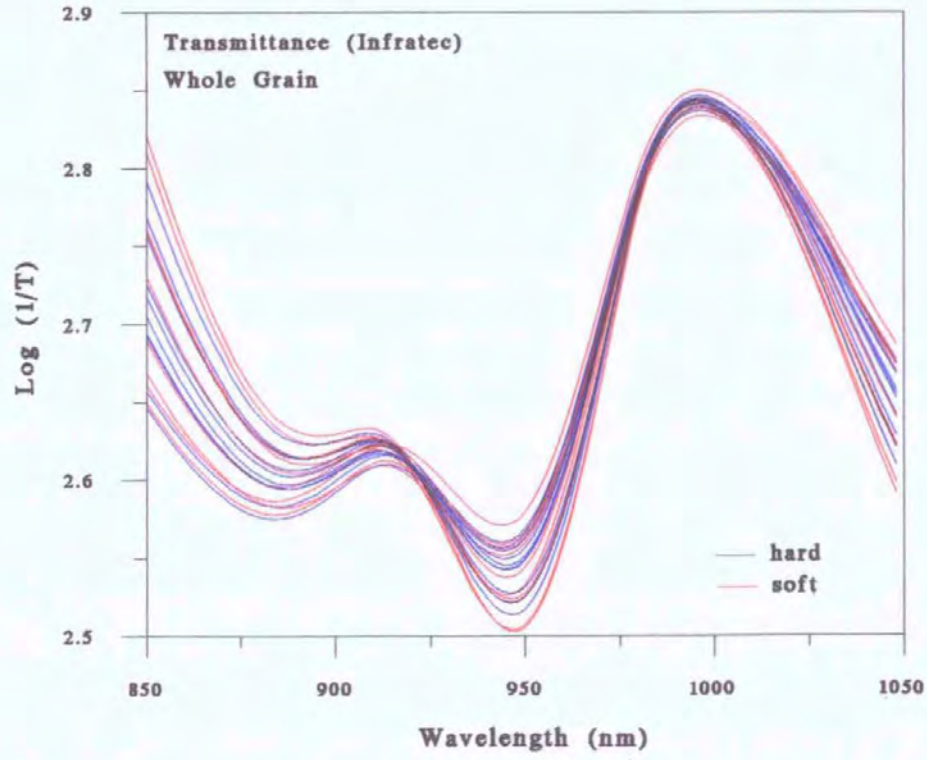

Figure 3.52 NIR transmittance spectra recorded on Infratec Model 1225 spectrophotometer of whole wheat grain after correction for multiplicative scattering

The relationship between the change in log 1/R values and particle size at selected log 1/R values and selected wavelengths in the reflectance spectra of ground wheat grain are shown in Figures 3.53 & 3.54, respectively.

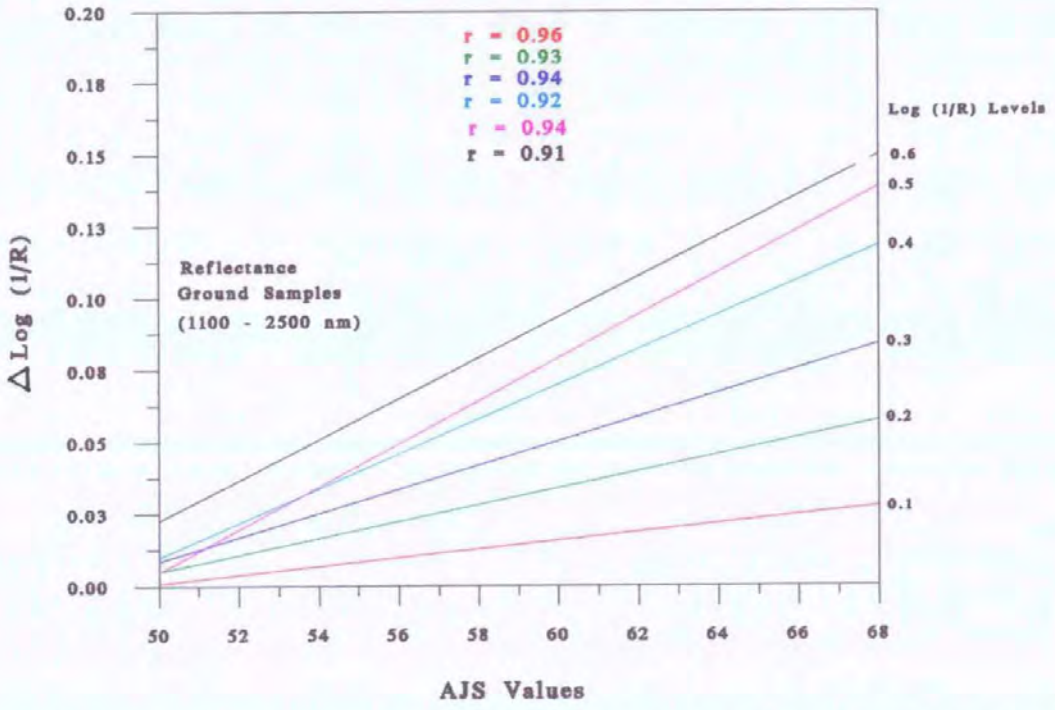

Figure 3.53 Relationship between the change in log 1/R and particle size in the reflectance spectra of ground wheat grain at selected log 1/R values

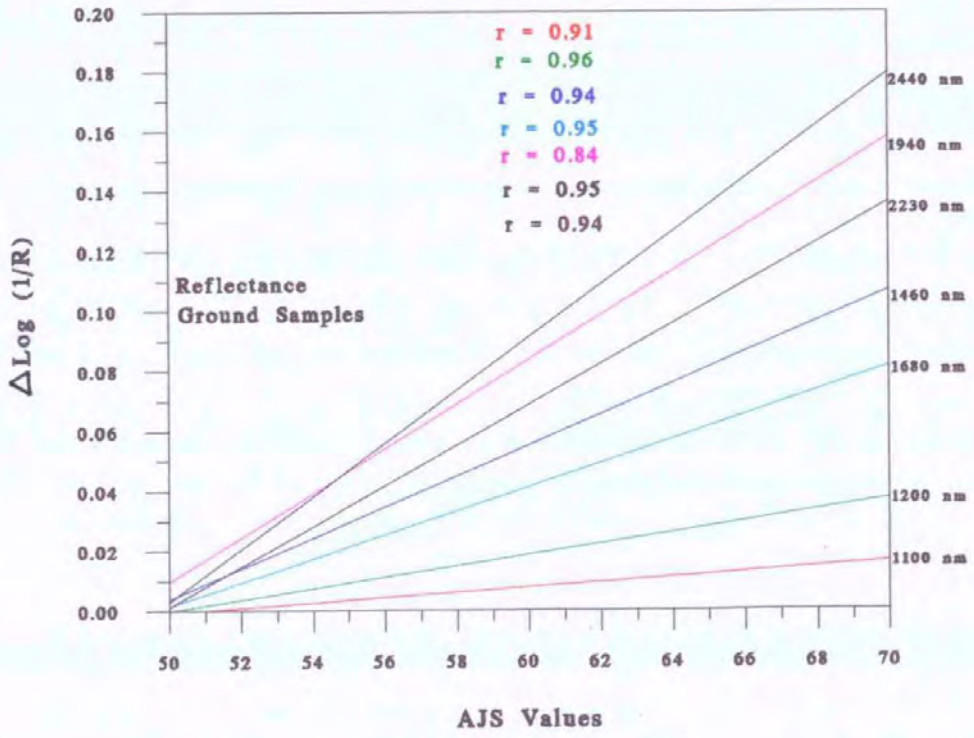

Figure 3.54 Relationship between the change in log 1/R and particle size in the reflectance spectra of ground wheat grain at selected wavelengths

The relationship between the change in log 1/R values and particle size at selected log 1/R values and selected wavelengths in the reflectance spectra of whole wheat grain are shown in Figures 3.55 & 3.56, respectively.

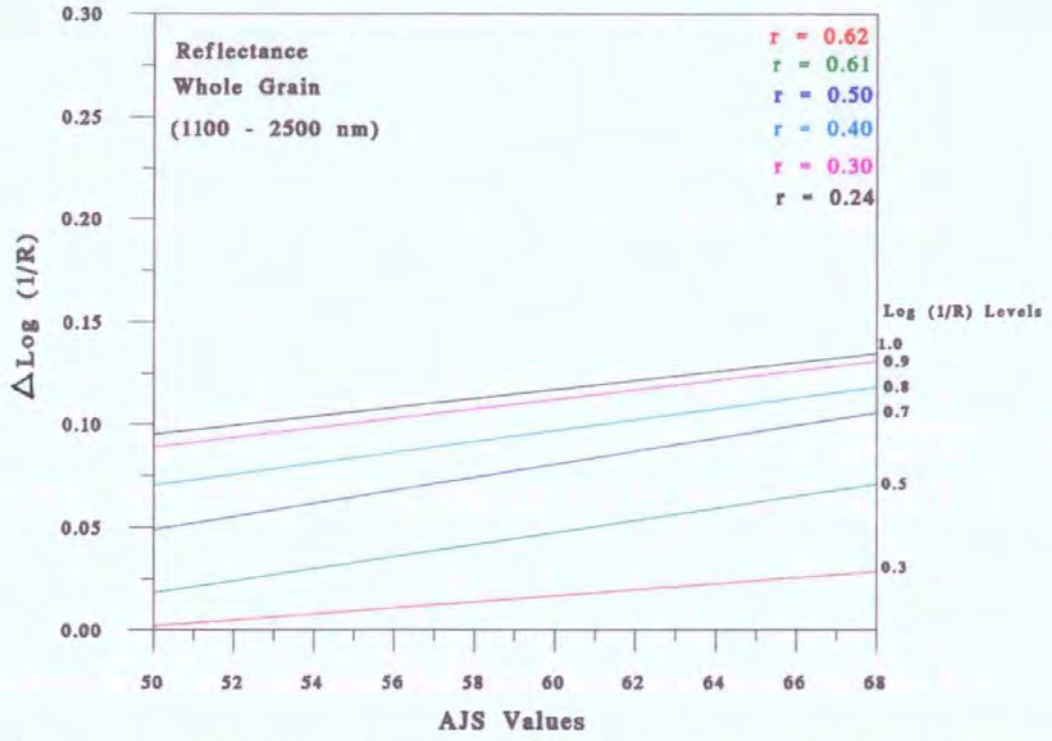

Figure 3.55 Relationship between the change in log 1/R and particle size in the reflectance spectra of whole wheat grain at selected log 1/R values

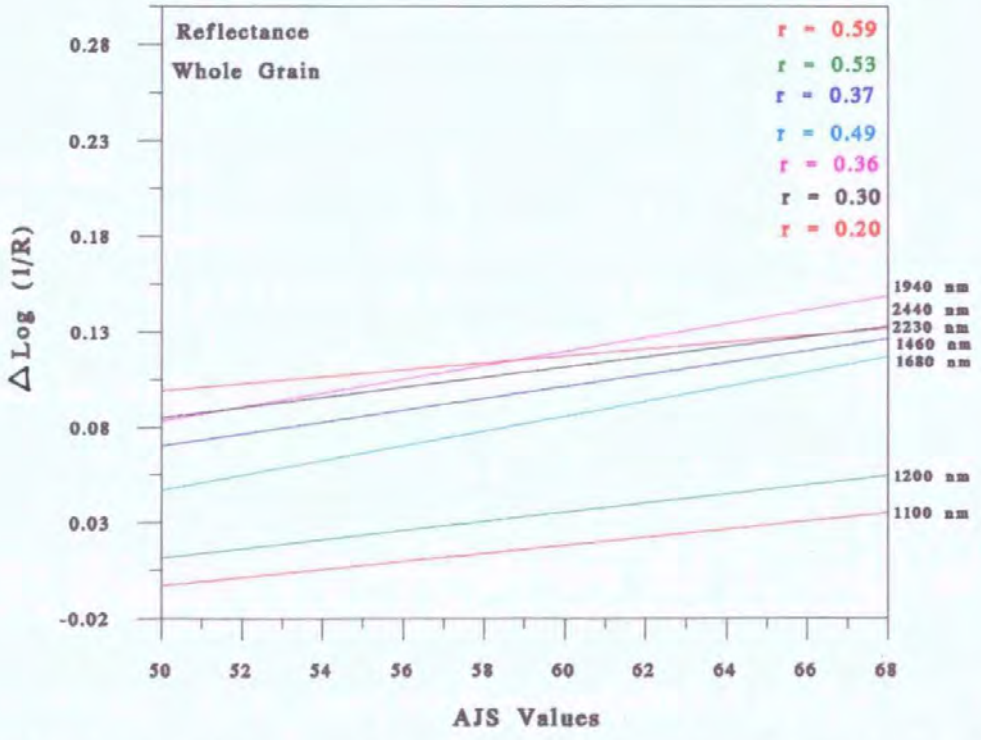

Figure 3.56 Relationship between the change in log 1/R and particle size in the reflectance spectra of whole wheat grain at selected wavelengths

The relationship between the change in log 1/R values and particle size at selected wavelengths (800 - 1100 nm) in the reflectance spectra of ground wheat grain and whole wheat grain are shown in Figures 3.57 & 3.58, respectively.

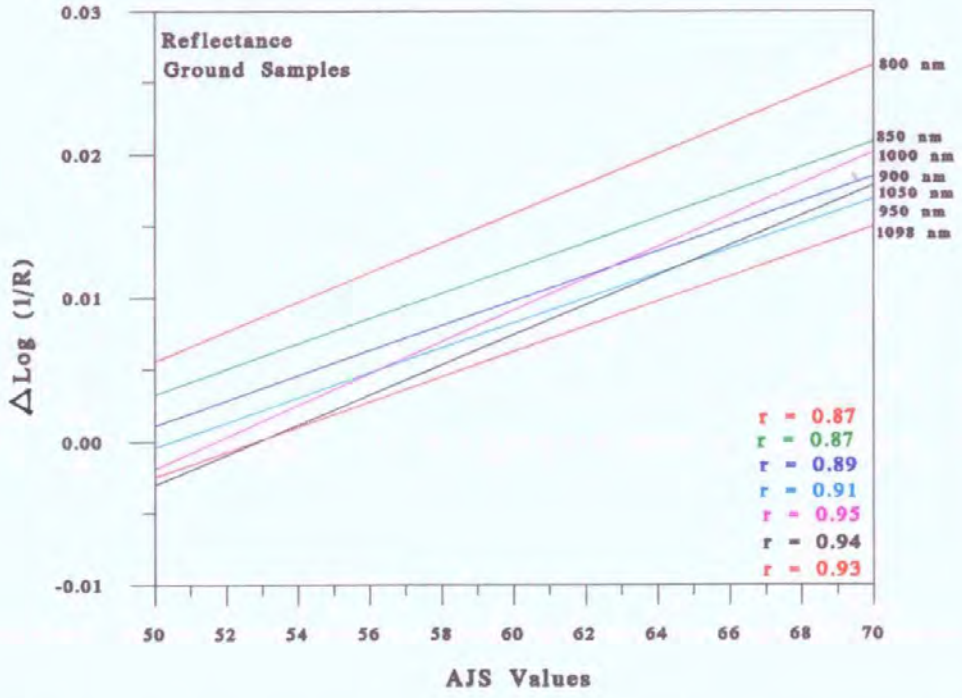

Figure 3.57 Relationship between the change in log 1/R and particle size in the reflectance spectra of ground wheat grain at selected wavelengths

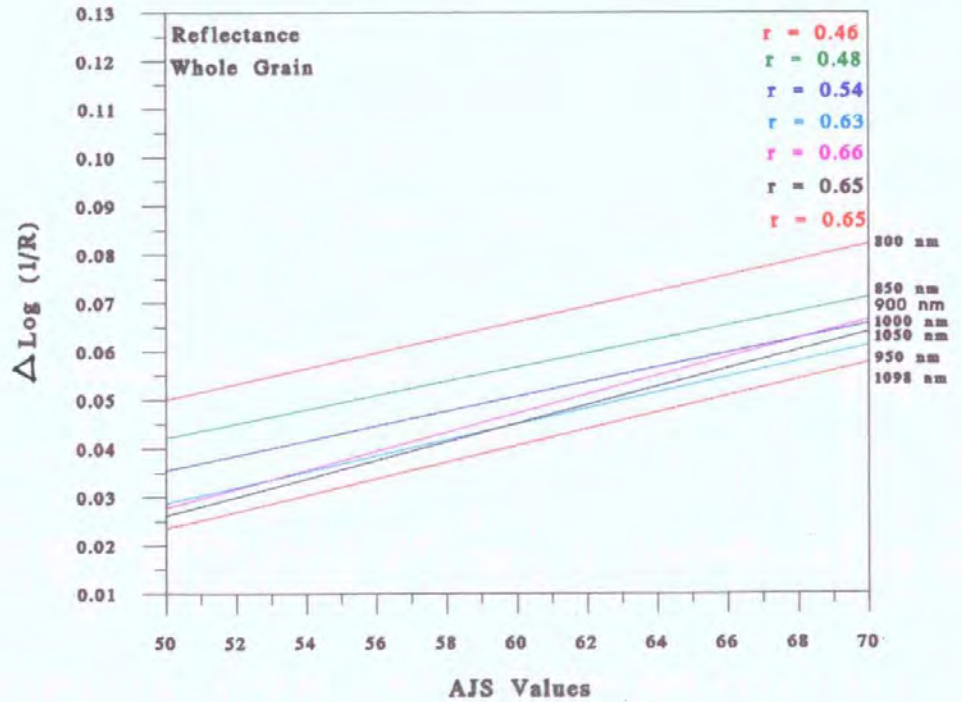

Figure 3.58 Relationship between the change in log 1/R and particle size in the spectra of reflectance whole wheat grain at selected wavelengths

The relationship between the change in log 1/R values and particle size in the transmittance spectra of whole wheat grain at selected wavelengths is shown in Figure 3.59 .

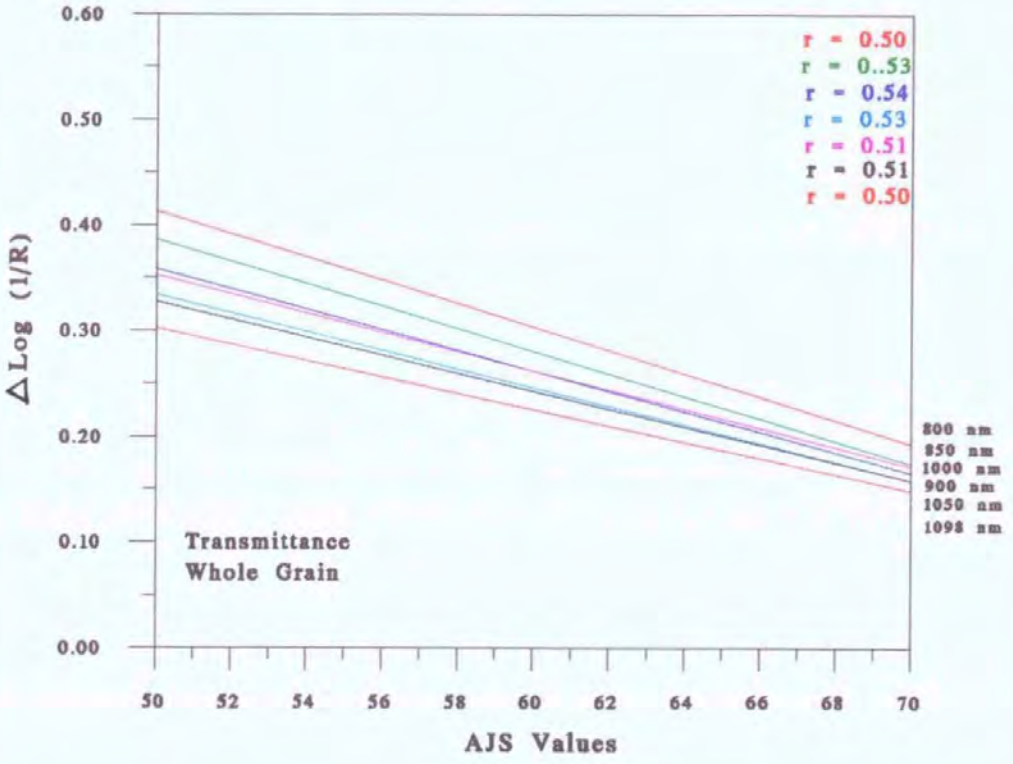

Figure 3.59 Relationship between the change in log 1/R and particle size in the transmittance spectra of whole wheat grain at selected wavelengths

3.6 The effect of protein content and growing season on two wheat varieties

Figures 3.60 to 3.67 illustrate the effect of protein content and growing season on the AACC NIR wheat hardness test and the spectral data of ground grain, whole grain reflectance and whole grain transmittance in terms of the 1st and 2nd principal components, respectively.

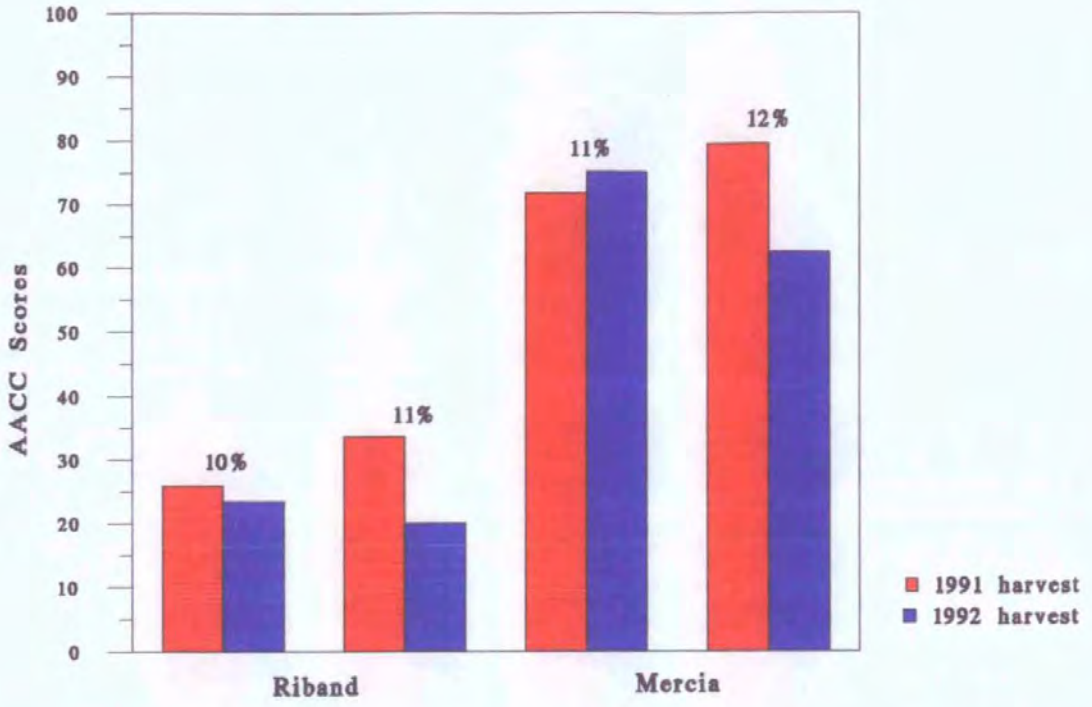

Figure 3.60 Bar graph to illustrate the effect of protein content and growing season on the AACC NIR wheat hardness test

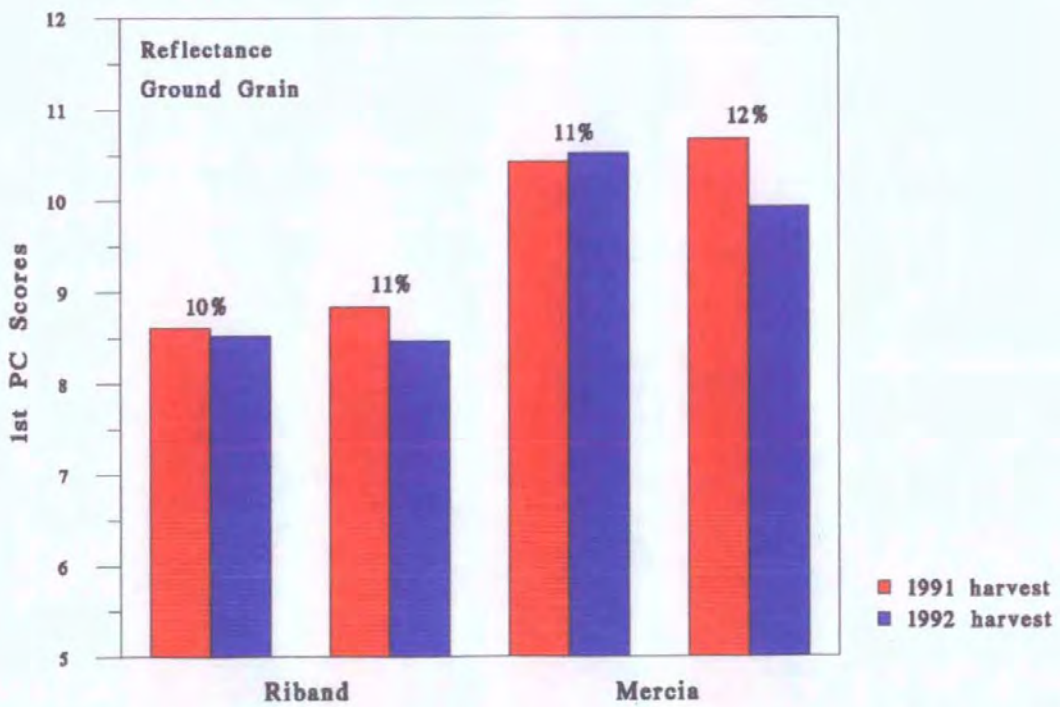

Figure 3.61 Bar graph to illustrate the effect of protein content and growing season on the 1st PC of ground grain reflectance spectra

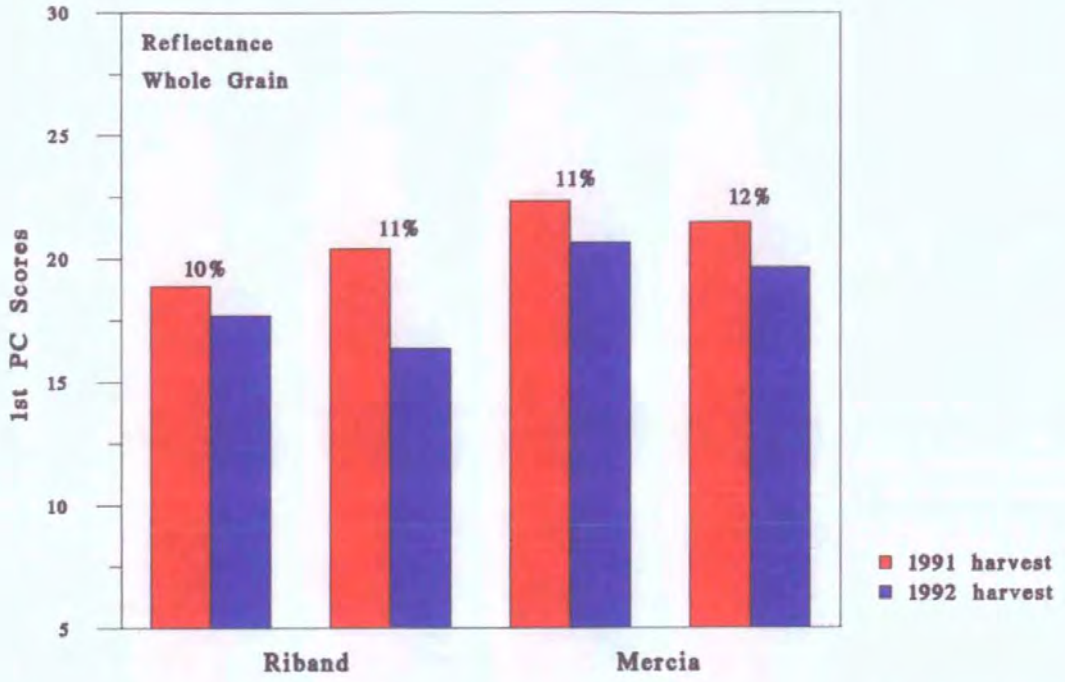

Figure 3.62 Bar graph to illustrate the effect of protein content and growing season on the 1st PC of whole grain reflectance spectra

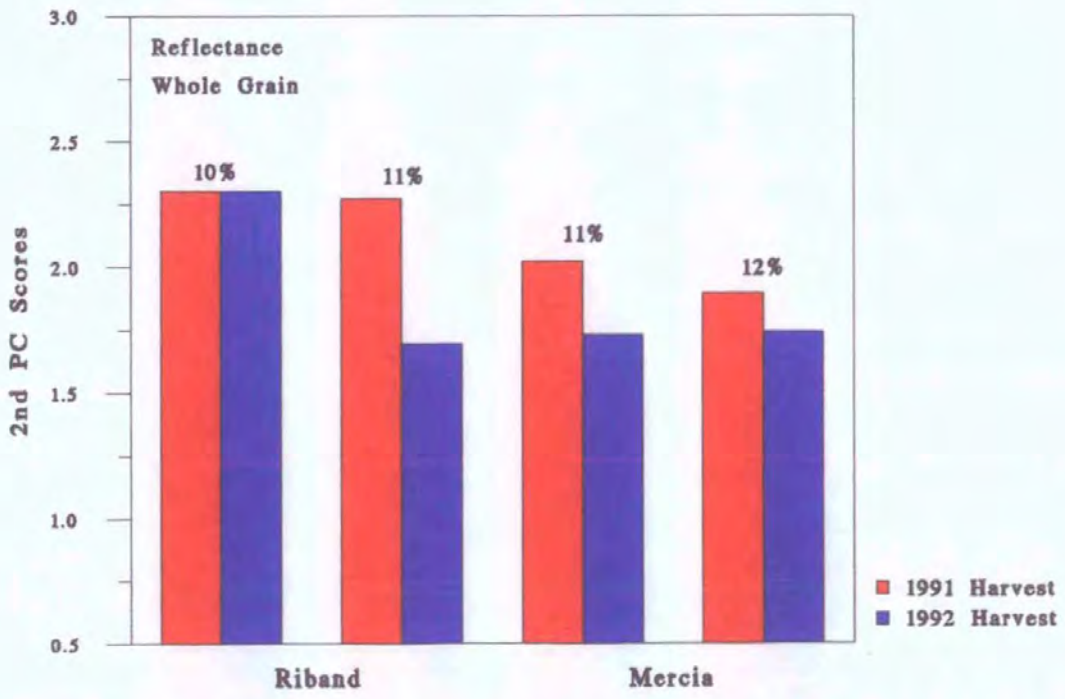

Figure 3.63 Bar graph to illustrate the effect of protein content and growing season on the 2nd PC of whole grain reflectance spectra

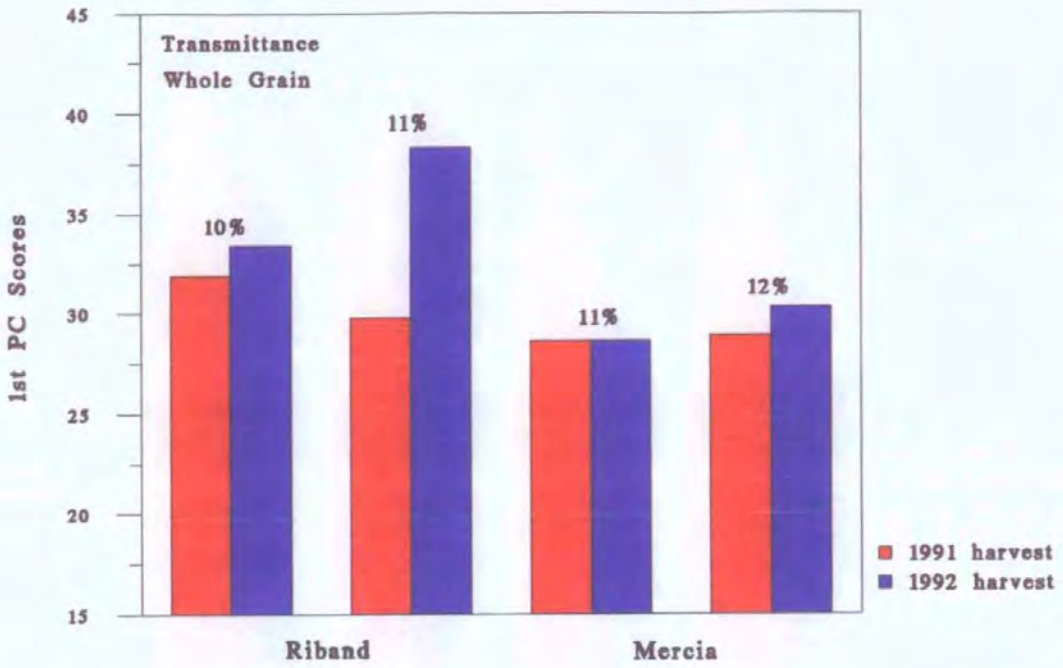

Figure 3.64 Bar graph to illustrate the effect of protein content and growing season on the 1st PC of whole grain transmittance spectra recorded on the NIRSystems Model 6500 spectrophotometer

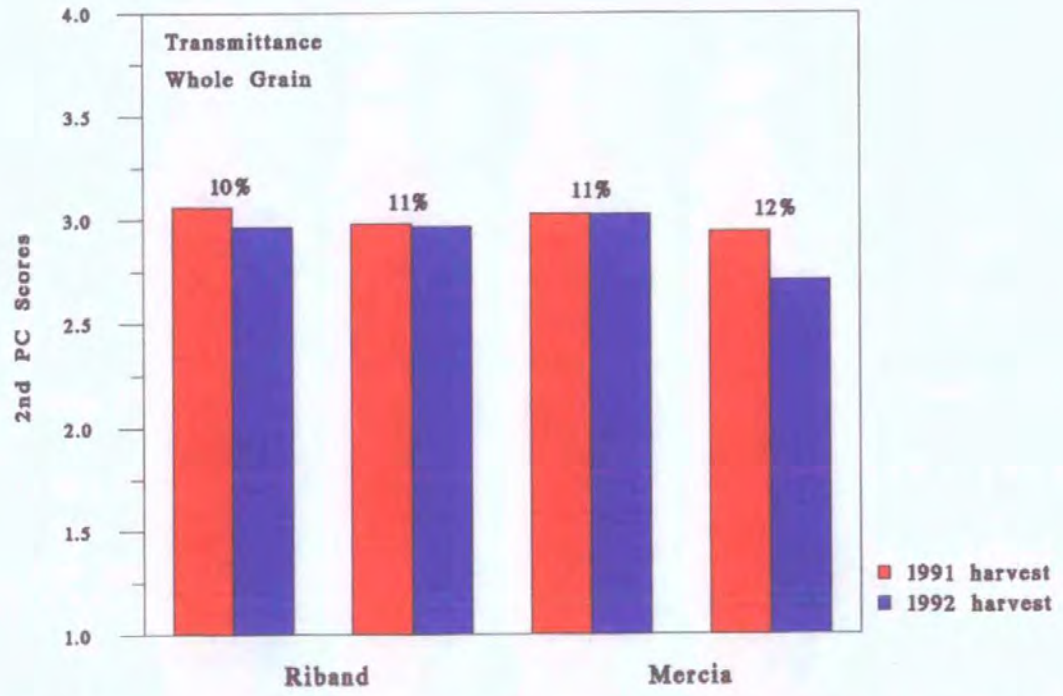

Figure 3.65 Bar graph to illustrate the effect of protein content and growing season on the 2nd PC of whole grain transmittance spectra recorded on the NIRSystems Model 6500 spectrophotometer

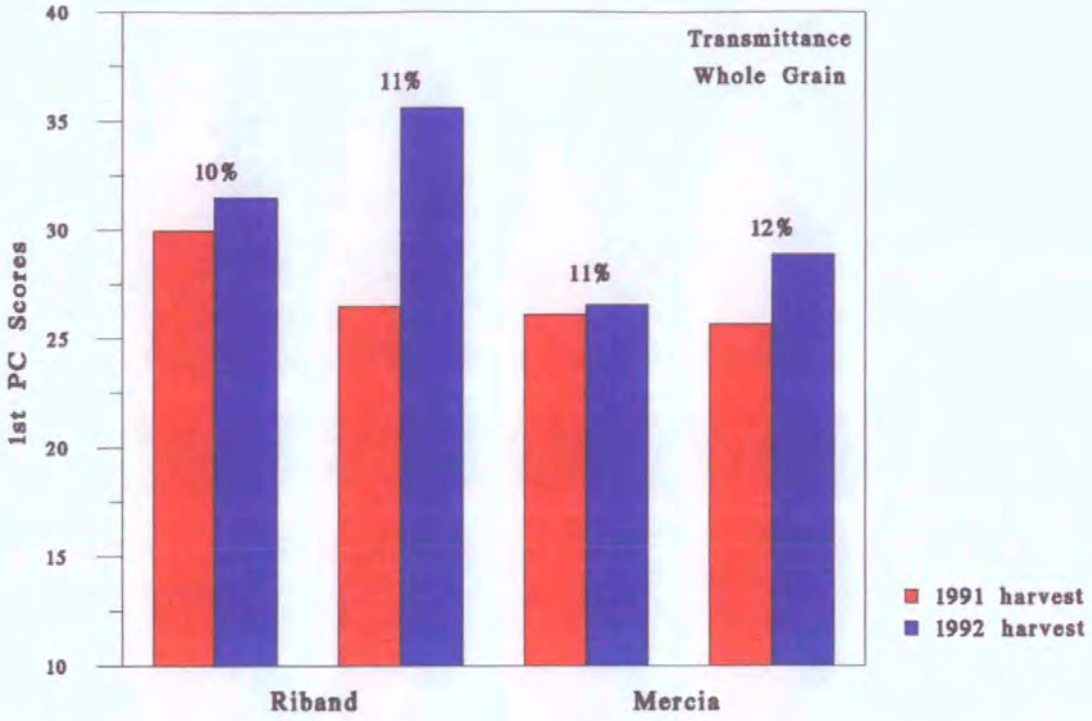

Figure 3.66 Bar graph to illustrate the effect of protein content and growing season on the 1st PC of whole grain transmittance spectra recorded on the Infratec Model 1225 spectrophotometer

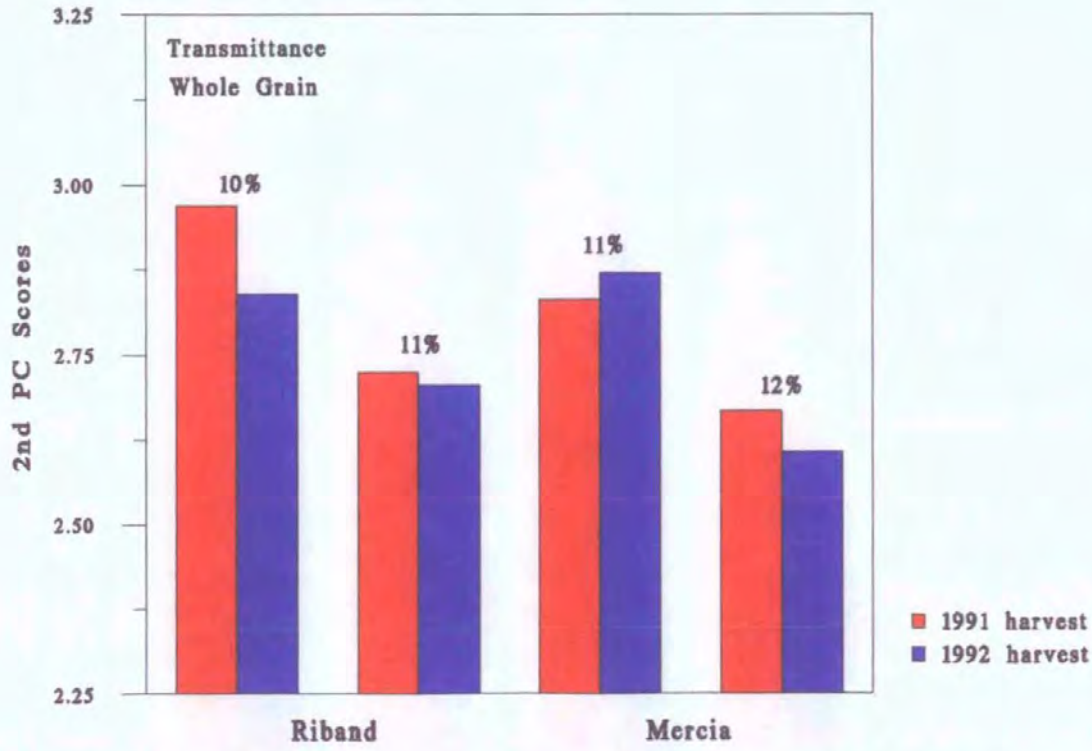

Figure 3.67 Bar graph to illustrate the effect of protein content and growing season on the 2nd PC of whole grain transmittance spectra recorded on the Infratec Model 1225 spectrophotometer

3.7 Relationship between NIR measurements and physical property measurements

Correlations between NIR measurements (1st PC and AACC NIR wheat hardness) and the physical property measurements (Parameter A and Parameter B) are shown in Figures 3.68 to 3.75.

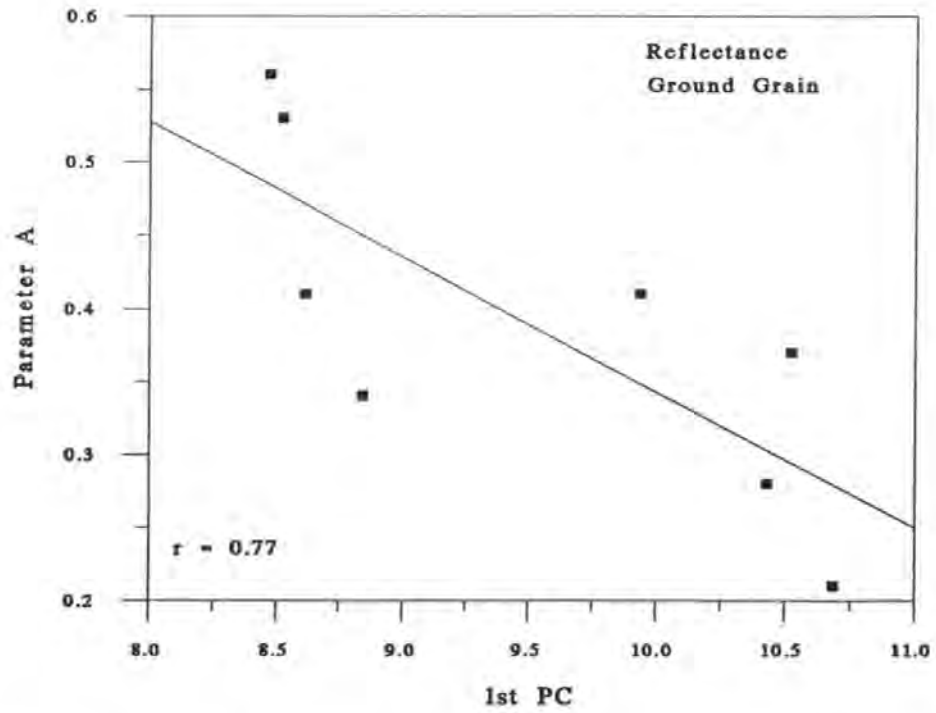

Figure 3.68 Correlation plot of Parameter A and 1st PC scores for ground grain reflectance

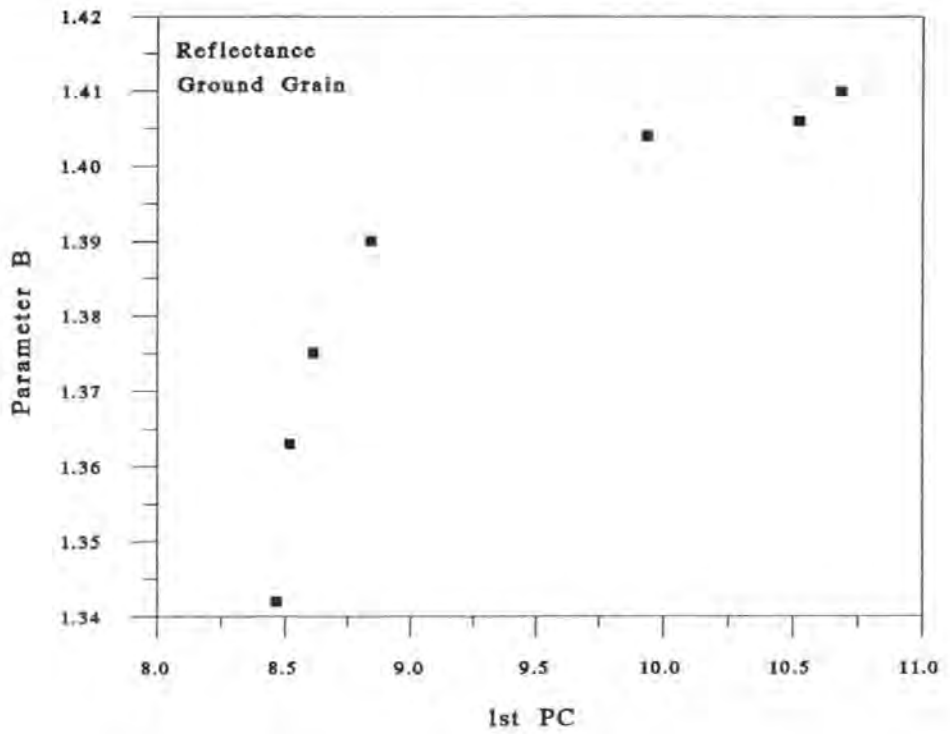

Figure 3.69 Correlation plot of Parameter B and 1st PC scores for ground grain reflectance

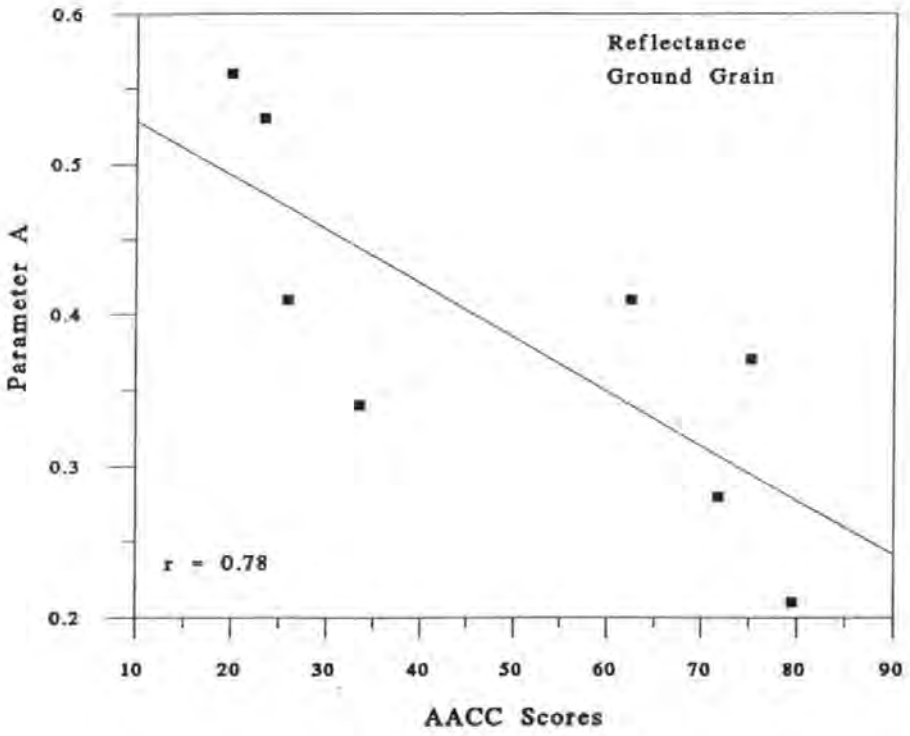

Figure 3.70 Correlation plot of Parameter A and AACC scores for ground grain reflectance

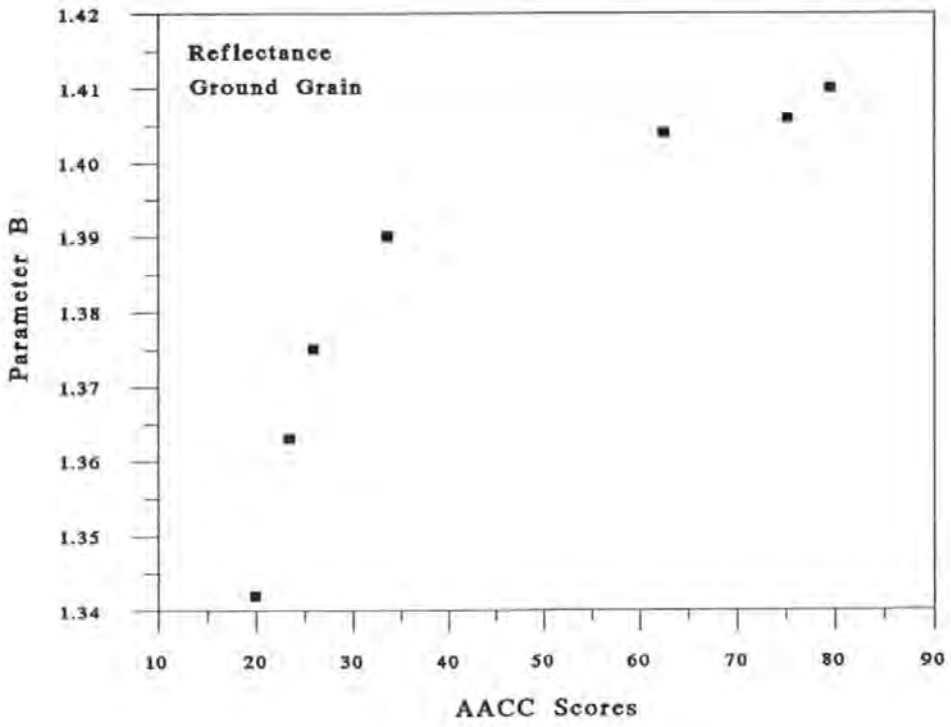

Figure 3.71 Correlation plot of Parameter B and AACC scores for ground grain reflectance

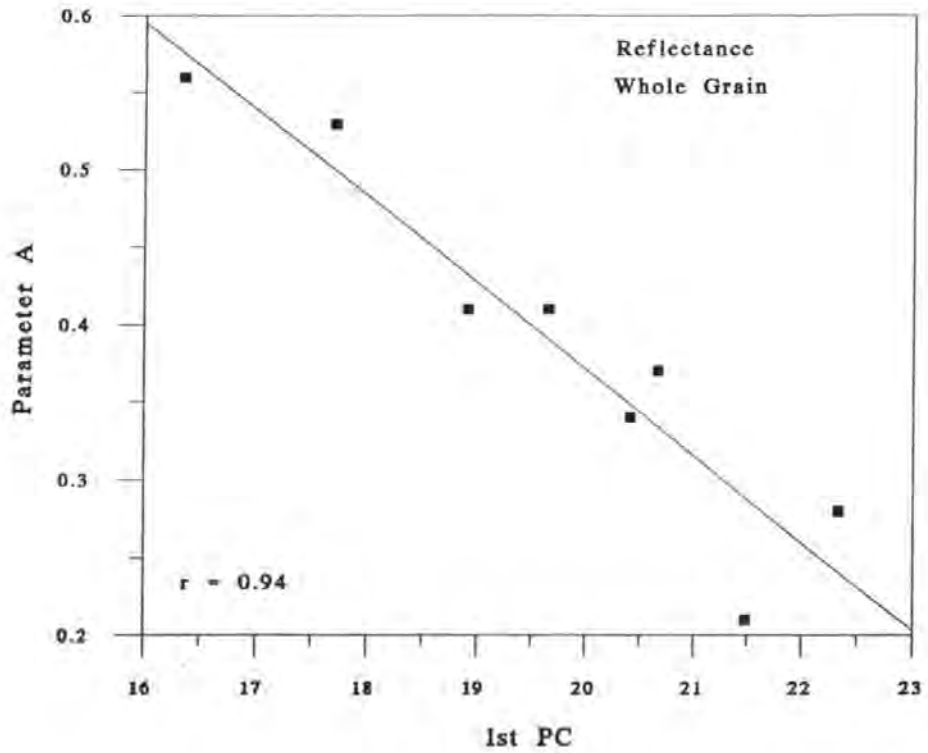

Figure 3.72 Correlation plot of Parameter A and 1st PC scores for whole grain reflectance

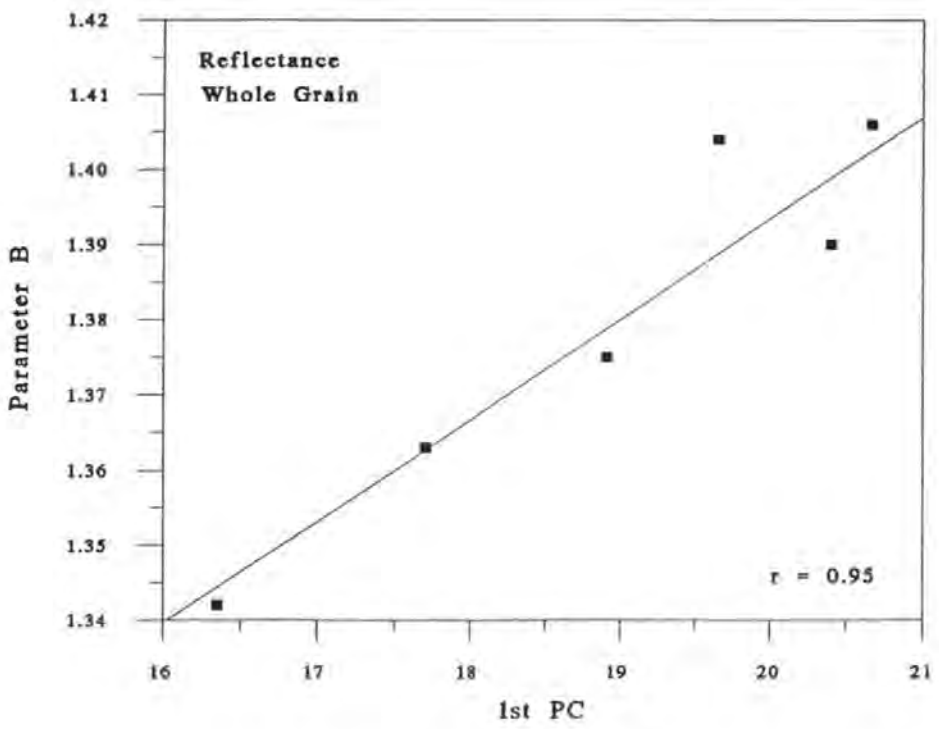

Figure 3.73 Correlation plot of Parameter B and 1st PC scores for whole grain reflectance

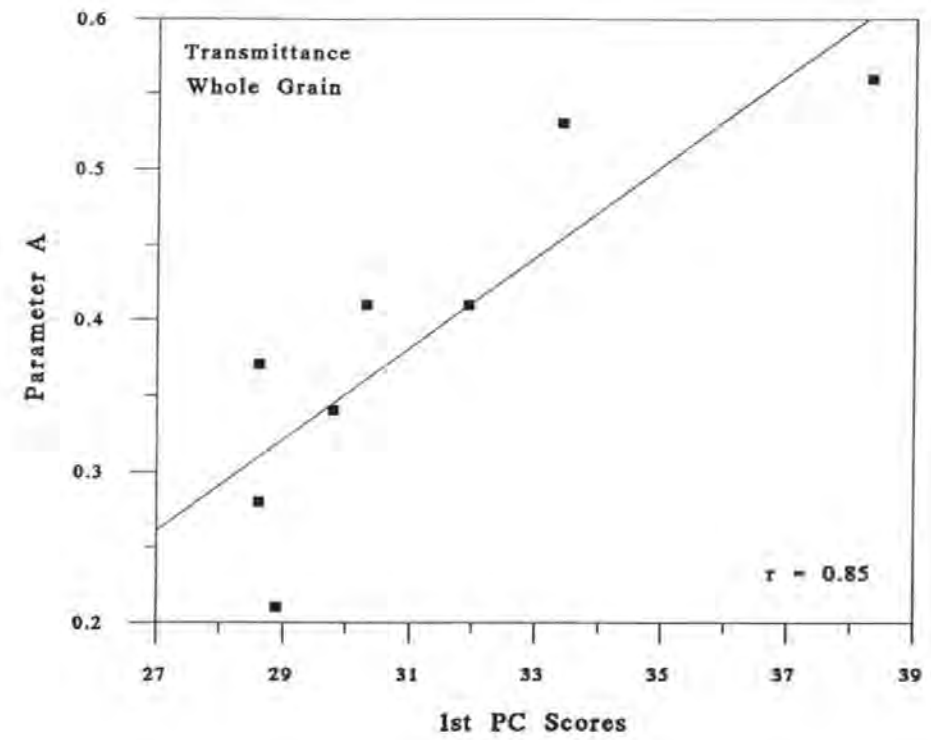

Figure 3.74 Correlation plot of Parameter A and 1st PC scores for whole grain transmittance

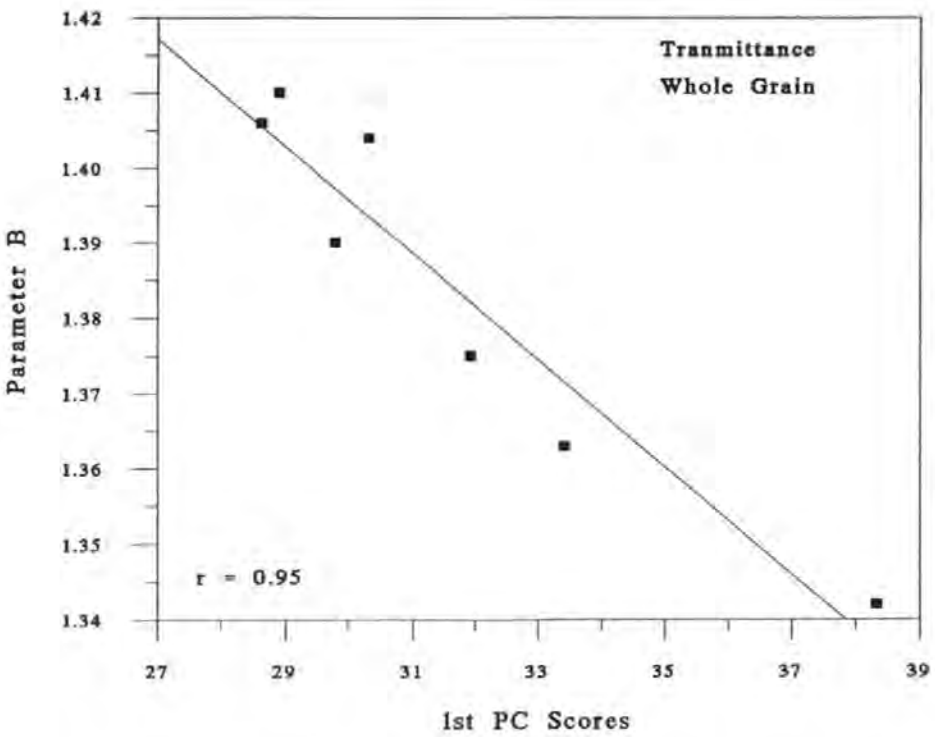

Figure 3.75 Correlation plot of Parameter B and 1st PC scores for whole grain transmittance

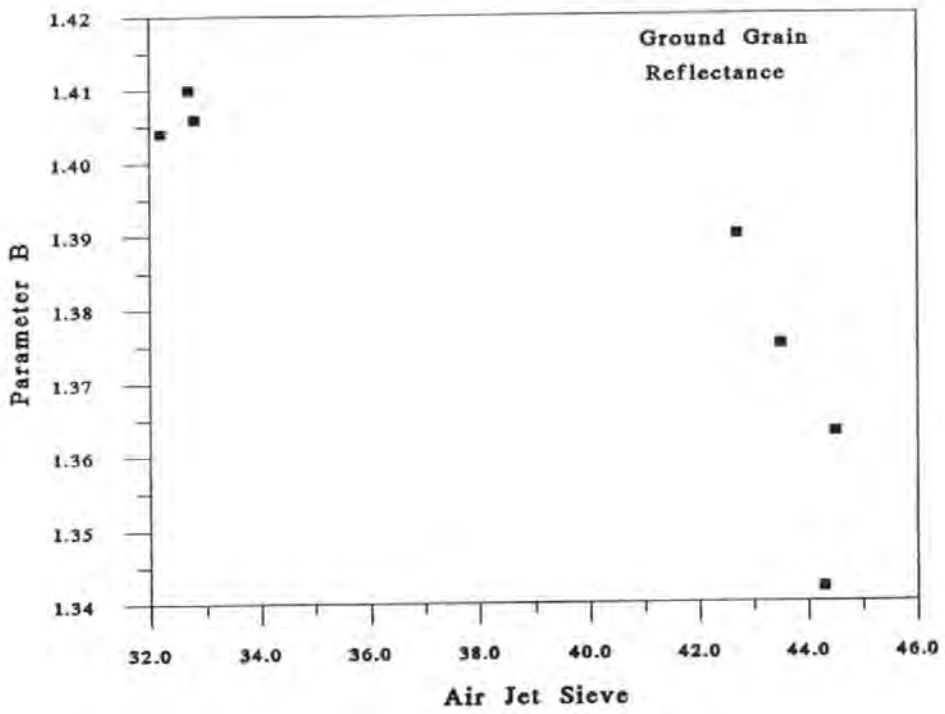

Figure 3.75 Correlation plot of Parameter B and Air Jet Sieve values

3.8 Single kernel analysis

Figures 3.77 to 3.86 show single kernel spectra of hard and soft UK home-grown wheats and hard, soft and durum Canadian home-grown wheats, respectively.

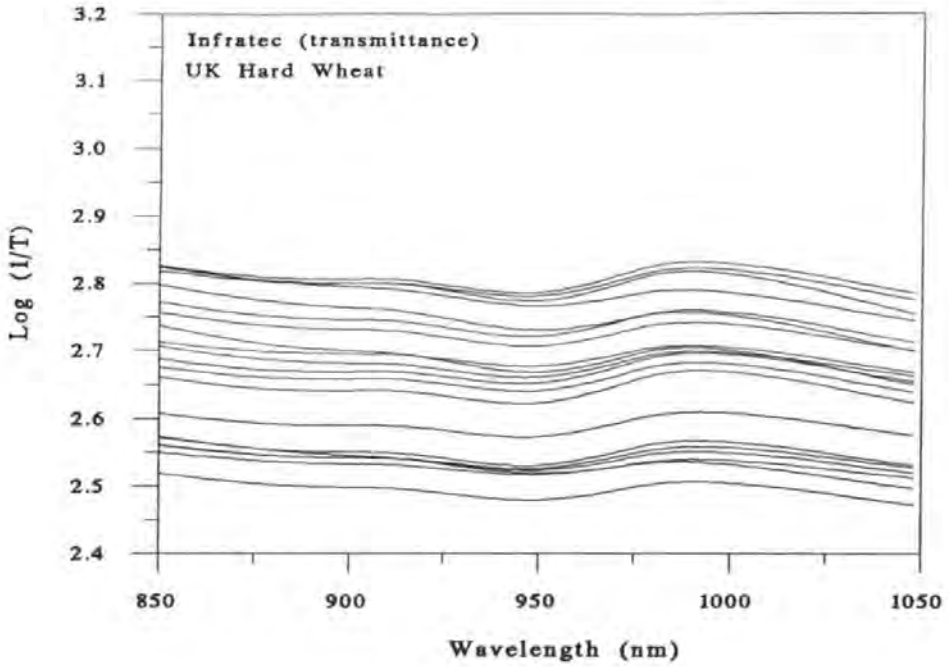

Figure 3.77 Single kernel, transmittance spectra of an UK home-grown hard wheat (20 kernels of Mercia) recorded on the Infratec Model 1225

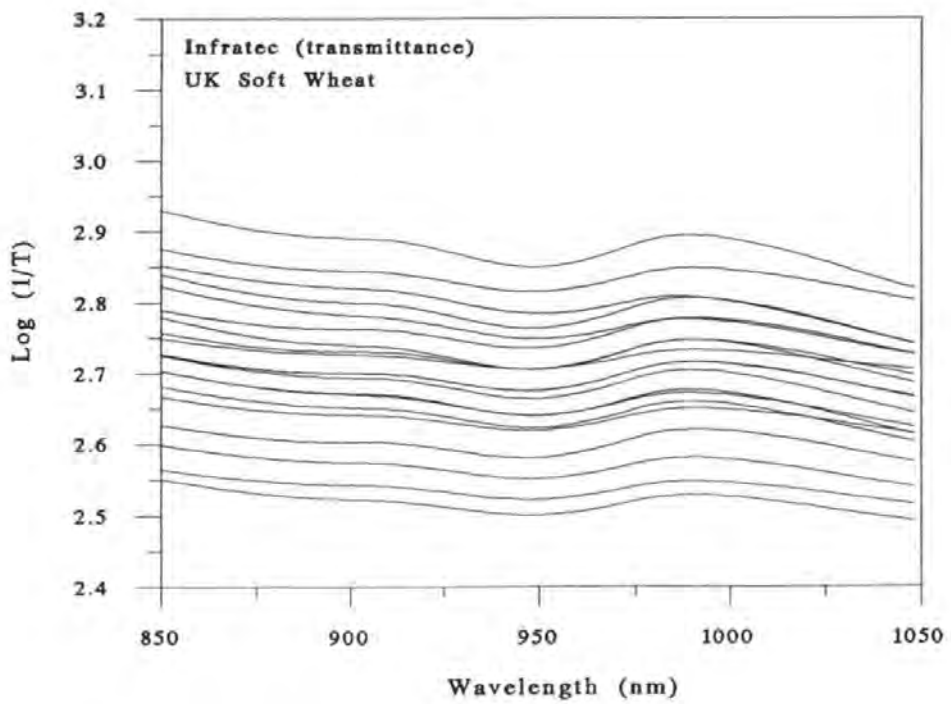

Figure 3.78 Single kernel, transmittance spectra of an UK home-grown soft wheat (20 kernels of Riband) recorded on the Infratec Model 1225

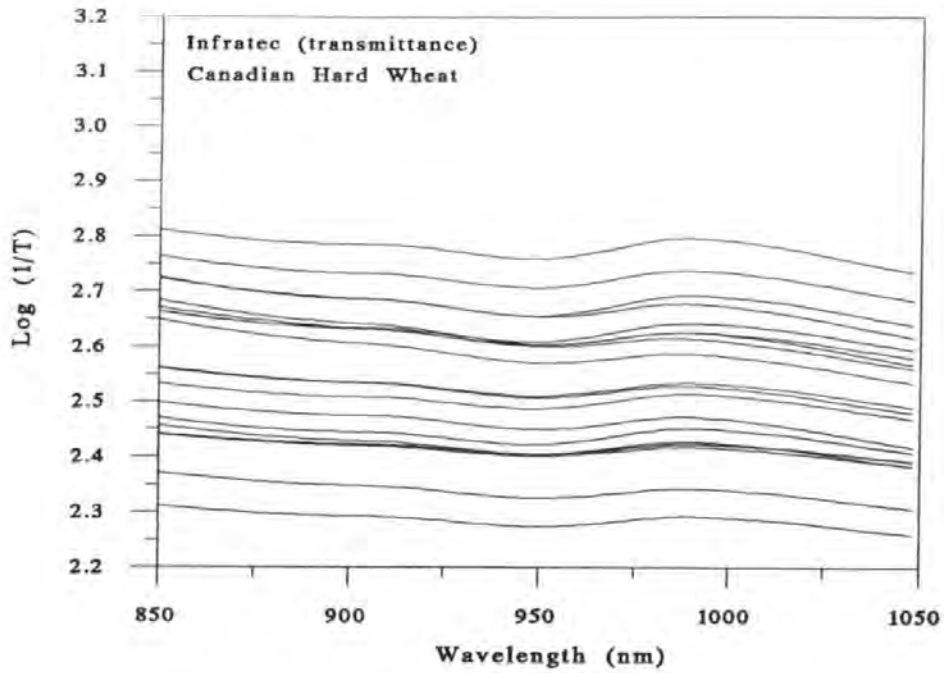

Figure 3.79 Single kernel, transmittance spectra of a Canadian home-grown hard wheat (20 kernels of HRS PC86) recorded on the Infratec Model 1225

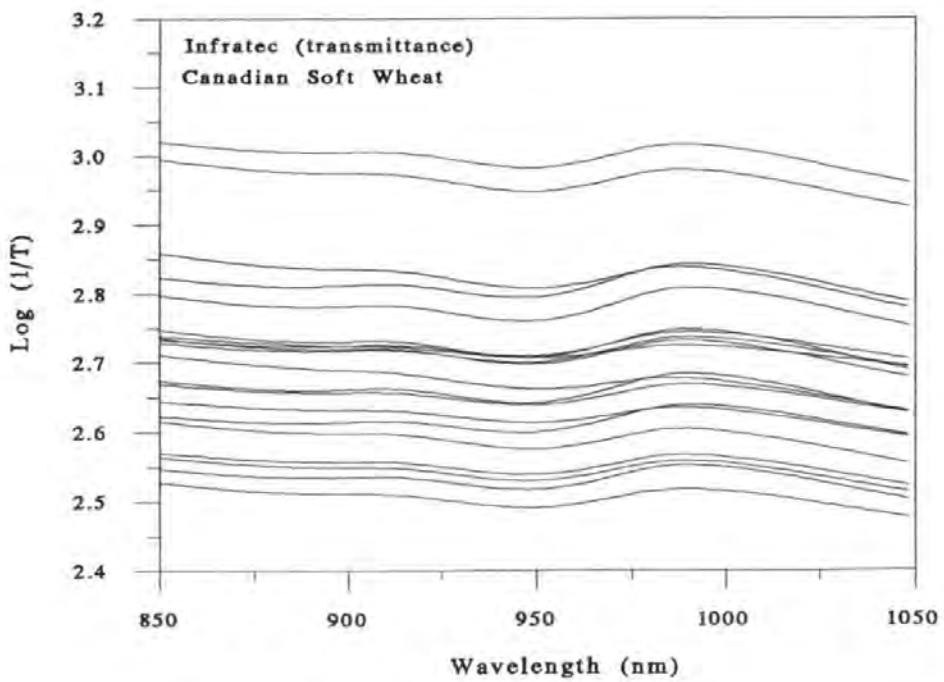

Figure 3.80 Single kernel, transmittance spectra of a Canadian home grown soft wheat (20 kernels of Augusta) recorded on the Infratec Model 1225

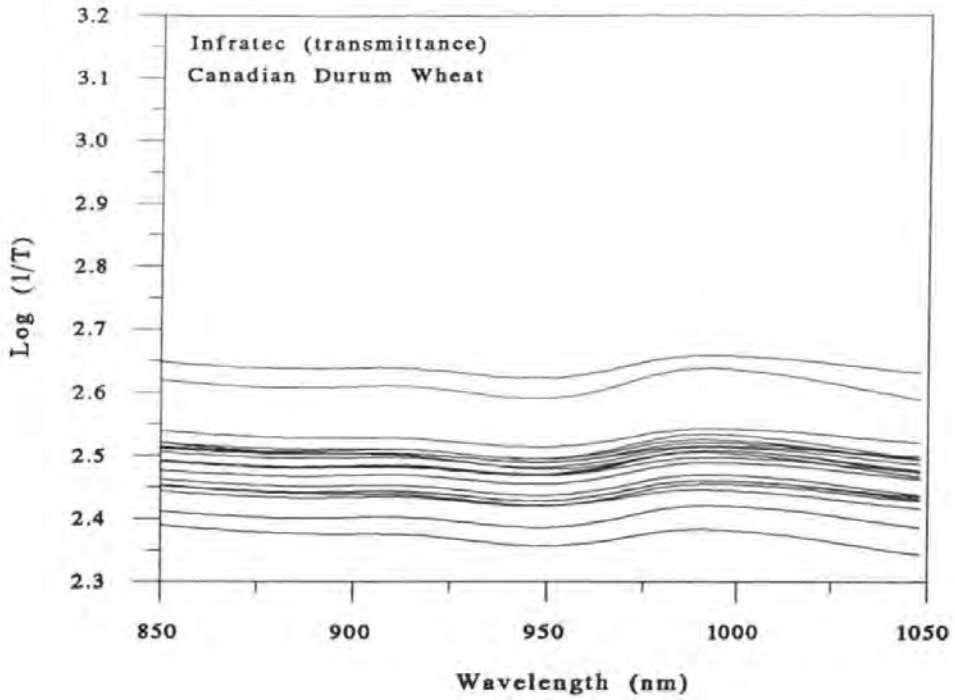

Figure 3.81 Single kernel, transmittance spectra of a Canadian home-grown durum wheat (20 kernels of 1CWAD) recorded on the Infratec Model 1225

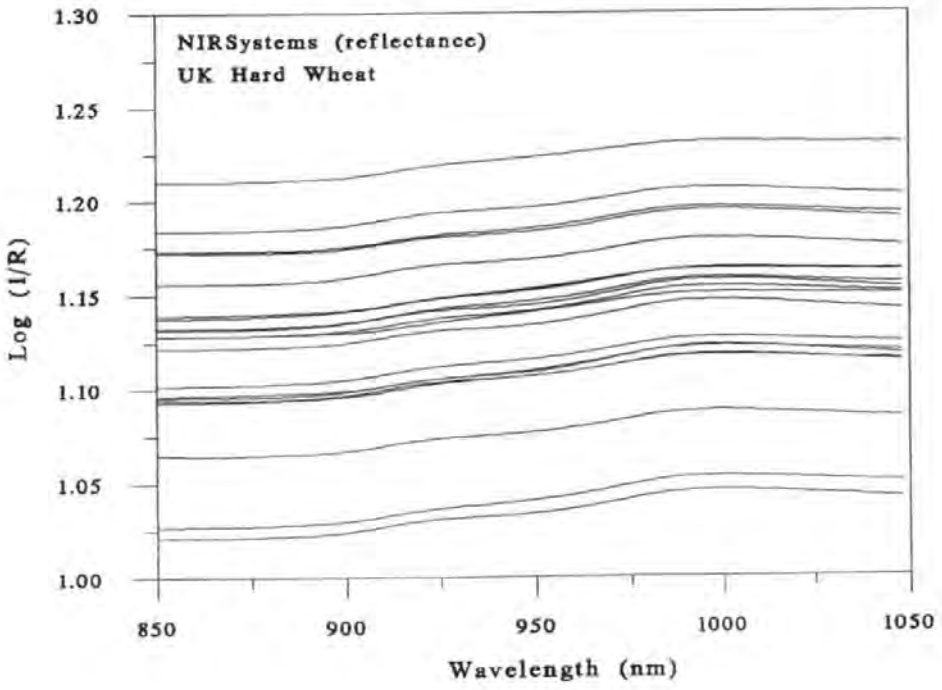

Figure 3.82 Single kernel, reflectance spectra of an UK home-grown hard wheat (20 kernels of Mercia) recorded on the NIRSystems Model 6500

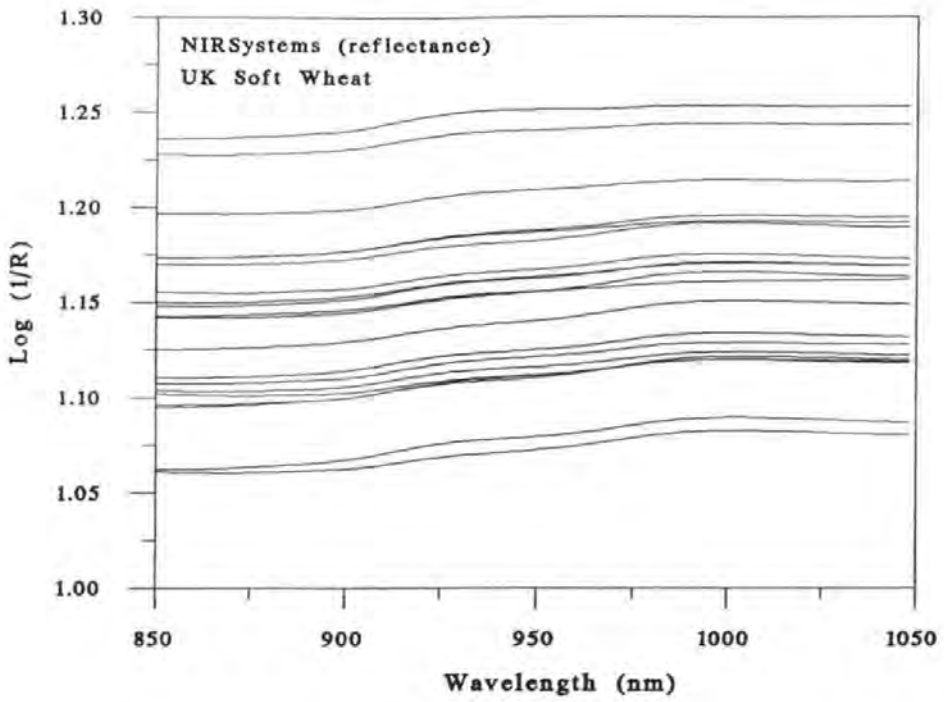

Figure 3.83 Single kernel, reflectance spectra of an UK home-grown soft wheat (20 kernels of Riband) recorded on the NIRSystems Model 6500

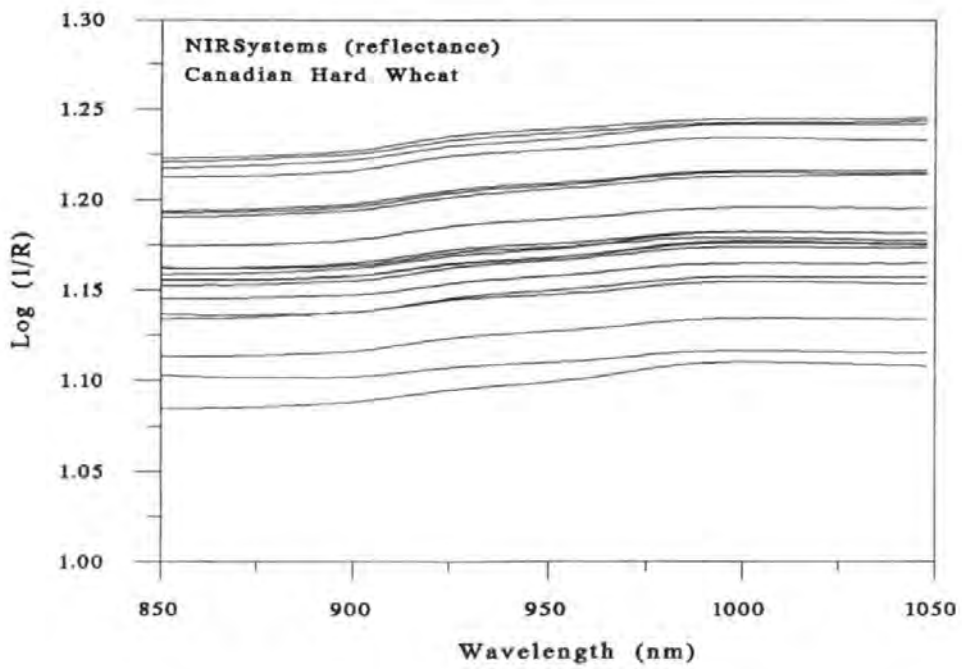

Figure 3.84 Single kernel, reflectance spectra of a Canadian home-grown hard wheat (20 kernels of HRS PC86) recorded on the NIRSystems Model 6500

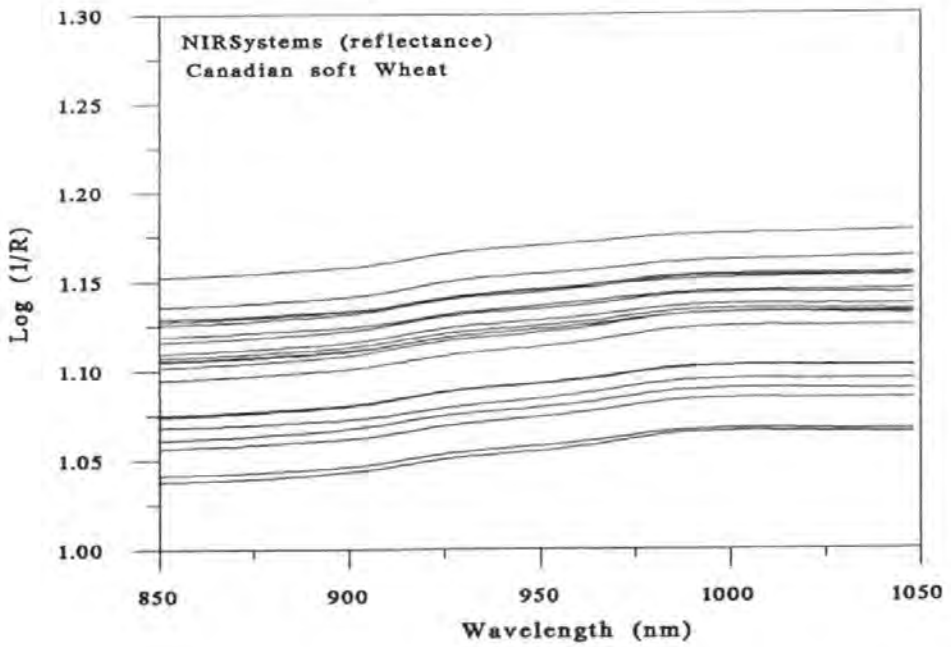

Figure 3.85 Single kernel, reflectance spectra of a Canadian home-grown soft wheat (20 kernels of Augusta) recorded on the NIRSystems Model 6500

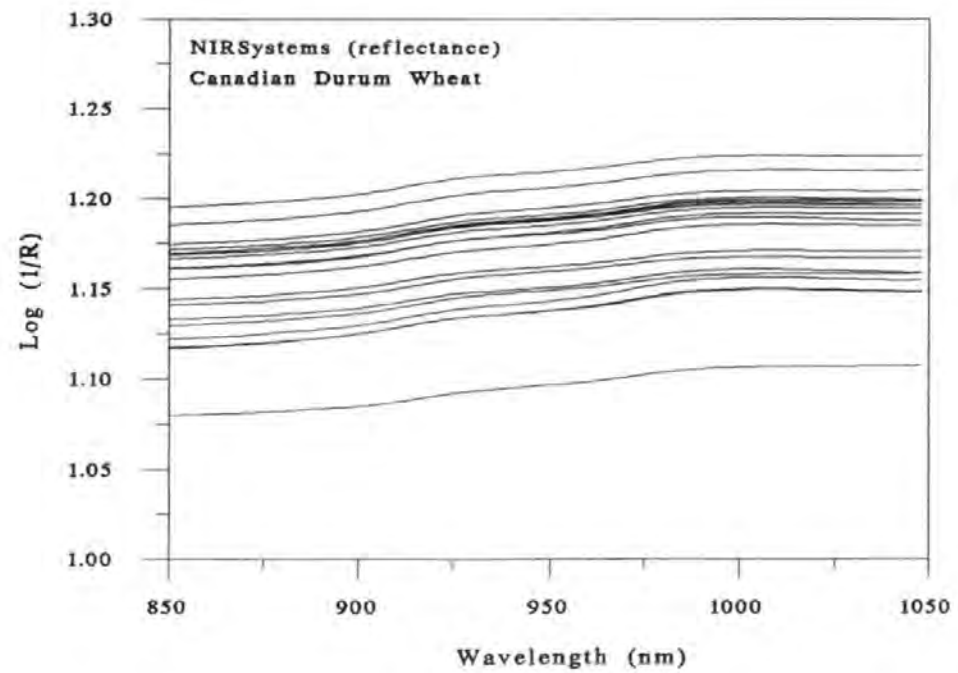

Figure 3.86 Single kernel, reflectance spectra of a Canadian home-grown durum wheat (20 kernels of 1CWAD) recorded on the NIRSystems Model 6500

Figure 3.87 to 3.89 show the mean spectrum and the first three principal components, respectively, for single kernel transmittance spectra recorded on the Infratec Model 1225 and Figure 3.90 the mean spectrum and the standard deviation for the same spectra.

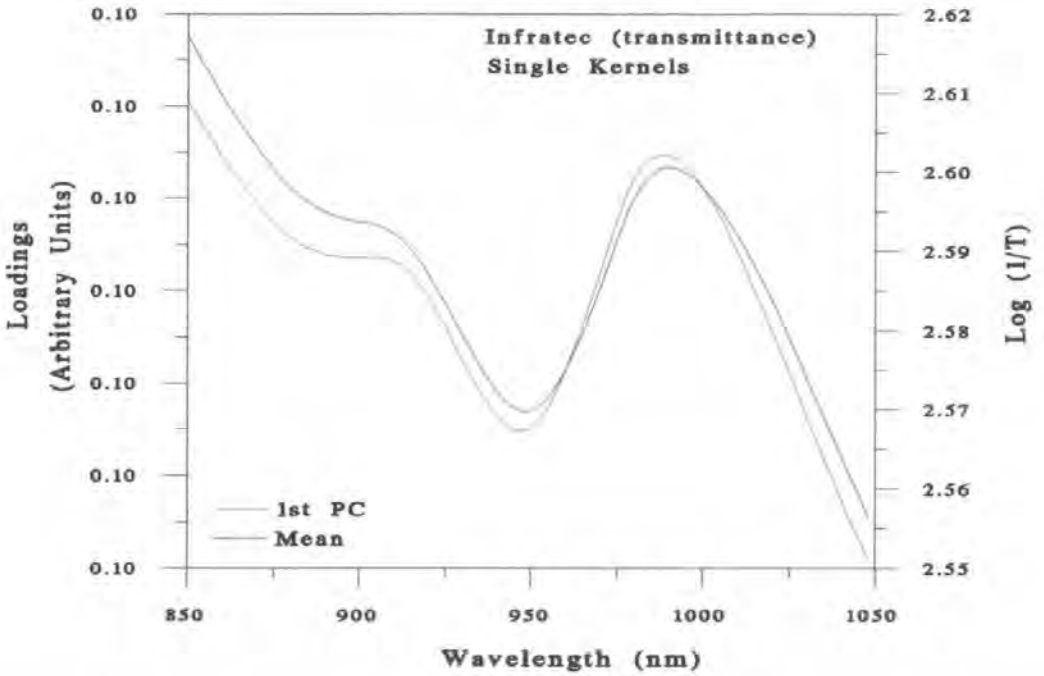

Figure 3.87 Plots of the mean spectrum and the loadings of the 1st PC for single kernel transmittance spectra

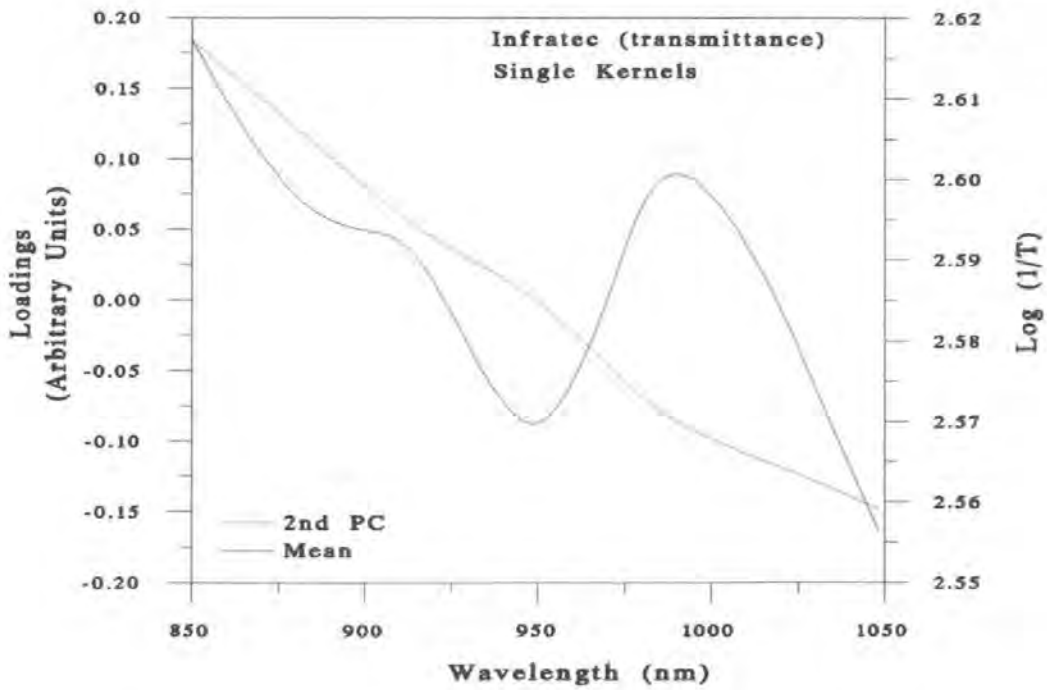

Figure 3.88 Plots of the mean spectrum and the loadings of the 2nd PC for single kernel transmittance spectra

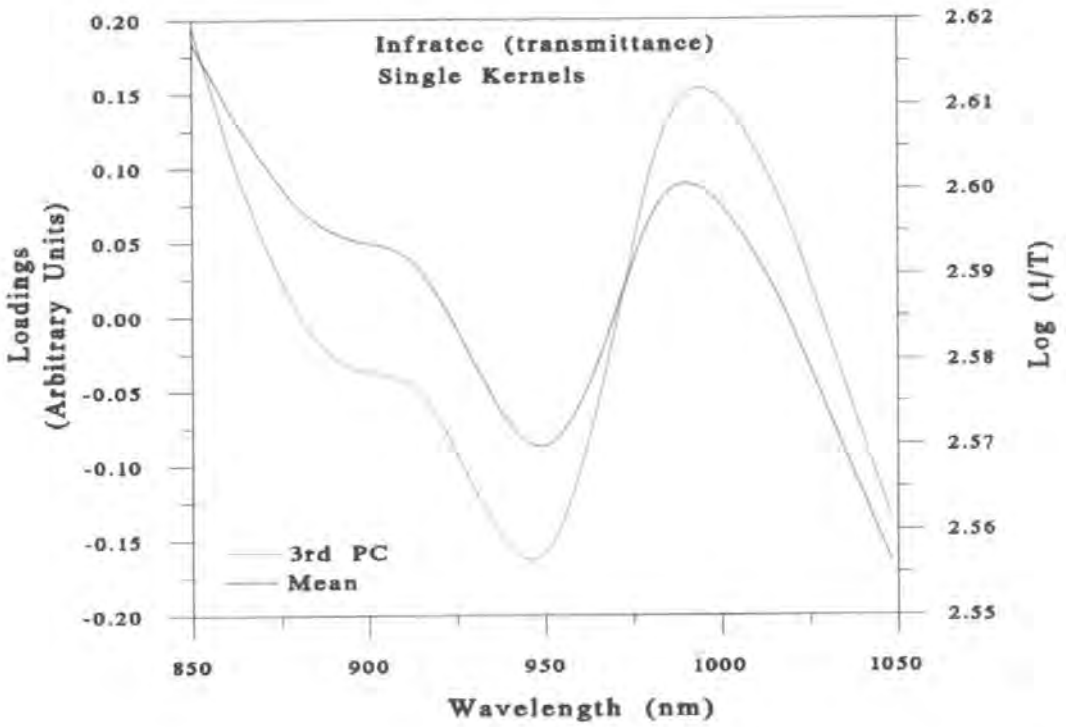

Figure 3.89 Plots of the mean spectrum and the loadings of the 3rd PC for single kernel transmittance spectra

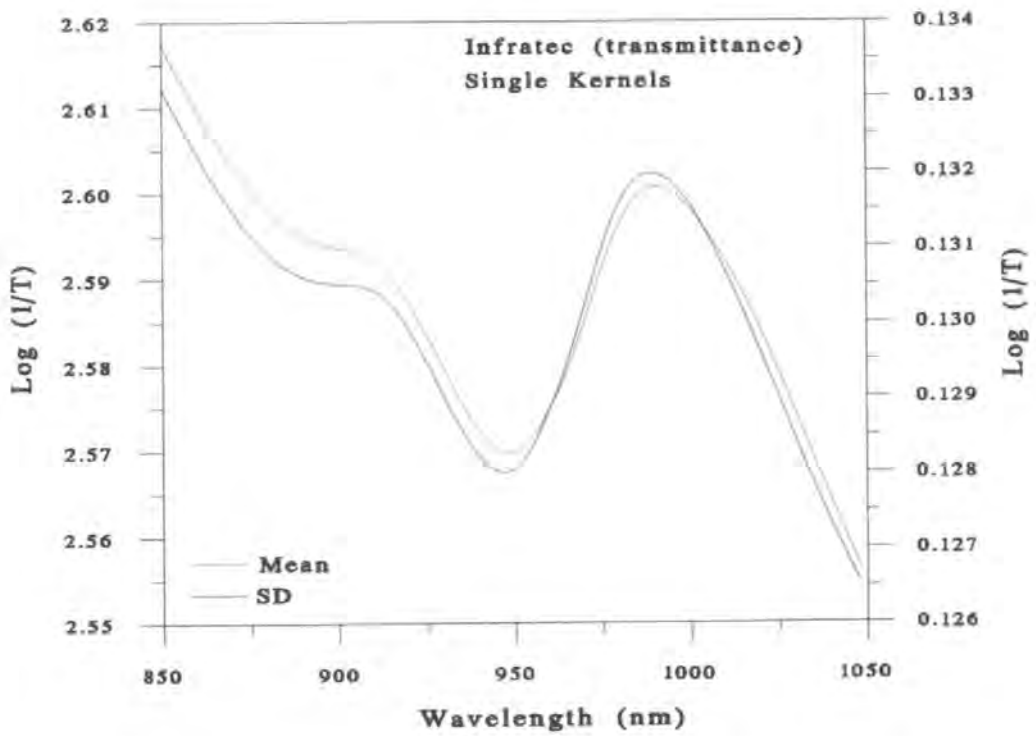

Figure 3.90 Plots of the mean spectrum and the standard deviation for single kernel transmittance spectra

Figure 3.91 to 3.93 show the mean spectrum and the first three principal components, respectively, for single kernel reflectance spectra recorded on the NIRSystems Model 6500 and Figure 3.94 the mean spectrum and the standard deviation for the same spectra.

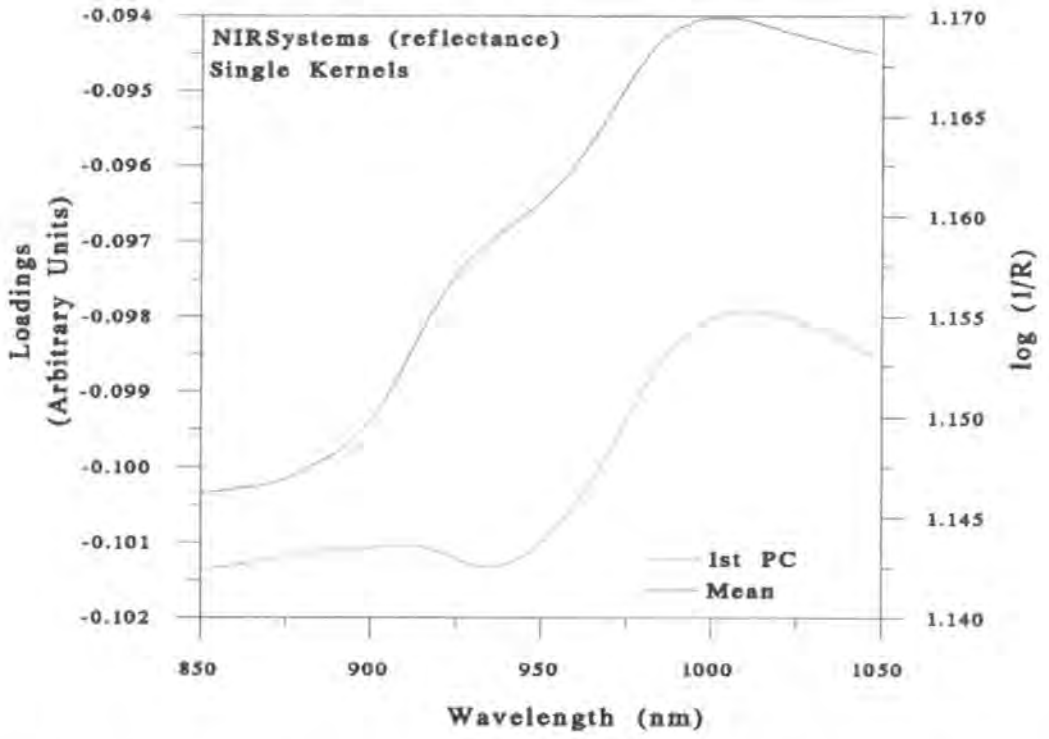

Figure 3.91 Plots of the mean spectrum and the loadings of the 1st PC for single kernel reflectance spectra

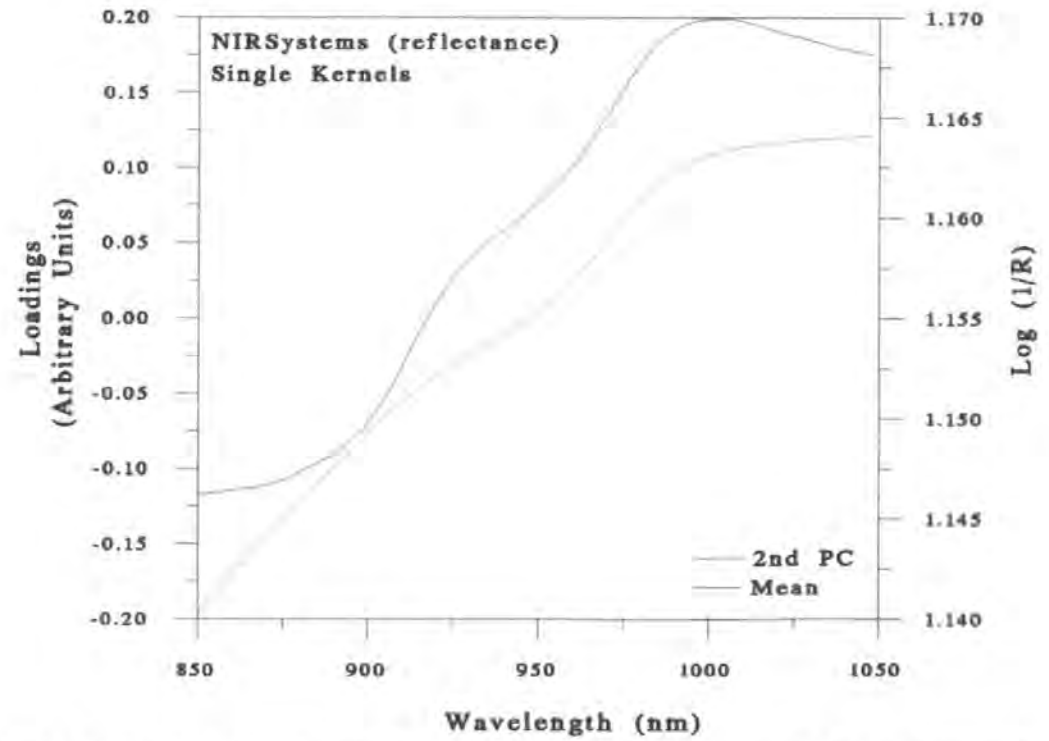

Figure 3.92 Plots of the mean spectrum and the loadings of the 2nd PC for single kernel reflectance spectra

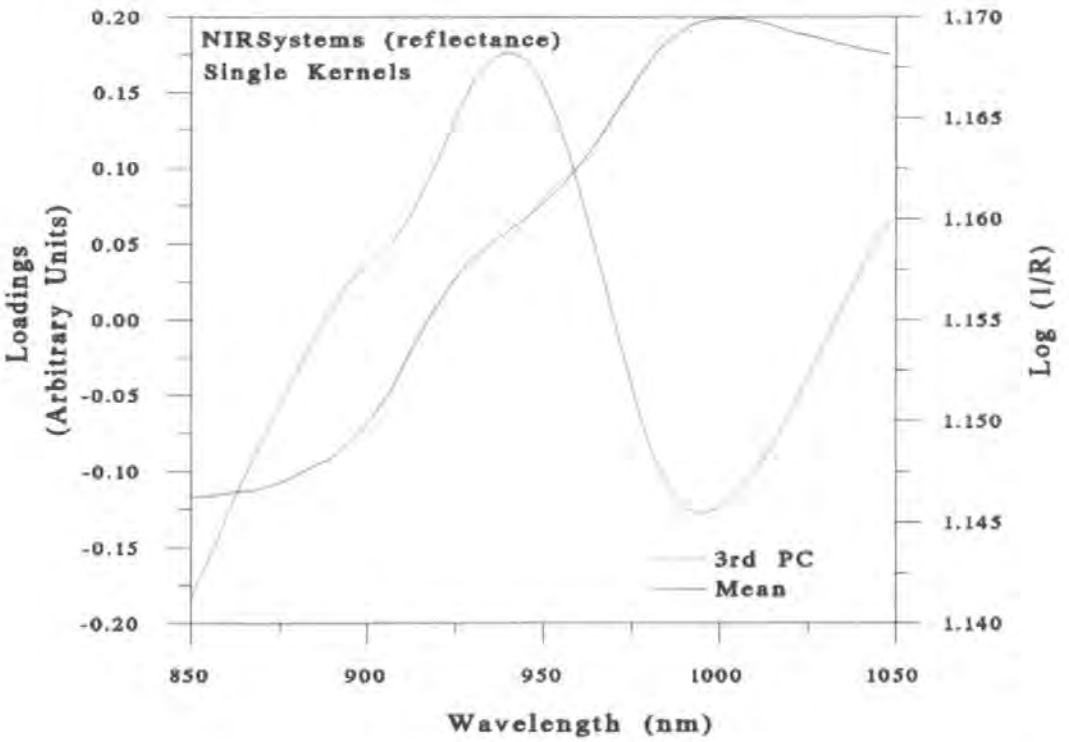

Figure 3.93 Plots of the mean spectrum and the loadings of the 3rd PC for single kernel reflectance spectra

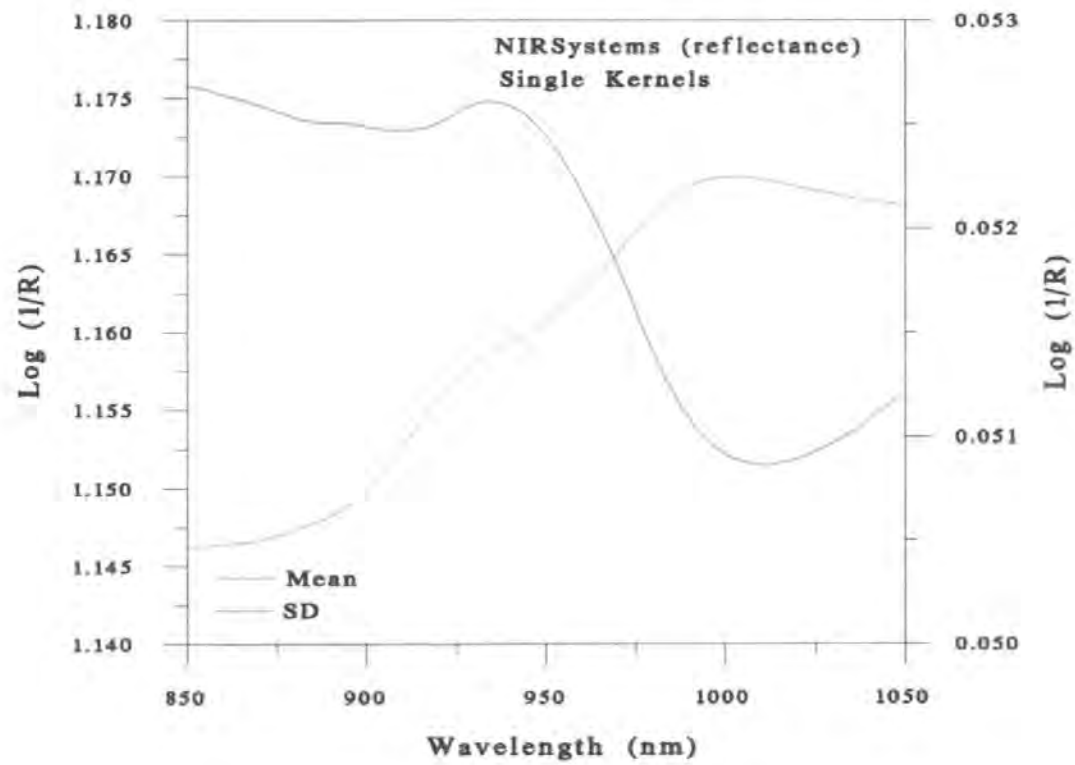

Figure 3.94 Plots of the mean spectrum and the standard deviation for single kernel reflectance spectra

Chapter 4

Discussion

4.0 DISCUSSION

4.1 Wheat hardness measurements

The Air Jet Sieve (AJS) and Particle Size Index (PSI) tests are currently the two most commonly used tests for measuring wheat hardness. These methods are used successfully as reference methods (AJS used by CCFRA and PSI used by CGC) to calibrate the NIR spectrophotometer for hardness measurements on flour as illustrated by Williams & Sobering (1986). The NIR wheat hardness test is internationally accepted by the AACC (AACC, 1989).

The AJS, PSI and AACC NIR wheat hardness test results, measured for all 104 wheat samples are presented in Chapter 3, Tables 3.1 to 3.4 and the correlations between AJS and PSI and AJS, PSI and AACC NIR wheat hardness tests are shown in Figures 3.1 & 3.2, respectively. Table 3.5 shows descriptive statistical results for the AJS, PSI and the AACC NIR wheat hardness test results for all of the 104 samples and Tables 3.6 & 3.7 show similar wheat hardness measurement statistical results for the calibration set and validation set used for the NIR calibrations.

The AJS, PSI and AACC NIR wheat hardness methods are highly correlated to each other and so either could be used as a reference method ($r = 0.92$ (AJS vs PSI); $r = -0.92$ (AJS vs AACC); $r = -0.91$ (PSI vs AACC)). This is expected, as although these three methods are different to some extent, they are all based on the differences in the particle size of the ground wheat grain. The samples were divided into a calibration set and a prediction set, as shown in Tables 3.6 & 3.7, in such a way that both sets cover similar ranges of hardness with similar standard deviations, which is desirable. It is important that the calibration set

covers the same range as the samples that would be tested in future.

4.2 NIR spectroscopy measurements

4.2.1 Determination of accuracy and precision of the NIR spectrophotometer

As far as NIR measurements are concerned, the most important factor to ensure accurate results, apart from sampling, sample preparation and the reference data, is the instrument. It is therefore important to monitor the stability of the instrument at all times. The importance of measuring noise in spectrophotometers and understanding the noise sources have been stressed by Norris (1992). The NIRSystems Model 6500 spectrophotometer is provided with diagnostics software which enables the measurement of noise to monitor the stability of the instruments.

Typical reflectance and transmittance noise spectra for the NIRSystems Model 6500 are displayed in Chapter 3, Figures 3.3 and 3.5, respectively, as five replicates measured at the same time. Average reflectance and transmittance noise spectra of five replicates measured at the same time over a four month period are displayed in Figures 3.4 and 3.6, respectively.

The figures show that the noise spectra obtained from the Model 6500 over a four month period are typical of an instrument performing at a high degree of stability. The instrument performance was monitored throughout the study. Based on these noise spectra, it was decided that it was acceptable to combine spectra collected over a period of time into one sample set.

The Infratec Food and Feed Analyzer Model 1225 is not equipped with noise diagnostics software. The performance of the instrument would therefore only be monitored by

recording spectra of standards or control samples. Norris (1992) described a procedure on how the noise of a spectrophotometer can be extracted from a normal sample spectrum and could be a useful procedure to apply.

4.2.2 NIR measurements of wheat samples

The reflectance spectra of the ground wheat grain and the reflectance and transmittance spectra of the whole wheat grain of all 104 samples analyzed are presented in Chapter 3, Figures 3.7 to 3.26.

Visual inspection of wheat spectra

- *Ground grain reflectance spectra*

The ground grain spectra were illustrated in Figures 3.7, 3.11, 3.15, 3.16 & 3.23.

Hard wheat endosperm breaks down to larger particles than does that of soft wheat when ground to a meal or flour (Chapter 1, section 1.1.1). When irradiated by electromagnetic energy in the NIR region, larger particles absorb a higher proportion of energy while smaller particles cause more light scatter. The larger particles of the harder wheats will therefore give spectra with higher log 1/R values while the spectra of soft wheat exhibit lower log 1/R values. This effect can clearly be seen in the ground grain spectra shown in Figures 3.7, 3.11 & 3.23. Purely on visual inspection of the spectra, it is therefore easy to separate the genetically hard and soft wheats into two groups. However, it is not possible to separate visually the two groups in an increasing or decreasing range of hardness.

The spectra of Riband and Mercia illustrated in Figures 3.15 & 3.16 indicate different amounts of radiated energy absorbed for different protein levels as well as for the different

harvests within the same variety. It is, however, not possible to tell which of the two variables has the greater effect. The effect of moisture on the AACC NIR wheat hardness scores was reported by Brown *et al.* (1993) and found to be more variable than that of American wheats. The effect of protein content and growing season on the AACC wheat hardness scores were also reported.

- *Whole grain reflectance spectra*

The whole grain reflectance spectra are illustrated in Figures 3.8, 3.12, 3.17, 3.18 & 3.24.

Figures 3.8, 3.12 & 3.24 clearly illustrate that separating the genetically hard and soft wheats into two groups based on visual inspection is not possible. The spectra of the soft wheats tend to show slightly different absorption trends in the 1600 - 1700 nm and 2200 - 2300 nm regions. These differences, however, are not pronounced enough to allow accurate separation between hard and soft wheats.

The whole grain spectra of Riband and Mercia illustrated in Figures 3.17 & 3.18 show different amounts of radiated light absorbed for different protein levels as well as for the different harvests within the same variety. Again, it is not possible to tell which of the two variables has the greater effect, but it is evident that the effect of protein and different harvests is greater on whole grain than ground grain spectra.

- *Whole grain transmittance spectra recorded on the Model 6500 spectrophotometer*

The whole grain transmittance spectra recorded on the NIRSystems Model 6500 spectrophotometer are illustrated in Figures 3.9, 3.13, 3.19, 3.20 & 3.25.

The whole grain transmittance spectra allow no clear separation between genetically hard

and soft wheats based on visual inspection (Figures 3.9 & 3.13). However, this holds only for the UK home-grown wheat samples. The Canadian home-grown soft wheats, show distinct differences in the 850 - 925 nm region (Figure 3.25).

The whole grain transmittance spectra of Riband and Mercia illustrated in Figures 3.19 & 3.20 show different amounts of radiated light absorbed for different protein levels as well as for the different harvests within the same variety. In this case it is also not possible to tell which of the two variables has the greater effect, but it is evident that the effect of protein and different harvests on whole grain spectra is again greater than that for ground grain spectra. The effect of different harvests is more pronounced in the case of the soft wheat variety, Riband.

- *Whole grain transmittance spectra recorded on Model 1225 spectrophotometer*

The whole grain transmittance spectra recorded on the Infratec Model 1225 are illustrated in Figures 3.10, 3.14, 3.21, 3.22 & 3.26.

The same differences between the hard and soft Canadian home-grown wheats were found for the Model 1225 spectrophotometer as for the Model 6500 (Figure 3.26). However, the Model 1225 exhibited lower levels of noise than the Model 6500 spectrophotometer. Apart from the differences in the 850-900 nm region for the Canadian home-grown wheat samples, it is not possible to separate between genetically hard and soft wheats purely on visual inspection of the spectra (Figures 3.10 & 3.14).

The whole grain transmittance spectra of Riband and Mercia illustrated in Figures 3.21 & 3.22 show similar results to the Model 6500. It is interesting to notice that in reflectance mode, analysis of hard whole wheat grain results in spectra with higher log 1/R values and

soft whole wheat grain in lower log 1/R values, while in transmittance mode the results are reversed. Therefore, in transmittance mode the soft wheat must exhibit less scattering.

Purely on visual inspection it is therefore straightforward to distinguish between hard and soft wheats on ground wheat grain spectra. In the case of whole wheat grain reflectance or transmittance spectra the separation is, however, not as clear, except for the Canadian home-grown whole wheat grain samples measured by NIR transmittance, which exhibit a distinct difference in the 850 - 900 nm region between hard and soft samples. The effect of different protein levels and different harvests within the same variety on the NIR spectroscopic measurements, is clearly demonstrated.

4.3 NIR spectroscopy calibrations

Successful NIR wheat hardness calibrations on ground wheat grain have been reported by previous workers (Williams, 1979; Miller *et al.*, 1982; Williams & Sobering, 1986; Randall *et al.*, 1992). However, NIR wheat hardness calibrations on whole wheat grain have only been reported in limited cases for Canadian home-grown wheat samples (Williams, 1991; Williams & Sobering, 1993).

In this study, empirical wheat hardness calibrations were developed based on the published wheat hardness calibrations (Williams & Sobering, 1993). The purpose of this was to establish a link between the present study and current knowledge of whole wheat grain hardness measurements by NIR. Empirical wheat hardness calibration equations were derived by means of partial least squares (PLS) regressions on the raw data with no scatter correction and no mathematical treatment. Three different reference methods were used i.e. AJS, PSI and AACC NIR wheat hardness. The 'best' calibration equations were chosen based on:

- the lowest standard error of prediction (SEP)
- the equation selected by the software employing internal cross-validations

The calibration equations were derived for the same data set, using three different software packages.

4.3.1 Empirical calibrations

Calibration and validation results obtained for the empirical NIR calibrations for ground grain reflectance, whole grain reflectance and whole grain transmittance are shown in Chapter 3, Tables 3.8, 3.9 & 3.10, respectively. The SEC, r and SEP are as quoted by the different software packages for each of the three different reference methods.

(i) Ground grain reflectance

- *NIR Calibrations using AJS and PSI hardness tests as reference methods, respectively*

The results in Table 3.8 indicate that **hardness can be measured by NIR on ground grain with a high degree of accuracy**. The SEP for AJS is 1.45 % with r = 0.98. As expected, internal cross-validations selected a calibration equation resulting in a slightly higher SEP than the equations selected based on lowest SEP after external validation. However, cross-validation calibration equations did not always have fewer terms than the lowest SEP equation as one would have expected. Almost identical results were obtained for ISI, NSAS and UNSCRAMBLER software packages. The only differences were the slight difference in the SEC results of UNSCRAMBLER and the SEP results of NSAS. These differences will be discussed in more detail below.

(ii) Whole grain reflectance

- *NIR Calibrations using AJS, PSI and AACC NIR wheat hardness tests as reference methods*

The results in Table 3.9 indicate that **hardness cannot be measured by NIR reflectance on whole grain with the same degree of accuracy as in the case of ground grain** (SEP for AJS = 3.76; r = 0.90). In the first instance when calibrating for ground grain both the reference and the NIR measurements are based on particle size differences. Therefore, both methods employ the same characteristic. For whole grain NIR hardness measurements, particle size could not have been the characteristic measured as no grinding was involved. However, the reference methods used measure particle size and are currently the best available reference methods. The same characteristic was therefore not involved in these respective measurements. What characteristic is actually measured by NIR spectroscopy and used to predict whole wheat grain hardness is not clear as yet.

The same differences as for ground grain were observed between the different software packages.

(iii) Whole grain transmittance

- *NIR Calibrations using AJS, PSI and AACC NIR wheat hardness tests as reference methods*

The results in Table 3.10 indicate that **hardness cannot be measured by NIR transmittance on whole grain with the same degree of accuracy compared to both ground grain and whole grain reflectance** (SEP for AJS = 5.06; r = 0.83). The calibrations were developed on the spectra recorded on the NIRSystems Model 6500. The level of noise was higher than was the case for the Infratec Model 1225.

There are several possible explanations for the higher level of noise:

- The path length used was not optimum for the measurement.

- The detector was too far from the sample.
- One detector situated directly behind the sample was not adequate. Additional detectors in 45° orientations might decrease the noise and subsequently improve the measurement.
- Insufficient sub-scans were taken when recording the spectra, but as the purpose of using NIR spectroscopy is to enable rapid measurements, recording more sub-scans is not a practical solution.

The different software packages gave results with similar differences as for ground grain calibrations. When cross-validations were used to choose the 'best' equation, an equation with less terms were selected as would be expected.

(iv) Comparison of empirical NIR calibrations

It is not possible to compare the SEP results of the calibration results of the different reference methods as the SEP is expressed in the units of the respective reference method. However, a comparison is possible by taking the ratio of the standard deviation of the validation set to the SEP as suggested by Williams & Sobering (1993). This statistic is called the RPD provides a basis for standardising the SEP. Williams & Sobering (1993) suggested that the RPD should be as high as possible with a value of 10 or over being excellent and equivalent or better than the reference method. Values of 5 - 10 should be adequate for quality control and values of 2.5 and over satisfactory for screening. Values of as high as ten would not normally be encountered for whole grain.

The RPD statistics calculated for the equations with the lowest SEP as well as the RPD statistics for hardness measurements by NIR for whole wheat grain, reported by Williams & Sobering (1993) are listed in Table 3.11. Table 3.11 also includes the RPD statistics for

whole wheat grain transmittance using the Infratec Food and Feed Analyzer Model 1225.

Table 3.11 shows the RPD statistics for the whole grain reflectance and transmittance calibration equations. In this study, the RPD statistics derived with PSI as the reference method do not correspond to those reported by Williams & Sobering (1993) (1.80 vs 3.32 and 1.62 vs 3.29, respectively), although the SEP result for whole grain reflectance (3.96) was very similar to those previously reported (3.52). The reason for this lies in the large differences in the standard deviations of the data sets. The standard deviation of the validation set used by Williams & Sobering (1993) was 11.10 for whole grain reflectance whereas for this study it was 7.12. A much higher standard deviation with a similar SEP will result in a higher RPD indicating a better dispersion of data. Based on the RPD statistics, the PSI and AACC NIR wheat hardness tests resulted in more accurate calibration equations in the case of whole grain analysis, but using AJS as the reference method resulted in more accurate calibration equations in the case of ground grain.

The spectra recorded on the Infratec Model 1225 did not result in more accurate calibration equations than the NIRSystems Model 6500 as would be expected considering the higher level of noise of the Model 6500 in transmittance mode.

Results obtained for whole wheat grain do not predict hardness as accurately as is necessary for quantitative measurements, but still with acceptable accuracy. However, to illustrate whether it is possible, at least, to distinguish between the genetically hard and soft wheats from the calibration equations derived, the results were expressed as bar graphs.

The wheat hardness results of the validation set measured by the reference methods (AJS, PSI and AACC NIR wheat hardness, respectively) and the results predicted by the

calibration equations derived were plotted as bar graphs. Cut off points for genetically hard and soft wheats were as follows:

- percentage throughs higher than 40 indicate soft wheat samples for the AJS
- percentage throughs higher than 65 indicate soft wheat samples for the PSI
- scores lower than 50 indicate soft wheat samples for the AACC NIR wheat hardness method

As both the actual and predicted values were plotted it also gives a visual presentation of the accuracy of the wheat hardness predictions.

Figures 3.27 to 3.34 illustrate the results (calibration equations selected were based on lowest SEP) in Tables 3.8, 3.9 & 3.10 as bar graphs.

The degree of accuracy of the NIR hardness prediction on ground wheat grain is illustrated in Figures 3.27 & 3.28 and wheat hardness can clearly be measured quantitatively by NIR on ground grain. Figures 3.29 to 3.34 illustrate that the measurements on whole wheat grain were not as accurate as for ground grain and would not be adequate for quantitative measurements. However, in reflectance this measurement should be adequate as a screening method. With AJS as the reference method, only two soft samples out of the total of 41 samples have been incorrectly predicted to be hard and four samples were border-line cases (Figure 3.29). In cases like this it might be necessary to repeat this border-line cases using a conventional reference method. With PSI as the reference method one hard sample and three soft samples were incorrectly predicted (Figure 3.30). With AACC as the reference method, two soft and two hard samples were predicted incorrectly (Figures 3.31 & 3.32). In transmittance, a considerably larger amount of samples were predicted incorrectly which suggests that it might not even be accurate enough for a

screening method (Figures 3.33 & 3.34).

(v) Comparison of software packages

The slight difference in the SEP results obtained from the ISI and NSAS software can be explained in terms of the equation used to calculate the SEP. ISI calculates the SEP using equation 4.1 whereas NSAS calculates the SEP using equation 4.2. If one re-calculates either of these two the calibration and validation results obtained by ISI and NSAS are identical. UNSCRAMBLER calculates the SEP also using equation 4.1 and is therefore identical to the SEP quoted by ISI.

$$SEP = \sqrt{\frac{\sum_{i=1}^{n} (y_i - \hat{y}_i)^2}{n}} \qquad \text{.....} \quad 4.1$$

$$SEP = \sqrt{\frac{\sum_{i=1}^{n} (y_i - \hat{y}_i)^2}{n-1}} \qquad \text{.....} \quad 4.2$$

The terminology relating to molecular spectroscopy published by the American Society for Testing and Materials (ASTM) defined the SEP according to equation 4.2 (ASTM, 1992). However, in the circumstances of a prediction set and with no bias correction equation 4.1 should be used to calculate the SEP.

The SEC results obtained by UNSCRAMBLER were also slightly different to those obtained from ISI and NSAS. The reason for the difference is not clear.

It can be concluded that when the same data set was analysed by three different software packages, results not significantly different were obtained. It is, however, important to realise that great care has to be taken when interpreting the statistical summaries of the software. Different terms are used by different software packages to quote, for example, the standard error of prediction and as mentioned above there is also sometimes slight differences in the equations used.

Tables 3.12, 3.13 & 3.14 illustrate the different ways in which the ISI, NSAS and UNSCRAMBLER software packages summarize the validation statistics, respectively.

Comparing these three statistical summaries it is clear **how important it is to define the statistical results quoted**. In the above-mentioned three examples, the term SEP is representing three different values. It is therefore important to make clear exactly what is meant by the SEP. ISI quotes the standard error of prediction as SEP, NSAS as root mean square (RMS) and UNSCRAMBLER as RMSEP. UNSCRAMBLER also quotes the term SEP, but it refers to the standard error of prediction corrected for bias. NSAS quotes the standard error of performance, but in this case it indicates specifically the SEP after correction for slope and bias.

The differences in selecting calibration equations using cross-validations were expected because different packages would select the random cross-validation groups in different ways and it is not possible to perform identical cross-validations using different software packages. It is, however, interesting to note that the results obtained from ISI and

UNSCRAMBLER after 20 cross-validations were identical for the whole grain reflectance and transmittance results, but not for ground grain reflectance.

4.3.2 Empirical calibrations for UK home-grown wheat

Successful wheat hardness calibrations on whole grain have only been reported for Canadian home-grown whole wheat grain (Williams, 1991; Williams & Sobering, 1993). The sample set used in this study contains a majority of UK home-grown wheat, but also a few Canadian home-grown wheat samples. It was decided to remove the Canadian wheat samples from the sample set and attempt predicting whole grain wheat hardness on UK home-grown wheat only.

Descriptive statistical analyses for AJS, PSI and AACC NIR wheat hardness tests are shown in Table 3.15 and similar statistical analyses for the calibration and prediction sets in Tables 3.16 & 3.17, respectively. Removing the Canadian home-grown wheat samples resulted in a sample set with a narrower range and a smaller standard deviation. The Canadian home-grown samples contain durum wheats, which are much harder than the hardest of the UK home-grown wheat. Calibration and validation results in terms of SEC, r and SEP, including the RPD statistics are shown in Tables 3.18, 3.19 & 3.20 for ground grain reflectance, whole grain reflectance and whole grain transmittance respectively.

Based on these results the calibration equations for UK home-grown whole wheat grain tend to be slightly worse (RPD = 1.80 vs 1.56 for AJS). **This confirms that, for this sample set, wheat hardness cannot be measured by NIR on whole wheat grain quantitatively, but with acceptable accuracy for grain trading.**

It is interesting to note that the correlation coefficient is lower for the UK home-grown

wheats (r = 0.90 vs 0.87 for whole grain reflectance; r = 0.83 vs 0.39 for whole grain transmittance). In terms of the multiple determination coefficient (R^2), this means that less of the variation within the data set is described by the model. This indicates that **these equations would not be as robust as for the sample set including Canadian home-grown wheat**.

4.3.3 Alternative calibrations

Empirical NIR spectroscopy calibrations are often performed without knowing what is measured or understanding the basis of the measurement. The plots of PLS factors were examined, but proved impossible to interpret. In other words the NIR spectrophotometer is often used as a "black box". This is the case for all of the calibrations discussed so far.

Successful NIR hardness measurements on ground wheat grain are based on light scattering. If NIR hardness measurements on whole grain are also based on light scattering this light scattering effect could be used to predict hardness on whole grain. Potentially useful techniques not previously applied to whole wheat grain are:

- multiplicative scatter correction (MSC)
- principal components analysis (PCA)
- area under the second derivative curve (AREA).

The empirical calibration results were used as a comparison to monitor the ability of these alternative calibration techniques to predict the wheat hardness on whole wheat grain by NIR spectroscopy. Alternative calibration equations were derived on ground grain to provide a direct comparison with successful empirical calibrations.

Calibration and validation results obtained by these alternative NIR calibrations (MSC,

PCA & AREA) for ground grain reflectance, whole grain reflectance and whole grain transmittance are shown in Chapter 3, Tables 3.21, 3.22 & 3.23, respectively, in terms of SEC, r and SEP according to equations 2.1, 2.2 & 2.3 in Chapter 2. A comparison between the alternative and the empirical calibration results are shown in Tables 3.24, 3.25 & 3.26.

The results in Tables 3.21 to 3.26 indicate that these alternative calibrations do not show any significant ($p < 0.05$) improvement on the results compared to the empirical calibrations. Although not significant at $p < 0.05$, the 1st and 2nd principal components for whole wheat grain reflectance and transmittance and the AREA for transmittance whole wheat grain by AJS did show an improvement in SEP compared to the empirical calibrations. These results and particularly those obtained for the whole wheat grain reflectance spectra will be discussed in more detail.

- *multiplicative scatter correction (MSC)*

Multiplicative scatter correction (MSC) has been discussed in detail in Chapter 1 and the development of the calibrations in detail in Chapter 2. A summary of the results compared to empirical calibrations are shown in Table 3.24.

Multiplicative light scatter occurs due to differences in the particle sizes of the ground samples. By applying MSC to the spectra all or most of the effect of multiplicative scatter is removed. It would therefore be expected that by separating the effect of multiplicative scatter and using that to predict hardness, results similar to the empirical calibrations would be obtained. It is shown in Table 3.24 that this was not the case for ground grain reflectance. It is possible that MSC did not remove all of the effect of light scattering, therefore the slightly worse result for the alternative calibration on ground grain. However,

the calibration derived with AJS as the reference method would be acceptable to predict wheat hardness for grain trading (SEP = 2.59). The results obtained for whole wheat grain reflectance and transmittance spectroscopy using this technique were not significantly *($p < 0.05$)* better than the empirical calibrations. This raises the question as to whether the scattering of light in the case of whole grain is multiplicative or not and whether the scattering properties for whole grain in reflectance and transmittance modes would be similar. **These results suggested a need for further investigation into the effect of light scatter on whole grains analysis by NIR spectroscopy.**

- *principal components analysis (PCA)*

Principal components analysis (PCA) has been discussed in detail in Chapter 1 and the development of calibrations in detail in Chapter 2. A summary of the results compared with empirical calibrations are shown in Table 3.25.

It is known that the plot of the loadings of the 1st PC normally has the shape of the mean spectrum (Cowe & McNicol, 1985) indicating that the scatter represents the largest single source of variation in the data. When calibrating for any other constituent but hardness this would be an indication that the spectra must be corrected for scatter before calibration. This was also the case in this sample set as can be seen in Figures 3.35, 3.36 & 3.37. Figure 3.35 illustrates the mean spectrum for ground grain reflectance and the standard deviation. Figure 3.36 shows the similarities between the plots of the mean spectrum and the loadings of the 1st PC (accounts for variation due to scatter) and Figure 3.37 the mean spectrum and the plot of the loadings of the 2nd PC (accounts for variation due to moisture). As a result of this and the fact that the 1st PC accounts for most of the variation within the data set, the 1st PC was selected *a priori* to calibrate for hardness on ground wheat grain using AJS and PSI as reference methods. As in the case of MSC, the AJS

calibration equation derived to predict wheat hardness would be acceptable for grain trading (SEP = 2.08). The 1st PC accounts for most (99.01 %), but not all of the variation in the data set (0.60 % of the variation accounted for by the 2nd PC and 0.31 % accounted for by the 3rd PC). However, for hardness measurements on ground wheat grain the 1st PC accounts for all of the variation that describes wheat hardness.

Figures 3.38, 3.39 & 3.40 illustrate similar figures for whole grain reflectance. It is clear that the plot of the loadings of the 1st PC only have the same shape as the mean spectrum up to about 1900 nm. However, the 2nd PC also has a similar shape to the mean spectrum apart from the difference at 1200 nm. It could be concluded that what is measured in the prediction of hardness, is the effect of light scatter, and that is reflected in the 1st PC in ground grain. In the case of whole grain the 1st PC does not seem to account for all of this light scatter, but in fact the 2nd PC contributes to a large extent. This can be concluded from the results in Table 3.22. **Calibrating for hardness on whole grain in reflectance mode using the 2nd PC gives better results than using the 1st PC and consequently using both results in an even lower SEP. Using both the 1st & 2nd principal components also results in a lower SEP than for the empirical calibration.** Therefore although the 1st PC accounts for most of the variation, it does not account for all of the variation that describes wheat hardness. The 2nd PC of whole wheat grain reflectance spectra also describes wheat hardness. The 1st PC account for 92.80 % of the variation in the data set and the 2nd PC for 6.3 %, which is more than the variation accounted for by the 2nd PC of ground grain spectra.

Whole grain transmittance spectra do not have as many prominent features as reflectance spectra. It is therefore more difficult to make conclusions from the plots of the loadings of the principal components of whole grain transmittance spectra. Figures 3.41, 3.42 &

3.43 show, respectively, the mean spectrum and standard deviation, the mean spectrum and the plot of the loadings of the 1st PC and the mean spectrum and the plot of the loadings of the 2nd PC. **As in the case of whole grain reflectance using both the 1st and 2nd principal components derived from the whole grain spectra in transmittance mode give better results than using only the 1st PC as well as better results than the empirical calibrations.** The 1st PC account for 96.86 % of the variation in the data set and the 2nd PC for 2.97 %.

- *Area under the second derivative curve (AREA)*

Area under the second derivative curve (AREA) has been discussed in Chapter 1 and the development of calibrations in detail in Chapter 2. A summary of the results compared with empirical calibrations are shown in Table 3.26.

As for the MSC and 1st PC calibrations the AREA calibration of wheat hardness for ground grain reflectance with AJS as the reference method would be acceptable for grain trading. **In this case only the calibrations for whole grain transmittance give better results than the empirical calibrations.**

Using principal components regressions (1st PC for ground wheat grain and the 1st and 2nd PCs for whole wheat grain) tend to describe the variation in the data set due to hardness better than does MSC and AREA.

There is no significant difference between the empirical and alternative calibrations ***($p < 0.05$)***. Therefore for ground grain the three alternative calibrations i.e. MSC, 1st PC and AREA are all equivalent and the wheat hardness prediction results are acceptable for grain trading (Osborne *et al.*, 1993; Williams & Norris, 1984). An excellent correlation

found between AREA and AACC NIR wheat hardness scores (r = 0.99) as well as AREA and 1st PC scores (r = 0.99) confirms the expectation that AREA is a function of scatter. This proves that the measurement of hardness on ground wheat grain is related to scatter.

For whole wheat grain reflectance using the 1st and 2nd principal components proved to be the best (although not significantly $(p < 0.05)$ better than the empirical calibrations). This indicates that pure scatter as measured in the case of MSC and AREA is inadequate to describe hardness.

For whole grain transmittance the measurements were worse than for ground grain reflectance and whole grain reflectance. The alternative calibrations apart from AREA were slightly worse than the empirical calibrations.

The fact that for the empirical calibrations the best equation was selected out of 15 terms, it is quite likely that overfitting could have occured. The benefit of the alternative calibrations is that fewer terms were used therefore no risk of overfitting.

The analysis of variances followed by Tukey's test showed that for any given calibration method the wheat hardness predictions by AJS for ground wheat grain reflectance were significantly better than whole wheat grain reflectance and both ground and whole wheat grain reflectance significantly better than whole wheat grain transmittance $(p < 0.05)$. For PSI wheat hardness predictions ground wheat grain reflectance were significantly better than both whole wheat grain reflectance and transmittance, but whole wheat grain reflectance was not significantly better than whole wheat grain transmittance $(p < 0.05)$. In the case of AACC NIR wheat hardness predictions whole grain reflectance were shown to be significantly better than whole wheat grain transmittance $(p < 0.05)$.

4.3.4 NIR calibrations of damaged starch on flour

It is known that the damaged starch potential of flour is directly related to the hardness of the wheat. Therefore, it was decided to investigate the measurement of damaged starch using alternative calibrations. The damaged starch calibration results are shown in Tables 3.27 to 3.31. Tables 3.28 to 3.30 show descriptive statistical summaries of the whole sample set and the calibration and validation sets, respectively.

Osborne & Douglas (1981) reported damaged starch NIR calibrations on Bühler-milled flours with SEP = 4.2 Farrand units and r = 0.95. Recently Morgan & Williams (1995) reported NIR calibration results for starch damaged in wheat flour with SEP = 3.0 Farrand units and r = 0.96. Finney, Kinney & Donelson (1988) suggested that NIR analysis of ground wheat grain could be used to predict damaged starch. A high correlation was shown between the NIR analysis and the enzymatic method used. In this study, damaged starch calibration equations for flour were derived by AACC NIR wheat hardness, 1st PC scores and the area under the second derivative curve with the Farrand method as reference method. The results were SEP = 5.89 and r = 0.72, SEP = 5.76 and r = 0.71 and SEP = 5.58 and r = 0.71, respectively (Table 3.31). **Predicting damaged starch of flour from AACC NIR wheat hardness, 1st PC scores and AREA, respectively did not result in accurate predictions**

4.4 The dependence of NIR wheat hardness measurements on chemical composition and scatter

Measurement of wheat hardness of whole wheat grain by NIR spectroscopy cannot be based on the same principle as for ground grain as no grinding is involved. The current theory of wheat hardness suggests that the way in which hard and soft wheats break down to flour and meal result from variation in the continuity of the protein matrix, starch-protein adhesion and intercellular spaces within the endosperm. It is therefore likely that these

structural differences would result in differences in scatter when NIR radiation is transmitted through the kernel. Based on previous results (principal component and AREA regressions) there must be some scattering effect that is related to hardness. It would therefore be interesting to establish whether the NIR measurement of hardness is based on only the scatter properties of the samples or on the chemical composition, too. Comparison of the two corresponding NIR signals may reveal any contribution that chemical composition makes to the hardness measurements, given that the scattering effect is different for ground and whole wheat grain samples. This comparison was performed by using canonical correlation analysis (CCA) which identifies the correlation between two groups of variables and consequently describes the information that is common to these two groups of variables (ground wheat grain and whole wheat grain in this case).

The results are shown in Chapter 3, Tables 3.32, 3.33 and Figures 3.44 to 3.48, respectively.

The correlation coefficients in Tables 3.32 & 3.33 indicate that the 1st PC would have the highest ability to measure wheat hardness in the case of ground grain and the 1st and 2nd PCs in the case of the whole grain. This supports the principal component regression results given in section 4.3.3. According to the correlation coefficients, the 3rd PC would be the best choice to plot a similarity map for ground grain with the 1st PC (Figure 3.44). Projecting all the data points on the 1st PC axis indicate that the first PC on its own would be adequate to separate between hard and soft wheats. The 1st PC accounts for 98.98 % of the total variation of the spectral data and the 2nd and 3rd for 0.60 and 0.33 %, respectively. Similarity maps were therefore plotted between the 1st and 2nd PCs for whole grain (Figure 3.45).

The similarity map of the 1st and 2nd PCs for the whole wheat grain show a large overlap between the samples. The 1st PC accounts for 92.45 % of the total variation of the spectral data and the 2nd and 3rd PCs for 6.55 and 0.69 %, respectively.

As discussed earlier, the 1st PC for ground grain has the same shape as the average wheat spectrum and therefore describes the scatter effect (Figure 3.36). Figure 3.40 shows that the 2nd PC for whole wheat grain has the same shape as the average wheat spectrum, therefore describing some of the scatter effect and being correlated with hardness to some extent.

Canonical correlation analysis was applied to the first 10 principal components of ground and whole grain reflectance spectra and high canonical correlation coefficients were observed between the first three pairs of variates (R^2 = 0.99, R^2 = 0.97 and R^2 = 0.94). The similarity map for the canonical variates showed a huge overlap between the hard and soft wheat samples. The canonical variate plots (Figures 3.46 to 3.48) show that the spectral patterns for the ground and whole grain were similar and exhibited absorption bands at 1900, 1925 and 1960 nm. These spectral patterns indicated that the variation in the first two canonical variates are mainly due to the water content. The hardness data were shown to be slightly correlated to the 2nd, 3rd, 4th & 5th CV. The 3rd CV was difficult to interpret as different absorption bands were revealed by the ground and whole grain spectra.

The only common chemical information was variation in the water content. The raw spectra of the ground wheat grain showed that wheat hardness could mainly be related to the particle size and the scattering effect. This was also revealed in the 1st PC which was highly correlated to the hardness measurements. The raw spectra of the whole wheat grain

did not reveal any scattering effect that could be related to hardness, neither did the 1st PC. However, the 2nd PC which is also highly correlated to the hardness measurement did reveal some effect of scatter, which could be related to wheat hardness to some extent. **This analysis did not show any chemical composition related to wheat hardness as measured by NIR.**

4.5 The effect of light scattering on whole grain wheat

All the above-mentioned results clearly necessitated a further investigation into the effect of light scattering on whole grains. This effect was therefore investigated based on work published by Norris & Williams (1984).

The spectra of the four sets of data are shown in Chapter 3, Figures 3.7 to 3.10, with the spectra after correction for multiplicative scattering, shown in Figures 3.49 to 3.52. It is apparent from these sets of spectra that the scattering is multiplicative in the case of the ground grain, but not in the case of whole grain. Figure 3.7 shows typical spectra of ground grain exhibiting the multiplicative scatter effect, where as in Figures 3.8 to 3.10 there is a linear baseline shift across the whole wavelength range. Figure 3.50 shows that correcting the whole grain reflectance spectra for multiplicative scattering as described in section 2.2.4 (iii) is not as successful as for the ground grain spectra (Figure 3.49). Correcting for multiplicative scattering on whole grain transmittance spectra is even less successful (Figures 3.51 & 3.52).

Norris & Williams (1984) have shown that the log 1/R values of reflectance spectra of ground grain samples are affected by particle size, with coarser samples having higher absorption and higher log 1/R values. The particle size effect is also greater at longer wavelengths. However, Olinger & Griffiths (1993) did not find an increase in log 1/R

levels with increasing particle size. They could not explain this discrepancy but suggested that it could be due to the different optical geometries used in the two measurements. Norris & Williams (1984), demonstrated that the particle size effect increases consistently with log 1/R, indicating that the primary relationship is to log 1/R rather than to wavelength.

The results of the present experiment confirmed the existence of a multiplicative scatter effect of different particle sizes of ground wheat, expressed as percentage throughs, as well as the consistent relationship with log 1/R values, but not with wavelengths (Figures 3.53 & 3.54). In fact, these results are almost identical to the results previously published by Norris and Williams (1984). It can therefore be concluded that the spectral properties of the sample set used (at least for reflectance spectra on ground wheat) are as expected from results published previously.

In the case of reflectance spectra of whole grain, the effect was only proportional for log 1/R values up to 0.7 in the 1100-2500 nm region (correlation coefficients 0.50 to 0.61) (Figure 3.55) and wavelengths up to 1200 nm (correlation coefficients 0.53 to 0.59) (Figure 3.56); above this value, there was no longer a consistent relationship.

In the 800-1100 nm region, the correlation coefficients for the regressions at different wavelengths in the reflectance spectra varied from 0.86 to 0.95 for ground grain and from 0.46 to 0.65 for whole grain but the slopes were essentially constant (as were the slopes of the regression lines in the 1100-2500 nm region for reflectance whole grain spectra) and there was no consistent relationship with increasing wavelengths as shown in Figures 3.57 and 3.58. **There appears to be some scatter effect, but it is clearly not multiplicative**. There was no relationship at different log 1/R values with correlation coefficients ranging

from 0.05 to 0.67 for ground grain and 0.03 to 0.56 for whole grain. A similar result was found for transmittance spectra of whole grain with correlation coefficients of 0.50 to 0.54 and 0.06 to 0.12 for wavelengths (Figure 3.59) and log 1/R values, respectively. This might be explained to some extent by similar findings by Birth (1986). He computed the Kubelka-Munk scatter coefficient for ground and whole wheat grains. He reported a relatively small wavelength dependence of the Kubelka-Munk scatter coefficient for ground wheat in the 750-1050 nm region but a large standard deviation in the values due to the heterogeneous nature of the samples. The Kubelka-Munk scatter coefficient was found to change more with wavelength in the case of whole grain. Less scattering was observed with whole grains than ground grains. This was ascribed to the large voids between the whole grains which will be different with each repack of the sample as will the orientation of the individual kernels. Both of these factors will influence the scatter effect.

4.6 The effect of protein content and growing season on two wheat varieties

Figures 3.15 to 3.22 in Chapter 3 shows that **NIR hardness measurements are affected by the effect of protein content and growing season within a single variety**. Figures 3.60 to 3.67 illustrate the effect of protein content and growing season on the AACC NIR wheat hardness test and spectra of ground grain, whole grain reflectance and whole grain transmittance in terms of the 1st and 2nd principal components, respectively. Figure 3.60 illustrates an excellent discrimination between the soft and hard wheat samples based on the AACC NIR wheat hardness scores. These scores mainly reflect differences in the particle size of ground samples, but a recent study of the AACC NIR wheat hardness test by Brown *et al.* (1993) showed that the results of this method depended on the protein and moisture contents of the different samples within a single variety. As AACC scores cannot be obtained from whole wheat grain samples, the 1st PC was chosen *a priori* as it accounts for most of the variation within the data set. The 2nd PC was chosen to relate to whole

grain reflectance and transmittance measurements based on previous results obtain by principal component regressions which indicated that inclusion of the 2nd PC improved the calibrations.

Comparing Figures 3.60 & 3.61 it is possible to distinguish between the hard and soft wheats in both cases, however, the 1st PC is less affected by protein content and growing season than the AACC NIR wheat hardness test.

The bar graphs of the 1st and 2nd principal components of the whole grain reflectance spectra does not group the hard and soft wheats as clearly as in the case of ground grain (Figures 3.62 & 3.63), although it is easier to tell between hard and soft wheats in the case of the 2nd PC. Both the 1st and the 2nd principal components are affected by protein content and environmental conditions.

The 1st PC for whole grain transmittance (spectra recorded on the NIRSystems Model 6500) is less affected by protein content and growing season than whole grain reflectance. It is also easier to tell between Riband and Mercia (Figure 3.64). The 2nd PC is more affected by growing season, but less so by protein content (Figure 3.65).

Figures 3.66 & 3.67 illustrate the equivalent plots for whole grain transmittance with the spectra recorded on the Infratec Model 1225. These spectra are much more affected by protein content and growing season than in the case of the Model 6500.

It was observed that the hectolitre weight decreased drastically from the 1991 season to the 1992 season, resulting in shrivelled grains. This could be a possible explanation for the effect of season on the NIR measurements. The discrimination between hard and soft

wheats is hugely affected by protein content and growing season. This is, however, not the only reason for lack in discrimination.

4.7 Relationship between NIR measurements and physical property measurements

Glenn *et al.* (1991) reported positive, but non-linear, correlations between the variation in fracture mechanical properties of a wheat and its hardness as measured by NIR.

Correlations between NIR measurements (1st PC scores) and the physical property measurements (Parameter A and Parameter B) are shown in Chapter 3, Figures 3.68 to 3.75.

Fracture mechanics can be used to predict milling performance of wheat, but the measurements are difficult and time consuming. Therefore the possibility of relating NIR measurements to the fracture mechanics measurements either directly of indirectly was investigated, the benefit of NIR being the speed of the measurements possible on-line measurements in the flour mill and the fact that most mills already have NIR instruments. Unfortunately sufficient data were only available in the case of Parameter A and Parameter B. It was therefore only possible to attempt correlations between NIR measurements and these two sets of data. However, the results turned out to be quite promising. Using only eight samples for the correlations were valid due to the fact that only one term (1st PC) was selected *a priori* and not because it fits the data set the best.

A linear relationship was found between Parameter A and the 1st PC scores ($r = 0.78$) (Figure 3.68), for ground grain reflectance, but not between Parameter B and the 1st PC scores (Figure 3.69). The same trend was shown for correlations with AACC NIR wheat hardness scores (Figures 3.70 & 3.71).

Highly correlated linear relationships were observed for the 1st PC scores derived from reflectance whole grain spectra and Parameter A ($r = 0.94$) as well as Parameter B ($r = 0.95$) (Figures 3.72 & 3.73). The 1st PC scores derived from the transmittance whole grain spectra also exhibited a linear relationship with Parameter A ($r = 0.77$) (Figure 3.74) and Parameter B ($r = 0.95$) (Figure 3.75).

A linear relationship between NIR measurements and Parameter A would be expected. The correlation plot between Parameter B and AJS values (Figure 3.76) show a similar non-linear plot than in the case of Parameter B and the 1st PC scores of ground wheat grain reflectance spectra. Air Jet Sieve values depend on scatter due to different particle sizes. It is therefore clear that Parameter B does not vary linearly with scatter. This justifies the non-linear plots of Parameter B and 1st PC scores and AACC NIR wheat hardness scores, respectively. It was, however, encouraging to see the high linear correlations between the NIR measurements and these two physical property measurements for whole wheat grain reflectance and transmittance. These linear plots for the whole grain measurements might indicate that Parameter B vary linearly with the scatter as observed in the case of whole wheat grain. This could be due to the differences in physical properties in the endosperm which will be different for hard and soft wheats. **Physical property measurements correlate with wheat hardness and NIR whole wheat grain measurements correlate positively with the physical property measurements**. It is therefore highly likely that fracture properties of wheat could, indirectly, be measured by NIR. This work, however, needs to be expanded using larger sample sets.

An additional benefit of these two methods is that both could be performed on single

kernels and as NIR spectroscopy is a non-destructive method the measurements could be performed on the same kernel. Fracture mechanics methods are time consuming, it would therefore be beneficial if the NIR spectrophotometer could be calibrated for hardness measurements using physical property measurements as reference methods. This approach could also be of further assistance in the fundamental understanding of wheat hardness measurement by NIR.

OPTIMILL results have shown that wheat hardness is related to the vitreousness or mealiness of the sample and that the overall hardness of the sample would be due to the ratio of vitreous and mealy grains (Dobraszczyk, 1994). The effect of environment on the vitreousness of a sample is well known. Vitreousness is strongly influenced by environmental factors such as the availability of nitrogen and water and the air temperature during maturation of the grain. A specific sample would appear vitreous or mealy due to the way it reflects light. Although it is not proven yet, there might be a possibility that the NIR reflectance of light from the sample or NIR transmittance of light from or through the sample could be related to the vitreousness of the sample which in turn relates to the hardness.

4.8 Single kernel analysis

The phenomenon that the range in hardness of single kernels can overlap even though their bulk hardness scores do not, has been reported by Glenn & Johnston (1992) and Delwiche (1993). This variation between single kernels within a single variety can also be seen visually as shown in Chapter 3, Figures 3.77 to 3.86.

The plots of the first three principal components and the mean spectrum for single kernel transmittance spectra are shown in Chapter 3, Figures 3.87 to 3.89 and the mean spectrum

and the standard deviation in Figure 3.90. Similar plots for single kernel reflectance spectra are shown in Figures 3.91 to 3.93 and Figure 3.94, respectively.

It is known that the plot of the loadings of the 1st PC normally has the shape of the mean spectrum (Cowe & McNicol, 1985). However, this was not the case for transmittance spectra of bulk samples (Figure 3.42). In the case of single kernels the 1st PC, however, does follow the shape of the mean spectrum as does the 3rd PC. To be able to record spectra from single kernels in transmittance mode, it is clear that the energy must be transmitted through the kernel. Scattering would therefore occur inside the kernel. **The differences between the principal components for single kernels and bulk samples could be due to the fact that in bulk samples scattering also occur between the kernels and that the energy is not transmitted through the kernels with scattering only inside the kernels as in the case of single kernel analysis.**

The differences in the spectral patterns of the principal components for reflectance and transmittance single kernel spectra could indicate that the absorption and scattering for these two measurements are different. It is therefore likely that for single kernel and bulk samples analysis in reflectance mode, only partial penetration of energy into the kernels would take place. This is, however, a much more complicated matter and more sophisticated work is needed to really understand the fundamentals behind NIR spectroscopic analysis of whole wheat grain.

Chapter 5

Conclusions

CHAPTER 5

5.0 Conclusions

The objectives of this study were to:

- investigate the measurement of whole wheat grain hardness by NIR spectroscopy
- investigate the measurement of whole wheat grain hardness by NIR spectroscopy on UK home-grown samples only
- predict damaged starch by NIR spectroscopy
- investigate the dependence of NIR wheat hardness measurements on chemical composition and scatter
- investigate the scatter properties of whole wheat grain as measured by NIR transmittance and reflectance spectroscopy
- attempt to provide a fundamental understanding of the measurement by NIR spectroscopy on whole wheat grains

The following observations were made in the discussion of the work performed during the course of this study:

- hardness can be measured by NIR on ground grain with a high degree of accuracy
- hardness cannot be measured by NIR reflectance on whole grain with the same degree of accuracy as in the case of ground grain
- hardness cannot be measured by NIR transmittance on whole grain with the same degree of accuracy compared to both ground grain and whole grain

reflectance

- comparing different software packages it is clear how important it is to define the equations used and statistical results quoted
- NIR calibration equations derived for wheat hardness on UK home-grown wheat would not be as robust as in the case of sample sets including Canadian home-grown wheat
- alternative regressions for predicting wheat hardness by NIR using techniques which separate the effect of light scatter, suggested the need for further investigation into the effect of scatter on whole wheat grain
- calibrating for hardness on whole grain in reflectance mode using the 2nd PC gave better results than using the 1st PC and consequently using both result in an even lower SEP. Using both the 1st & 2nd principal components also result in a lower SEP than for the empirical calibration
- as in the case of whole grain reflectance, using both the 1st and 2nd principal components of whole grain in transmittance mode gave better results than using only the first as well as better results than the empirical calibrations
- calibrations using the area between the second derivative curve and the wavelength axis for whole grain transmittance result in better predictions for hardness than the empirical calibrations
- no significant difference was found between the empirical and alternative calibrations $(p < 0.05)$
- predicting damaged starch of flour from AACC NIR wheat hardness, 1st PC scores and AREA, respectively did not result in accurate predictions
- applying canonical correlation analysis to ground and whole wheat grain did not show any chemical composition related to wheat hardness as measured by NIR

- investigation into the effect of light scatter on whole wheat grain did show a scatter effect, but it was clearly not multiplicative
- NIR spectral measurements are affected by the effect of protein and growing season within a single variety
- NIR whole wheat grain measurements (in terms of 1st PC) correlate positively with the physical property measurements
- preliminary single kernel analysis indicate that in whole grain transmittance of bulk samples scattering also occur between the kernels and the energy is not transmitted through the kernels with scattering only inside the kernels as in the case of single kernel transmittance analysis

For the sample set investigated, whole wheat grain hardness could not be measured by NIR with the same degree of accuracy as for ground grain. However, although the measurement on whole wheat grain was not suitable for quantitative measurements the hardness measurements could be performed at an acceptable accuracy and it could, for example, be used as a screening method for wheat hardness in a wheat breeding programme.

Wheat hardness can be measured on ground grain with a high degree of accuracy, even with a limited number of samples in the calibration set. Using the same sample set for whole grain calibrations succeeded in predictions with acceptable accuracy for grain trading. Using the NIR as a "black box" there is currently no fundamental understanding of the measurement of wheat hardness on whole grain by NIR. It is quite likely that for whole grain calibrations many more samples are needed to achieve more accurate predictions. It is, however, important that the "right" samples are included, meaning that the full range of hardness that would be measured in future, adequately dispersed, needs

to be included.

It was interesting to note the decrease in robustness (lower R^2) of the calibration equations derived after the Canadian home-grown samples were removed from the sample set. Investigating only UK home-grown samples, the effect of protein content and growing season within a single variety on NIR spectral measurements were shown. The effect of environmental conditions on the vitreousness and mealiness of a sample is also well known. Fracture mechanics results have shown that within a single variety the wheat hardness depends on the ratio of vitreous and mealy kernels. Canadian home-grown wheat samples are usually totally vitreous or totally mealy. However, this is not the case in UK home-grown wheat samples. More often than not the samples are a mixture of vitreous and mealy kernels and quite often the kernels are found to be half vitreous and half mealy. This effect is seldom or never observed in Canadian home-grown wheat. This must be due mainly to the inconsistency of the weather conditions in the UK. This variation due to vitreous and mealy kernels must affect the NIR spectral measurements and even more so the hardness measurements by NIR. As inclusion of Canadian home-grown wheat samples improved the robustness of the calibration equations, this might be a way of improving calibrations of UK home-grown whole grain wheat.

In contrast with the current methods of measuring wheat hardness, mentioned above, using the NIR as a "black box", additional techniques which do have a theoretical basis were investigated. Multiplicative scatter correction can be applied to spectral data to remove the effect of light scatter. The first principal component accounts for most of the variation in the data set which in the case of ground grain is due to scatter. The area between the second derivative curve and the wavelength axis is a function of path length and therefore scatter. High correlations between 1st PC, AACC NIR wheat hardness scores and AREA

confirms that AREA is a function of scatter. Applying these techniques to whole grain (which has not been done before) to separate the effect of scatter and then regressing this scatter effect against reference hardness measurements, did suggest a scatter effect to be involved in the measurement of wheat hardness on whole grain by NIR.

It was shown that the 1st PC of ground wheat grain is highly correlated to hardness measurements and that it accounts for most of the variation within the data set and that this variation is due to multiplicative scatter. It was interesting to observe that for whole grains both the 1st and 2nd PC correlated highly to hardness measurements and that the 2nd PC also account for the variation due to the effect of scatter in the case of whole grain as well as the 1st PC. This was confirmed by the improvement of the predictions after inclusion of the 2nd PC as well as the similarity between the 2nd PC spectral pattern and the mean spectrum of whole grain. It was also shown that for ground grain only the 1st PC correlated highly to hardness measurements where for whole grain both the 1st PC and 2nd PC correlated highly with hardness measurements. Regressing the 1st PC and 2nd PC of whole grain against wheat hardness proved to give better predictions than the empirical methods.

Regressing the calculated area between the second derivative curve and the wavelength axis against hardness measurements for whole grain in transmittance mode proved to give better predictions than the empirical calibrations. A possible solution could be to use reference methods which measure the actual wheat hardness i.e. fracture mechanics and not a reference method that is based on particle size. No significant differences were observed between the empirical and alternative calibrations. The benefit of the alternative calibrations are that less terms are used and therefore no risk of overfitting as could be the case for empirical calibrations.

Canonical correlation analysis indicated that no chemical composition was related to wheat hardness as measured by NIR for ground and whole wheat grain, suggesting that the measurement of wheat hardness by NIR is based only on scattering. As the above-mentioned techniques are usually associated with ground grain applications, the scatter involved would be assumed to be multiplicative. Investigating this effect of light scatter on whole grain suggest that the light scatter was not multiplicative. The question now is whether the light scatter that was separated applying these above-mentioned techniques to whole wheat grain to predict hardness was the correct "type of scatter" as it has been shown that the effect of light scatter is different on ground grain and whole grain reflectance and transmittance. It can be concluded that the measurement of wheat hardness on whole grain is due to scattering, however, whether the correct "type of scatter" was separated to predict hardness is questionable. More work is needed to investigate the effect of scatter on whole grain and possible development of techniques to separate the effect of scatter on whole grains.

In this study NIR spectral measurements were correlated with two physical property measurements i.e. Parameter A and Parameter B. The high positive linear correlations observed between NIR spectral measurements and the physical property measurements were quite promising. The ideal would be to use physical property measurements, which do have a theoretical basis, as reference measurements for NIR calibrations. This work needs to be expanded on bigger sample sets as well as more different physical property measurements.

It can therefore be concluded that the measurement of wheat hardness on whole grain is based purely on scattering. In contrast with NIR hardness measurements on ground grain, the scattering involved is not multiplicative. New techniques need to be developed to

separate this specific effect of scatter to predict hardness on whole grain. Using reference methods with a theoretical basis then might improve the predictions. This will also contribute to the fundamental understanding of measuring whole grain wheat hardness by NIR.

Analysis of single kernels did show a difference between the measurements made on single kernels and bulk samples as well as between single kernels analysed in reflectance and transmittance modes, respectively based on spectral analysis of principal component loadings. There is an indication that in the case of the bulk sample NIR transmittance the radiation is not transmitted through the samples, but that scattering between the samples also occurs. However, this was only preliminary work and the fundamental understanding of the properties of whole wheat grain using NIR spectroscopy is a much more complicated matter and much more sophisticated work is required to solve this problem.

Although this study did not completely solve the problem of measuring whole grain wheat hardness by NIR, new insights were provided. Hopefully these new insights and observations made would encourage further work in this area which might lead to a more complete fundamental understanding of the properties of whole wheat grain hardness using NIR spectroscopy.

Future Work

- Investigate the spectral differences observed for Canadian home-grown soft wheats in the 850 - 925 nm region
- Additional techniques to separate light scatter for whole grain to predict wheat hardness needs further investigation
- Expanding the investigation into the use of physical property measurements as

reference methods for wheat hardness calibrations on whole grain

- Fracture mechanics suggested that wheat hardness depends on the ratio of mealy and vitreous kernels within a single variety. Preliminary work showed that mealy and vitreous kernels within a single variety exhibited different NIR spectral absorbances. Continuing this work is strongly suggested.
- If a large enough sample set is available over as wide a range of wheat hardness as possible a modelling technique known as "match calibrations" could be used. This model is based on H-distances. Instead of deriving a global calibration equation the software is allowed to select the, say, 50 closest spectra to the unknown sample spectra based on the H-distances. Those 50 spectra would then be used to derive a calibration equations and the unknown sample predicted. This sequence would be performed for each unknown sample to be predicted.

References

REFERENCES

AACC, 1989. Method 39-70A: Wheat hardness as determined by near infrared reflectance. In: *Approved Methods of the American Association of Cereal Chemists.* St. Paul, Minnesota. USA. American Association of Cereal Chemists.

ASTM, 1992. *Terminology relating to molecular spectroscopy.* Designation E 131 - 91a. American Society for Testing and Materials. Philadelphia, USA.

BARLOW, K.K., BUTTROSE, M.S., SIMMONDS, D.H. & VESK, M., 1973. The nature of the starch-protein interface in wheat endosperm. *Cereal Chem.*, **50**, 443-454.

BEN-GERA, I. & NORRIS, K.H., 1968a. Determination of moisture content in soybeans by direct spectrophotometry. *Isr. J. Agric. Res.*, **18**, 125-132.

BEN-GERA, I. & NORRIS, K.H., 1968b. Direct spectrophotometric determination of fat and moisture in meat products. *J. Fd. Sci.*, **33**, 64-67.

BENNION, E.B., 1969. *Breadmaking.* 4th Edition. Oxford University Press. London. pp 391.

BIRTH, G.S., 1986. The light scattering characteristics of ground grains. *Int. Agrophysics*, **2**, 59-67.

BLACKMAN, J.A. & PAYNE, P.I., 1987. Grain quality. In: Lupton, F.G.P. (ed). *Wheat Breeding: Its scientific basis.* Chapman and Hall Ltd. Chapter 15.

BROWN, G.L., CURTIS, P.S & OSBORNE, B.G., 1993. Factors affecting the measurement of hardness by near infrared reflectance spectroscopy of ground wheat. *J. Near Infrared Spectrosc.* **1**, 147-152.

BURNS, D.A., 1992. Indicator variables: How they may save time and money in NIR analysis. In: Burns, D.A. & Ciurczak, E.W., (eds). *Handbook of Near-Infrared Analysis.* Practical Spectroscopy Series, Volume 13, Marcel Dekker, Inc. New York. Chapter 12.

BURNS, D.A. & CIURCZAK, E.W. (eds), 1992. *Handbook of Near-Infrared Analysis.* Practical Spectroscopy Series, Volume 13, Marcel Dekker, Inc. New York. pp 681.

CIURCZAK, E.W., 1992. Principles of near infrared spectroscopy. In: Burns, D.A. & Ciurczak, E.W., (eds). *Handbook of Near-Infrared Analysis.* Practical Spectroscopy Series, Volume 13, Marcel Dekker, Inc. New York. Chapter 2.

COBB, N.A., 1896. The hardness of the grain in the principal varieties of wheat. *Agricultural Gazette of NSW*, 7, 279-299.

COBLENTZ, W.W., 1905. *Investigations of infrared spectra, Part I.* Publication No 35, Carnegie Institute of Washington: Washington DC (republished under the joint sponsorship of the Coblentz Society and the Perkin-Elmer Corporation, 1962).

COVENTRY, A.G., 1988. The development and application of NIR with particular reference to the food industry. *Fd. Sci. & Technol. Today*, **2**, 130-131.

COWE, I.A. & McNICOL, J.W., 1985. The use of principal components in the analysis of near infrared spectra. *Appl. Spectrosc.*, **39**, 257-266.

COWE, I.A., McNICOL, J.W. & CUTHBERTSON, 1990. Principal component analysis: A chemometric approach to the analysis of near infrared spectra. *Anal. Proc.*, **27**, 61-63.

CUTLER, G.H. & BRINSON, G.A., 1935. The granulation of whole wheat meal and a method of expressing it numerically. *Cereal Chem.*, **12**, 120-129.

DEVAUX, M.F., ROBERT, P., QANNARI, A., SAFAR, M. & VIGNEAU, E., 1993. Canonical correlation analysis of mid- and near infrared oil spectra. *Appl. Spectrosc.*, **47**, 1024-1029.

DELWICHE, S.R., 1993. Measurement of single-kernel wheat hardness using near infrared transmittance. *Trans. ASAE.*, **36**, 1431-1437.

DELWICHE, S.R. & NORRIS, K.H., 1993. Classification of hard red wheat by near infrared diffuse reflectance spectroscopy. *Cereal Chem.*, **70**, 29-35.

DiFOGGIO, R., 1995. Examination of some misconceptions about near infrared analysis. *Appl. Spectrosc.*, **49**, 67-75.

DOBRASZCZYK, B.J., 1994. Fracture mechanics of vitreous and mealy wheat endosperm. *J. Cereal Sci.*, **19**, 273-282.

ECKHOFF, S.R., SUPAK, W.A. & DAVIS, A.B., 1988. A rapid single-kernel wheat hardness tester. *Cereal Chem.*, **65**, 503-508.

FARRAND, E.A., 1964. Flour proteins in relation to the modem bread process in the United Kingdom, with special reference to α-amylase and starch damage. *Cereal Chem.*, **15**, 15-27.

FARIDI, H.A., FINLEY, J.W. & LEVEILLE, G.A., 1987. Wheat hardness: A user's view. *Cereal Foods World*, **32**, 327-329.

FINNEY, P.L., KINNEY, J.E. & DONELSON, J.R., 1988. Prediction of damaged starch in straight-grade flour by near infrared reflectance analysis of whole ground wheat. *Cereal Chem.*, **65**, 449-452.

FMBRA, 1992. Introduction of wheat and milling Short Course Handouts. FMBRA, Chorleywood, Hertfordshire, UK.

FREEMAN, G.H.C., 1992. Physical standards for calibrating NIR instruments. Murray, I. & Cowe, I.A. (eds). *Making Light Work: Advances in Near Infrared Spectroscopy*. Ian Michael Publications, Chichester, 115-123.

GELADI, P., MacDOUGAL, D. & MARTENS, H., 1985. Linearization and scatter-correction for near infrared reflectance spectra of meat. *Appl. Spectrosc.*, **39**, 491-

500.

GLENN , G.M. & JOHNSTON, R.K., 1992. Mechanical properties of starch, protein and endosperm and their relationship to hardness in wheat. *Fd. Structure*, **11**, 187-199.

GLENN, G.M. & SAUNDERS, R.M., 1990. Physical and structural properties of wheat endosperm associated with grain texture. *Cereal Chem.*, **67**, 176-182.

GLENN, G.M., YOUNCE, F.L. & PITTS, M.J., 1991. Fundamental physical properties characterizing the hardness of wheat endosperm. *J. Cereal Sci.*, **13**, 179-194.

GREENWELL, P. & SCHOFIELD, J.D., 1986. A starch granule protein associated with endosperm softness in wheat. *Cereal Chem.*, **63**, 379-380.

HALVERSON, J. & ZELENY, L, 1988. Criteria of wheat quality. In: Pomeranz, Y. (ed). *Wheat chemistry and technology*, Volume 1. American Association of Cereal Chemists, Inc., St. Paul, Minnesota, USA. Chapter 2.

HERSCHEL, F.W., 1800. Investigation of the power of the prismatic colours to heat and illuminate objects; with remarks, that prove the different refrangibility of radiant heat. To which is added, an inquiry into the method of viewing the sun advantageously with telescopes of large apertures and high magnifying powers. *Phil. Trans. Roy. Soc. (London)*, **90**, 255-283.

HOSENEY, R.C., 1994. *Principles of cereal science and technology*. 2nd Edition. American Association of Cereal Chemists. St. Paul, Minnesota, USA. pp 378.

HOSENEY, R.C. & SEIB, P.A., 1973. Structural differences in hard and soft wheat. *Bakers Digest*, **47**, 26-28, 56.

ILARI, J.L., MARTENS, H. & ISAKSSON, T., 1988. Determination of particle size in powders by scatter correction in diffuse near infrared reflectance. *Appl. Spectrosc.*, **42**, 722-728.

ISI, 1991. Routine operation and calibration software for Near Infrared Instruments. Infrasoft International, Silver Spring, Maryland, USA.

KENT, N.L. & EVERS, A.D., 1994. *Technology of Cereals*. 4th Edition. Pergamon. Elsevier Science Ltd, Oxford, UK. pp 334.

KENT-JONES, D.W. & AMOS, A.J., 1967. *Modern Cereal Chemistry*. Food Trade Press Ltd., London. pp 730.

KRZANOWSKI, W.J., 1988. Principal multivariate analysis: A User's perspective. Clarendon Press, Oxford. pp

KUBELKA, P., 1948. New contributions to the optics of intensely light-scattering materials. Part 1. *J. Opt. Soc. Am.*, **38**, 448-457

KUBELKA, P. & MUNK, F., 1931. Ein Beitrag zur Optik der Farbanstriche. *Z. Tech. Physik.*, **12**, 593-604.

LAI, F.S., ROUSSER, R., BRABEC, D & POMERANZ, Y., 1985. Determination of hardness in wheat mixtures. II. Apparatus for automated measurement of hardness of single kernels. *Cereal Chem.*, **62**, 178-184.

MAHALANOBIS, P.C., 1936. On the generalized distance in statistics. *Proc. Natl. Inst. Sci. India*, **2**, 49-55.

MANLEY, D.J.R., 1983. *Technology of biscuits, crackers and cookies.* Ellis Horwood Ltd., Chichester, England. pp 446.

MARK, H.L. & TUNNELL, D., 1985. Qualitative near infrared reflectance analysis using Mahalanobis distances. *Anal. Chem.*, **57**, 1449-1456.

MARTENS, H., JENSEN, S.A. & GELADI, P., 1983. Multivariate linearity transformations for near infrared reflectance spectrometry. *Proc. Nordic Symp. on Applied Statistics*, Stavenger, Stokkand Forlag, 205-233.

MARTENS, H. & NÆS, T., 1987. Multivariate calibration by data compression. In: Williams, P.C. & Norris, K.H. (eds). *Near Infrared Technology in the Agricultural and Food industries.* American Association of Cereal Chemists, Inc., St. Paul, Minnesota, USA. Chapter 4.

MARTIN C.R., ROUSSER, D.L. & BRABEC, D.L., 1993. Development of a single-kernel wheat characterization system. *Trans. of the ASAE*, **36**, 1399-1404.

MASSIE, D.R., SLAUGHTER, D.C., ABBOTT, J. & HRUSCHKA, W.R., 1993. Acoustic, single-kernel wheat hardness. *Trans. ASAE*, **36**, 1393-1398.

MATTERN, P.J., 1988. Wheat hardness: A microscopic classification of individual grains. *Cereal Chem.*, **65**, 312-315.

MILLER, B.S., AFEWORK, S., POMERANZ, Y., BRUINSMA, B.L. & BOOTH, G.D., 1982. Measuring the hardness of wheat. *Cereal Foods World*, **27**, 61-64.

MILLER, R., 1991. Professor Harry Willis and the history of NIR spectroscopy., *NIR news*, **2**, 12-13.

MORGAN, J.E. & WILLIAMS, P.C., 1995. Starch damage in wheat flours: A comparison of enzymatic, iodometric and near infrared reflectance techniques. *Cereal Chem.*, **72**, 209-212.

MULLER, K.E., 1982. Understanding canonical correlation through the general linear model and prinicpal components. *The American Statistician*, **36**, 342-354.

MURRAY, I., 1988. Aspects of the interpretation of near infrared spectra. *Fd. Sci. & Technol. Today*, **2**, 135-139.

MURRAY, I., & HALL, P.A., 1983. Animal feed evaluation by use of near infrared reflectance (NIR) spectrocomputer. *Anal. Proc.*, **20**, 75-79.

NABIM, 1994. National Association of British and Irish Millers Facts and Figures Leaflet. 21 Arlington street, London.

NÆS, T. & ISSAKSON, T., 1994. Some aspects of scatter correction in calibration. Part 1. *NIR news*, **5**, 4-5, 15.

NORRIS, K.H., 1962. Instrumentation of infrared radiation. *Trans. ASAE.*, **5**, 17-20

NORRIS, K.H., 1964. Reports on the design and development of a new moisture meter. *Agricultural Engineers (St Joseph, Michigan)*, **45**, 370-372.

NORRIS, K.H., 1992. A closer look at noise. *NIR news*, **3**, 4-6.

NORRIS, K.H., HRUSCHKA, W.R., BEAN, M.M. & SLAUGHTER, D.C., 1989. A definition of wheat hardness using near infrared reflectance. *Cereal Foods World*, **34**, 696-705.

NORRIS, K.H. & KUENSTNER, J.T., 1995. Rapid measurement of analytes in whole blood with NIR transmittance. In: Batten, G.D., Flinn, P.C., Welsh, L.A. & Blakeney, A.B. (eds). *Leaping ahead with near infrared spectroscopy*. NIR Spectroscopy Group, Royal Australian Chemical Institute. North Melbourne, 431-436.

NORRIS, K.H. & WILLIAMS, P.C., 1984. Optimization of mathematical treatments of raw near infrared signal in the measurement of protein in hard red spring wheat. I. Influence of particle size. *Cereal Chem.*, **61**, 158-165.

NSAS, 1991. NIRSystems spectral analysis software. Version 3.25. Perstorp Analytical Inc. Maidenhead, United Kingdom.

OLINGER, J.M. & GRIFFITHS, P.R., 1992. Theory of diffuse reflectance in the NIR region. In: Burns, D.A. & Ciurczak, E.W. (eds). *Handbook of Near-Infrared Analysis.* Practical Spectroscopy Series, Volume 13, Marcel Dekker, Inc. New York. Chapter 3.

OLINGER, J.M. & GRIFFITHS, P.R., 1993. Effects of sample dilution and particle size/morphology on diffuse reflection spectra of carbohydrate systems in the near- and mid-infrared. Part II: Durum wheat. *Appl. Spectrosc.*, **6**, 695-701.

OSBORNE, B.G., 1981. Principles and practice of near infrared (NIR) reflectance analysis. *J. Fd. Technol.*, **16**, 13-19.

OSBORNE, B.G. & DOUGLAS, S., 1981. Measurement of degree of starch damage in flour by near infrared reflectance analysis. *J. Sci. Fd. Agric.*, **32**, 328-332.

OSBORNE, B.G., 1991. Measurement of the hardness of wheat endosperm by near infrared spectroscopy. *Postharvest News and Information*, **2**, 331-334.

OSBORNE, B.G., 1992. NIR analysis of baked products. In: Burns, D.A. & Ciurczak, E.W. (eds). *Handbook of Near-Infrared Analysis.* Practical Spectroscopy Series, Volume 13, Marcel Dekker, Inc. New York. Chapter 19.

OSBORNE, B.G., DOUGLAS, S., FEARN, T. & WILLIS, K.H., 1982. The development of universal calibrations for measurement of protein and moisture in UK home-grown wheat by near infrared reflectance spectroscopy. *J. Sci. Fd. Agric.*, **33**, 736-740.

OSBORNE, B.G., FEARN, T. & HINDLE, P.H., 1993. *Practical NIR Spectroscopy with application in food and beverage analysis.* 2nd Edition. Longman, Scientific and Technical, Harlow. pp 227.

POMERANZ, Y., MARTIN, C.R., ROUSSER, R., BRABEC, D. & LAI, F.S., 1988. Wheat hardness determined by a single kernel compression instrument with semiautomated feeder. *Cereal Chem.*, **65**, 86-94.

POMERANZ, Y., PETERSON, C.J. & MATTERN, P.J., 1985. Hardness of winter wheats grown under widely different climatic conditions. *Cereal Chem.*, **62**, 463-467.

POMERANZ, Y. & WILLIAMS, P.C., 1990. Wheat hardness: its genetic, structural, and biochemical background, measurement, and significance. In: Dickinson. E & Stainsby. G. (eds). *Advances in Cereal Science and Technology.* Elsevier Applied Science publishsers Ltd., London. Chapter 8.

RANDALL, P.G., KRIEG, H.M., McGILL, A.E.J., 1992. Calibration comparison between South African and Federal Grain Inspection Service and European calibrations. *S. Afr. J. Food Sci. Nutr.*, **4**, 33-35.

REEVE, P.T.V. & WHITE, F.H., 1988. In-line measurement of beer original gravity by NIR analysis. *Fd. Sci. & Technol. Today*, **2**, 131-135.

SHENK, J.S. & WESTERHAUS, M.O., 1993. *Analysis of agriculture and food products by near infrared reflectance spectroscopy.* Monograph. Penn State University, PA, USA. pp 116.

SHENK, J.S., WORKMAN, J.J. & WESTERHAUS, M.O., 1992. Applications of NIR spectroscopy to agricultural products. In: Burns, D.A. & Ciurczak, E.W. (eds). *Handbook of Near-Infrared Analysis.* Practical Spectroscopy Series, Volume 13, Marcel Dekker, Inc. New York. Chapter 15.

SHEWRY, P.R. & MIFLIN, B.J., 1985. Seed storage proteins of economically important cereals. In: Pomeranz, Y. (ed). *Advances in Cereal Science and Technology.* Volume VII. American Association of Cereal Chemists, Inc., St Paul, Minnesota. Chapter 1.

SIMMONDS, D.H., BARLOW, K.K. & WRIGLEY, C.W., 1973. The biochemical basis of grain hardness in wheat. *Cereal Chem.*, **50**, 553-562.

STARK, E., LUCHTER, K. & MARGOSHES, M., 1986. Near infrared analysis: A technology for quantitative and qualitative analysis. *Appl. Spectrosc. Rev.*, **22**, 335-

399.

STENVERT, J.L. & KINGSWOOD, K., 1977. The influence of the physical structure of the protein matrix on wheat hardness. *J. Sci. Fd. Agric.*, **28**, 11-19.

SYMES, K.J., 1961. Classification of Australian wheat varieties based on the granularity of their wholemeal. *Aust. J. Exp. Agric. Anim. Husb.*, **1**, 18-23.

TIPPLES, K.H., KILBORN, R.H., & PRESTON, K.R., 1994. Bread-wheat quality defined. In: Bushuk, W. & Rasper, V.F. (eds). *Wheat production, properties and quality*. Chapman & Hall, Glasgow. Chapter 3.

UNSCRAMBLER, 1993. Software for multivariate data analysis applying PCA, PCR and PLS including experimental design. CAMO A/S. Trondheim, Norway.

WALL, J.S., 1979. The role of wheat proteins in determining baking quality. In: Laidman, D.L. & Wyn Jones, R.G. (eds). *Recent advances in the biochemistry of cereals*. Academic Press, New York. Chapter 11.

WETZEL, D.L., 1983. Near infrared reflectance analysis of major food components in foods. *Instrumental Analysis of Food.*, **1**, 183-202.

WIBBERLEY, J.E., 1989. *Cereal husbandry.* Farming Press Books. Ipswich. pp 258.

WILLIAMS, P.C., 1973. The application of the neotec grain quality analyzer to the analyses of cereal grains and oilseeds. 1. Preliminary observations (abstr.). *Cereal Sci. Today.*, **18**, 284-285.

WILLIAMS, P.C., 1975. Application of near infrared reflectance spectroscopy to analysis of cereal grains and oilseeds. *Cereal Chem.* **52**, 561-576.

WILLIAMS, P.C., 1979. Screening wheat for protein and hardness by near infrared reflectance spectroscopy. *Cereal Chem.* **56**, 169-172.

WILLIAMS, P.C., 1991. Prediction of wheat kernel texture in whole grains by near infrared transmittance. *Cereal Chem.*, **68**, 112-114.

WILLIAMS, P.C. & NORRIS, K.H. (eds), 1987. *Near Infrared Technology in the Agricultural and Food industries.* American Association of Cereal Chemists, Inc., St. Paul, Minnesota, USA. pp 330.

WILLIAMS, P.C. & SOBERING, D.C., 1986. Attempts at standardization of hardness testing of wheat. II. The near infrared method. *Cereal Foods World*, **31**, 417-420.

WILLIAMS, P.C. & SOBERING, D.C., 1993. Comparison of commercial near infrared transmittance and reflectance instruments for analysis of whole grains and seeds. *J. Near Infrared Spectrosc.* **1**, 25-32.

WILLIAMS, P.C. & THOMPSON, B.N., 1978. Influence of whole meal granularity on analysis of HRS spring wheat for protein and moisture by near infrared reflectance spectroscopy. *Cereal Chem.* **55**, 1014-1037.

WORKMAN, J.J., 1992. NIR spectroscopy calibration basics. In: Burns, D.A. & Ciurczak, E.W. (eds). *Handbook of Near-Infrared Analysis.* Practical Spectroscopy Series, Volume 13, Marcel Dekker, Inc. New York. Chapter 10.

WORKMAN, J. & ANDREN, H., 1993. NIR spectroscopy for at-line meat product measurements. *International Laboratory.*, April, 26-32

WORKMAN, J.J. & BURNS, D.A., 1992. Commercial NIR instrumentation. In: Burns, D.A. & Ciurczak, E.W. (eds). *Handbook of Near-Infrared Analysis.* Practical Spectroscopy Series, Volume 13, Marcel Dekker, Inc. New York. Chapter 4.

Appendices

APPENDIX 1

Table 1 Wheat hardness characteristics of samples used to construct AACC NIR wheat hardness calibration

Sample Number	Wheat Variety	hard/soft
1	Riband	soft
2	Fresco	hard
3	Mercia	hard
4	Apollo	soft
5	Hereward	hard
6	Hunter	soft
7	Mercia	hard
8	Acier	hard
9	Galahad	soft
10	Admiral	soft
11	Festival	hard
12	Apollo	soft
13	Admiral	soft
14	Alexandria	hard
15	Beaver	soft
16	Wasp	soft
17	Torfrida	hard
18	Riband	soft
19	Talon	hard
20	CWRS[#]	hard

[#] Canadian Western Red Spring (class)

Table 2 Wheat hardness characteristics of UK home-grown samples from different localities

Sample Number	Wheat Variety	hard/soft	Other Comments (localities)
1	Cadenza	hard	Morley
2	Hunter	soft	Cambridge (ADAS)
3	Spark	hard	Morley
4	Andante	soft	Holbeach
5	Hereward	hard	Morley
6	Flame	hard	Holbeach
7	Hunter	soft	Holbeach
8	Cadenza	hard	Holbeach
9	Riband	soft	Cambridge 2
10	Brigadier	hard	Cambridge 2
11	Mercia	hard	Holbeach
12	Andante	soft	Cambridge (ADAS)
13	Flame	hard	Morley
14	Prophet	hard	Cambridge (ADAS)
15	Cadenza	hard	Cambridge 2
16	Mercia	hard	Horncastle
17	Genesis	hard	Horncastle
18	Cadenza	hard	Horncastle
19	Mercia	hard	Cambridge 2
20	Spark	hard	Cambridge 2
21	Spark	hard	Holbeac
22	Rialto	hard	Holbeach
23	Hunter	soft	Horncastle
24	Flame	hard	Cambridge (ADAS)
25	Riband	soft	Horncastle
26	Prophet	hard	Horncastle
27	Brigadier	hard	Cambridge (ADAS)
28	Mercia	hard	Morley
29	Riband	soft	Cambridge (ADAS)
30	Hereward	hard	Cambridge (ADAS)
31	Hereward	hard	Horncastle
32	Rialto	hard	Morley
33	Hunter	soft	Cambridge 2
34	Andante	soft	Horncastle
35	Riband	soft	Morley
36	Prophet	hard	Cambridge 2
37	Mercia	hard	Cambridge (ADAS)
38	Flame	hard	Cambridge 2
39	Cadenza	hard	Cambridge (ADAS)
40	Genesis	hard	Cambridge 2
41	Genesis	hard	Holbeach
42	Hunter	soft	Morley
43	Hereward	hard	Cambridge 2
44	Brigadier	hard	Holbeach
45	Rialto	hard	Cambridge (ADAS)
46	Rialto	hard	Cambridge 2
47	Riband	soft	Holbeach
48	Genesis	hard	Cambridge (ADAS)
49	Spark	hard	Cambridge (ADAS)
50	Andante	soft	Morley
51	Brigadier	hard	Morley
52	Andante	soft	Cambridge 2
53	Hereward	hard	Holbeach
54	Brigadier	hard	Horncastle

Table 3 Wheat hardness characteristics of the varieties Riband and Mercia at different protein levels from two harvests

Sample Number	Wheat Variety	hard/soft	Other Comments
1	Riband	soft	10 % protein, 1991 harvest
2	Riband	soft	11 % protein, 1991 harvest
3	Mercia	hard	11 % protein, 1991 harvest
4	Mercia	hard	12 % protein, 1991 harvest
5	Riband	soft	10 % protein, 1992 harvest
6	Riband	soft	11 % protein, 1992 harvest
7	Mercia	hard	11 % protein, 1992 harvest
8	Mercia	hard	12 % protein, 1992 harvest

Table 4 Wheat hardness characteristics of Canadian home-grown wheat samples

Sample Number	Wheat Variety	hard/soft
1	URBAN	hard
2	CREW	soft
3	DAWS	soft
4	Len	hard
5	Wheaton	hard
6	Marshall	hard
7	Perlo	hard
8	Absolvent	hard
9	Max	hard
10	Frankenmuth	soft
11	Vic 1985	durum
12	Vic 1987	durum
13	Augusta	soft
14	HRS PC86	hard
15	Fielder 85 HP	soft
16	2 CPS CK	hard
17	ICEWW	soft
18	1CWAD	durum
19	2CWAD	durum
20	ARW	hard
21	ARW	hard
22	unknown	hard

APPENDIX 2

2.0 Determination of wheat hardness by Air Jet Sieve

2.1 Preparation of grain samples

A representative sample of wheat (ca. 50 g) must be ground. The Model 3100 hammer mill (Falling Number AB, Huddinge, Sweden) fitted with a 1 mm screen must be fed carefully with grain to avoid heating and overloading. Grinding should be continued for 30-40 seconds after the last of the sample has entered the mill. Small quantities of bran particles remaining on the sieve may be discarded. The ground grain must be carefully mixed before use.

2.2 Determination

2.2.1 Check that the 75 μm sieve is in place on the Alpine Air Jet Sieve (as set up at the CCFRA).

2.2.2 Check that the manometer gives a pressure reading between 100 and 110 mm with the apparatus turned on and the perspex lid in place, if not adjust the air valve accordingly and if necessary replace the filter paper. After 5 or 6 tests or earlier if it proves impossible to obtain a satisfactory manometer reading it will be necessary to clean or replace the filter paper again.

2.2.3 Weigh 10.0 g ground wheat. Remove the perspex lid, scatter the ground wheat onto the sieve and replace the lid.

2.2.4 Start the timer and air jet sieve simultaneously. If any ground wheat adheres to the underside of the perspex lid, free by gently rapping the lid with the mallet. Check that the manometer is reading between 100 and 110 mm, if not adjust the air valve accordingly.

2.2.5 Run the sieve for 90 seconds then turn off, remove the perspex lid and transfer any particles adhering to the underside to the sieve.

2.2.6 Remove the sieve. Brush out any material remaining on top of the mesh onto the paper. Transfer the contents of the paper to a previously weighed or tared off container. Weigh and record the weight to the nearest 0.01g.

2.3 Expression of results

2.3.1 Calculate the weight of throughs by subtracting the weight obtained in 1.3.5 from the initial sample weight, 10.0 g.

2.3.2 The particle size of ground wheat increases with hardness, therefore the higher the weight of throughs the softer the wheat, a weight less than 4.0 g indicates a hard wheat while a weight of 4.0 g or more indicates a soft wheat.

2.3.3 Express the final result as percentage throughs.

APPENDIX 3

3.0 Determination of wheat hardness by Particle Size Index test

(Williams & Sobering, 1986)

3.1 Preparation of grain samples

A representative sample of wheat must be ground. Set the grinder at its finest setting. Grind 22 - 23 g of wheat. The wheat should contain no more than 1 % foreign material and should have a moisture content of 11-13 % whole grain basis. (This moisture range has a negligible influence on the PSI test). The ground grain must be carefully mixed before use.

3.2 Determination

3.2.1 Accurately weigh 10.0 g ground wheat to the nearest 0.01 g. Transfer the ground wheat to a 74 μm sieve with a receiving pan and add approximately 50 g of whole wheat kernels or sieve cleaners to prevent clogging of the sieve and cover with lid.

3.2.2 Sieve for exactly 10 minutes on an automatic sieve shaker, preferably fitted with a percussion device.

3.2.3 Transfer all throughs, including those adhering to the bottom of the sieve, into the receiving pan. Weigh throughs to the nearest 0.01 g.

3.3 Expression of results

3.3.1 Calculate the weight of throughs.

3.3.2 The particle size of ground wheat increases with hardness, therefore the higher the weight of throughs the softer the wheat, a weight less than 7.0 g indicates a hard wheat while a weight of 7.0 g or more indicates a soft wheat.

3.3.3 Express the final result as percentage throughs

APPENDIX 4

4.0 Determination of wheat hardness by near infrared spectroscopy

(AACC, 1989)

4.1 Standard samples

Two sets of 10 wheat samples covering a range of hardness (5 hard and 5 soft) to construct the initial calibration and validate the equation, respectively.

4.2 Preparation of grain samples

A representative sample of wheat must be ground. The mill must be fed carefully with grain to avoid heating and overloading. Grinding should be continued for 30-40 seconds after the last of the sample has entered the mill. Small quantities of bran particles remaining on the sieve may be discarded. The ground grain must be carefully mixed before use.

4.3 Constructing initial calibration

4.2.1 Enter the following initial constants into the instrument:

K0 = 0.0, K1 = -1099 and K2 = 1475

where K1 is the constant at 1680 nm and K2 is the constant at 2230 nm.

4.2.2 Insert each of the ground calibration samples into the NIR instrument and record the predicted AACC wheat hardness score for each of these samples based on the equation above.

4.4 Constructing final calibration

4.4.1 Calculate the mean hardness scores for the five hard (MH) samples and five soft (MS) samples, respectively.

4.4.2 Calculate new constants as follows by making the MH equal to 75 and the MS equal to 25:

slope correction, b = 50/(MH - MS)

bias correction, a = 25 - (b x MS)

New K0" = a, new K1" = b x K1 and new K2" = b x K2

4.4.3 Enter these new constants into the instrument. It is now standardised to measure AACC wheat hardness scores.

4.5 Expression of results

The absorption of near infrared energy increases with particle size and the particle size of ground what increases with hardness. Therefore near infrared reflectance can be used to indicate the hardness of wheat.

4.5.1 Express the results as AACC wheat hardness scores

APPENDIX 5

Table 5 Detailed regression results for multiplicative scatter correction calibration

Sample Number	Ground grain (reflectance)		Whole grain (reflectance)		Whole grain (transmittance)	
	intercept	slope	intercept	slope	intercept	slope
1	0.019700	1.170	0.15000	0.941	-0.9270	1.190
2	0.017500	1.280	0.16100	0.960	-0.9610	1.210
3	0.017300	1.180	0.13200	0.920	-0.9120	1.200
4	-0.000949	1.130	0.06690	0.856	0.5130	0.828
5	0.016200	1.110	0.10600	0.861	0.0229	1.050
6	0.014100	1.090	0.02780	1.050	-1.2100	1.370
7	0.001240	1.050	0.02020	1.010	-0.0349	0.947
8	0.011400	1.080	0.08040	0.993	-0.5410	1.100
9	-0.001810	1.010	-0.02430	1.060	0.1030	0.918
10	0.008880	1.060	0.10600	0.816	0.4460	0.877
11	-0.002760	1.000	-0.00378	0.998	0.2010	0.922
12	-0.003050	1.090	-0.06120	1.080	0.2960	0.929
13	-0.004390	1.070	0.03380	0.936	0.5450	0.796
14	0.002930	1.010	0.02740	0.885	0.8820	0.713
15	0.010300	1.030	0.13400	0.925	-0.0562	0.927
16	-0.000177	1.070	0.03960	0.917	-0.3080	1.050
17	-0.003550	1.040	-0.03830	1.050	0.8310	0.727
18	-0.001250	1.030	-0.02140	0.971	0.6430	0.828
19	-0.000154	1.060	0.00746	1.060	-0.5680	1.140
20	-0.001690	1.030	0.05200	0.951	0.3830	0.822
21	0.011600	1.010	0.02790	1.010	-0.1070	1.390
22	-0.001160	1.070	-0.01220	1.070	-0.2820	1.050
23	-0.002190	1.020	-0.01810	1.080	0.2230	0.913
24	-0.003040	1.080	0.00411	1.090	-0.3090	1.050
25	-0.002940	1.050	0.00722	0.992	0.0554	0.961
26	-0.002340	1.010	0.03590	0.907	0.7090	0.772
27	-0.002350	1.060	-0.04480	1.040	0.3220	0.955
28	-0.000616	1.010	0.02500	0.931	0.4870	0.819
29	-0.003630	1.000	-0.03010	1.050	0.3120	0.871
30	-0.001620	1.020	0.01270	0.965	0.4940	0.830
31	-0.002710	1.080	0.01590	1.060	-0.7940	1.220
32	-0.007780	1.020	-0.14800	1.200	0.1220	1.030
33	-0.004130	1.070	0.00358	1.030	0.1430	0.914

Table 5 continued/...

34	-0.003710	1.090	-0.01880	0.957	-0.3850	1.160
35	-0.005820	1.060	0.02740	1.030	0.5330	0.774
36	-0.002630	1.080	0.02650	0.951	-0.1480	1.000
37	-0.004090	1.070	0.02020	1.010	-0.6110	1.170
38	-0.002470	0.973	0.00733	0.902	0.7970	0.704
39	-0.003390	0.964	-0.04090	0.992	0.5030	0.886
40	0.008550	0.948	0.07450	0.860	-0.0913	1.040
41	-0.006390	1.010	-0.08460	1.130	0.2590	0.957
42	-0.004620	1.080	-0.06790	1.120	0.0240	1.010
43	0.000096	0.896	-0.00594	0.987	0.5750	0.824
44	-0.005160	0.917	-0.00189	1.000	0.8810	0.705
45	-0.004320	0.889	-0.03660	1.080	0.5530	0.837
46	-0.004110	0.976	-0.06920	1.140	-0.9040	1.260
47	-0.004580	0.931	-0.02690	0.995	0.2450	1.260
48	-0.005320	0.883	-0.07840	1.020	0.2450	0.911
49	-0.006340	0.933	-0.02880	1.020	0.6440	0.887
50	-0.006800	0.865	-0.14700	1.140	-0.0361	1.090
51	-0.006410	0.899	-0.05640	1.030	0.6730	0.808
52	-0.006150	0.890	-0.02910	0.986	0.3090	0.908
53	-0.002950	0.890	-0.02980	0.966	0.8260	0.817
54	0.003200	0.856	0.00941	0.755	2.6900	0.377
55	-0.005540	0.906	-0.00816	1.000	-0.4730	1.100
56	-0.007230	0.904	-0.09520	1.040	-0.8160	1.320
57	-0.004860	0.853	0.00092	0.880	0.5560	0.798
58	-0.004610	0.863	-0.02030	1.070	-0.7870	1.240
59	0.009760	0.870	-0.01910	1.070	-2.0100	1.680
60	0.005780	0.852	0.01600	1.040	-0.3450	1.210
61	0.004380	0.868	-0.03220	1.000	-2.3100	1.790
62	-0.006320	0.832	-0.08090	1.090	0.5310	0.873
63	0.005360	0.847	-0.02910	1.000	-1.6800	1.620

Multiplicative scatter correction regression equations:

(a = intercept; b = slope)

Ground grain reflectance

AJS = 97.9 - 141a - 61.4b

PSI = 129 + 14.8a - 67.8b

Whole grain reflectance

AJS = 66.3 - 95.7a - 29.7b

PSI = 102 - 97.3a - 40.4b

AACC = -85.1 + 393a + 144b

Whole grain transmittance

AJS = 0.55 + 10.4a + 35.7b

PSI = 21.8 + 12.2a + 39.3b

AACC = 187 - 42.8a - 127b

Table 6 Detailed results for mulitplicative scatter correction calibration equation validation

Sample Number	Ground grain (reflectance)		Ground grain (reflectance)		Ground grain (reflectance)	
	intercept	slope	intercept	slope	intercept	slope
1	0.00915	1.080	0.09350	0.966	0.0008	0.925
2	0.00174	1.120	0.07350	0.858	0.7110	0.754
3	0.01090	1.110	0.15500	0.906	0.7040	0.693
4	0.01210	1.100	0.08060	0.851	0.3470	0.937
5	0.01040	1.100	0.11800	0.909	0.2770	0.854
6	0.00099	1.040	0.02020	0.956	0.1460	0.910
7	-0.00427	1.050	0.04480	0.899	0.5600	0.788
8	0.01170	1.100	0.09990	0.886	0.1530	1.010
9	0.00221	0.976	0.02010	0.955	0.2070	0.912
10	0.00072	1.090	0.02720	0.966	-0.1230	1.000
11	-0.00128	1.030	-0.01770	0.962	0.6280	0.833
12	-0.00149	0.991	-0.01190	1.030	0.0121	0.947
13	-0.00062	1.060	0.02110	1.010	0.5100	0.812
14	0.00129	1.060	0.02060	1.010	-0.3570	1.070
15	-0.00285	1.020	0.03020	0.909	0.1540	0.884
16	-0.00359	1.050	-0.05710	1.070	0.1020	0.986
17	-0.00717	1.060	-0.02900	1.060	0.0821	0.969
18	-0.00480	1.100	0.07060	0.903	0.4860	0.784
19	-0.00272	1.060	0.02860	1.070	-0.3300	1.000
20	-0.00498	1.010	-0.05640	1.020	0.4560	0.873
21	-0.00416	1.070	0.00764	1.020	0.1290	0.919
22	-0.00239	1.030	0.05920	0.915	0.6470	0.766
23	-0.00291	1.030	-0.03180	1.100	-0.3140	1.060
24	-0.00419	1.050	-0.00916	1.020	0.4520	0.840
25	0.00711	1.040	0.08500	0.996	0.2300	0.878
26	-0.00548	1.020	-0.01010	1.060	-0.1540	1.030
27	-0.00455	0.997	-0.02470	1.010	0.7390	0.792
28	-0.00292	0.927	0.00517	1.020	0.3410	0.873
29	-0.00500	0.906	-0.05840	1.030	0.5220	0.897
30	-0.00426	0.906	-0.01790	0.917	1.3600	0.664
31	-0.00453	0.913	-0.03400	0.989	-0.0406	1.000
32	-0.00621	0.880	-0.08200	1.070	0.3810	0.934
33	0.00608	0.908	-0.05440	1.160	-2.4800	1.770
34	-0.00354	0.887	-0.05290	0.943	0.3510	0.943
35	-0.00314	0.877	-0.06670	0.905	0.9360	0.797

Table 6 continued/...

36	-0.00626	0.877	-0.06920	1.030	1.0100	0.633
37	0.00648	0.880	-0.02210	0.957	-1.0900	1.370
38	-0.00713	0.911	-0.03030	0.967	-0.0427	1.010
39	-0.00608	0.840	-0.05060	1.020	0.5920	0.830
40	-0.00434	0.876	-0.03850	0.979	-0.1500	1.060
41	-0.00582	0.842	-0.01390	0.956	0.5370	0.819

APPENDIX 6

Table 7 Detailed regression results for principal component calibrations

Sample Number	Ground grain (reflectance) 1st PC	Ground grain (reflectance) 2nd PC	Whole grain (reflectance) 1st PC	Whole grain (reflectance) 2nd PC	Whole grain (transmittance) 1st PC	Whole grain (transmittance) 2nd PC
1	-11.946588	0.134140	-24.965321	-1.177564	26.718596	2.409528
2	-12.940772	-0.016358	-25.021841	-1.076193	26.890972	2.391913
3	-11.990660	0.101772	-23.506571	-1.077618	27.065434	2.400296
4	-11.075635	-0.142338	-20.141943	-1.194761	30.160086	1.944855
5	-11.317241	-0.017956	-21.586758	-1.159868	32.090000	2.261924
6	-11.002854	-0.112325	-23.341068	-1.898884	29.095575	2.539629
7	-10.369346	-0.159756	-22.242554	-1.641891	28.263205	1.952518
8	-10.889919	-0.112481	-23.437748	-1.507772	27.819239	2.184057
9	-9.837719	-0.075037	-22.211477	-1.939419	28.785872	1.930440
10	-10.582386	-0.003249	-20.541098	-1.112277	30.987982	1.941355
11	-9.771867	-0.048433	-21.398783	-1.741703	29.890598	1.960492
12	-10.613857	-0.163659	-21.632309	-2.173174	31.039616	2.001138
13	-10.433714	-0.000018	-21.033642	-1.448952	29.527220	1.848461
14	-9.934754	-0.153122	-19.755974	-1.412879	30.387140	1.779402
15	-10.336615	0.016887	-24.082033	-1.227111	27.449142	1.921361
16	-10.520906	-0.171238	-20.768408	-1.390745	28.709608	2.144080
17	-10.155630	-0.108264	-21.630623	-2.009384	30.326672	1.718313
18	-9.891143	-0.050473	-21.536587	-1.852796	30.423904	1.702596
19	-10.424286	-0.123987	-23.105532	-1.778383	28.634518	2.187549
20	-10.054148	-0.131211	-21.813976	-1.402421	28.694454	1.804096
21	-10.156131	0.059995	-23.240637	-1.823075	31.345240	2.641690
22	-10.502978	-0.142054	-22.720089	-1.900711	28.912016	2.162851
23	-9.925179	-0.026746	-22.907204	-1.923496	29.825487	1.903045
24	-10.565039	-0.123101	-23.610325	-1.829373	28.711660	2.129965
25	-10.272280	-0.142879	-21.543594	-1.699345	29.588570	2.099049
26	-9.863538	-0.121905	-20.446384	-1.437986	30.463341	1.845527
27	-10.326969	-0.152242	-21.247637	-2.027602	32.099796	2.104918
28	-9.912212	-0.128640	-20.687292	-1.504837	29.654711	1.842998
29	-9.757918	-0.031795	-21.857023	-1.944699	29.454622	1.919863
30	-9.932524	-0.099184	-21.120693	-1.600280	30.048708	1.843409
31	-10.480819	-0.092042	-22.366405	-1.886243	28.804171	2.264308
32	-9.805094	-0.071670	-22.091438	-2.825534	32.205334	2.141688
33	-10.189909	-0.134049	-22.124119	-1.717418	30.480164	1.766327
34	-10.638790	-0.117838	-20.298080	-1.717099	31.047197	2.352421

Table 7 continued/...

35	-10.225714	-0.119094	-22.965805	-1.615902	28.739719	1.739619
36	-10.506010	-0.134204	-21.166325	-1.515515	28.717262	2.057503
37	-10.424335	-0.123782	-22.894506	-1.856624	29.100241	2.262768
38	-9.481025	-0.000758	-19.618320	-1.545840	29.270851	1.692673
39	-9.369641	-0.028289	-20.318933	-1.932500	31.816757	1.963649
40	-9.505239	-0.024631	-20.208227	-1.277094	30.518114	2.114088
41	-9.704583	-0.046272	-22.212730	-2.367534	31.504559	2.000907
42	-10.493829	-0.155710	-22.363420	-2.265173	30.663738	2.025680
43	-8.784720	-0.116053	-21.102238	-1.751696	30.681194	1.908970
44	-8.873065	-0.145720	-21.495127	-1.740263	30.153425	1.716895
45	-8.614141	-0.085840	-22.226353	-2.035204	30.844309	1.854737
46	-9.469341	-0.109785	-22.824793	-2.312856	28.907990	2.368699
47	-9.022524	-0.147465	-20.725338	-1.876354	29.976620	1.974977
48	-8.528495	-0.045122	-20.047823	-2.178725	33.261852	1.997428
49	-8.998233	-0.156971	-21.288525	-1.905534	30.515532	1.992897
50	-8.319610	-0.037675	-20.683533	-2.732047	32.436222	2.270186
51	-8.665327	-0.133895	-20.669815	-2.088087	31.161686	1.963358
52	-8.580606	-0.134975	-20.474289	-1.870860	30.525253	1.995906
53	-8.661480	-0.110723	-20.038927	-1.840409	32.981617	1.947734
54	-8.468971	-0.174183	-16.465368	-1.377886	38.395641	1.825570
55	-8.751063	-0.084792	-21.414917	-1.767919	28.623123	2.154888
56	-8.690296	-0.129611	-19.922132	-2.300888	31.614597	2.548259
57	-8.243854	-0.011905	-18.976080	-1.543652	29.714567	1.780318
58	-8.353862	-0.083862	-22.476673	-1.928308	29.497477	2.395504
59	-8.764208	0.131184	-23.172651	-2.211734	30.500412	3.014321
60	-8.493293	0.134755	-23.178579	-1.974116	33.130352	2.564970
61	-8.617631	0.060370	-20.796038	-2.079575	31.016836	3.208808
62	-8.004599	-0.025243	-21.431776	-2.297155	31.707047	1.936645
63	-8.435912	0.041270	-21.075897	-1.995474	32.056473	2.987750

Principal components analysis regression equations:

(x = 1st PC; y = 2nd PC)

Ground grain reflectance

AJS = 97.5 + 6.22x

AJS = 36.6 + 0.4y

AJS = 97.6 + 6.22x + 0.42y

PSI = 123 + 6.24x

PSI = 61.2 -3.9y

PSI = 122 + 6.24x - 3.9y

Whole grain reflectance

AJS = 81.6 + 2.08x

AJS = 18.7 - 10y

AJS = 63.7 + 2.08x - 10y

PSI = 113 + 2.4x

PSI = 46.2 - 8.54y

PSI = 98.2 + 2.4x - 8.54y

AACC = -139-9.15x

AACC = 123+36y

AACC = -74.9 - 9.15x + 36y

Whole grain transmittance

AJS = -24.8 + 2.03x

AJS = 26.9 + 4.62y

AJS = -34.5 + 2.03x + 4.62

PSI = -5.6 + 2.22x

PSI = 53.4 + 3.83y

PSI = -13.7 + 2.22x + 3.83y

AACC = 303 - 8.1x

AACC = 66.7 - 3.8y

AACC = 311 - 8.1x - 3.79y

Table 8 Detailed results for principal component calibration equation validation

Sample Number	Ground grain (reflectance) 1st PC	Ground grain (reflectance) 2nd PC	Whole grain (reflectance) 1st PC	Whole grain (reflectance) 2nd PC	Whole grain (transmittance) 1st PC	Whole grain (transmittance) 2nd PC
1	10.800240	-00.186820	-23.287900	-01.288600	27.946650	01.973676
2	10.985020	00.110473	-20.433500	-01.180760	29.934000	01.815888
3	11.103950	-00.015480	-23.571800	-00.881910	28.001250	01.641114
4	11.050560	00.050880	-20.454400	-01.187270	31.783680	02.019776
5	11.002750	-00.013690	-22.685200	-01.076270	28.572110	01.837854
6	10.197340	00.144089	-21.192000	-01.599150	28.979610	01.933380
7	10.171330	00.028758	-20.584300	-01.375660	29.434330	01.778923
8	11.016470	00.001259	-21.703300	-01.153160	32.142850	02.244757
9	09.624007	00.111224	-21.151700	-01.609200	29.630030	02.001526
10	10.680790	00.172016	-21.589200	-01.552750	28.979560	02.051446
11	10.057910	00.161696	-20.355300	-01.793180	31.468550	01.912744
12	09.671897	00.055213	-22.026500	-01.882780	28.743580	01.979887
13	10.334370	00.139646	-22.351800	-01.643000	29.673230	01.782389
14	10.428370	00.161401	-22.437500	-01.665020	28.710410	02.148778
15	09.950161	00.023486	-20.425900	-01.455140	28.270830	01.862817
16	10.232040	00.139204	-21.601300	-02.163660	30.835420	02.031454
17	10.186440	00.083684	-22.135800	-01.989480	30.094790	02.014292
18	10.638060	00.134101	-21.342400	-01.260890	28.578950	01.794156
19	10.363140	00.086308	-23.892500	-01.697170	27.037570	02.008656
20	09.775449	00.074395	-20.627200	-02.089680	30.964200	01.966159
21	10.412440	00.149819	-22.322300	-01.732470	29.054170	01.932059
22	10.072930	00.031044	-21.299900	-01.335930	29.641430	01.799229
23	10.014120	00.031846	-22.964100	-02.087620	28.930390	02.152027
24	10.191340	00.128173	-21.745600	-01.838500	29.912440	01.818230
25	10.401460	-00.008360	-23.716400	-01.385250	28.842150	01.866669
26	09.875302	00.041774	-22.617300	-01.898750	29.552990	02.098709
27	09.657533	00.091975	-21.172400	-01.904360	31.344260	01.875589
28	09.014145	00.127590	-22.248500	-01.750190	29.803320	01.896559
29	08.761470	00.048374	-20.782700	-02.112870	32.344680	01.967095
30	08.776649	00.089282	-19.358600	-01.743560	33.737490	01.838602
31	08.840230	00.147576	-20.517800	-01.925210	29.873600	02.059899
32	08.474726	00.035846	-20.989900	-02.294130	32.038500	01.998260
33	09.041943	-00.047300	-23.580200	-02.351900	28.592170	03.104004
34	08.611025	00.142971	-19.024700	-01.967010	32.008380	02.077469
35	08.519975	00.160796	-17.821200	-01.980970	33.489640	01.937537
36	08.442873	00.081242	-20.550800	-02.186040	29.287080	01.764529
37	08.777752	00.020679	-20.104500	-01.891300	30.357320	02.73083

Table 8 continued/...

38	08.753591	00.119492	-20.127200	-01.869080	30.051210	02.060263
39	08.085545	00.056709	-20.708500	-02.049920	31.027720	01.880508
40	08.477450	00.106343	-20.180300	-01.926790	30.459460	02.109549
41	08.105256	00.043160	-20.324400	-01.759540	30.153010	01.828764

APPENDIX 7

Table 9 Detailed results for the AREA under the second derivative curve calibration

Sample Number	Ground grain (reflectance)	Whole grain (reflectance)	Whole grain (transmittance)
1	3.956105	3.620997	2.060018
2	4.327933	3.614851	2.077621
3	3.996861	3.465485	2.139927
4	3.895900	3.128077	1.979986
5	3.794264	3.363437	2.271941
6	3.759191	4.015727	2.487925
7	3.634938	3.648698	2.014922
8	3.677157	3.622752	2.074539
9	3.555259	3.832201	2.097887
10	3.591400	3.311381	2.300694
11	3.508948	3.633696	2.181625
12	3.795028	3.884770	2.232849
13	3.738897	3.418313	2.009652
14	3.433071	3.139962	1.845546
15	3.520162	3.694228	2.055318
16	3.692350	3.286239	2.088637
17	3.646419	3.763194	2.035096
18	3.540097	3.734218	2.092151
19	3.656253	3.717008	2.237404
20	3.544855	3.505147	1.965045
21	3.522083	3.910763	2.744504
22	3.723833	3.808783	2.078709
23	3.567290	3.863985	2.374615
24	3.766831	3.839292	2.163078
25	3.655122	3.565130	2.008279
26	3.509147	3.375108	1.905866
27	3.695236	3.756407	2.232766
28	3.509895	3.418709	1.989070
29	3.514066	3.743252	2.160623
30	3.539823	3.440779	2.158281
31	3.728909	3.712600	2.430008
32	3.628633	4.489585	2.558011
33	3.628873	3.626683	2.066831
34	3.714502	3.352326	2.297431
35	3.663754	3.576545	2.039643

Table 9 continued/...

36	3.719627	3.404761	2.115034
37	3.740535	3.815143	2.345037
38	3.394414	3.302548	2.010541
39	3.406220	3.663372	2.270491
40	3.302580	3.384906	2.347183
41	3.551508	4.135534	2.477210
42	3.743169	4.007442	2.403489
43	3.156209	3.537863	2.026048
44	3.212587	3.507174	1.960066
45	3.145596	3.858063	2.220826
46	3.448312	4.120272	2.412997
47	3.292584	3.644414	2.087161
48	3.138312	3.761650	2.657844
49	3.282834	3.660517	2.183334
50	3.141952	4.328769	2.538311
51	3.206215	3.752576	1.935527
52	3.185647	3.602152	2.088966
53	3.136050	3.512033	2.281149
54	3.042003	2.933970	1.831220
55	3.195136	3.590857	2.306710
56	3.246514	3.892939	2.525972
57	3.004770	3.251588	2.181247
58	3.073414	3.722889	2.351271
59	3.114746	4.143379	3.010916
60	3.036098	4.033339	2.681652
61	3.100878	3.946275	3.011524
62	2.971514	4.001484	2.369094
63	3.087876	3.967123	3.076638

Area under the second derivative curve regression equations:

(a = area)

Ground grain reflectance

AJS = 112 - 21.6a

PSI = 140 - 22.4a

Whole grain reflectance

AJS = 13.8 + 6.21a

PSI = 46 + 4.2a

AACC = 127 - 18.6a

Whole grain transmittance

AJS = 9.75 + 12a

PSI = 39.3 + 9.88a

AACC = 129 - 31.5a

Table 10 Detailed results for the AREA under the second derivative curve calibration equation validation

Sample Number	Ground grain (reflectance)	Whole grain (reflectance)	Whole grain (transmittance)
1	3.663307	3.616895	2.223921
2	3.856852	3.148992	1.923079
3	3.753353	3.420810	1.886387
4	3.742871	3.305861	2.304705
5	3.746211	3.452351	2.085024
6	3.604455	3.483826	2.041115
7	3.656096	3.270647	2.095123
8	3.731037	3.358872	2.248791
9	3.401255	3.519657	2.000184
10	3.742277	3.409549	2.120841
11	3.580695	3.493071	2.148600
12	3.488989	3.784068	2.132233
13	3.641038	3.575202	2.078862
14	3.659372	3.542617	2.126739
15	3.537841	3.322729	2.084992
16	3.675159	3.874813	2.316841
17	3.687898	3.828495	2.291912
18	3.798076	3.296509	1.914266
19	3.646681	3.746624	2.050989
20	3.536503	3.757182	2.129951
21	3.702386	3.609655	2.124602
22	3.583000	3.365640	2.001760
23	3.613647	3.983409	2.285687
24	3.636707	3.669250	2.148529
25	3.592541	3.760101	2.171609
26	3.586435	3.851892	2.305272
27	3.466155	3.623024	2.097190
28	3.242564	3.615268	2.082861
29	3.203428	3.795271	2.360834
30	3.193941	3.375704	2.174191
31	3.218622	3.606303	2.203384
32	3.142644	3.918375	2.393449
33	3.255027	4.508751	2.875307
34	3.163163	3.548550	2.186588
35	3.117209	3.424882	2.159635
36	3.160890	3.870178	1.529075
37	3.164732	3.869475	2.355030

Table 10 continued/...

38	3.212360	3.580375	2.284584
39	3.013177	3.742080	2.239212
40	3.110366	3.589592	2.353201
41	3.008332	3.477012	2.196245

Copyright Statement

Marena Manley
28/7/95